NUMERICAL AND EXPERIMENTAL STUDY OF TRANSIENT HEAT TRANSFER THROUGH CONCRETE

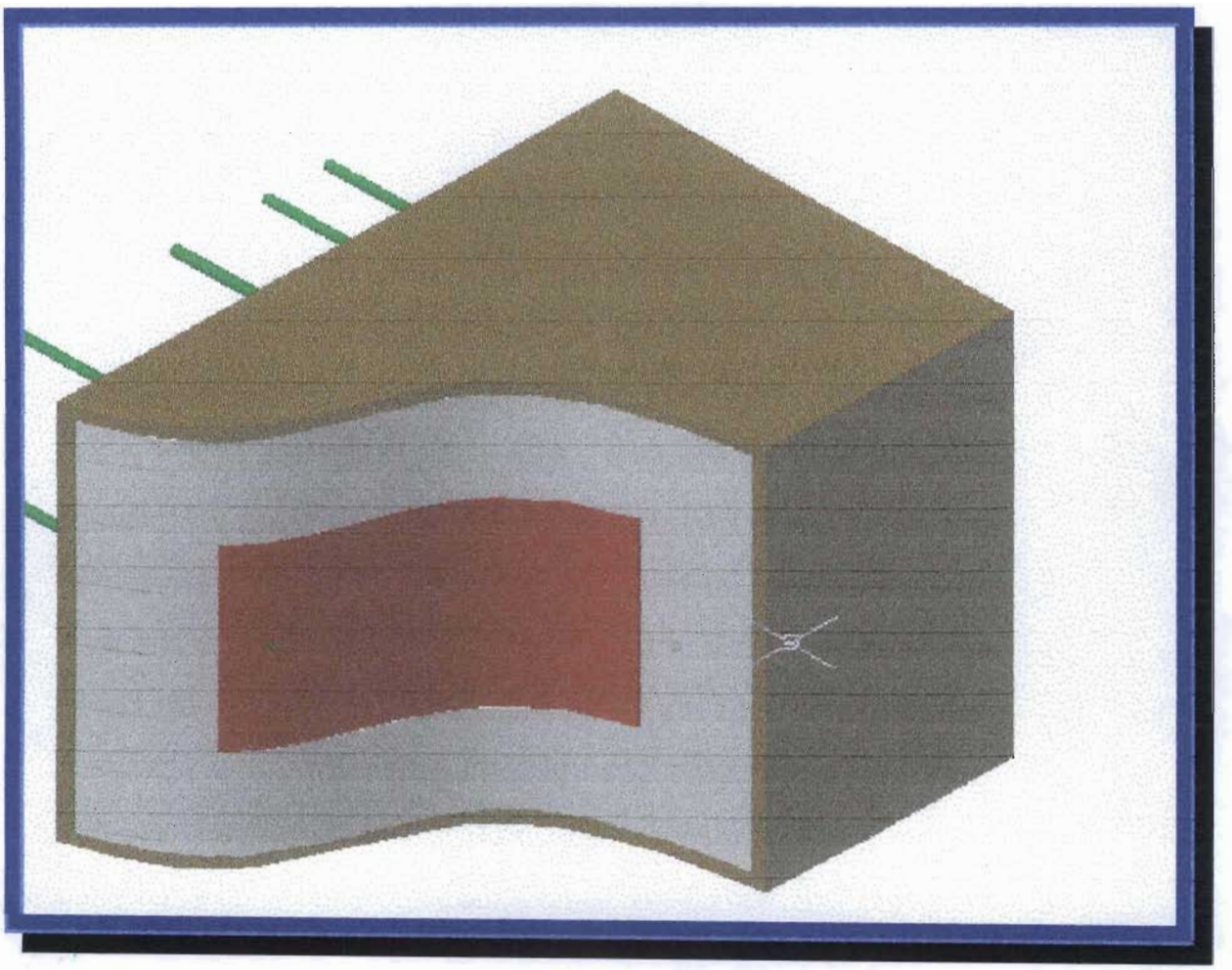

STUDENT: T. G. MABUYA

STUDENT NUMBER: 9306369

SUPERVISOR: PROF O. O. ONYEJEKWE

NUMERICAL AND EXPERIMENTAL STUDY OF TRANSIENT HEAT TRANSFER THROUGH CONCRETE

GORDON THABO MABUYA (9306369)

PROFESSOR O.O. ONYEJEKWE (Supervisor)

August 2001

DECLARATION

I declare that this thesis is my own, unaided work, except where otherwise acknowledged. It has not been submitted before for any degree or examination purpose at any other institution.

.....
Thabo Gordon Mabuya
Student

.....
Date

Certification

A Thesis submitted to the Faculty of Engineering, School of Civil Engineering, University of Durban Westville for a fulfillment of the requirements for the degree of Masters of Science in Engineering.

.....	.....	.....
Prof. O.O. Onyejekwe	Dr. F. Orulosongo	Thabo Gordon Mabuya
(Supervisor)	(Discipline Chair)	(Student)
20 - IX - 2001	27 Sept. 01.	

ABSTRACT

The increase in temperature of developing concrete as a result of heat liberated by cementing reactions is the primary cause for thermally induced cracks in large concrete elements. It is very essential, in engineering to predict the temperature rises in order to be able to minimise the potential of crack formation. This thesis covers the experimental determination of the heat of hydration curve using the adiabatic calorimeter and experimental determination of transient heat transfer obtained from measurement of temperature variations in concrete at its early ages of hydration. The measured temperature profiles from a one-dimensional heat transfer scenario are then compared with the predicted temperature profiles.

The adiabatic hydration curve of a concrete beam sample is used as input into a numerical technique known as the Green Element Method for the calculation of temperature profiles. Time-based boundary conditions are imposed on the equation governing the model and will be solved using the Green Element Method coded in Fortran Power Station 4.0.

ACKNOWLEDGEMENTS

I would like to express greatest praises to the Lord Who has been my greatest inspiration and this work could not have been achieved without His Will and Blessings.

My greatest thanks goes to my supervisor, Professor O.O. Onyejekwe for the courage, confidence, understanding, advices and guidance that he has offered me since my undergraduate studies up to this far. I only pray and hope that this should not end at this point, and will endeavor to work with him in the near future.

I also like to thank Professor Y Bhalim, from the Witwatersrand University for his time, knowledge and guidance in conducting the laboratory analysis and the research material. Without his assistance, this work could not have been achieved. I also like to thank Peter Graham and Fana for assisting me with the laboratory work and relevant material.

Finally I thank my family for being supportive and understanding throughout my research. Special thanks goes to my grandmother who has shown a lot of interest and support by asking me from time to time about the progress of my studies.

CONTENTS

APPENDICES

LIST OF TABLES

LIST OF FIGURES

ABBREVIATIONS

SYMBOL	DESCRIPTION
t	time variable.
x	space variable.
k	thermal conductivity of concrete.
Q'	rate of heat of hydration (heat rate).
T	temperature.
ρ	density of concrete.
C	specific heat capacity of concrete.
D	thermal diffusivity of concrete.

CHAPTER 1 - INTRODUCTION

1.1 Background.

The prediction of temperature variations that are likely to occur in a concrete structure becomes of great importance to their design. Research conducted by C.L.D Huang, N.A Gamal and D.L.Fenton[1] considers that understanding the phenomena of coupled heat transfer in concrete structures subject to high temperatures in short duration, has essential application in safety assessment of nuclear reactors and of tall buildings at elevated temperatures as a result of fire. The problem of mass and heat transfer in concrete that is subjected to high temperatures such as fire involves temperature and moisture content distribution, strong couplings of pressure, nonlinearly dependence of various material properties such as density, conductivity, and specific heat etc. on temperature, pressure and moisture.

K van Breugel[2] indicates that in order to enhance the quality and performance of concrete structures, control of temperature variations and of the associated thermal stresses is of paramount importance. It is apparent that temperature differentials are among the key-factors considered in thermal analysis of concrete structures.

The knowledge of temperature prediction may be used in numerous applications such as development of strategies that may used to minimise the risk of thermal cracking of concrete. Early age thermal cracking, occurs when the restrained thermal contraction strain exceeds the tensile strain capacity of the concrete, and can be minimised by the understanding of the thermal behaviour of the structure.

Harrison[3] confirms the fact that early age thermal cracking is caused by the restraint to contraction on cooling from temperature peak, which is associated with the release of heat of hydration. In simple terms, as cements hydrates, it generates heat known as the heat of hydration. Some of this heat is retained in the concrete, resulting to a temperature rise in concrete. Once the rate of heat loss exceeds the rate of heat generation the concrete starts to cool and contract.

P Moraito[4] states that in order to minimise the risk of thermal cracking in concrete structures, knowledge of the expected temperature rise during hydration of cement is desirable. He gives factors controlling the rate of temperature rise such as, the rate of heat of hydration, proportion and composition of cement, environmental conditions temperature of concrete at placing, concrete mix proportions and aggregate type.

In order to develop the transient temperature profiles of concrete it is necessary to obtain a measure of the rate of heat generation as well as the thermal conductivity of a particular concrete mix. Various methods (which are discussed in chapter 2) have been developed to determine the rate and the extent of heat generation of concrete mixes. Results from these tests are used in conjunction with numerical methods, to determine the transient temperature profiles. E.A.B Koenders and K van Breugel[5] points out that several computer programs have been developed to evaluate thermal problems in hardening concrete. For most of these programs the adiabatic hydration curve of the concrete mix is an essential part of the input data.

1.2 Objectives of the research.

This research covers the adiabatic calorimeter test for a concrete beam to determine the rate of hydration curve that will be used to as an input to a Green Element Method will be used to achieve the following:

- Prediction of time based temperature profiles.
- Solving a governing equation that is defined by time dependent boundary conditions.
- Provide a solution to a governing equation that contains time dependent recharge/source term, which in this case is the heat of hydration curve in this case.

1.3 Methodology and approach to the research.

The research consists of the following:

- Literature review on previous and current researches undertaken.
- Perform a Calorimeter test to determine the rate of heat of hydration curves.

- Perform a laboratory experiment for measuring ternperatures at various positions of a concrete beam, at various times.
- Apply the Green element method to predict the measured temperatures.
- Coding of the Green element method solution in Fortran program.
- Comparison of the experimental and predicted results.
- Recommendations from this research.

The methodology and approaches used in the study will be detailed in the relevant chapters that follow.

CHAPTER 2 - LITERATURE REVIEW

2.1 Introduction

The data was collected through previous papers, journals and books obtained from various libraries, concrete institutions as well as from some researchers.

The most important aspect of the research was to understand the topic of heat flow in concrete structures. Chapter 13 of the Fultrons' Concrete Technology[6] provides basic information that may be required for understanding the subject of heat transfer in concrete. An extensive list of references covering most of the topics that are related to this research was obtained from this submission. Majority of the references deal mainly with the laboratory methods used to determine the heat hydration curves and measurement of temperature profiles of a developing concrete. Very few references describe numerical models that may be used to predict temperature profiles that are obtained from laboratory results. Previous research undertaken on studies that are related to heat transfer is discussed on the following sections.

2.2 Heat of hydration

Chapter 13 of the Fultrons' Concrete Technology[6] provides description of three test methods that are used to determine the rate of heat liberated by reacting cement and extenders. Isothermal methods are used to measure heat generated by samples that are kept at constant temperature while the semi adiabatic methods monitor the rate of heat evolution while heat exchange with the surrounding environment is kept minimal. The problem with these two methods is that the rate of heat evolution is itself temperature dependent, and hence the heat lost to the environment is not available to increase the temperature of the sample and thus affect the rate of heat of hydration of the concrete sample.

This problem has led to investigation of the third method known as the adiabatic calorimeter. The adiabatic calorimeter is described as a method in which heat exchange between the sample and its environment is largely eliminated. For a known specific heat capacity of a particular concrete mix, the results of the measured adiabatic calorimeter can be used determine the total amount of heat liberated by the hydrating cement over time.

P Morabito and F Barberis[7] confirm problems that are encountered in the isothermal and semi-adiabatic tests. They stated that isothermal tests do not reflect the real condition in the structure where the rate of heat of hydration changes with the changing temperature. The adiabatic calorimeter us considered to be an alternative and more reliable approach. Several adiabatic calorimeters have been developed in the past research.

The Enel-Cris Adiabatic Calorimeter described by P Morabito and F Barberis[7] is constituted of three parts, the calorimetric cell, a conditioning unit that regulates the temperature of an anti-freeze, and an automatic data control system. A more detailed description of the system can be obtained from this paper. The Enel-Cris Adiabatic Calorimeter was designed to satisfy essential requirements. The dimensions of the sample are such that the integral massive concretes can be tested. The tests enable initial starting temperature to be varied in order to evaluate the influence on the rate of hydration. The equipment used is such that the non-adiabatic tests can also be performed.

The research outlines the causes of error arising in an adiabatic calorimeter. The temperature rise of a concrete sample hydrating in an adiabatic calorimeter is affected from the residual heat losses that are mainly due to the defects of adiabatism and heat capacity of the calorimeter, regarded as the more significant error. The heat capacity of the calorimeter is considered to be the main source of error. This paper provides ways in which the two errors can be compensated.

In order to minimise the errors that are caused by heat capacity of the cell a new technique was developed. It consists of in supplying additional heat to the sample while the test is in progress to compensate the hydration heat absorbed from the thermal capacity of the calorimeter. The procedure has been carefully verified by tests on different types of concrete exhibiting adiabatic temperature rise ranging from about 17^{0}C to 40^{0}C. The adopted testing method allows to determine the adiabatic temperature rise and to measure the heat capacity of concrete with repeatability of 3% and 4% respectively.

The research recommends use of an adiabatic calorimeter with an electrical heater that allows to perform an accurate calibration of equipment to measure the heat capacity of concrete and to compensate the heat capacity of the cell

G.Y. Gibbon, Y Ballim and G.R.H. Grieve[8] investigated on the availability of adiabatic calorimeters suitable for the testing of concrete samples and found out that the cost of available calorimeters was expensive. The research demonstrated how a low-cost computer controlled adiabatic calorimeter test could be used to determine the heat of hydration of concrete. The paper described the design and operation of a low cost, computer controlled adiabatic calorimeter used for determination of heat of hydration of concrete mixes using small samples of concrete. The basis of the operation of the adiabatic was that water surrounding the test concrete sample is kept at the same temperature as the sample.

A low cost calorimeter with a personal computer as the data control system was designed and manufactured. In a brief description, the adiabatic calorimeter consisted of the computer and power supply the temperature sensors used to measure the temperature of the sample and that of the tank filled with water, were the sample was kept. The heater was placed in the tank holding the sample to regulate the temperature of the water. This system enables the temperature of water in the tank to be kept the same as the temperature of the sample so as to minimise any heat transfer between the sample and water. This simply meant that no heat is lost from, or gained by the sample, implying that the heat measured during the test is the result of hydrating of the cement.

Heat measurements were started at ten minutes after water was added to the concrete and a continuous plot of the rate of heat generation was obtained. The adiabatic calorimeter that performed appears to be a useful, low cost tool for the determination of heat development of concrete during the early ages of hydration. It allows for more engineering properties of concrete to be determined under conditions of temperature-matched curing.

A paper submitted by P Morabito[4] reviews various methods that are used to measure heat of hydration. He mentions that numerous laboratory techniques have been developed to measure the temperature rise in concrete, ranging from sophisticated calorimeters that, are used in monitoring temperature in small samples of cement to temperature measurements at the centre of large insulated block of concrete. An important point to note in addition to the description of isothermal methods is that they are applied to pure cement pastes and thus make them possible to measure the heat generated by samples kept at a constant temperature. The paper deals mainly with the review of various adiabatic methods.

Two adiabatic calorimeters were compared, one that uses air and the other that uses water as the insulating medium. Comparison was made on temperature measurements taken at the centre of a large insulated block. Measurements are taken at the centre of a large concrete block in order make the surrounding concrete act as an insulation medium. The result showed that the temperature rise measurements using water as an insulating material compared very well with that from the large block. The results obtained from the apparatus using air were lower when compared to the temperature measurement taken from the large block.

From this comparison, adiabatic calorimeter that uses water as the insulating medium takes the preference. The adiabatic calorimeter that uses air as the insulating medium is easily constructed as opposed to the adiabatic calorimeter that uses water as the insulating medium.

The other type is the adiabatic calorimeter that uses heated container as the insulating medium. Some of the problems encountered with this calorimeter are that it is sometimes difficult to construct particularly where the specimen holder is heated and this in turn heats any gap that may exist between it and the specimen. There are different types of heat insulated adiabatic calorimeters that have been developed.

Comparison of temperature measurements taken using the adiabatic calorimeters and semi adiabatic calorimeters indicated that the measured curve of an adiabatic calorimeters is slightly lower than the corrected adiabatic curve, whereas opposed to the semi adiabatic calorimeters curve which is far lower.

Errors that arise out of any adiabatic semi adiabatic calorimeters are mainly influenced by the design of the calorimeter, the thermal loss from adiabatic calorimeter and heat capacity of the calorimeter, the sensitivity of the temperature controller and the concrete sample size.

P Morabito[4] obtained a relationship that may be used for calibration of thermal losses and effects of the heat capacity, the expression is given as follows:

$$\theta_{ad} = \left(1 + \frac{C_{cal}}{C_c}\right)\left[\theta_s(t) + \int_0^t a(t)dt\right] \tag{2.1}$$

where

t		is the time.
C_{cal}	(J/K)	apparent heat capacity of the calorimeter.
C_c	(J/K)	apparent heat capacity of the sample respectively.
$\theta_s(t)$		is the measured temperature rise.
$a(t)$	(K/h)	is the co-efficient of temperature loss.

If $\theta_s(t)$ is measured by an adiabatic calorimeter, then $T_{ad}(t)$, represents the adiabatic temperature rise of concrete. If the test is performed by semi adiabatic calorimeter, then equation 2.2.1 leads to a lower estimate of the adiabatic temperature rise.

The challenge to note is that, in a concrete structure, temperature varies at different points and the rate of reaction at a point at any instant depends on the total amount of heat already liberated and the temperature at the time of consideration. In order to determine the rate of heat of hydration at any time in a concrete element, maturity of concrete, as opposed to the clock time should be used. This implies that from the heat rate vs. time curve obtained from the adiabatic test must be translated into a heat rate-maturity relationship. The most commonly used relationship, known as the Nurse-Saul relationship, uses a datum temperature of -10°C, being a temperature at which cement hydration is considered to cease. The function is given as:

$$M = \sum_{i=1}^{t} (T_i + 10)\Delta t_i \tag{2.2}$$

where M is the maturity of concrete up to time t, and T_i is the average temperature of concrete during the time interval Δt_i.

Research reveals that various maturity functions developed are used to describe the relationship between the temperature and the engineering properties of concrete. The research by Wang and Dingler[9] considers apparent that the total cement hydration heat of a concrete mix depends on the cement type and content. This implies that for a particular cement, the hydration rate at any moment depends on the total heat already released and this is known as the concrete maturity. One of the most commonly known maturity functions is known as the Arrhreneius Function.

By studying the test results on adiabatic temperature rise with time for a concrete mix, the cement hydration rate at a standard temperature of 20°C and any other temperature can be derived and applied to a computer model. The relationship between the rate of heat of hydration and concrete maturity at 20°C for an ordinary Portland cement is given below:

$$q = 0.5 + 0.54M^{\,0.5} \qquad \text{for} \qquad M \leq 10 \text{ hours} \tag{2.3}$$

$$q = 2.2e^{[-0.0286(M-10)]} \qquad \text{for} \qquad M \succ 10 \text{ hours} \tag{2.4}$$

where M is the maturity of concrete in hours and is determined using Arrhreneius Function for maturity.

When the temperature is constantly 20°C, the concrete maturity equals its clock age, and when it is different from 20°C, it is given as:

$$M = \int_0^{\infty} H(t)dt \tag{2.6}$$

where $H(t)$ is the temperature function and t is the clock time.

The research on various methods that are used to determine provides useful information that is required for the determination of heat of hydration curve.

2.3 Thermal Conductivity

The study of factors influencing thermal conductivity of concrete is very useful in the analysis of heat transfer in concrete. Thermal conductivity plays a vital role as an input parameter when a numerical method is applied to predict temperature distribution in concrete.

According to Chapter 13 of the Fultrons' Concrete Technology[6], thermal conductivity is defined as a measure of ability of a material to conduct heat and indicates heat flow under a given temperature gradient. Thermal conductivity depends mainly on the moisture content of concrete, type of aggregates, density, and porosity of concrete. It also depends on the temperature of concrete but the effects are negligible over the range of temperatures that are commonly encountered.

Typical values of thermal conductivities for concrete made with a range of aggregate types presented on Chapter 13 of the Fultrons Concrete Technology[6], are given on the Table 2.1 below:

Table 2.1: Thermal conductivities of concrete made with a range of aggregate types.

Type of Aggregate	Thermal Conductivity of Concrete in (W/m.K)
Quartzite	3.5
Dolomite	3.2
Limestone	2.6 - 3.3
Granite	2.6 - 2.7
Rhyolite	2.2
Basalt	1.9 - 2.2

It is also important to note that thermal conductivity will vary with the progress of cementing reactions. Previous researches reveal that the nature of variations for thermal conductivity may either decrease or increase as the reactions proceed.

More research has been undertaken to study the effects of the moisture content of concrete, type of aggregates, density, and porosity of concrete and limited research on the temperature effects on thermal conductivity.

The paper written by D Campbell and C.P. Thorne[10] covers the experimental work that deals with the effects of moisture content on the thermal conductivity of concrete made with various aggregates. Also presented from this paper is the theoretical derivation of the thermal conductivity expression used to calculate thermal conductivity of concrete as a function of the aggregates, mix proportions and the experimental values of the conductivity of mortar. The expression thermal conductivity of concrete is given as:

$$k = k_m\left(2M - M^2\right) + \frac{k_m k_a \left(1-M\right)^2}{k_a M + k_m\left(1-M\right)} \tag{2.7}$$

where: $M = \sqrt[3]{1-P}$

k_m is the thermal conductivity of mortar.

k_a is the thermal conductivity of aggregate.

P is the volume of mortar per unit volume of concrete.

The experimental work consisted of the following:

- The experimental determination of relation between thermal conductivity and the moisture content of mortar made from quartz sand and Portland cement capillary pores.

- The values of thermal conductivity of mortar for the sand and Portland cement were obtained experimentally. By substituting of k_m values into equation (2.3.1) enables the calculation of the relation between the thermal conductivity of concrete (k) and the thermal conductivity of aggregate (k_a), for any given moisture content.

The agreement between experimental and predicted results obtained using the procedure given above, was satisfactory. The research presents the development of a theory for giving the thermal conductivity of concrete in terms of thermal conductivity of constituents. This theory consists of two parts, one that relates to conductivity of cement paste to that of hydrated cement and to the percentage by volume of free water. The second part describes the relation between the conductivity of cement paste and aggregates.

Both the theories are said to show consistency with experimental results, and provide reliable indication of the relative importance of various factors that influence the thermal conductivity of concrete.

The paper further concludes that the conductivity of any given concrete varies approximately linearly with the moisture content, for a higher concrete conductivity, the greater is the percentage drop in conductivity resulting from the loss of given percentage by volume of water. An increase in conductivity of aggregates causes a smaller decrease in concrete conductivity. For light aggregates the thermal conductivity of concrete will be higher, whereas for heavy aggregates the thermal conductivity of concrete will be lower. Generally, higher water/cement will yield cement pastes with low conductivities.

A research on the effects of time on the thermally conductivity was submitted by G.J. Gibbon[11]. This work presents development of a program from which mainly the heat of hydration data can be processed. The program also calculates the results of thermally conductivity from the specific heat and density of the sample. Three different types of cement were used and results compared. The results show that the effects of time on conductivity may be minimal as opposed to other effects that have been discussed above.

2.4 Temperature Measurement Prediction

Various models that enable the prediction of measured temperatures have been developed in the past. In order to allow predictions of time-based variation in temperature of concrete, it is very essential to develop the heat of hydration and conductivity measurements.

The good foundation in understanding the equation that governs the flow of heat in concrete is obtained in Chapter 13 of the Fultrons' Concrete Technology[6]. The flow of heat in concrete is governed by a Fourier equation in three dimensional form, and is given as:

$$k\left(\frac{d^2T}{dx^2}+\frac{d^2T}{dy^2}+\frac{d^2T}{dz^2}\right)+Q^{\cdot}=\rho C\frac{dT}{dt} \tag{2.8}$$

Where:

ρ is the density of concrete,

t is time.

k is thermal conductivity of concrete.

$Q^{\cdot}$ is the rate of heat of hydration.

C is the specific heat capacity of concrete.

T is the temperature and

x, y, z are coordinates at a particular point in a structure.

Wang and Dingler[9] presented work that deals with development of a computer model to predict the temperature distribution in hardening concrete. They considered a two dimensional finite element thermal analysis which was used to model a transient heat transfer between concrete and the environment by taking into account the cement type and content, boundary and environmental conditions including the solar radiation and artificial heating. The work was limited to the two dimensional form of equation (2.4.1), as given below:

$$k\left(\frac{d^2T}{dx^2}+\frac{d^2T}{dy^2}\right)+Q^{\cdot}=\rho C\frac{dT}{dt} \tag{2.9}$$

Two types of boundary conditions are defined for equation (2.9). The first is that the temperature along the boundary or portion of the boundary is known. The second states that the energy transfer through boundary is known. The expression for the latter conditions was given as:

$$k\left(\frac{dT}{dx}n_x + \frac{dT}{dx}n_y\right) + Q_b = 0 \qquad (2.10)$$

where: n_{xy} are the direction cosines of the unit outward normal to the boundary surfaces.

Q_b total boundary heat gain or loss including solar radiation, thermal radiation and convection.

It was noted at this point that the main difficulty in solving equation (2.9), was to establish the boundary heat transfer conditions that are time dependent. The heat transfer conditions takes up five forms: solar radiation, thermal radiation and convection, evaporation and condensation, where the last two are least significant and are neglected in this model. The amount of solar radiation that reaches the concrete surface can be estimated from the structures' geographical location, orientation, altitude and atmospheric conditions, time of the day and day of the year. The convection heat transfer is the heat loss to or gain from the surrounding sir as a result of the air environment and depends on speed and temperature difference between the concrete surface and bulk air. Thermal radiation is the heat radiation emission by the concrete body and is a function of surface temperature and thermal emissivity of concrete.

They described a model in which temperature field of the cross section at each time step is obtained by the variational finite element method combined with Galerkin weighted residual method for time domain solution. The non-linearity problem of the thermal radiation heat transfer through the boundary is bypassed by converting the non-linear radiation heat transfer into quasi-linear radiant convection.

Changes that are undergone by concrete at early ages, which are, removal of formwork and/or insulation material and multi-lift casting, were accounted for by automatically transferring of element nodal temperature and concrete maturity data from the end of the previous stage to the beginning of the current stage. This analysis was carried out by a computer program known as FETAB and is coded in Fortran 77. An important factor to note is that the refinement of the program was made in order to account for the time varying boundary heat transfer conditions. It was further developed to handle the changes of boundary conditions, structure configurations and the prediction of maturity and strength development of the structure.

The basic input of the computer analysis included the cement content and type, thermal properties of each conduction material and boundary environmental conditions, initial concrete temperature and maturity as well finite element mesh of the structure. The time step length was chosen as one hour for the first two days and increased for the rest of the time. The computed temperature compared very well with measured temperature. The model and the program were subsequently used in the design and construction planning of the 13.5km long bridge.

G.Y. Gibbon and Y Ballim[12] made another valuable contribution into this field of study. The work presented results obtained from the laboratory tests that were developed to determine the heat of hydration and thermal conductivity of concrete samples were used to predict the temperature profile in a concrete structure.

A simple heat model was developed to predict the temperature in an infinitively large concrete structure with one surface exposed to the ambient temperature conditions. The model was developed for structures with least dimensions between the exposed surfaces greater than 1,0 m as approximately adiabatic conditions are considered to exist at depths greater than 0,5 m, for a first few days after casting. Mat lab program was used to read the heat of hydration and thermal conductivity information determined during a test and plots temperature at each finite element node against time. The predicted temperature was found to be accurate to within 2^{0}C when compared with the measured temperature.

Y Ballim[13] presented further research on the prediction of temperature profiles in mass concrete. The work described the development and operation of a finite difference heat model for predicting time-based temperature profiles in mass concrete elements. The significance of this research was that the model represented a two dimensional solution to the Fourier heat flow equation which was simple enough to be run on a commercially available spreadsheet package.

The model further resolves the complexity that the rate of heat of hydration at any point in the concrete element is dependent on mix parameters, time and location. This is achieved using, as input, the results of a rate of heat of hydration determination using low-cost adiabatic calorimeter together with Saul-Nurse maturity relationship to indicate the extent of heat of hydration at any time and position.

The paper presented the numerical solution for a rectangular block of concrete that has a z direction significantly larger than the x and y dimension. The final form of the finite difference equation for the different situations in the concrete block and associated boundary conditions was presented. The equation to be solved is similar to the two-dimensional Fourier heat flow equation (2.4.2), mentioned above.

The modelling of the environmental ambient temperature that has been incorporated within the heat prediction model takes the form:

$$T_A = \sin\left(\frac{2\pi(\tau_d + \tau_m)}{24}\right)\left(\frac{T_{\max} - T_{\min}}{2}\right) + \left(\frac{T_{\max} + T_{\min}}{2}\right) \qquad (2.11)$$

where: τ_d is the clock time of day at which the prediction is being made (0-24 hours).

τ_m is the time at which the minimum overnight temperature occurs.

$T_{\max}$ and $T_{\min}$ are the maximum and minimum temperatures for the day under consideration.

From the finite difference equations for each condition of the nodes, i.e. internal, bottom surface, corner and exposed surface nodes, predicted temperature values were obtained. Generally the finite difference equation takes the form:

$$T_{m,n}^{P+1} = \frac{k\Delta t}{pC\Delta x^2}(\,)\left(T_{m+1,n}^{P} + T_{m-1,n}^{P} + T_{m,n+1}^{P} + T_{m,n-1}^{P}\right) + \left(1 - \frac{4k\Delta t}{pC\Delta x^2}\right)T_{m,n}^{P} + \frac{\Delta x \Delta t Q'}{pC} \qquad (2.12)$$

The predicted temperature profiles compared very well with the measured profiles. The early age drying from the surface of the concrete causes the model to over estimate the temperatures near the surface.

There is limited research that handles a three-dimensional analysis. A.B. Fernando, A Pedro and E. Mirambell[14] are one of the few researchers that have looked into the solution of a three-dimensional heat transfer problem. Their work entailed a numerical method that considers environmental interaction and concreting phases to obtain the hydration temperatures. They obtained a heat of hydration characteristics from a study in which insulated concrete cubes were tested.

2.5 Conclusion

Extensive work on the heat of hydration methods has been done in the past and most researchers seem to recommend the adiabatic calorimeter mainly because of its advantages. Previous researchers have properly documented these advantages. This gives an opportunity to a future research on the choice of the method to be used.

Various numerical models have been used in the past to predict temperature profiles. It is evident that most researchers have preferred using the finite element method. There is limited research on other available numerical techniques that may be used for temperature predictions.

CHAPTER 3 – LABORATORY PROCEDURES

3.1 Introduction

In order to enable verification of the predicted temperature in a concrete, an adiabatic calorimeter test was performed. The temperatures of the concrete model at early ages of hydration are also measured. The verification of the predicted temperature is achieved by comparing them with the measured temperatures.

The adiabatic calorimeter test was used in this research mainly because the adiabatic conditions approximately exist during the early ages of hydration. The test is performed to measure the heat of hydration of a mass concrete beam. The mass concrete beam was cast with temperature probes placed at various positions to monitor the temperature rise and decline as a result of the heat of hydration.

3.2 Concrete Mix Design

The concrete beam used in the laboratory test had a nominal compressive strength of 25Mpa, a maximum aggregate size of 13mm, a slump of 100mm and the binder consisted of plain Portland cement (220 kg/m^3). The slump and aggregate size were selected to ensure that the thermal probes were not displaced during casting.

The concrete constituents for the heat beam per cubic metre are as follows:

Table 3.1: Concrete Beam mix proportions.

Description	Mass in kg or L
Cement	340
Granite Stone	750
Granite Sand	1000
Water	220

3.3 Adiabatic Calorimeter

3.3.1 Introduction

The calorimeter is similar to the one used by G.Y. Gibbon, Y Ballim and G.R.H. Grieve[3].The control software was written by G.J. Gibbon[7] and one calorimeter was constructed by the University of the Witwatersrand for routine laboratory test work. It was developed as an inexpensive alternative to commercially available adiabatic calorimeters. Mr Peter Graham and Mr T Mabuya performed the test under the supervision of Prof Bhallim.

3.3.2 General Description

A schematic arrangement of a calorimeter, showing the major components and their relationships is given in figure 3.1.The equipment was designed to measure heat of hydration temperature rises and, if required to carry out simultaneous temperature matched curing exercises.

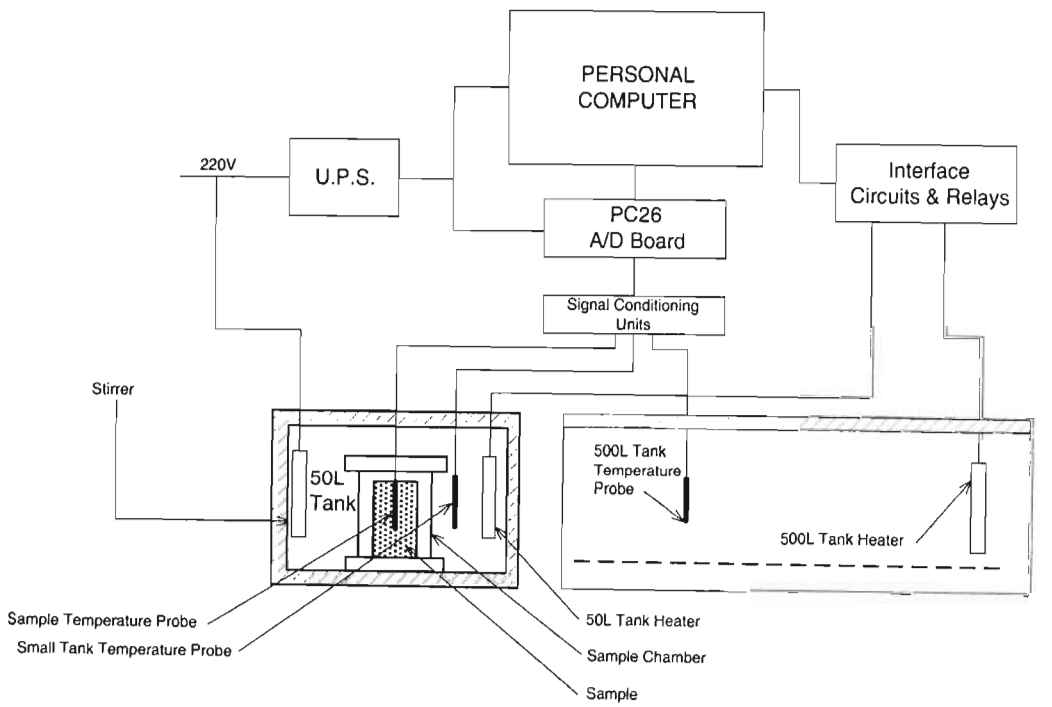

Fig.3.1 Schematic Arrangement of Adiabatic Calorimeter

The apparatus basically consists of two tanks, which are filled with water to appropriate levels during the test procedures. Each tank is equipped with a heater, which controls the temperature of the water in accordance with instructions received from the personal computer shown. When measuring temperature rises due to cement hydration, a concrete sample is cast in a light plastic mould and a thermal probe is embedded in the sample. The sample is then placed in the sample container, which in turn is placed in the 50-litre tank so that the Perspex top of the sample container is well below the level of the water in the tank.

The temperatures of the sample and the water are continuously measured and recorded by the personal computer. As hydration progresses the temperature of the sample increases and the computer responds by accurately matching the temperature of the water to the temperature of the sample. Adiabatic conditions are thus created at the sample because with a zero temperature difference between the sample and its environment, it is not possible for it to gain or lose heat.

The 500-litre tank is used for temperature matched curing and is not an essential part of the apparatus. The temperature of the water in this tank can be controlled to match the sample temperature to provide for curing of concrete test cubes under adiabatic conditions. The software also caters for other curing regimes, such as those obtained from site observations.

The entire apparatus is housed in an air-conditioned room. Ambient conditions are kept constant in order to minimize heat losses or gains due changes in the environment.

3.3.3 Components of the System

The main components of the apparatus are detailed below.

3.3.3.1 Sample Chamber

The sample chamber is shown diagrammatically in Fig. 3.2 below which includes all of the pertinent dimensions. It consists of a plastic tube, which constitutes the walls of the chamber. The top and bottom ends of the tube are sealed by means of two thick square perspex plates, which are tightened against each other and the plastic tube by means of six long bolts (not shown).

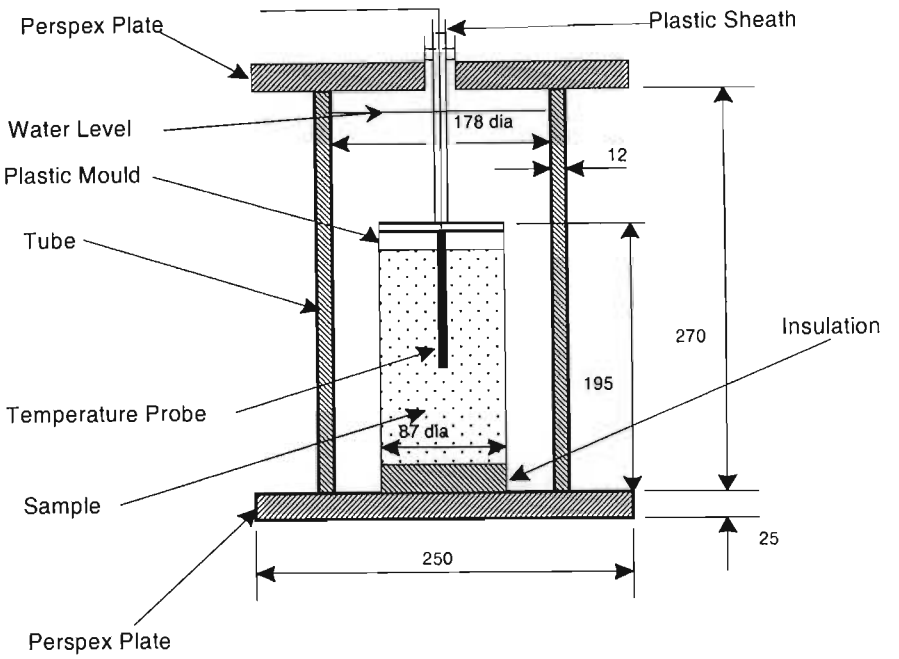

Figure. 3.2: Sample chamber

Before assembly, the newly cast concrete sample in its plastic mould is placed in the chamber on top of a layer of insulation. The temperature probe is inserted into the sample and the wires are led from the container through a plastic sheath.

The top and bottom perspex plates are then tightened against the plastic tube and the whole assembly is placed below the water level in the small tank.
Because the concrete sample is appreciably smaller than the chamber, it is, with the exception of the insulation pad on which it rests, surrounded by an air space.

This arrangement has proved effective in damping the transmission of heat from the small tank to the sample and vice versa.

3.3.3.2 Temperature Probes

The temperatures of the sample, water in the 50 litre tank and water in the 500 litre tank are measured by means of temperature sensors manufactured by Pyrotemp (Pty) Ltd and have the following specification:

Type:	PT100
Containment:	Copper tube 6mm diameter and 100mm long.
Guaranteed Accuracy	0.5 ^{0}C with an output voltage of 10mV/^{0}C
Supply Voltage:	4 to 30 Volts

The length of the probes was chosen to be about half the sample length in order to enable an average temperature within the sample to be measured. The sample probe is smeared with petroleum jelly before insertion in the sample in order to facilitate removal on completion of the test.

3.3.3.3 Signal Conditioning Units

The signal conditioning units convert 0 to 100 ^{0}C from the temperature probes to a 0 to 10 volt output. This is accomplished by three commercially available signal converters, the details of which are provided below:

Manufacturer:	Quanta Instruments
Model:	1100L
Supply:	220V 50Hz
Input:	PT100; 0- 100^{0}C; 3 Wire
Output:	0 – 10 Volts

3.3.3.4 Analogue to Digital Converter Board

The output voltage from the signal conditioning units is read by the computer using a digital to analogue converter board. The key specifications of this board are:

Manufacturer:	Eagle Technologies
Type:	PC26
A/D Resolution:	12 bit
Non-linearity:	Less than +/- -0.75 LSB
A/D full scale input ranges:	0 to +10 V, -5 to +5 V and –10 to + 10V jumper selectable.
Number of A/D inputs:	16 single ended
A/D throughput rate:	25KHz

This A/D card gives a resolution of 0.024 ^{0}C.

3.3.3.5 Personal Computer

The computer is an IBM compatible PC with a 486 mother board, 640 K byte RAM, 1.44 M byte floppy disk drive and a 609 M byte hard disk drive. The analogue to digital card and the digital interface (I/O card), detailed in 3.2.4 and 3.2.6 respectively, were fitted into the computer.

3.3.3.6 Interface circuits and Relays

The heaters in both tanks are controlled by the computer via a PC36A digital I/O board. An in-house designed interface is included in the circuitry to provide a buffer between the I/O board and two solid state relays which control the power supply to the tank water heaters. The system is designed to fail safe, in the off position, in the event of computer failure and also includes a 5 V power supply to monitor power failure conditions.

3.3.3.6 Uninterruptible Power Supply

Power to the PC and the signal conditioning units is supplied by means of a 950 W, 220V, 50Hz Uninterruptible Power Supply. This arrangement allows tests to continue through power failures of up to 45 minutes. Although the software provides for re-starts of tests after power failures of longer than 15 minutes, Gibbon's experience indicated that after long delays the temperature of the water in the tank dropped to the extent that conditions were no longer adiabatic and results had to be discarded. The unit has sufficient capacity to supply power for the systems of both calorimeters simultaneously.

3.3.3.8 50 Litre Tank

The 50 litre or small tank is double walled and manufactured from stainless steel. The space between the walls is insulated to reduce heat loss. In addition the tank is mounted on a wooden platform to reduce heat loss to the floor. The tank is equipped with a 2.0 KW heater that is capable of heating the water in the tank at a rate of 12^{0}C per hour. An electric stirrer keeps the water in motion and minimises temperature variations in the tank.

Evaporation losses are made up by means of a float valve, which controls the level of water in the tank and a 150mm thick polystyrene cover reduces heat and evaporation losses through the top of the tank.

3.3.3.9 500 Litre Tank

When required the large 500 litre tank can be used to cure concrete cubes at the same temperature as the sample in the small tank or at any other desired temperature. It is not insulated and made from a single thickness of galvanized mild steel sheeting. An expanded metal shelf, situated near the bottom of the tank is provided to ensure that the concrete cubes are completely surrounded by water at the required temperature throughout the curing period.
The tank is equipped with a 2 KW heater and circulating pump, which minimises temperature variations in the tank. A 100mm thick polystyrene cover reduces heat and evaporation losses.

3.3.4 Software

The software to control the calorimeter was developed by Gibbon. It was written in Turbo Pascal 6.0 and the menu system was based on libraries developed by the Software Engineering Applications Laboratory of the Department of Electrical Engineering at the University of the Witwatersrand.

The program allows the operator to enter information about the sample being tested and to modify various test parameters and control constants. The test parameters can be altered while a test is being conducted. The program also provides for calibration of the calorimeter and setting of calibration parameters.
The results can be plotted and are saved for further use.

The temperature of the water in the small and large tanks is matched to the temperature of the sample in the chamber by means a simple ON/OFF switching system. This would be described as an explicit steering algorithm because the temperature of the control medium is adjusted stepwise to meet the temperature at the core of the sample. It is recommended that the use of an implicit steering algorithm whereby the temperature of the water or control medium is adjusted gradually on the basis of the rate of temperature rise in the preceding time period, using extrapolation techniques. They have noted that heat losses to the environment are almost completely prevented by this method.

Earlier versions of the calorimeter provided for proportional control of the heaters. Whilst developing this and earlier calorimeters, the proportional control is not necessary because of the slow rate of change in temperature of the concrete and the damping effect caused by the insulating air surrounding the sample and the water in the bath.

3.3.5 Calibration

Compatible results from the calorimeter were a pre-requisite. In order to achieve this it was necessary to a dual calibration method. In essence the calibration of the calorimeter is accomplished in three steps. In the first step the signal conditioners for each computer are calibrated to ensure equal response to temperature changes. The second step calibrates the temperature probes to ensure correct readings and accurate control of the calorimeters. When this has been achieved, the heater control system is adjusted to provide an adiabatic environment for the sample.

3.3.5.1 Signal Conditioner Adjustment

The three thermal probes for the calorimeter are connected to the personal computer via three individual signal conditioners and each unit has a facility for span adjustment.
This part of the procedure is accomplished by placing all 6 probes (3 from each calorimeter) in a freezing point ice – water mixture and then adjusting the software factors for the computer to read 0^0C. The probes are then placed in water at a temperature 70^0C, which is normally above the required operating temperature of the calorimeters. The spans of the individual signal conditioners are then adjusted to match the temperature reading on a thermometer placed in the water.

3.3.5.2 Thermal Probe Calibration

In this procedure, the probes for measuring the temperature of the sample, small tank and large tank are tied together with a calibrating thermometer by means of elastic bands and placed in the small tank. They are positioned so that the extremities of the probes and the bulb of the thermometer are at the same depth in the water and the tops of the probes are just below the water level. The computer is then set to maintain a steady temperature in the tank. Then the temperature readings of the probes on the computer screen are compared with the calibration thermometer. The differences are determined and entered into the computer in order to equalise the readings for the three probes on the screen and simultaneously to align them with the actual temperature of the water in the tank.

When the temperature probes have been satisfactorily correlated, the calorimeter is set in heating mode and the water in the small tank is heated to 70 ^{0}C to encompass its normal operating range. During this phase, the temperature readings from the probes are recorded by the computer for analysis. Since adiabatic control of the calorimeter is effected by the difference between sample and small tank readings, this parameter may require further adjustment to compensate for any measurement discrepancies related to temperature in the operating range of the apparatus.

The data from the computer is extracted and the differences in temperature between the sample and the small tank probes are calculated. These results are then plotted against the sample temperature. Fig. 3.3 shows a typical result.

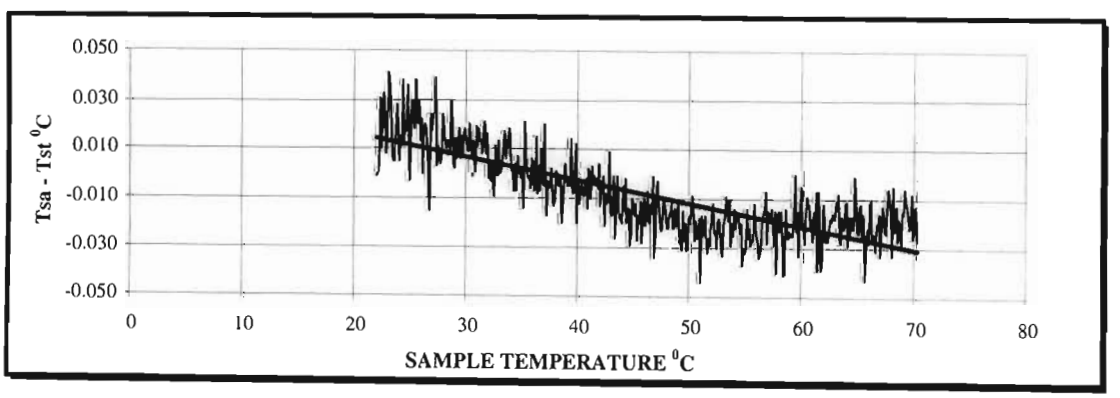

Figure. 3.3: Thermal Probe Calibration.

In the example shown above it can be noted that the readings have a characteristic fluctuation of about 0.02 ^{0}C and there is a slight negative drift in the probe temperature difference with increasing temperature.

The software accommodates corrections for this drift when the slope and intercept from a simple straight line regression of the calibration data are entered into the computer.
When the slope and intercept corrections have been made the calorimeter is again calibrated as per the foregoing procedure in order to check on the validity of these corrections. Figure 3.4 shows the results obtained after making the corrections suggested by the regression of the data that was used for figure 3.3.

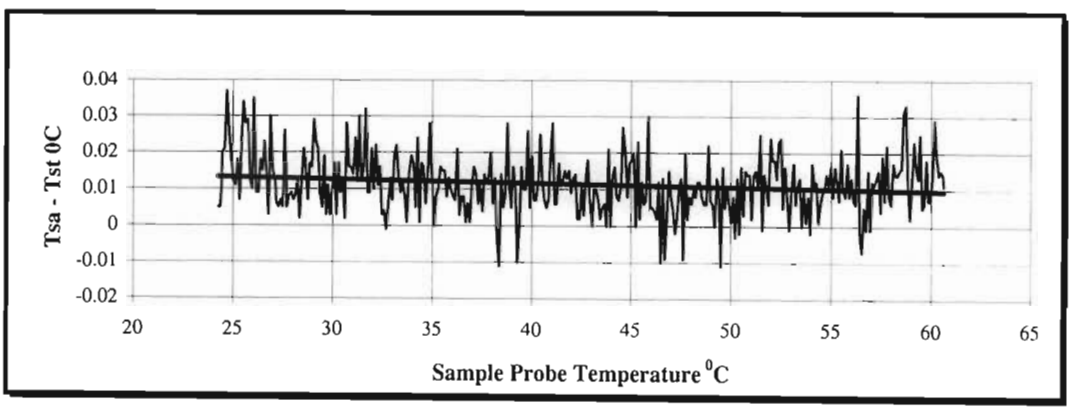

Figure 3.4: Corrected Thermal Probe Calibration

3.3.5.1 Adiabatic Performance Calibration.

The preceding procedure ensures that the temperatures in the calorimeter are measured accurately. In order to complete the calibration it is necessary to ensure that the calorimeter behaves adiabatically. This is accomplished by adjusting the switching parameters of the heaters until the calorimeter can maintain an inert sample a fixed temperature over a sustained period.
This step is necessary because a number of external factors, which are difficult to quantify, can de-stabilize the temperatures of the system. Such factors include:

- the temperature difference between ambient and the small tank.
- heat induced to the tank water by the stirring mechanism.
- heat losses from the sample via the thermal probe cable.

An inert sample of silica sand with a thermal probe is installed in the sample chamber that is in turn placed in the small tank. The system is then set to heat to a pre-determined temperature. When the sample reaches this temperature, the system is set in adiabatic mode. The temperatures of the tank water and the sample are then allowed to equalise.

At this point the heater parameters are adjusted until the sample maintains a constant temperature. The temperatures in the system are then monitored over a period of 18 hours to ensure that the calorimeter can maintain the sample at the constant temperature.

This process is repeated at every 10 degree interval in the operating range of the calorimeter. Fig.3.5 shows the results of a typical test where the sample has been maintained at a temperature of approximately 60 ^{0}C.

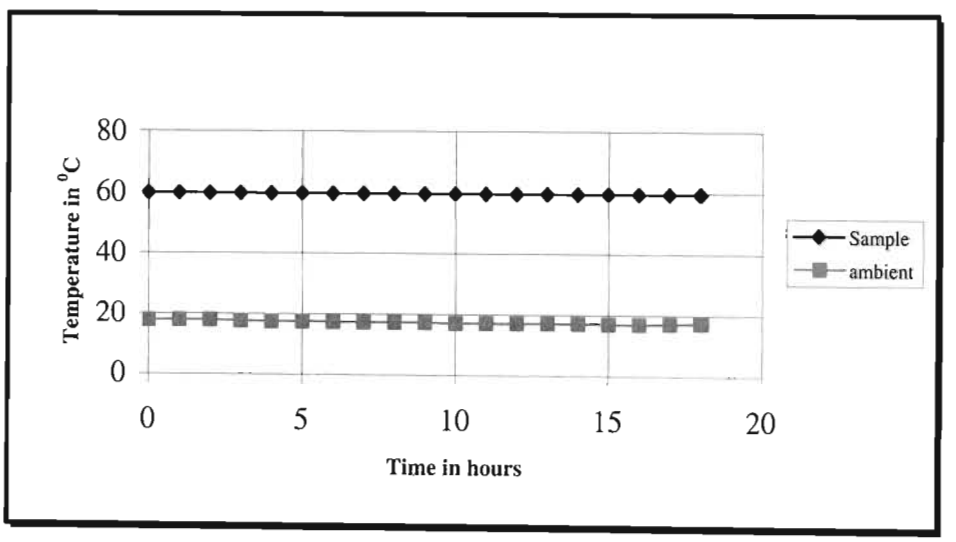

Figure 3.5: Adiabatic Calibration.

3.3.6 Discussions.

It was noted earlier that a comprehensive calibration and adjustment of the calorimeter is carried in 2 steps. The first step being the calibration of the thermal probes and the calorimeter is adjusted for adiabatic performance in the second step.

Accurate control of the calorimeter is dependent upon the readings from the sample and small tank probes being as close as possible to each other when exposed to the same temperature environment.

Fig. 3.3 shows an initial calibration of the difference between the two probes plotted against the sample probe temperature (or in this case the temperature of the water in the small tank) for most of the operating range of the calorimeter.

As can be seen the readings have a very small, regular fluctuation which is probably a characteristic of the electronics of the system. This fluctuation has a spread of about 0.04 ^{0}C. It can also be noted that the differences between the probes show a small negative drift with increasing temperature. The statistics obtained from the regression and analysis of the readings is shown in Table 3.2 below.

Calibration after correction for the regression parameters as shown in fig. 3.4 demonstrates that the negative drift is virtually cancelled by this step. The statistics obtained from the reading used for fig. 3.4 are also given in Table 3.

Table 3.2: Effect of Regression Correction in Calibration.

	Initial Calibration	After Correction for Regression Parameters
Slope	-0.00093	-0.0001
Intercept	0.034312	0.015687
r^2	0.615836	0.016499
r	-0.78475	-0.12845
Mean	-0.008	0.11405
Standard Deviation	0.1655	0.000283
High	0.041	0.037
Low	-0.044	-0.011
Range	0.085	0.048

The value of r obtained from the regression of the initial calibration data indicates a reasonable correlation between the temperature being measured and the difference the two probes. However it is interesting to note that after correction the value for r is very low which implies that there is now little or no correlation between the measured temperature and the difference between the probes. It also suggests that the fluctuations are random and supports the conclusion that they are a characteristic of the system. More importantly the measured temperature has been removed as a variable.

It can also be noted that the regression correction considerably reduced the spread of the readings from 0.085 ^{0}C to 0.048 ^{0}C, which now represents the characteristic fluctuation. The standard deviation is also significantly reduced to 0.000286 ^{0}C and the difference in temperature between the probe readings can be said to be 0.011405 +/- 0.0086 ^{0}C at 95% confidence. In terms of temperature measurement this is a very small error and is certainly well within the guaranteed accuracy of the probes.

Figure. 3.5 demonstrates the capability of the calorimeter to perform adiabatically after suitable adjustment of the heater switching parameters. It can be seen that an inert sample was held at a constant temperature of about 60 ^{0}C for a period of 18 hours. At this temperature, close to the upper end of the operating range of the calorimeter, the temperature differential with ambient is high and potential heat losses from the system are near to maximum.

Nevertheless under these conditions the calorimeter was able to maintain the sample at a virtually constant temperature. Over the 18-hour period the temperature only fell by 0.145 ^{0}C or 0.00856 ^{0}C per hour that can be accepted as adiabatic performance for the purposes of this work. When the inert sample was being heated for the adiabatic performance test, an overall coefficient of heat transfer between the water in the tank and the sample was calculated for steady state conditions. The mean value of this coefficient was found to be 726 J/^{0}C hr.

A typical cement sample of the size used here will generate about 264 KJ over a 90 hour period. If a worst-case scenario is considered where a sample continuously loses temperature at the rate measured above for the period of 90 hours then the temperature loss would be:

Temp. loss	= 0.00856 x 90= 0.7704 ^{0}C
Mean temp. loss	= 0.3852 ^{0}C
Heat loss	= 0.3852 x 726 x 90= 25169 J
Potential error	= 25169 x 100/264000
	= 9.53%

In practice the temperature loss would never be as large as indicated above because the temperature drift used in the calculation was for a tank temperature of 60 ^{0}C at the upper end of the calorimeter's range. When is operating at lower temperatures it is unlikely that the sample will lose heat in fact it is possible that it will experience a slight gain of heat, negating some of the heat loss that occurs at higher temperatures.

The 9.53% potential error should therefore be considered as the outer edge of the envelope of experimental error of the calorimeter. The output curves are discussed under section 3.5. Even though the calorimeter was developed as a low cost alternative to commercially available adiabatic calorimeters, it has been shown that it can be calibrated to read temperatures accurately and to respond to very small temperature differences. As a result it is able to maintain the sample in a very close to adiabatic environment for sustained periods and a such it is a suitable tool for measuring heats of hydration of cement.

3.4 Temperature Profiles Readings

3.4.1 Introduction

This section describes the laboratory test procedure that was used for measuring temperature in a concrete beam.

3.4.2 General description of the experiment

A Concrete beam comprising 0,135m³ of concrete was cast with dimensions as shown in Figure 3.4.6. The block was cast onto a concrete floor in the laboratory and the formwork for the one 300 x 300 mm surface (near the probe placed at 0 mm) was removed at 18 hours after casting. These surfaces were then coated with a wax-based curing compound.

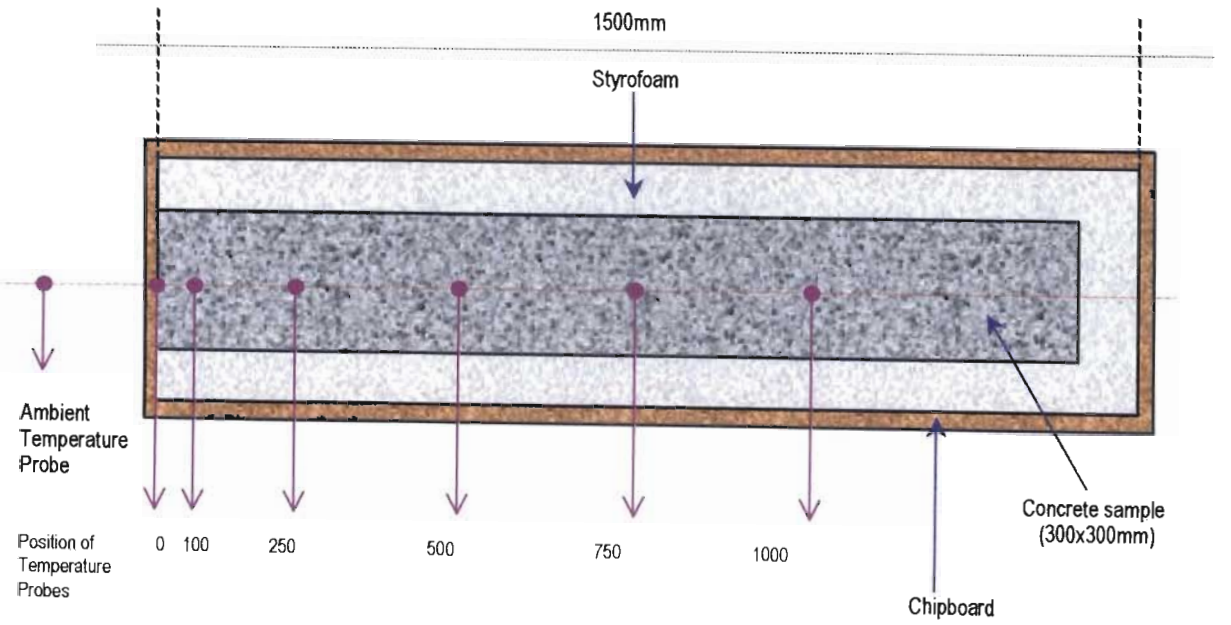

Figure 3.6: Schematic representation of the heat concrete beam and arrangement of probes.

The block was insulated on the four opposite 300 x 1500mm faces and one 300 x 300 mm surface in order to ensure 1-dimensional heat flow. The outer insulation comprised of a12mm thick chipboard covering the five faces of the beam. The internal insulator, also covering five faces, was by means of a 150mm thick Styrofoam.

Thermal probes were placed in the centre of the concrete at the node points shown in Figure 3.6. Concrete was cast to a depth of 150mm and temperature probes were put in place. The remaining portion of the beam was cast to a full depth of 300mm. This was done to ensure that the probes were placed in the required position. A probe was also placed on the outside of the concrete block to monitor the ambient temperature.

The thermal probes were manufactured from inexpensive integrated circuits (ic) units which require a dc input voltage of 10V and have an output of 0-1V, representing a temperature of 0° to 100°C. The IC units were connected to doubly insulated telephone cables. The assembly was encased in epoxy, to form a probe measuring 6mm in diameter and approximately 1200mm long.

The probes were all connected to an automatic data-logging facility and a constant voltage supply unit as shown on figure 3.7.

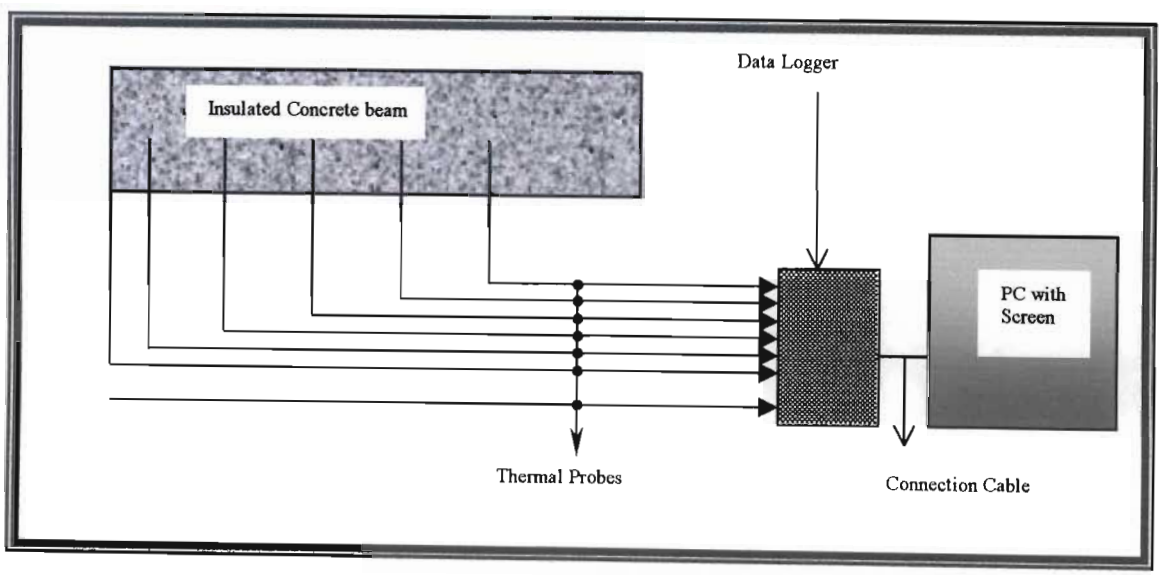

Figure 3.7: Schematic representation of temperature measurement experiment.

Temperatures at each of the probes were then recorded at 1-hour intervals up to 46 hours, 2 hours after casting. During this period, the ambient temperature varied between 16ºC and 21ºC. The recording was stopped for 20 minutes to download the recorded temperature from the computer. The temperature recording was continued at 2-hour intervals up to 284 hours. The recording was again stopped for 20 minutes to download the recorded temperature from the computer. Finally the temperature recording was continued at 2-hour intervals up to 475 hours.

At the time of casting, a small sample of the concrete was obtained for the adiabatic calorimeter test, which was conducted at the same time as the heat monitoring of the test. The measured temperature curves are discussed under section 3.5.

3.5 Discussion and Conclusions

3.5.1 Adiabatic Calorimeter

From the measured temperature readings of the calorimeter test, a plot of temperatures versus time is obtained as shown in Figure 3.8, below.

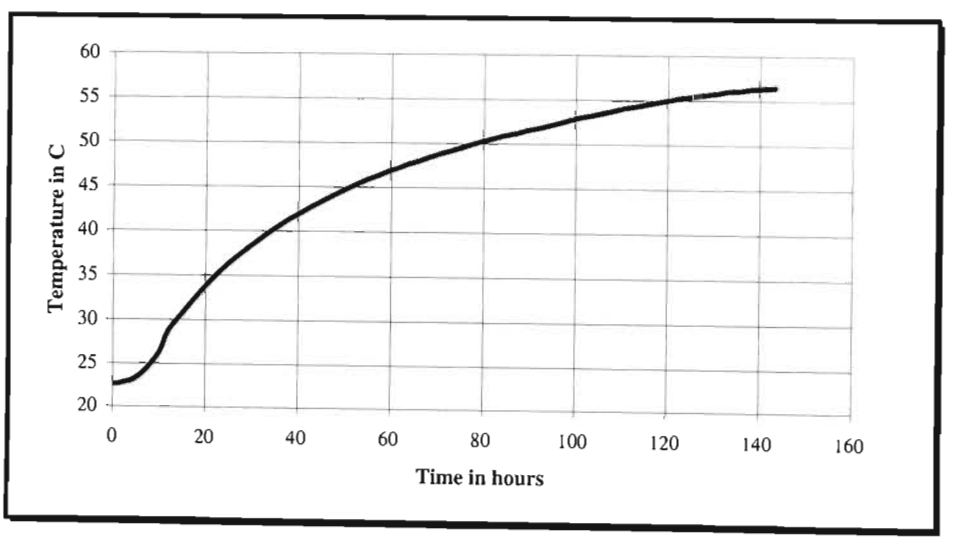

Figure 3.8: Temperature versus time

As expected the results show that, at early ages, concrete is subjected to rise in temperature. The derivative of the measured temperature values enables the temperature to be converted into the temperature rate. These results are shown in figure 3.9.

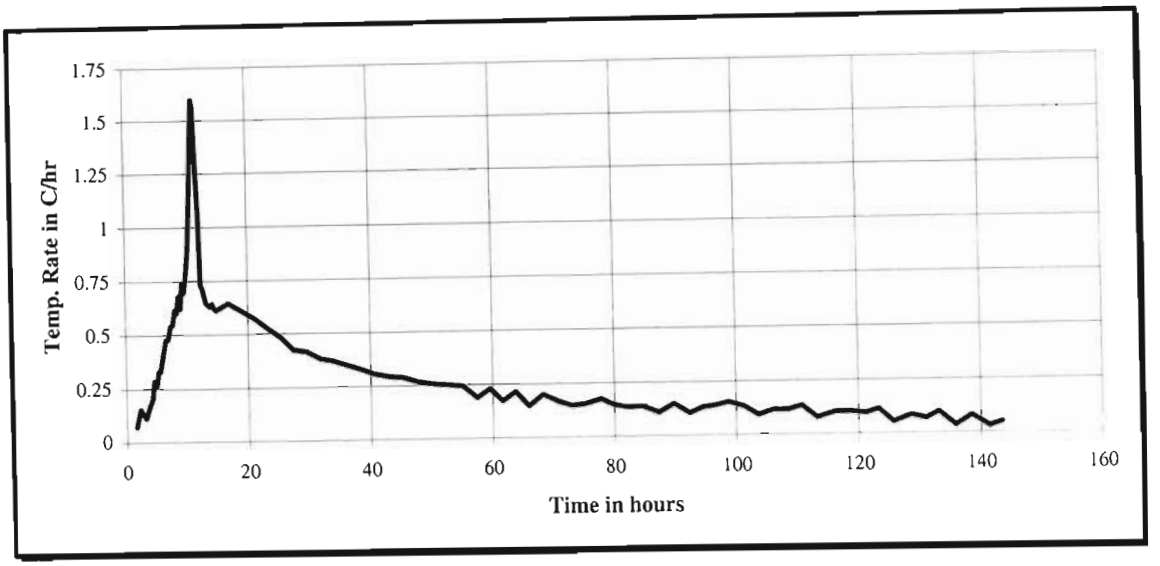

Figure 3.9: Temperature rate versus time.

The rate for the heat of hydration versus time curve is obtained by converting the temperature rate into heat rate and the results are shown on figure 3.10.

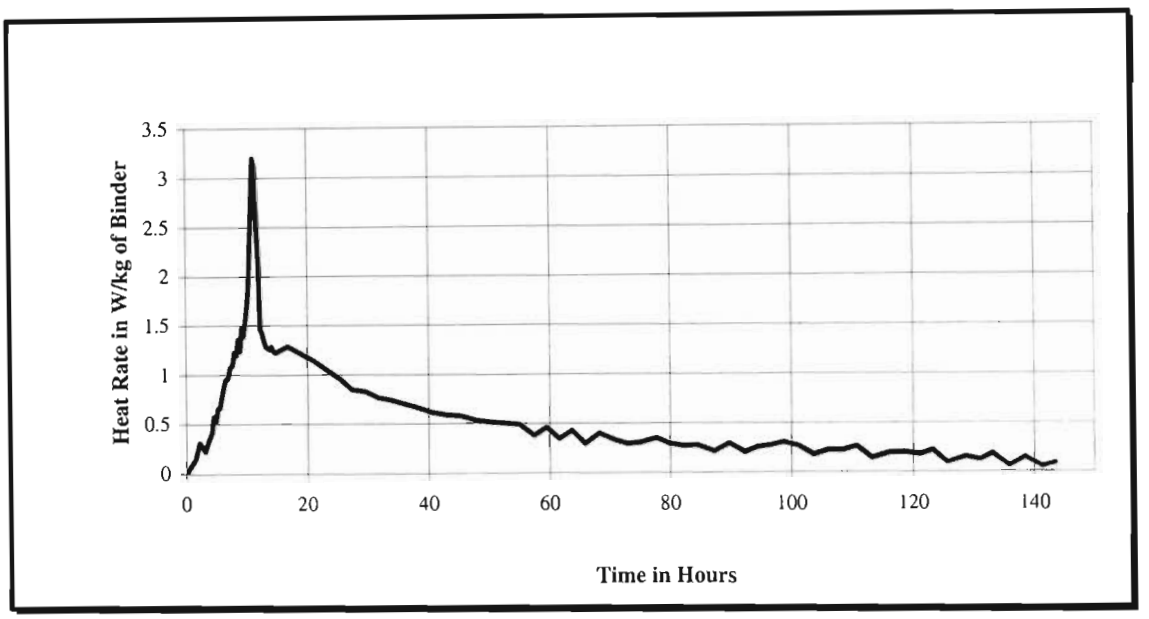

Figure 3.10: Heat rate versus time.

Using the Nurse-Saul and Arrhenius maturity function, the time is transferred into maturity by using Nurse-Saul and Arrhenius equivalent hours to obtain the Heat Rate-Nurse/Saul maturity and Heat Rate-Arrhenius maturity curves, the results are presented in figure 3.11 and 3.12 respectively.

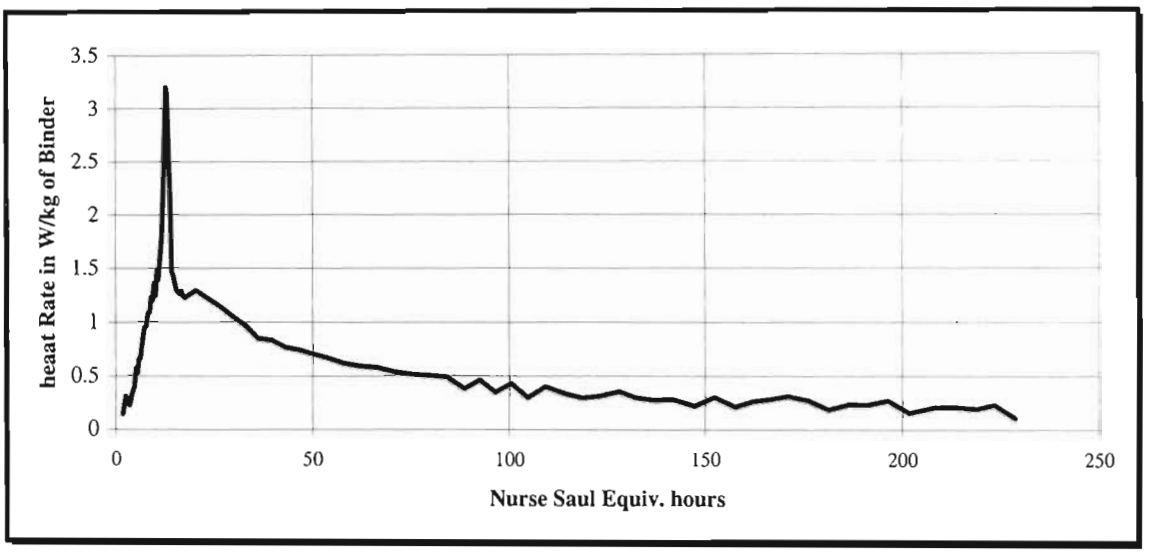

Figure 3.11: Heat rate vs Nurse-Saul Equivalent time.

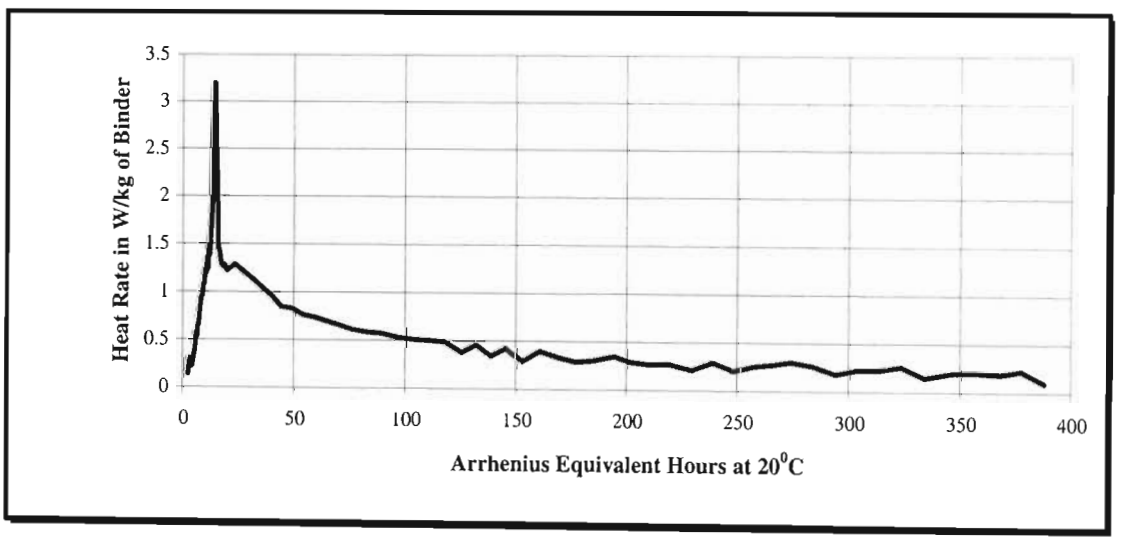

Figure 3.12: Heat rate versus Arrhenius Equivalent time.

For the purpose of this research, the heat rate versus Nurse-Saul maturity curve will be used as the input to the numerical model for prediction of the temperature profiles.

3.5.2 Temperature Measurements.

The measured temperature values from the concrete beam were downloaded from the data logger. Figure 3.13 gives the temperature versus time curves for thermal probe positions, 0mm to 1000mm and the probe measuring the ambient temperature

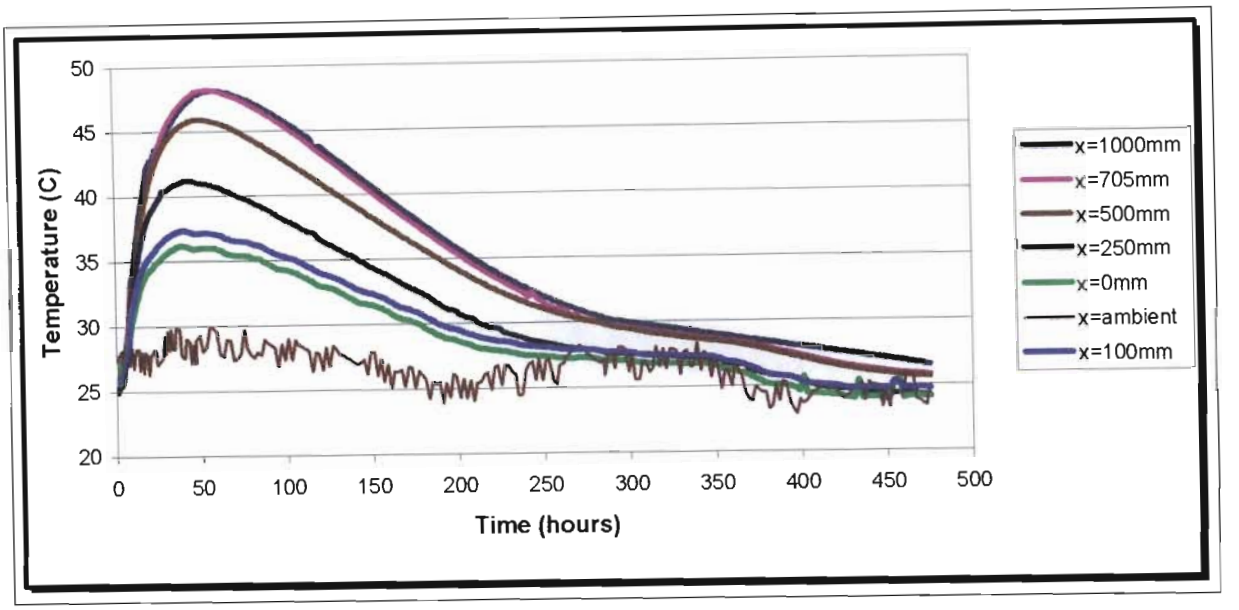

Figure 3.13: Measured Temperature versus Time.

The profiles indicate that at the position closest to the insulated surface (x=1000mm) the temperature reaches the highest peak as opposed to the exposed surface (x=0mm). The shape of the curves, except for the ambient temperature curve, show a steep temperature gradient at the start of temperature measurement i.e. at the initial time =0.

The exposed position reaches a peak earlier than the insulated position, this is associated with the greater rate of heat loss at the exposed surface as opposed to the lesser heat loss at the position that is closer to the insulated surface.

The shape of the curves shows a peak between 40 and 60 hours for various positions, the peak is associated with the effects of the heat of hydration. The peaks for these curves occur later than that of the heat rate curve observed in figure 3.10 that occurs at approximately 12 hours. The curves for positions x=1000mm and x=0mm will be used later as boundary conditions in the numerical model. This will be achieved by obtaining the analytical expression that best describes this relationship.

CHAPTER 4 – APPLICATION OF THE GREEN ELEMENT METHOD (GEM)

4.1 Introduction.

The theoretical development of the Boundary Element Method (BEM) can be traced back to the eighteenth century when the related theory of ideal flow and integral transforms was formulated. The technique involves subdividing the boundary of the problem domain into segments and obtaining system of discreet equations from the integral equation. The early research in BEM was done by Nardini and Brebbia[15], Wrobel *et al*[16], and Brebbia and Nardini[17]. More detailed review of literature can be obtained from the research covering the topic of BEM submitted by Dargush and Banerjee[18], Banerjee and Butterfield[19], Brebbia *et al*[20], and Azevedo and Wrobel[21].

Later the Finite Element method was developed to try and deal with problems involving non-linearity, heterogeneity and body force terms that the BEM could not handle. Some engineering problems are complex and very practical, and require both the BEM and FEM to be combined in order to obtain simple way to attain the solution. This led to the birth of the Green element Method (BEM) which is founded on the on the BEM theory of element-by-element approach to obtain solutions for a specific problem domain. This new theory has been given special attention by the works of Onyejekwe[22-33] Taigbenu and Onyejekwe[34-37], Karama *et al*[38], and Teshome and Onyejekwe[39] and have manage to obtain great success.

The Green Element Method is a new approach of implementing in an element-by-element fashion, the singular Boundary Integral Theory, by enhancing the capabilities of the theory in terms of ease in solving non-linear and heterogeneous problems, and achieving sparseness in the global co-efficient matrix.

The Green Element Method provides solutions to linear, non-linear, steady and transient engineering problems in one and two-dimensional domains.

The next section describes the basic formulation of the GEM.

4.2 Basic Formulation of the Green Element Method.

The one-dimensional second order Poisson's equation used in most engineering applications is given as:

$$\frac{d\phi(x,t)}{dt} + f(x,t) = K(x,h)\frac{d^2\phi(x,t)}{dx^2} \qquad 4.1$$

where:

$\phi(x,t)$	is the primary variable which is a function of time and space.
x	is the independent or space variable.
t	is the time variable.
$K(x,h)$	is the hydraulic conductivity.
$f(x,t)$	is the external or internal recharge term.

General properties of the equation (4.1)

- The equation is **linear** if the conductivity K is **not** a function of the primary or dependent variable.
- The equation is **non linear** if the conductivity K is a function of the primary or dependent variable.
- The equation is **homogeneous** if the conductivity K is **not** a function of the independent or space variable.
- The equation is **heterogeneous** if the conductivity K is a function of the independent or space variable.
- The equation is **steady** if the primary variable ϕ is a function of the independent or space variable.
- The equation is **transient** if the primary variable ϕ is a function of the independent or space variable and the time variable.

The procedure that the Green Element Method uses to solve differential equations is summarized in Figure 4.2, below.

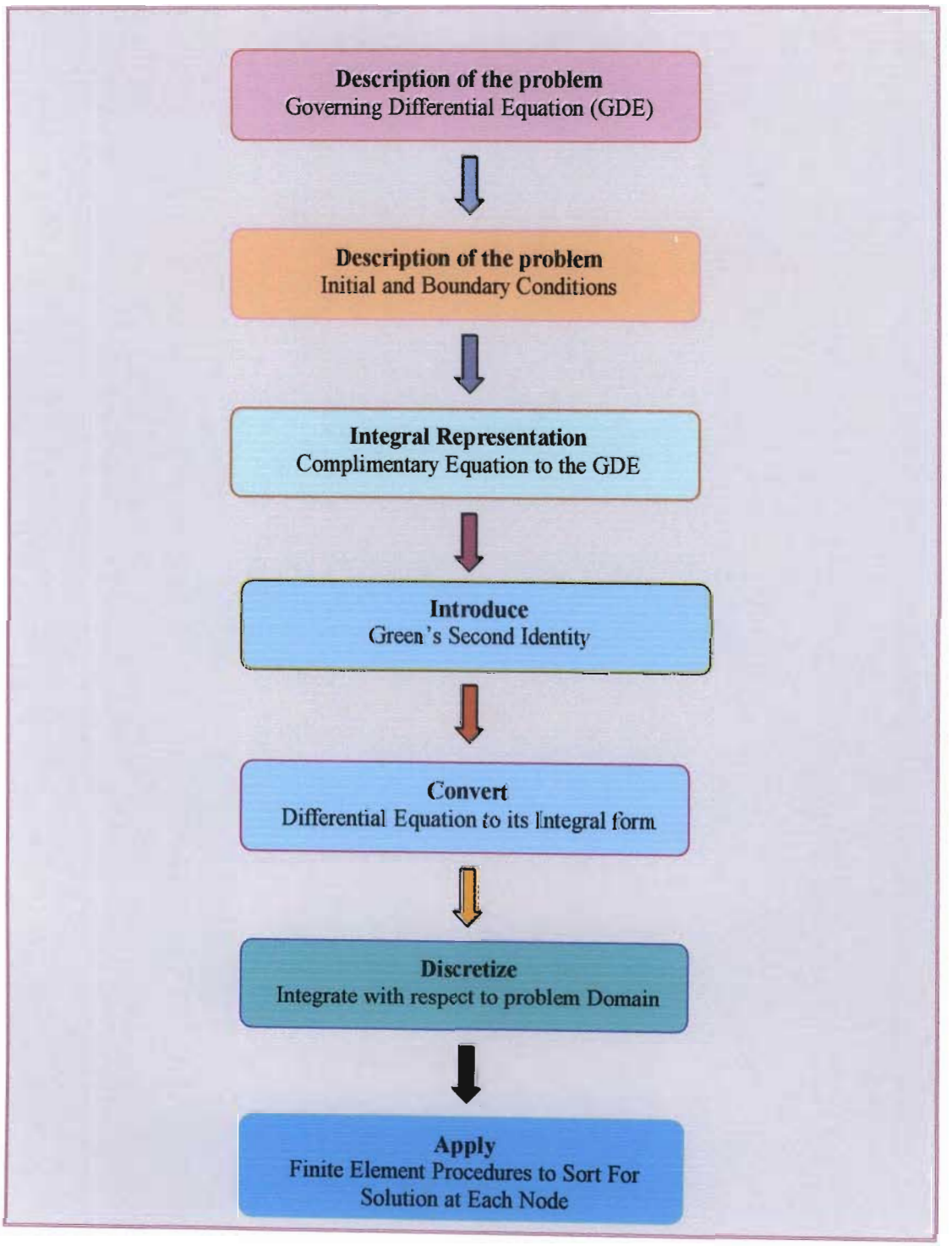

Figure 4.1: Schematic Representation of Green Element Procedure.

4.2.1 Steady Linear Homogeneous Equation

For a domain that is steady and homogeneous, K is constant (neither a function of the independent nor primary variable), and primary variable is not a function of time, equation (4.1) reduces to:

$$K\frac{d^2\phi}{dx^2} = f(x) \tag{4.2}$$

4.2.2 Boundary Conditions

These conditions describe the activity occurring at the start and end points of any given domain of a differential equation. The length of the domain, L, is obtained by subtracting the start point (x_0), from the end point (x_L), i.e. L = $x_L - x_0$.

Conditions are imposed at these points on the primary variable, ϕ and/or its derivative $\frac{d\phi}{dx}$, in order to obtain a unique solution of the differential equation.

Three types of boundary conditions are described below:

- *Dirichlet or Essential Conditions*
  This conditions specifies the value of the primary variable ϕ, at a boundary position as follows:

$$\phi(x = x_0) = \phi_0 \text{ and } \phi(x = x_l) = \phi_L \tag{4.3}$$

- *Neumann or Flux Condition*
  This conditions specifies the value of the flux or derivative of the primary variable ϕ, at a boundary position as follows:

$$-K\left[\frac{d\phi}{dx}\right]_{x=x_0} = \varphi_0 \text{ and } -K\left[\frac{d\phi}{dx}\right]_{x=x_L} = \varphi_L \tag{4.4}$$

- *Cauchy Condition*

  This conditions specifies the value for a linear combination of the primary variable ϕ, and the flux, $\frac{d\phi}{dx}$ at a boundary position as follows:

$$\left[a_0\phi + b_0 K\frac{d\phi}{dx}\right]_{x=x_0} = v_0 \text{ and } \left[a_L\phi + b_L K\frac{d\phi}{dx}\right]_{x=x_L} = v_L \tag{4.5}$$

  where a_0, b_0, a_L and b_L are known co-efficients.

4.2.3 Integral Representation

In numerical computations, it is usually easier to work with an integral equation than a differential one. Therefore we shall try to formulate integral representation of equation (4.2).

In order to derive an integral representation of equation (4.2) we shall first introduce a complimentary equation. Our complimentary differential equation is

$$\frac{d^2G}{dx^2} = \delta(x - x_i) \tag{4.6}$$

Eq. (1.3) is called a Dirac-delta function and has the following properties

$$\delta(x - x_i) = \begin{cases} \infty, & x = x_i \\ 0, & x \neq x_i \end{cases} \tag{4.7}$$

$$\int_{-\infty}^{\infty} \delta(x - x_i)dx = \int_{x_i-\epsilon}^{x_i+\epsilon} \delta(x - x_i)dx = 1 \tag{4.8}$$

$$\int_{-\infty}^{\infty} f(x)\delta(x - x_i)dx = \int_{x_i-\epsilon}^{x_i+\epsilon} f(x)\delta(x - x_i)dx = f(x_i) \tag{4.9}$$

Dirac delta function has a symmetric shape, and the following relations hold

$$\int_{x_i}^{\infty} \delta(x-x_i)dx = \int_{x_i}^{x_i+\in} \delta(x-x_i)dx = \frac{1}{2} \tag{4.10}$$

$$\int_{-\infty}^{x_i} \delta(x-x_i)dx = \int_{x_i-\in}^{x_i} \delta(x-x_i)dx = \frac{1}{2} \tag{4.11}$$

$$\int_{x_i}^{\infty} f(x)\delta(x-x_i)dx = \int_{x_i}^{x_i+\in} f(x)\delta(x-x_i)dx = \frac{f(x_i)}{2} \tag{4.12}$$

4.2.4 Green' Second Identity

The only information required now before deriving the integral representation of equation (4.2) is the statement of one of Green's identities. For any two functions, U and V, which are twice differentiable with respect to x, Green's identity states

$$\int_{x_0}^{x_L}\left(U\frac{d^2V}{dx^2} - V\frac{d^2U}{dx^2}\right)dx = U\frac{dV}{dx}\Bigg|_{x_0}^{x_L} - V\frac{dU}{dx}\Bigg|_{x_0}^{x_L} \tag{4.13}$$

Setting U to ϕ and V to G, and substituting equations (4.2) and (4.6) into eq. (4.13) yields

$$\int_{x_0}^{x_L}\left(\phi\frac{d^2G}{dx^2} - G\frac{d^2\phi}{dx^2}\right)dx = \phi\frac{dG}{dx}\Bigg|_{x_0}^{x_L} - G\frac{d\phi}{dx}\Bigg|_{x_0}^{x_L} \tag{4.14}$$

We can now substitute the values of d^2G/dx^2 and $d^2\phi/dx^2$ into eq. (4.14), thus resulting in

$$\int_{x_0}^{x_L}\left(\phi\delta(x-x_i) - G\frac{f(x)}{K}\right)dx = \phi\frac{dG}{dx}\Bigg|_{x_0}^{x_L} - G\frac{d\phi}{dx}\Bigg|_{x_0}^{x_L} \tag{4.15}$$

4.2.5 Numerical conversion of the governing equation.

Using the definition for the Dirac delta function from equation. (4.9), eq. (4.15) becomes

$$-\lambda\phi_i + \phi\frac{dG}{dx}\Big|_{x_0}^{x_L} - G\frac{d\phi}{dx}\Big|_{x_0}^{x_L} + \int_{x_0}^{x_L} G\frac{f(x)}{K}dx = 0 \tag{4.16}$$

The parameter λ =1 when x_i is within the domain $[x_0, x_L]$ and

λ =0.5 when x_i is at the end points x_0 and x_L.

Equation (4.16) is the integral representation of eq. (4.2)

The next step is the numerical implementation of eq. (4.16).

In one dimension, solution to eq. (4.6) is given as

$$G(x, x_i) = \frac{|x - x_i| + k}{2} \tag{4.17}$$

In which k is an arbitrary constant

$$\frac{dG(x, x_i)}{dx} = \frac{1}{2}[H(x - x_i) - H(x_i - x)] \tag{4.18}$$

In which H is the Heaviside function which has the following representation

$$H(x - x_i) = \begin{cases} 1, & x \succ x_i \\ 0, & x \prec x_i \end{cases} \tag{4.19}$$

Introducing eqs. (4.16) and (4.17) into eq. (4.18) yields

$$\begin{aligned} &-2\lambda\phi_i + [H(x_L - x_i) - H(x_i - x_L)]\phi(x_L) - [H(x_0 - x_i) - H(x_i - x_0)]\phi(x_i) \\ &-(|x_L - x_i| + k)\frac{d\phi}{dx}\Big|_{x=x_L} + (|x_0 - x_i| + k)\frac{d\phi}{dx}\Big|_{x=x_0} + \int_{x_0}^{x_L}(|x - x_i| + k)\frac{f(x)}{K}dx = 0 \end{aligned} \tag{4.20}$$

Or

$$-2\lambda\phi_i + [H(x_L - x_i) - H(x_i - x_L)]\phi_L - [H(x_0 - x_i) - H(x_i - x_0)]\phi_i$$
$$-(|x_L - x_i| + k)\varphi_L + (|x_0 - x_i| + k)\varphi_0 + \int_{x_0}^{x_{iL}} (|x - x_i| + k)\frac{f(x)}{K}dx \qquad (4.21)$$
$$+ \int_{x_i}^{x_L} (|x - x_i| + k)\frac{f(x)}{K}dx = 0$$

In which $\phi_L=\phi(x_l)$, $\phi_O=\phi(x_O)$, $\varphi_L=d\phi(x=x_L)/dx$, $\varphi_O=d\phi(x=x_O)/dx$

The Heaviside equation can be extended so that eq. (4.21) can be evaluated

$$H(x_L - x_i) - H(x_i - x_L) = \begin{cases} 1, & x_i \prec x_L \\ 0, & x_i = x_L \end{cases} \qquad (4.22a)$$

$$H(x_0 - x_i) - H(x_i - x_0) = \begin{cases} 1, & x_i \prec x_0 \\ 0, & x_i = x_0 \end{cases} \qquad (4.22b)$$

4.2.6 Discretization with respect to problem domain.

The solution domain between x_O and x_L is subdivided into subdomains or M elements. The integral representation can be expressed as a summation of the integral representation of eq. (4.21) in each element. That is

$$\sum_{e=1}^{M} -2\lambda^{(e)}\phi_i^{(e)} + \left[H\left(x_2^{(e)} - x_i^{(e)}\right) - H\left(x_i^{(e)} - x_2^{(e)}\right)\right]\phi_2^{(e)} - \left[H\left(x_1^{(e)} - x_i^{(e)}\right) - H\left(x_i^{(e)} - x_1^{(e)}\right)\right]\phi_1^{(e)}$$
$$-\left(\left|x_2^{(e)} - x_1^{(e)}\right| + k\right)\varphi_2^{(e)} + \left(\left|x_1^{(e)} - x_1^{(e)}\right| + k\right)\varphi_1^{(e)} + \frac{1}{K}\int_{x_1^{(e)}}^{x_2^{(e)}} \left(\left|x - x_i^{(e)}\right| + k\right) f(x)dx = 0 \qquad (4.23)$$

From eq. (4.23) there are 4 unknown quantities in the typical element - $\phi_1^{(e)}$, $\varphi_1^{(e)}$, $\phi_2^{(e)}$ and $\varphi_2^{(e)}$, which implies 2 degrees of freedom at each node. Eq. (4.23) can be split into 2 equations and by evaluating it with $x_i^{(e)} = x_1^{(e)}$ and $x_i^{(e)} = x_2^{(e)}$

$$\sum_{e=1}^{M} -\phi_1^{(e)} + \phi_2^{(e)} + k\varphi_1^{(e)} - (k + \ell^{(e)})\varphi_2^{(e)} + \frac{1}{K}\int_{x_1^{(e)}}^{x_2^{(e)}} f(x)\left(x - x_1^{(e)} + k\right)dx = 0 \qquad (4.24)$$

$$\sum_{e=1}^{M} \phi_1^{(e)} - \phi_2^{(e)} + (k + \ell^{(e)})\varphi_1^{(e)} - k\varphi_2^{(e)} + \frac{1}{K}\int_{x_1^{(e)}}^{x_2^{(e)}} f(x)\left(x_2^{(e)} - x + k\right)dx = 0 \qquad (4.25)$$

Eqs. (4.24) and (4.25) can be combined into a matrix equation of the form

$$\sum_{e=1}^{M}\begin{bmatrix}-1 & 1\\ 1 & -1\end{bmatrix}\begin{Bmatrix}\phi_1^{(e)}\\ \phi_2^{(e)}\end{Bmatrix}+\begin{bmatrix}k & -\left(k+\ell^{(e)}\right)\\ \left(k+\ell^{(e)}\right) & -k\end{bmatrix}\begin{Bmatrix}\varphi_1^{(e)}\\ \varphi_2^{(e)}\end{Bmatrix}+\begin{Bmatrix}F_1^{(e)}\\ F_2^{(e)}\end{Bmatrix}=\begin{Bmatrix}0\\ 0\end{Bmatrix} \tag{4.26}$$

Or

$$\sum_{e=1}^{M} R_{ij}^{(e)}\phi_j^{(e)}+L_{ij}^{(e)}\varphi_j^{(e)}+F_i^{(e)}=0 \tag{4.26}$$

in which,

$$R_{ij}^{(e)}=\begin{bmatrix}-1 & 1\\ 1 & -1\end{bmatrix}=(-1)^{i+j-1} \tag{4.27}$$

$$L_{ij}^{(e)}=\begin{bmatrix}k & -\left(k+\ell^{(e)}\right)\\ \left(k+\ell^{(e)}\right) & -k\end{bmatrix} \tag{4.28}$$

$$F_1^{(e)}=\frac{1}{K}\int_{x_1^{(e)}}^{x_2^{(e)}} f(x)(x-x_1^{(e)}+k)dx \tag{4.29}$$

$$F_2^{(e)}=\frac{1}{K}\int_{x_1^{(e)}}^{x_2^{(e)}} f(x)(x_2^{(e)}-x+k)dx \tag{4.30}$$

For the choice of the value of k, the domain should be uniformly discretised so that

$$k=\bar{\ell}=\ell \tag{4.31}$$

where $\bar{\ell}$ =length of the longest domain. For a computational domain that is uniformly discretised

$$L_{ij}^{(e)}=L_{ij}=\begin{bmatrix}1 & -2\\ 2 & -1\end{bmatrix} \tag{4.32}$$

Evaluation of the recharge term for distributed source/sink is,

$$F_1^{(e)}=\frac{1}{K}\int_{x_1^{(e)}}^{x_2^{(e)}} f(x)\left(x-x_1^{(e)}+\bar{\ell}\right)dx \tag{4.33}$$

$$F_2^{(e)} = \frac{1}{K}\int_{x_1^{(e)}}^{x_2^{(e)}} f(x)\left(x_2^{(e)} - x + \bar{\ell}\right)dx \tag{4.34}$$

and for concentrated source/sink

$$F_1^{(e)} = \frac{1}{K}\sum_{j=1}^{N_p^{(e)}} Q_j\left(x_j - x_1^{(e)} + \bar{\ell}\right) \tag{4.35}$$

$$F_2^{(e)} = \frac{1}{K}\sum_{j=1}^{N_p^{(e)}} Q_j\left(x_2^{(e)} - x_j + \bar{\ell}\right) \tag{4.36}$$

4.2.7 Global Matrix Assembly.

A problem domain that consist of M elements will result in N =M=1 number of nodes and will need to compute 2N unknown quantities. Consider a typical problem domain below:

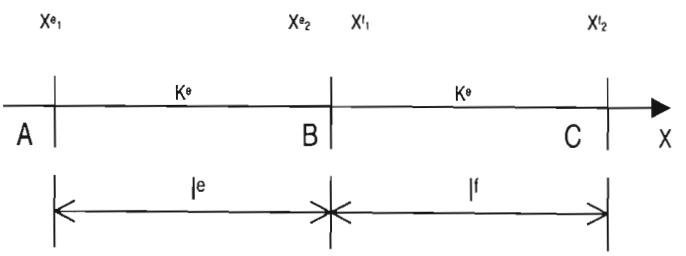

Figure 4.2: Typical elements of the problem domain.

Looking at node B, $X^e_2 = X^f_1$, this is because they appear at the same point, therefore the following can be concluded:

$$\phi_2^e = \phi_1^f \tag{4.37}$$

and $K^e\varphi_2^e = K^f\varphi_1^f$

where K^e and K^f are known as hydraulic conductivities of elements e and f respectively. For a homogeneous medium the following, $K^e = K^f$ holds.

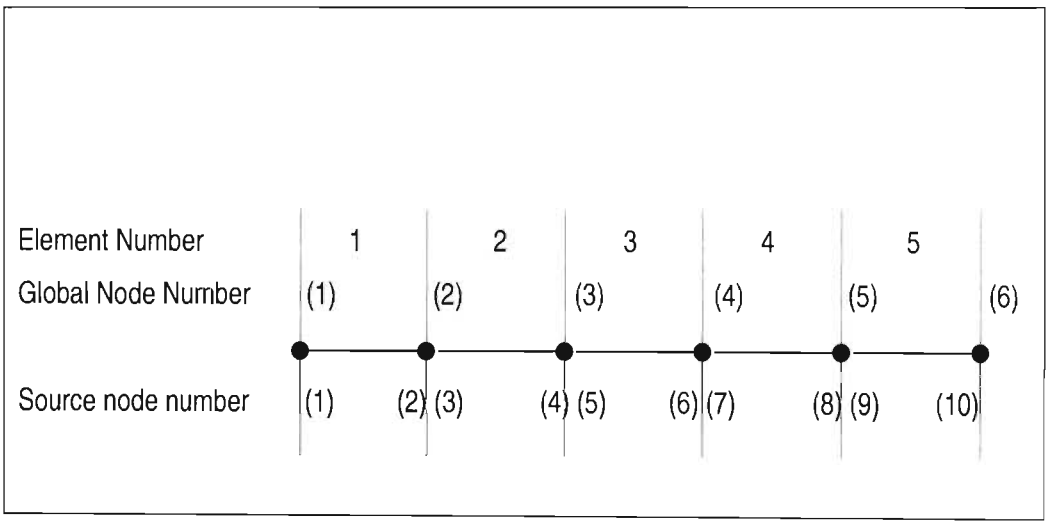

Figure 4.3: Typical elements of the problem domain.

If we assume that the boundary condition prescribed at node 1 is the primary variable and the flux is specified at node 6 then the following is applicable:

At node 1 $\quad \phi_{x=0} = \phi^1$

At node 2 $\quad \varphi_{x=l} = \varphi_6$

Then recalling equation (4.26), which is

$$\sum_{e=1}^{M} R_{ij}^{(e)} \phi_j^{(e)} + L_{ij}^{(e)} \varphi_j^{(e)} + F_i^{(e)} = 0$$

and can be written as follows:

$$\sum_{e=1}^{M} \begin{bmatrix} R_{11} & R_{12} \\ R_{21} & R_{22} \end{bmatrix} \begin{Bmatrix} \phi_1^{(e)} \\ \phi_2^{(e)} \end{Bmatrix} + \begin{bmatrix} L_{11} & L_{12} \\ L_{21} & L_{22} \end{bmatrix} \begin{Bmatrix} \varphi_1^{(e)} \\ \varphi_2^{(e)} \end{Bmatrix} + \begin{Bmatrix} F_1^{(e)} \\ F_2^{(e)} \end{Bmatrix} = \begin{Bmatrix} 0 \\ 0 \end{Bmatrix} \qquad (4.38)$$

Applying this equation to each element of the problem domain, For element 1 there are two equations and are as follows:

$$R^1_{11}\phi^1_1 + R^1_{12}\phi^1_2 + L^1_{11}\varphi^1_1 + L^1_{12}\varphi^1_2 + F^1_1 = 0 \tag{4.39}$$

$$R^2_{21}\phi^2_1 + R_{122}\phi^2_2 + L^2_{21}\phi^2_1 + L^2_{22}\phi^2_2 + F^2_2 = 0 \tag{4.40}$$

All the known terms can be moved to the right-hand side and the equations are written as:

$$R^1_{12}\phi^1_2 + L^1_{11}\varphi^1_1 + L^1_{12}\varphi^1_2 = -R^1_{11}\phi^1_1 - F^1_1$$

$$R_{122}\phi^2_2 + L^2_{21}\phi^2_1 + L^2_{22}\phi^2_2 = -R^2_{21}\phi^2_1 - +F^2_2$$

The same procedure will be followed for all nodes. For five elements, there will be 5 x 2 equations. The left-hand side of the equation consists of coefficient matrix multiplied by the unknown variable matrix. The right-hand side consists of known values. Hence the equation formed by matrices is given as:

$$\begin{bmatrix}
L^1_{11} & R^1_{12} & L^1_{12} & 0 & 0 & 0 & 0 & 0 & 0 & 0 \\
L^1_{21} & R^1_{22} & L^1_{22} & 0 & 0 & 0 & 0 & 0 & 0 & 0 \\
0 & R^2_{11} & L^2_{11} & R^2_{12} & L^2_{12} & 0 & 0 & 0 & 0 & 0 \\
0 & R^2_{21} & L^2_{21} & R^2_{22} & L^2_{22} & 0 & 0 & 0 & 0 & 0 \\
0 & 0 & 0 & R^3_{11} & L^3_{11} & R^3_{12} & L^3_{12} & 0 & 0 & 0 \\
0 & 0 & 0 & R^3_{21} & L^3_{21} & R^3_{22} & L^3_{22} & 0 & 0 & 0 \\
0 & 0 & 0 & 0 & 0 & R^4_{11} & L^4_{11} & R^4_{12} & L^4_{12} & 0 \\
0 & 0 & 0 & 0 & 0 & R^4_{21} & L^4_{21} & R^4_{22} & L^4_{22} & 0 \\
0 & 0 & 0 & 0 & 0 & 0 & 0 & R^5_{11} & L^5_{11} & R^5_{12} \\
0 & 0 & 0 & 0 & 0 & 0 & 0 & R^5_{21} & L^5_{21} & R^5_{22}
\end{bmatrix}
\begin{Bmatrix}
\varphi_1 \\ \phi_2 \\ \varphi_2 \\ \phi_3 \\ \varphi_3 \\ \phi_4 \\ \varphi_4 \\ \phi_5 \\ \varphi_5 \\ \phi_6
\end{Bmatrix} =
\begin{bmatrix}
R^1_{12} + F^1_1 \\ R^1_{21} + F^1_2 \\ 0 \\ 0 \\ 0 \\ 0 \\ 0 \\ 0 \\ R^5_{12} + F^5_1 \\ R^5_{12} + F^5_2
\end{bmatrix}$$

The general form of the matrix is given by:

$$[A]\begin{Bmatrix}\phi \\ \varphi\end{Bmatrix} = \{S\} \tag{4.41}$$

Examples of problems solved by hand using the Green Element Method are obtained in appendix D.

4.3 Solution of the Governing Equation For a non transient case

The GEM will now be used to solve a primary variable that is both space and time-dependent. As discussed in the section 4.1, the boundary conditions that will be used specify the primary variable T, at end nodes and are both time depended. The temperature-time curve that was obtained experimentally from the results produced from the temperature measurements experiment described in chapter 3 for positions 0mm and 1000mm will be converted into an analytical expression. Another condition that is required to solve the transient problem is known as the initial condition. This condition describes an earlier attained equilibrium state of the system at time=0 and specifies the primary variable, which is the temperature in this case, everywhere in the domain.

The recharge term which is represented by the F in the GEM notation is treated as the heat of hydration curve and will also obtained experimentally from the results produced from the calorimeter test in chapter 3 and will be converted into an analytical expression.

The procedure for solving the transient problem is the same as the one described in section 4.2, except that it will be dealt in a slightly different manner to accommodate its transient nature.

The transient one-dimensional second order equation is given as:

$$\frac{d\phi}{dt} + f(x,t) = K\frac{d^2\phi}{dx^2} \tag{4.42}$$

The equation is re-arranged to be:

$$\frac{d^2\phi}{dx^2} = \frac{1}{K}\left[\frac{d\phi}{dt} + f(x,t)\right] \tag{4.43}$$

Applying the Greens' Second Identity to convert equation 4.31 into an integral form yields:

$$\int_{x_0}^{x_L}\left(\phi(x,t)\frac{d^2G}{dx^2} - G\frac{d^2\phi}{dx^2}\right)dx = \phi(x,t)\frac{dG}{dx}\Big|_{x_0}^{x_L} - G\frac{d\phi}{dx}\Big|_{x_0}^{x_L}$$

Our complimentary differential equation is

$$\frac{d^2G}{dx^2} = \delta(x - x_i) \tag{4.44}$$

The solution to equation (4.44) is given as

$$G(x, x_i) = \frac{|x - x_i| + k}{2} \tag{4.45}$$

In which k is an arbitrary constant which is given the value of the longest element length.

The first derivative of $G(x, x_i)$, gives the Heaveside Function:

$$\frac{dG(x, x_i)}{dx} = \frac{1}{2}\left[H(x - x_i) - H(x_i - x)\right] \tag{4.46}$$

Introducing eqs. (4.46) and (4.45) into eq. (4.43) and simplifying yields

$$\begin{aligned} &-2\lambda\phi_i + \left[H(x_L - x_i) - H(x_i - x_L)\right]\phi_L - \left[H(x_0 - x_i) - H(x_i - x_0)\right]\phi_i \\ &-\left(|x_L - x_i| + k\right)\varphi_L + \left(|x_0 - x_i| + k\right)\varphi_0 + \frac{1}{K}\int_{x_0}^{x_L}\left(|x - x_i| + k\right)\left[\frac{d\phi}{dt} + f(x,t)\right]dx = 0 \end{aligned} \tag{4.47}$$

The terms within the integral are of great of concern and will be taken care of by approximating of the two terms, $\phi(x,t)$ and $f(x,t)$ using the linear interpolation as follows:

$$\phi(x,t) = \Omega_1^e(\xi)\phi_1^e(t) + \Omega_2^e(\xi)\phi_2^e(t) \tag{4.48a}$$

$$f(x,t) = \Omega_1^e(\xi)f_1^e(t) + \Omega_2^e(\xi)f_2^e(t) \tag{4.48b}$$

where $\Omega_1^e(\xi)$ and $\Omega_2^e(\xi)$ are linear element interpolating functions and $\phi_1^e(t)$, is for example the value of ϕ at node x_2^e at time t. The temporal derivative of ϕ is given as:

$$\frac{\phi(x,t)}{\partial t} = \Omega_1^e(\xi)\frac{\phi_1^e(t)}{dt} + \Omega_2^e(\xi)\frac{\phi_2^e(t)}{dt} \tag{4.49}$$

Note that the shape functions, $\Omega_1^e(\xi)$ and $\Omega_2^e(\xi)$ take care of the distance x component of ϕ and the derivative with respect to time is used in equation 4.47,Equations 4.48a and 4.48b are now implanted into equation 4.47 to get the following;

$$-2\lambda\phi_i + [H(x_L - x_i) - H(x_i - x_L)]\phi_L - [H(x_0 - x_i) - H(x_i - x_0)]\phi_i$$
$$-(|x_L - x_i| + k)\varphi_L + (|x_0 - x_i| + k)\varphi_0 + \frac{1}{K}\int_{x_0}^{x_L}(|x - x_i| + k)\Omega_j^e\left[\frac{d\phi_j}{dt} + f_j\right]dx = 0 \qquad (4.50)$$

Equation 4.50. above is split into two equation by evaluating $x_i = x_1$ and $x_i = x_2$, and using the ξ co-ordinate system:

$$-\phi_1^e + \phi_2^e + \bar{l}\,\varphi_1^e - (\bar{l} + l)\varphi_2^e + \frac{\bar{l}}{K}\int_0^1 \Omega_j^e\left[\frac{d\phi_j}{dt} + f_j^e\right]\left(\bar{l} + l^e\xi\right)d\xi = 0 \qquad (4.51a)$$

$$\phi_1^e - \phi_2^e - \bar{l}\,\varphi_2^e + (\bar{l} + l)\varphi_1^e + \frac{\bar{l}}{K}\int_0^1 \Omega_j^e\left[\frac{d\phi_j}{dt} + f_j^e\right]\left(\bar{l} + l^e(1 - \xi)\right)d\xi = 0 \qquad (4.51b)$$

The tensor matrix form of equations is given by:

$$R_{ij}^{(e)}\phi_j^{(e)} + L_{ij}^{(e)}\varphi_j^{(e)} + \frac{T_{ij}^e}{K}\left[\frac{d\phi_j}{dt} + f_j^e\right] = 0 \qquad (4.52)$$

The matrices R_{ij} and L_{ij} have been defined in sections 4.2, the min concern is evaluating T_{ij} and the temporal derivative $\frac{d\phi_j}{dt}$.

T_{ij} is a matrix used in interpolation of functions that uses the ξ co-ordinate system and is given by:

$$T_{ij}^{(e)} = \frac{l^e}{6}\begin{bmatrix} \bar{3}l + l^e & \bar{3}l + 2l^e \\ \bar{3}l + 2l^e & \bar{3}l + l^e \end{bmatrix} \qquad (4.53)$$

There are various methods of evaluating the temporal derivative. The different approximation method for a two and a three level time schemes will be used.

For a two level time schemes, the temporal derivative becomes:

$$\left.\frac{d\phi_j^{e,m+1}}{dt}\right|_{t=t_m+\alpha\Delta t} = \frac{\phi_j^e(t_m+\Delta t)-\phi_j^e(t_m)}{\Delta t} = \frac{\phi_j^{e,m+1}-\phi_j^{e,m}}{\Delta t} \qquad 0\le\alpha\le 1 \qquad (4.54)$$

For a three level time schemes, the temporal derivative becomes:

$$\left.\frac{d\phi_j^{e,m+1}}{dt}\right|_{t=t_m+\alpha\Delta t} = \frac{\alpha}{\Delta t}(\phi_j^{e,m+1}-\phi_j^{e,m}) + \frac{d\phi_j^m}{dt}(1-\alpha) \qquad 1\le\alpha\le 2 \qquad (4.55)$$

The two and a three level time schemes indicate that the temporal derivative will be evaluated at a time $t_m+\Delta t$, where t_m is the previous time level and $\Delta t = t_{m+1}-t_m$ is the time step or temporal element size and t_{m+1} is the current time level at which the numerical solution is desired. α is the time wheighing factor. The value of α positions the time level at which the temporal derivative has been evaluated at $t_m+\alpha\Delta t$, it is reasonable to evaluate the other terms of equation 4.52 at that time level using the weighed average of the form.

Two level time schemes is represented by:

$$\alpha\left[R_{ij}^{(e)}\phi_j^{(e)} + L_{ij}^{(e)}\varphi_j^{(e)} + \frac{T_{ij}^e}{K}\right]_{t=t_{m+1}} + (1-\alpha)\left[R_{ij}^{(e)}\phi_j^{(e)} + L_{ij}^{(e)}\varphi_j^{(e)} + \frac{T_{ij}^e}{K}\right]_{t=t_{m+1}}$$

$$+\left[\frac{T_{ij}^e}{K}\left(\frac{\phi_j^{e,m+1}-\phi_j^{e,m}}{\Delta t}\right)\right]_{t=t_m+\alpha\Delta t} = 0 \qquad i.j=1,2, \qquad 0\le\alpha\le 1 \qquad (4.56)$$

Three level time schemes is represented by:

$$\alpha\left[R_{ij}^{(e)}\phi_j^{(e)} + L_{ij}^{(e)}\varphi_j^{(e)} + \frac{T_{ij}^e}{K}\right]_{t=t_{m+1}} + (1-\alpha)\left[R_{ij}^{(e)}\phi_j^{(e)} + L_{ij}^{(e)}\varphi_j^{(e)} + \frac{T_{ij}^e}{K}\right]_{t=t_{m+1}}$$

$$+\frac{T_{ij}^e}{K}\left[\frac{\alpha}{\Delta t}(\phi_j^{e,m+1}-\phi_j^{e,m}) + \frac{d\phi_j^m}{dt}(1-\alpha)\right]_{t=t_m+\alpha\Delta t} = 0 \qquad i.j=1,2, \qquad 0\le\alpha\le 1 \qquad (4.57)$$

The time scale is shown in the figure below:

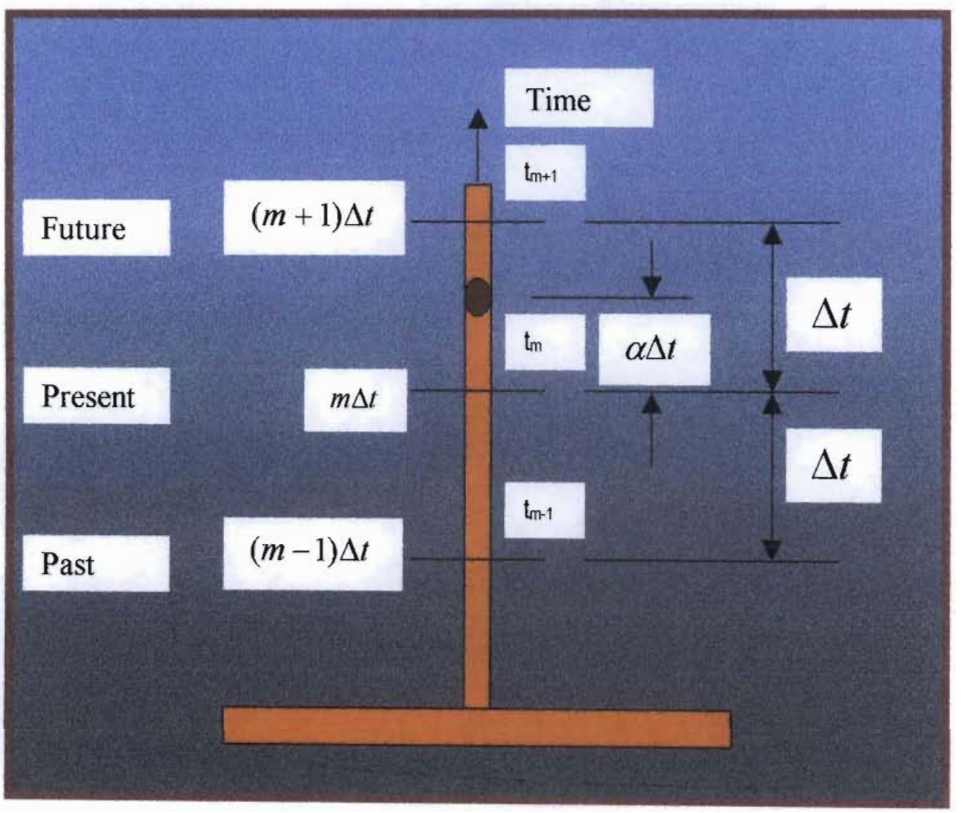

Figure 4.4: Graphical representation of time scale.

Equations 4.34 and 4.36 can be written eliminating the (e) and replacing it by time levels as follows: Two level time schemes is represented by:

$$\alpha\left[R_{ij}^{t_{m+1}}\phi_j^{t_{m+1}} + L_{ij}^{t_{m+1}}\varphi_j^{t_{m+1}} + \frac{T_{ij}^{t_{m+1}}}{K}\right]_{t=t_{m+1}} + (1-\alpha)\left[R_{ij}^{t_m}\phi_j^{t_m} + L_{ij}^{t_m}\varphi_j^{t_m} + \frac{T_{ij}^{t_m}}{K}\right]$$

$$+\left[\frac{T_{ij}^{e}}{K}\left(\frac{\phi_j^{e,m+1} - \phi_j^{e,m}}{\Delta t}\right)\right] = 0 \qquad i.j = 1,2, \qquad 0 \le \alpha \le 1 \tag{4.58}$$

Three level time schemes is represented by:

$$\alpha\left[R_{ij}^{t_{m+1}}\phi_j^{t_{m+1}} + L_{ij}^{t_{m+1}}\varphi_j^{t_{m+1}} + \frac{T_{ij}^{t_{m+1}}}{K}\right]_{t=t_{m+1}} + (1-\alpha)\left[R_{ij}^{t_m}\phi_j^{t_m} + L_{ij}^{t_m}\varphi_j^{t_m} + \frac{T_{ij}^{t_m}}{K}\right]$$

$$+\frac{T_{ij}^{e}}{K}\left[\frac{\alpha}{\Delta t}(\phi_j^{e,m+1} - \phi_j^{e,m}) + \frac{d\phi_j^m}{dt}(1-\alpha)\right] = 0 \qquad i.j = 1,2, \qquad 0 \le \alpha \le 1 \qquad (4.59)$$

The obtained matrix equation is represented by:

$$[A]\begin{Bmatrix}\phi^{m+1}\\ \varphi^{m+1}\end{Bmatrix} = \{\delta^m\} \qquad (4.60)$$

The unknown vector is evaluated at the present time (t_{m+1}) which then becomes the initial values for the evaluation of the unknowns in the subsequent time. Therefore the initial conditions will have to be specified in order to proceed with obtaining solutions at some desired time level which would be positioned by the value of α .

CHAPTER 5 – CODING OF THE SOLUTION USING FORTRAN PROGRAM

5.1 Governing Equation

The Green element solution is coded in a general Fortran program that is designed to handle any one-dimensional transient diffusion equation. The general form of the equation (equation 4.41) that the program has been designed to solve is described in chapter 4. The one dimensionality of the governing equation that describes the concrete beam was achieved by insulation of the beam in the y and the z directions to allow heat flow in the x direction only.

The temperature distribution within a one dimensional concrete beam governed by the equation similar to equation 4.43 in chapter 4, where the primary variable ϕ, is converted to temperature T, and the recharge term $f(x,t)$ to Q', and is represented as:

$$k\left[\frac{d^2T}{dx^2}+Q'\right]=\rho C\frac{dT}{dt} \tag{5.1}$$

Where:

t	is time.
x	is the space variable.
k	is thermal conductivity of concrete.
Q'	is the rate of heat of hydration (heat rate).
T	is the temperature.
ρ	is the density.
C	is the specific heat capacity.

Re-arranging equation 5.1 yields:

$$\frac{k}{\rho C}\frac{d^2T}{dx^2}+\frac{1}{\rho C}Q'=\rho C\frac{dT}{dt} \tag{5.2}$$

The term $\frac{k}{\rho C}$, is known as the thermal diffusivity, D and is evaluated in section 5.3.

5.2 Alteration made to the Main Program

Some alterations have been made to the main or original program to accommodate specific criteria. The new program known as "Heat Beam" is in appendix C. It consists of the main body and the subroutines. The program is executed using the input data and the output data which gives the predicted temperature and flux values. The input data is described in section 5.2.3, below.

The subroutines are used to define the boundary and initial conditions, the line integral, the coefficient matrix and the recharge. The purposes of the alterations to the program subroutines for the boundary conditions and the heat rate (recharge) term of the governing equation are described in the sections below.

5.2.1 Boundary Conditions Functions

The chosen boundary conditions represent the temperature that varies with time. The alterations are made to account for the transient nature of the boundary conditions.

The temperature versus time curves at nodes 0mm and 1000mm obtained experimentally, are converted into analytical functions that are later introduced in the subroutine for boundary conditions. The analytical expressions are obtained using the Microsoft Excel. Each temperature versus time curve has been divided into four parts that subsequently yields into four analytical functions.

This was done to enhance the highest degree of approximation of the curve resulting from the measured time base temperature profiles at the end nodes. The alterations to the main program are discussed in appendix C.

The time dependent Dirichlet boundary conditions have been considered in this case. The temperature time curves for the positions 0 and 1000mm are adopted to describe the boundary conditions of the problem domain. The curves at x=0mm and x=1000mm are obtained from figure 3.13 of chapter 3.

Figure 5.1 below gives the curves that describe the boundary conditions at the end nodes, i.e. positions, x=0mm and x=1000m.

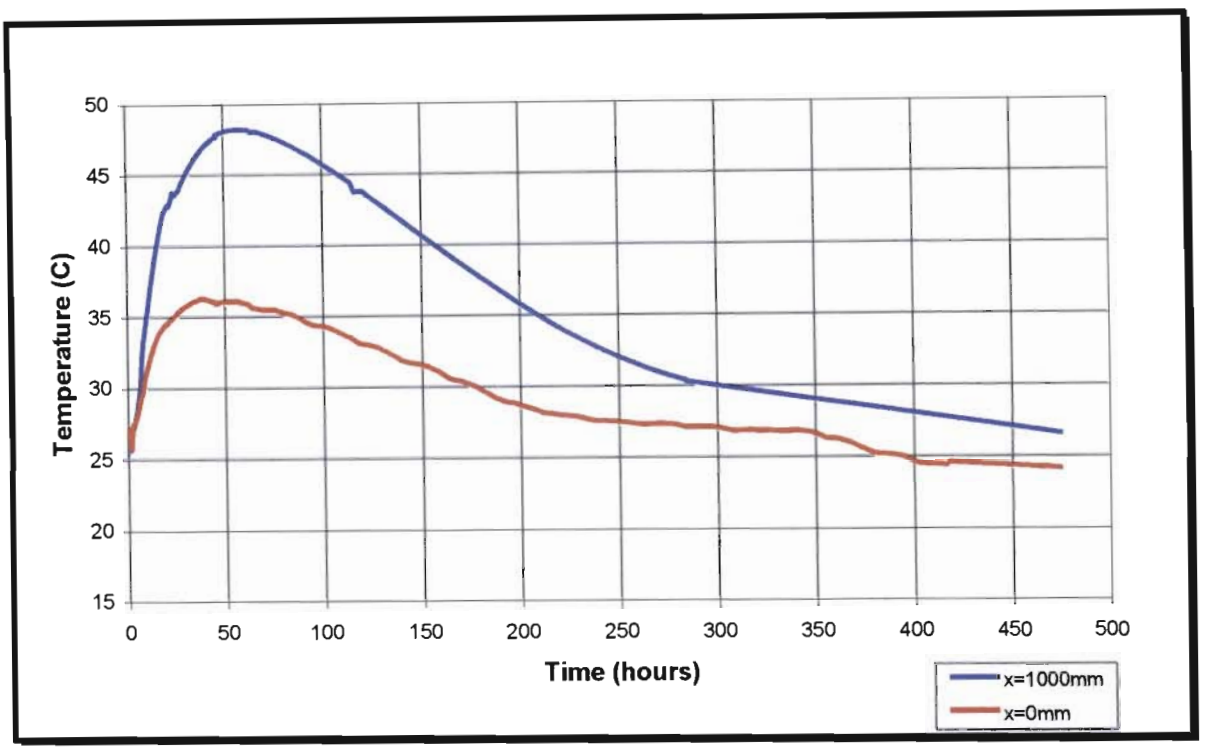

Figure 5.1: Boundary Conditions Curves.

Having obtained the boundary conditions curve, the next step was to divide each curve to into four sub curves operating at particular times in order to simplify the analytical representation of the boundary curves. Each sub-curve is then expressed into the analytical expression that will be used in a sub-routine that defines the boundary conditions at the end nodes. The analytical expressions are obtained using the trend-line fitting tool available in a Microsoft spreadsheet. The trend line approximates the measured temperature versus time curve, and gives analytical expression that best describes the curve. The sub curves, analytical expressions and subroutine names are given below:

- **Sub-routine Data4.**

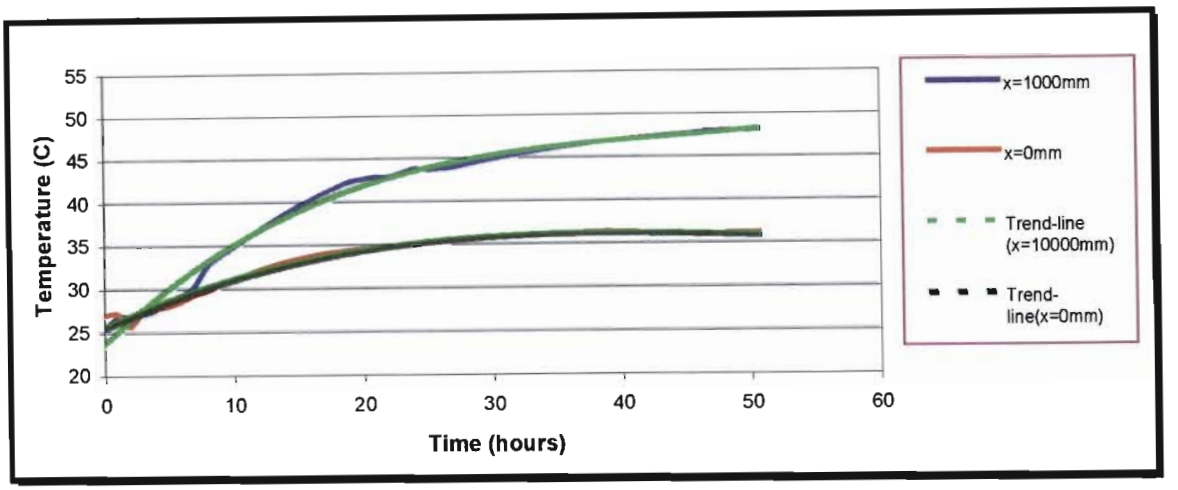

Figure 5.2: Sub-Routine Data4 Boundary Conditions Curve.

The resulting analytical functions are:

At x=0mm,

Temperature =0.000087*(TIME**3)-0.0137*(TIME**2)+0.6793*TIME+25.454 (5.3)

At x=1000mm,

Temperature =0.0001079*(TIME**3)-0.0196*(TIME**2)+1.1515 *TIME+25.325 (5.4)

These functions will be used in the program when the time is greater than 0 and less or equals to 50.6667 hours. This implies that the subroutine only operates between the said times.

- **Sub-routine Data5.**

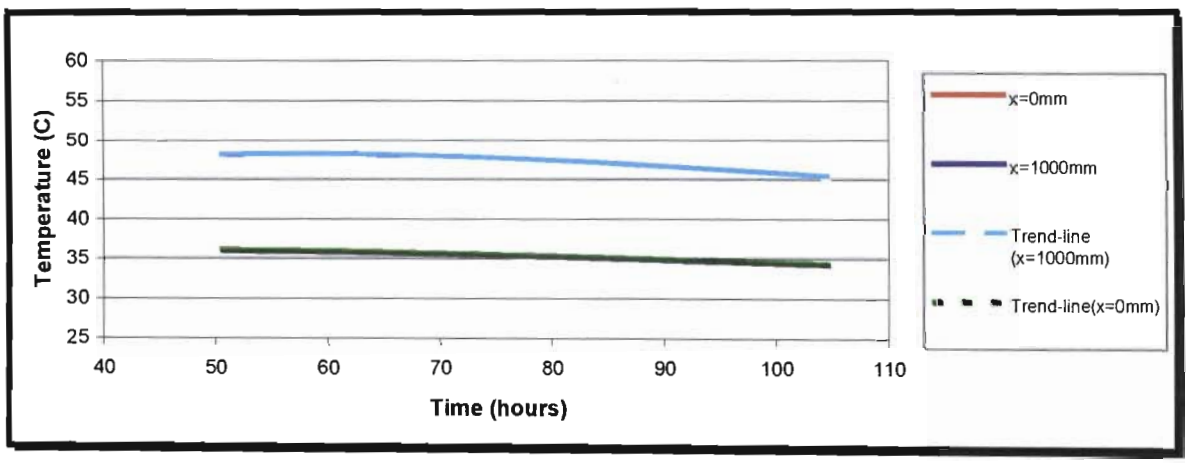

Figure 5.3: Sub-Routine Data5 Boundary Conditions Curve.

At x=0mm,

Temperature =0.0000044*(TIME**3)-0.0013*(TIME**2)+0.0874*TIME+34.267 (5.5)

At x=1000mm,

Temperature =0.0000153*(TIME**3)-0.0045*(TIME**2)+0.3657*TIME+38.926 (5.6)

These functions will be used in the program when the time equals or greater than 50.6667 hours and less or equals to 104.6667 hours.

- **Sub-routine Data6.**

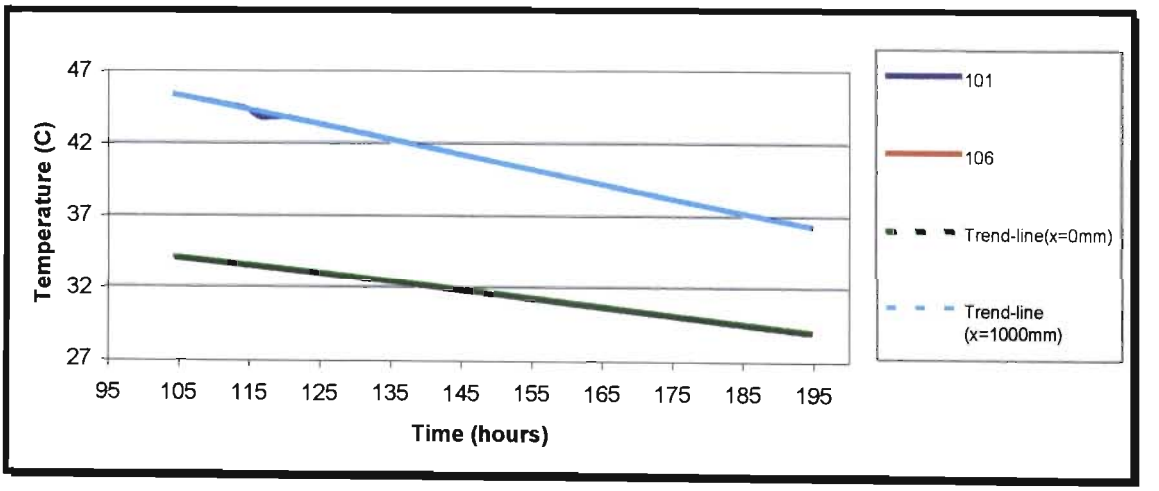

Figure 5.4: Sub-Routine Data6 Boundary Conditions Curve.

At x=0mm,

Temperature =0.000001*(TIME**3)-0.00047*(TIME**2)+0.0151*TIME+36.437 (5.7)

At x=1000mm,

Temperature =0.00000115*(TIME**3)-0.000494*(TIME**2)-0.0326*TIME+52.79 (5.8)

These functions will be used in the program when the time equals or greater than 104.6667 hours and less or equals to 194.6667 hours.

- **Sub-routine Data7.**

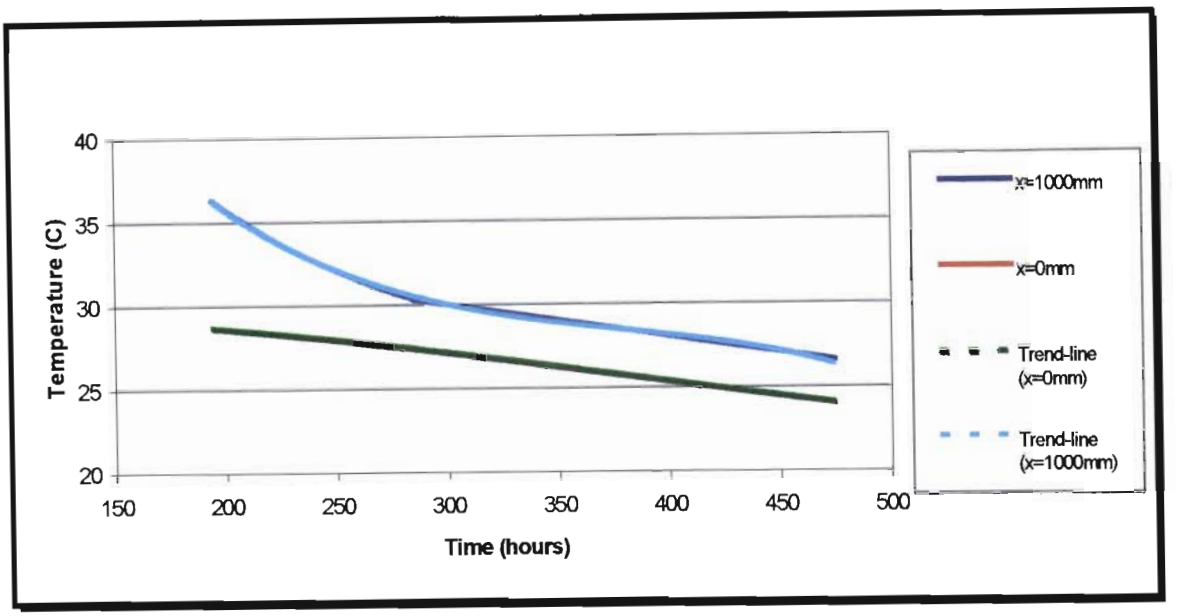

Figure 5.5: Sub-Routine Data7 Boundary Conditions Curve.

At x=0mm,

Temperature =0.00000005*(TIME**3)-0.00006*(TIME**2)+0.006*TIME+29.398 (5.9)

At x=1000mm,

Temperature =-0.0000008*(TIME**3)+0.000916*(TIME**2)-0.3645*TIME+78.262 (5.10)

These functions will be used in the program when the time equals or greater than 194.6667 hours and less or equals to 475.00 hours.

5.2.2 Recharge Functions.

An approach similar to the one in section 5.2.1 will be used to obtain analytical expressions. The Heat rate versus Nurse-Saul Equivalent time curve will be used to describe the heat of hydration and is obtained from figure 3.13 of chapter 3. The curve will be divided into three sub curves and the yielding analytical expressions will be inserted into the recharge subroutines that are used in the program.

The sub curves, analytical expressions and subroutine names are given below:

- **Sub-routine RechargeT1**

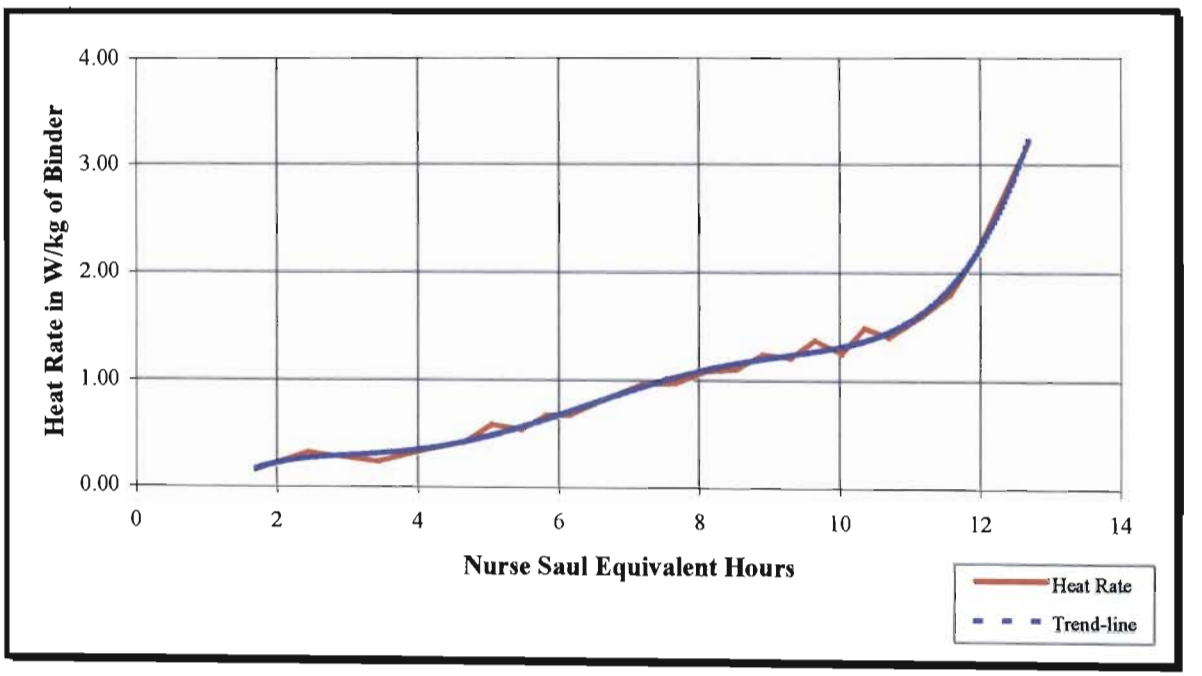

Figure 5.6: Sub-routine RrechargeT1 heat rate curve.

The resulting equation is,

Heat Rate =(0.0003*(TIME**5)-0.0106*(TIME**4)+0.1215*(TIME**3)-0.6175*(TIME**2)
+1.4715*TIME-1.0806)/2258704 (5.11)

Note that the term dividing equation (5.11) is the product of the specific heat and density of the concrete beam. This equation defines the heat rate curve and will be used in the program when the time is greater than 0 hours and less or equals to 12.6669 hours.

❖ **Sub-routine RechargeT2**

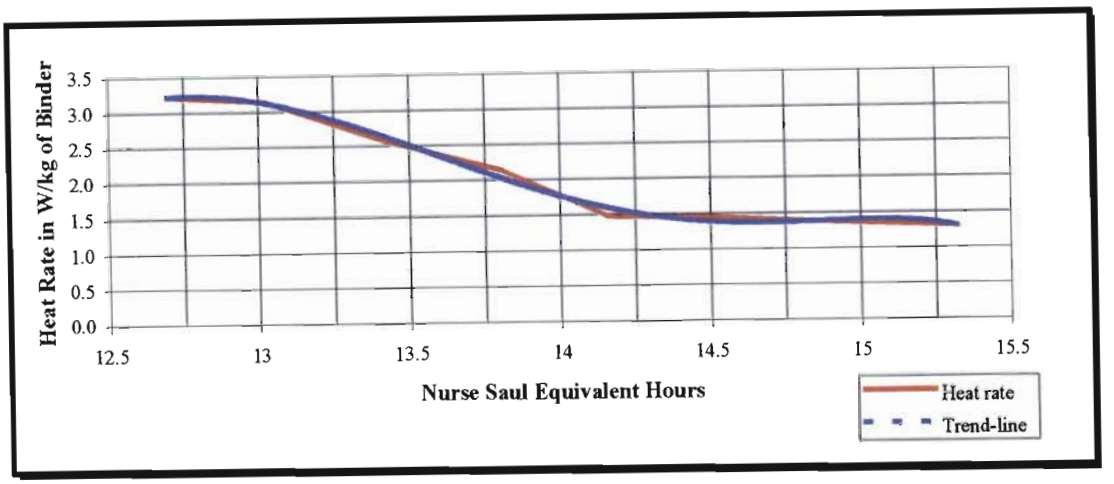

Figure 5.7: Sub-routine RrechargeT2 heat rate curve.

Heat Rate =(-0.0862*(TIME**5)+5.7354*(TIME**4)-151.84*(TIME**3)*

+1998*(TIME**2)-13061*TIME+33920)/ 2258704 (5.12)

This function will be used in the program when the time equals or greater than 12.6669 hours and less or equals to 15.3253 hours.

❖ **Sub-routine RechargeT3**

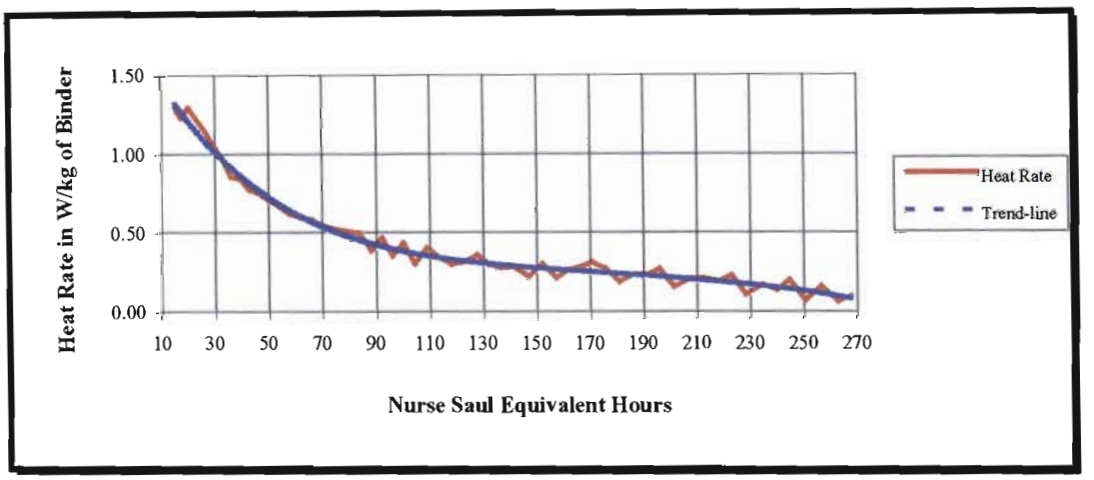

Figure 5.8: Sub-routine RrechargeT3 heat rate curve.

Heat Rate=(-0.000000000003*(TIME**5)+0.000000003*(TIME**4)-0.000001

*(TIME**3)+0.0003*(TIME**2)-0.0316*TIME+1.7307)/ 2258704 (5.13)

This function will be used in the program when the time equals or greater than 15.3253 hours and less or equals to 267.7307 hours.

5.3 Input File to the Program

The input file is formed by input variable that are determined in this section:

5.3.1 Thermal Diffusivity.

The thermal diffusivity is given by:

$$D = \frac{k}{\rho C} \tag{5.14}$$

Where $k = 2.7 J.s/m.K$, and is obtained from a table presented in a paper by E.A.B Koenders and K van Breugel[5]is for concrete made up of granite as its aggregate. $\rho = 2112 kg/m^3$, Is the proportioned density of concrete beam constituents. The specific heat capacity $C = 1069.5 J/kg.K$ is obtained by proportioning the specific heat capacities of the concrete beam constituents. Now the thermal diffusivity can be calculated as follows:

$$D = \frac{k}{\rho C}$$

$$D = \frac{J.s/m.K \times 3600 s/hour}{2310 kg/m^3 \times 1069.5 J/kg.K}$$

$$D = 0.004303 m^2/hour.$$

5.3.2 Initial temperature

The initial temperature is obtained by taking the average of measured temperature values at the start of taking readings.

The initial temperature, $T_0 = 26.0609^0 C$.

5.3.3 Discretization

The problem domain is discretized in relation to the position of the probes and is shown in figure 5.8 below.

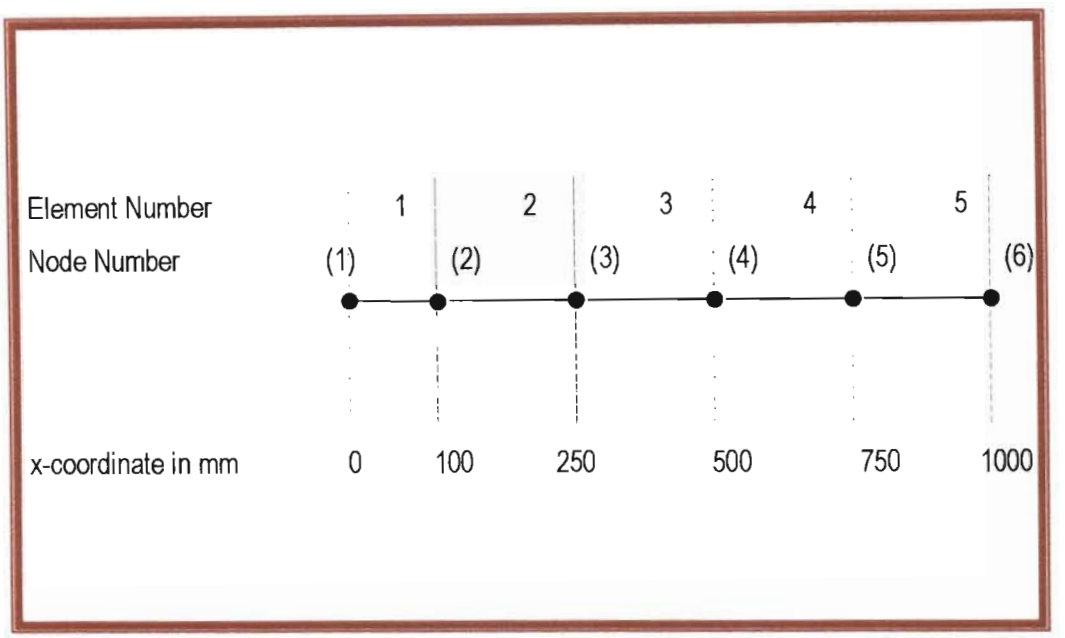

Figure 5.9: Discretization of the beam domain.

5.3.4 Input Data File

The variables into the input data file shown in Figure 5.9 are describe in a typical input data file that represent the calculation of temperature using a Green Element Solution coded in Fortran. Other input data files are found in appendix C. The corresponding output data file in Figure 5.10 prints the required solutions that were specified by the input file.

1-D. Diffusion-advection problem	
0	Key1, Key2
0.004303	DIFF
0.0	VELX
0.0	DECAY
1	Inat
1 1 0	nsub, time, icond
1 1 60	nwrite, tdiv, tlevel
3	TIME SCHEME
1.25	THETA
3	NSEG
0.0 0	X(1), NSP(1)
0.1 0	X(IEND), NSP(M)
0.25 2	X(1), NSP(1)
1.0 0	X(IEND), NSP(M)
0	NFINIT
26.0609	POT
0	NNODES
0	NRECH
0	RECH

Figure 5.10: Sample of the Fortran Input Data File.

The parameters in the input data file are explained as follows

- KEY1, KEY2 are the controls of how the title in the out put data file is arranged.
- DIFF represent the diffusivity D and has a value of 0.004303.
- VELX is the velocity co-efficient and is zero since velocity term of the governing equation is not applicable.
- DECAY represents the term for rate of first order decay, which is also not applicable.
- INAT controls the state of the program, it takes the value 0 for a steady state problem and 1 for the transient case. In this case INAT is 1.
- NSUB is the number of divisions of the time dimension.
- TIME represent the initial time, which is 1 hour in this case.

- NWRITE gives the number of time divisions that will be skipped before the solution is printed.
- TDIV is the length of each time division.
- TLEVEL is the time at which the program should consider the last time coordinate of each time division.
- TIME SCHEME is the value of the time levels, the two and the three time level scheme.
- THETA is the time weighing factor.
- NSEG is the number of segments into which the one dimensional problem domain is divided.
- X(x) is the coordinate at node (x). X(I) it describe the value of the first coordinate and XIEND describe the value of the last coordinate node of the discritized domain.
- NSP describe the number of nodes within the segment.
- NTYPE(I) describe the boundary condition, it assumes the value of 1 if it is the flux type and 2 if is dirichlet type.
- NFINIT tells the program where to read the initial condition value, it assumes 0 for a constant initial value and 1 for various positions of different initial values.
- POT is the value assigned to a constant initial condition.
- NNODES is the number of external nodes which the initial condition value should be specified.

1-D. Diffusion-advection problem

..... NUMBER OF NODES = 6

..... NATURE OF BOUNDARY CONDS. (STEADY=0; UNSTEADY=1) = 0

INITIAL TIME = 1.0000; TIME LIMIT = 60.0000

..... TIME .....= 2.0000

Node No.	Location	Primary Variable	Flux
1	.000	26.7585	-171.3985
2	.100	23.8421	32.7244
3	.250	25.8518	2.4305
4	.500	26.5060	7.3381
5	.750	20.8458	-91.8547
6	1.000	27.5505	372.6140

..... TIME .....= 3.0000

Node No.	Location	Primary Variable	Flux
1	.000	27.3709	6.9683
2	.100	25.5170	-20.2794
3	.250	25.6713	10.6021
4	.500	25.6293	-18.1050
5	.750	22.2755	21.0682
6	1.000	28.6060	-30.4470

Figure 5.11: Sample of the Fortran Output File.

5.4 Conclusions

Having defined the input parameters, the next step is to run the program and obtain output files containing the temperature values at various positions. The output files are found in appendix B.

Because the temperature reading were taken at different time intervals, the program requires that we have three input data files to account for the time as described in chapter 3. The temperature profiles resulting from the output data files will be presented in the next chapter for discussions.

The program is a very powerful tool because of one of its advantages to mention a few, to print required solutions at specific time limit and frequency. It also user friendly as one can vary parameter or part of the main program for greater depth of analysis of the problem being solved. The output data file can easily be converted into a spreadsheet for graph plotting and into word processors to allow easy report writing or whatever the requirement may be.

CHAPTER 6 – DISCUSSION OF RESULTS

6.1 Introduction

This chapter deals with the comparison of the measured and predicted (calculated) temperature profiles. The results are discussed and comments will be made based on the observations.

6.2 Comparison of Experimental and Numerical Results

The calculated temperature profile data obtained from the Fortran output file was converted into a spreadsheet data. The temperature versus time curves for various distances along the concrete beam and the temperature versus distance for particular times are plotted using the spreadsheet.

The measured temperature profiles obtained from the data logger were converted into a spreadsheet. The next sections provide the comparison of the two profiles.

6.2.1 Temperature-Time Profiles

The results for the predicted temperature profiles and the measured temperature profiles are presented at all six positions are presented below with the discussions.

- **Distance x=0mm(boundary condition)**

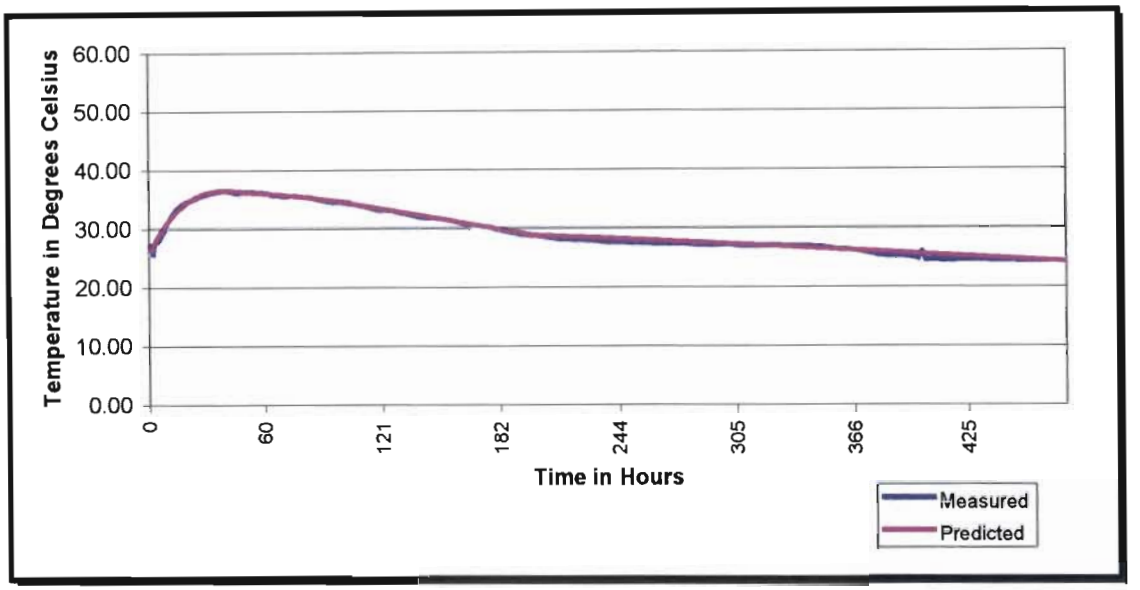

Figure 6.1: Comparison of measured and predicted temperature profiles at distance x=0mm.

The predicted curve at this distance compares very well with the measured temperature curve as was expected of a position where the boundary condition have been imposed. This clearly indicates that the approximation of the analytical expression for the boundary condition curve and the numerical analysis were successful.

An important aspect to note is that peak temperature at this boundary condition position is reached when temperature is approximately equal to 36.274°C at time of 43hours. Both temperature curves show a steep gradient at early ages and this is associated with the heat of hydration effects. The time and the value of the peak temperature will later be compared with the temperature peaks at other positions.

After the peak, both curves show a gradual decrease in temperature values and this occurs as a result of two things, the decrease in the rate of heat of hydration curve and the fact that since this position is at the exposed surface, some of the concrete heat is lost to the environment.

- **Distance x=100mm**

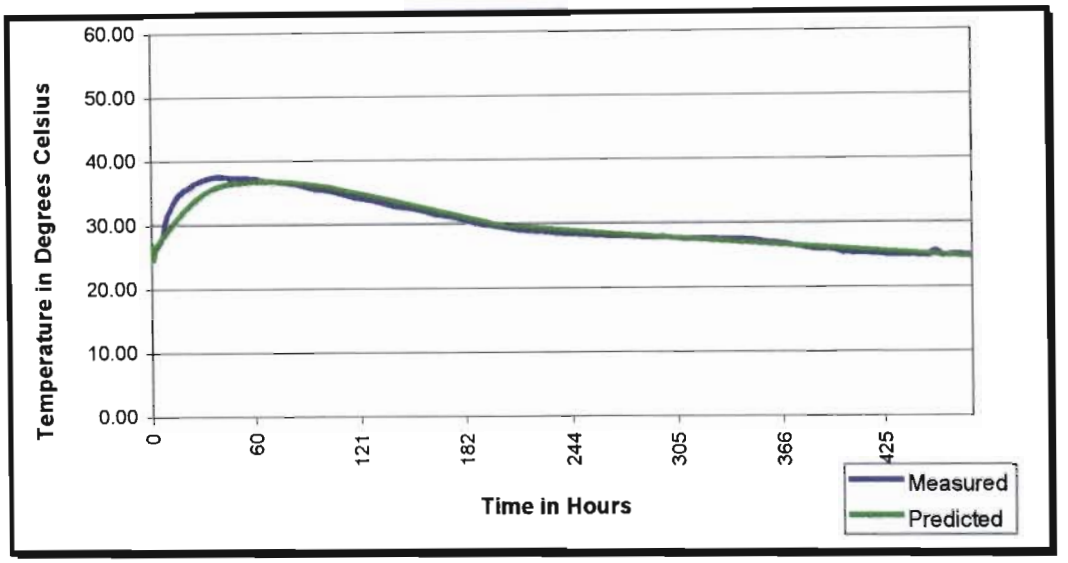

Figure 6.2: Comparison of measured and predicted temperature profiles at distance x=100mm.

The two curves compare well except that the predicted temperature curve is lower than the measured temperature curve between 10 and 60 hours. The difference in values between the two curves increases in value from time=10 hours and reaches its maximum at approximately 15 hours. As the time increases, the difference gradually decreases until it reaches 0 at time = 60 hours. The maximum error of the predicted curve values is 9.9331%. This error may be associated with various reasons mainly coming from the input parameters.

The one parameter that may be the cause of the error is the initial temperature. It must be recalled that, during the laboratory testing, the measurement for temperature was taken almost 2 hours after concrete mixing. This indicates that the initial temperature value should have been taken immediately after the concrete was mixed.

The value used in this analysis was obtained by taking the average of the first temperature reading at all positions, this may not have been the correct value. The correct value could have been higher than the value used as a result of the heat of hydration generated immediately when water combines with cement, immediately after mixing.

The other input parameter may have been the fact that the assumed value of thermal conductivity does not take account of other effects such as time and type of the cement and moisture content of the concrete. It was based on the aggregate type alone. The thermal conductivity could have been the main source of error as it also influences the thermal diffusivity of concrete.

Another observation to make is that the peak temperature of the measured temperature curve occurs at 38 hours, which is earlier than that of the predicted temperature occurring at 66.667 hours. The peak temperature has a value of 37.34°C that is higher than the value of 36.58 °C, for the predicted temperature curve.

- **Distance x=250mm**

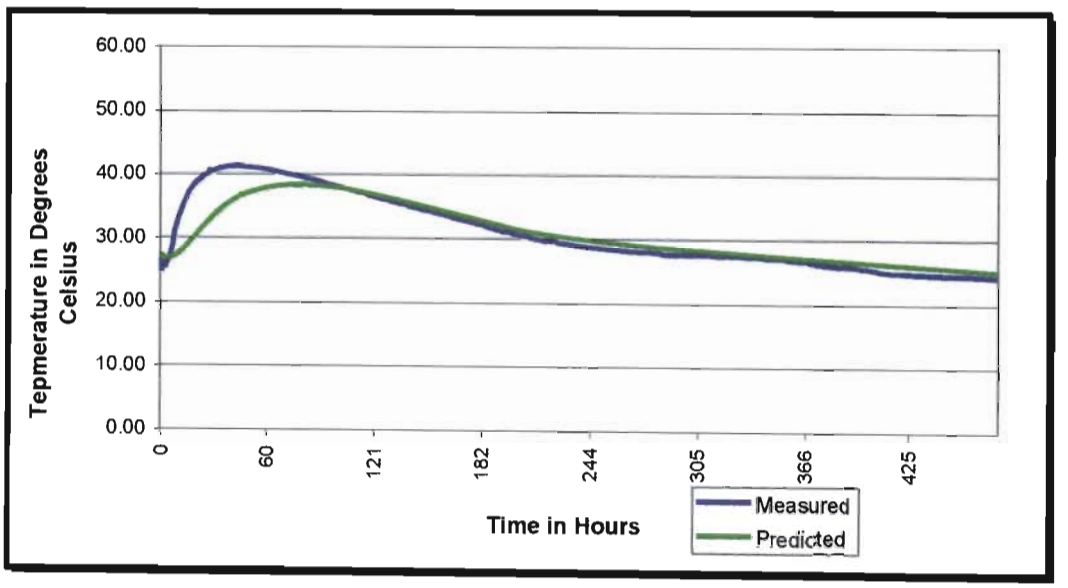

Figure 6.3: Comparison of measured and predicted temperature profiles at distance x=250mm.

Similar to the previous case, the two curves compare well except that the predicted temperature curve is lower than the measured temperature curve between 5 and 90 hours. The difference increases from time equals 5 hours and reaches its maximum at approximately 15 hours before it gradually decreases to 0°C at the time of 60 hours. The maximum error computed is 21.5105%. This error may be associated with various reasons mainly coming form the input parameters as described in the previous case.

The maximum error experienced at this position is greater than the error experienced before at 0mm. Also the length of the time at which the difference between the predicted and the measured temperature curves has increased from10-60 hours at position 100mm to 5-90 hours at position 250mm. This is associated with the thermal conductivity error.

The explanation to these observations is that the effects of thermal conductivity exhibit a vital role as we move away from the boundary conditions positions, hence the increase in error as well as the length of time at which the difference is experienced.

The peak temperature of the measured temperature curve occurs at 42 hours, which is earlier than that of the predicted temperature occurring at 78.667hours. The peak temperature of the measured temperature curve has a value of 37.34°C that is higher than the value of 36.58 °C for the predicted temperature curve.

- **Distance x=500mm.**

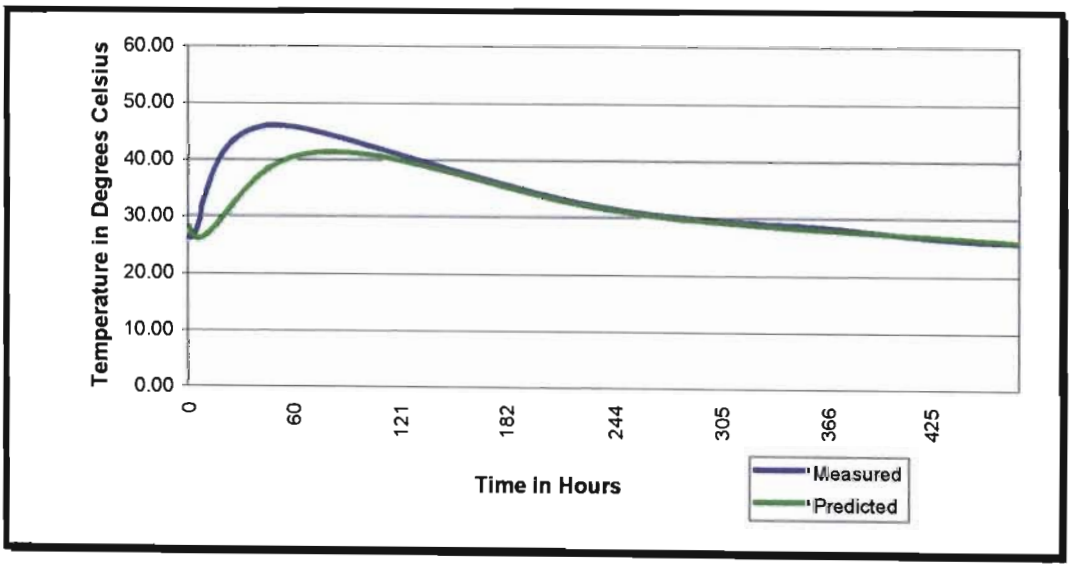

Figure 6.4: Comparison of measured and predicted temperature profiles at distance x=500mm.

Similarly to the previous cases, the two curves compare well except for the fact that predicted temperature curve is lower than the measured temperature curve between 5 and 132.6667 hours. The difference increases from at time of 5 hours and reaches its maximum at approximately 19 hours before it gradually decreases to almost nothing at the time of 132.6667 hours. The maximum error computed is 27.7377%.

A maximum error experienced at this position is greater than the error experienced in the latter cases. Also the length of the time at which the difference between the predicted and the measured temperature curves observed is between 5 and 132.667 hours at this position. The explanation to these observations is similar to the previous case.

The peak temperature of the measured temperature curve occurs at 50.6667 hours, which is earlier than that of the predicted temperature occurring at 84.667hours. The peak temperature of the measured temperature curve has a value of 45.9081°C that is higher than the value of 41.2431°C for the predicted temperature curve.

- **Distance x=750mm**

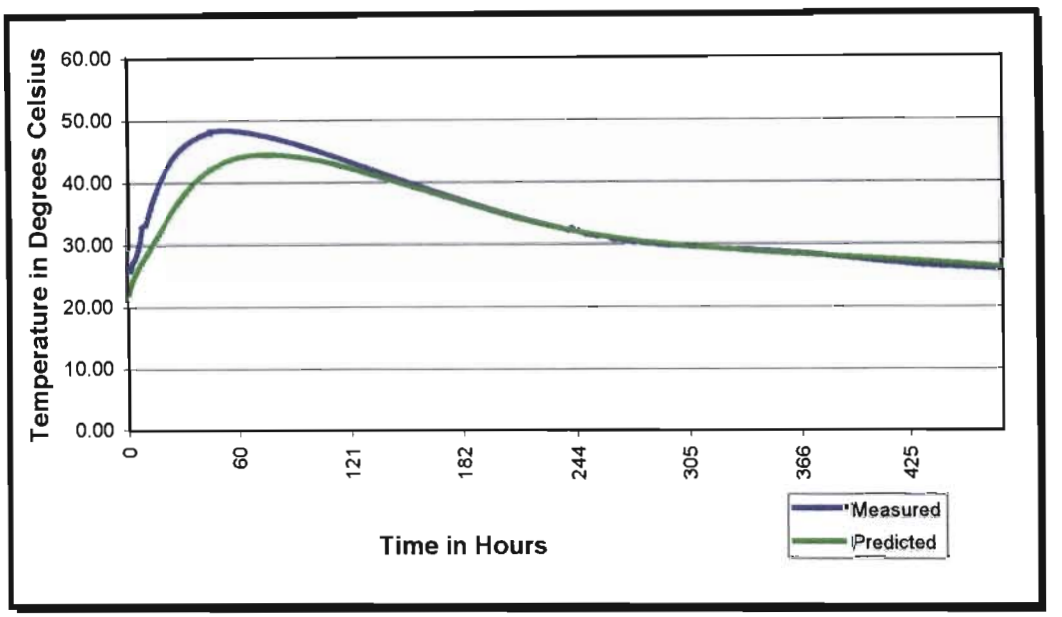

Figure 6.5: Comparison of measured and predicted temperature profiles at distance x=750mm

The two curves compare well except that the predicted temperature curve is lower than the measured temperature curve between 0 and 154.6667 hours. The difference increases from a time of 0 hours and reaches its maximum at approximately 154.6667 hours before it gradually decreases to almost nothing at the time of 154.6667 hours. The maximum error computed is 19.8466%. It is observed that the maximum error is less than the error observed at distances 250 and 500mm. This confirms the expectations that the maximum error should be experienced at distance 500mm, which is the position that is furthest from the boundary conditions.

The peak temperature of the measured temperature curve occurs at 54.6667 hours, which is earlier than that of the predicted temperature occurring at 76.667hours. The peak temperature of the measured has a value of 48.149°C that is higher than the value of 44.3114°C for the predicted temperature curve.

- **Distance x=1000mm(boundary condition)**

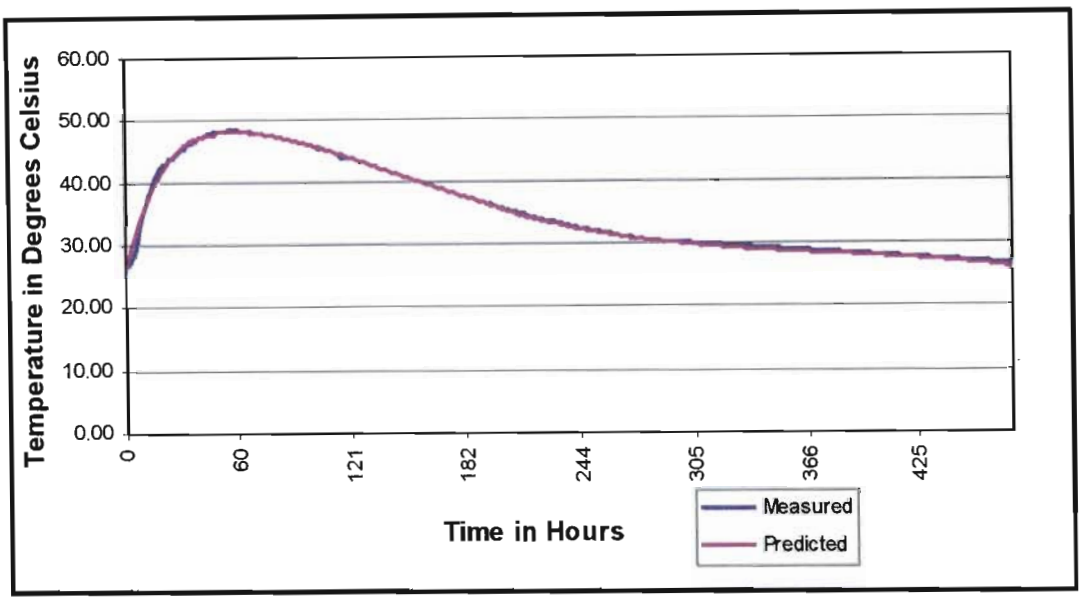

Figure 6.6: Comparison of measured and predicted temperature profiles at distance x=1000mm.

The predicted curve at this distance compares very well with the measure temperature curve as expected to be the case for the position where the boundary condition are imposed.

An important aspect to note is that peak temperature at this boundary condition position is reached when temperature is approximately equal to 47.9817°C at time of 55 hours which is higher and later than the peak observed at the other position were the boundary condition have been imposed (at distance x=0mm). This is associated with the fact that this position is at insulated surface hence the rate and amount of heat loss is lesser than the exposed surface. This will be confirmed by the comparison of temperature versus distance profiles for various times.

6.2.2 Temperature-Distance Profiles

The comparison of temperature versus distance profiles for various times is undertaken mainly to confirm the expectation that the rate of heat loss increases as we move away from the insulated surface towards the exposed surface. Three different times, namely at 15, 138.667 and 285 hours have been chosen arbitrarily.

- **At time = 15 hours**

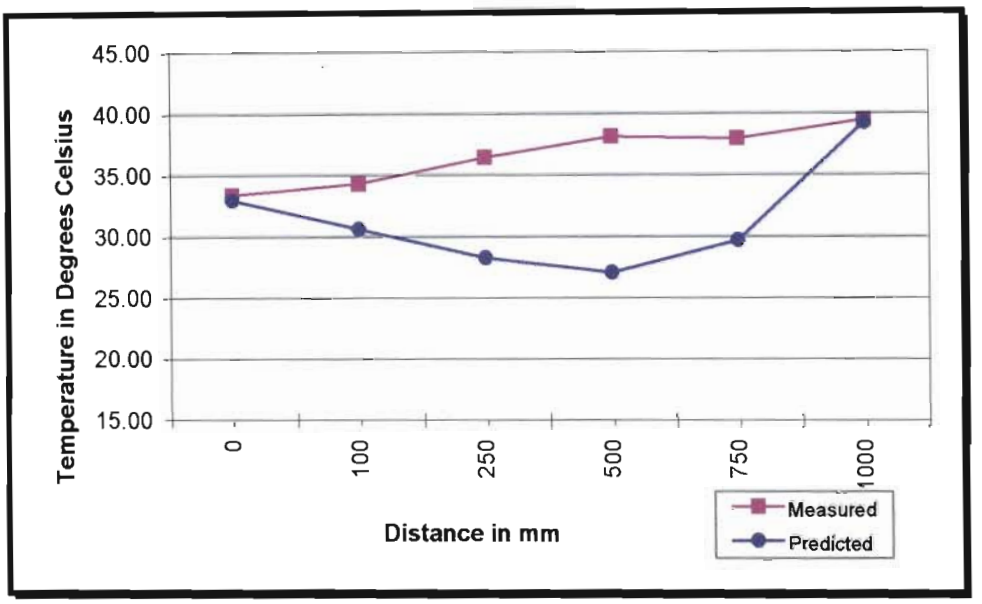

Figure 6.7: Comparison of measured and predicted temperature profiles at time=15 hours.

Because of the error occurring at early ages of concrete, the results presented for this time period do not meet the expectations. The predicted temperature curve indicates that that the rate of heat loss is defined by a parabolic function. This is not in agreement with the measured temperature curve that is defined by a linear function that indicates a decrease in temperature as we approach the exposed surface position. The results from the predicted temperature curve couldn't be used to confirm what is expected.

❖ **At time = 138.6667 hours**

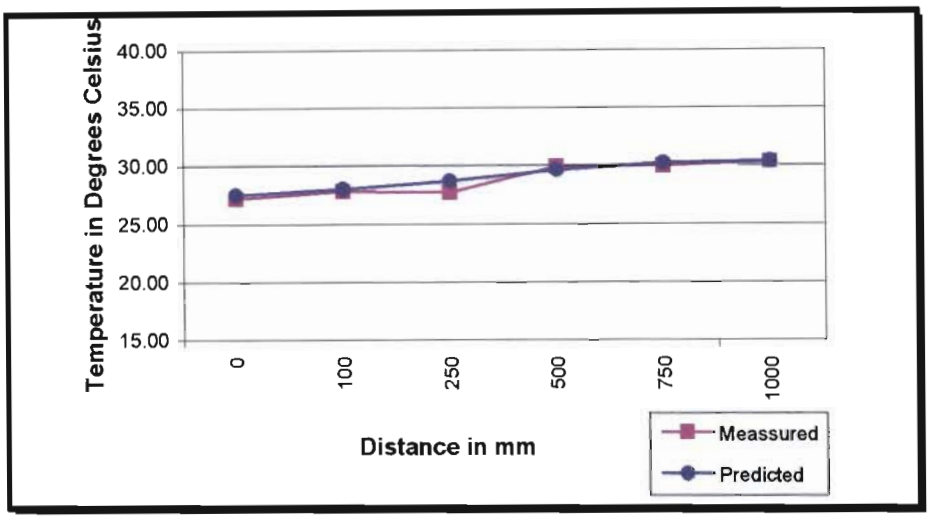

Figure 6.7: Comparison of measured and predicted temperature profiles at time=138.667hours.

The results observed above show a good agreement between the predicted and the measured temperature curves. The shape of the curves indicated that a temperature decrease is experienced as we move towards exposed surface, at 0mm. As indicated earlier, this is associated with the expected results indicating that the rate at which heat is lost to the atmosphere is greater at the exposed surface than the insulated surface.

❖ **At time = 285hours**

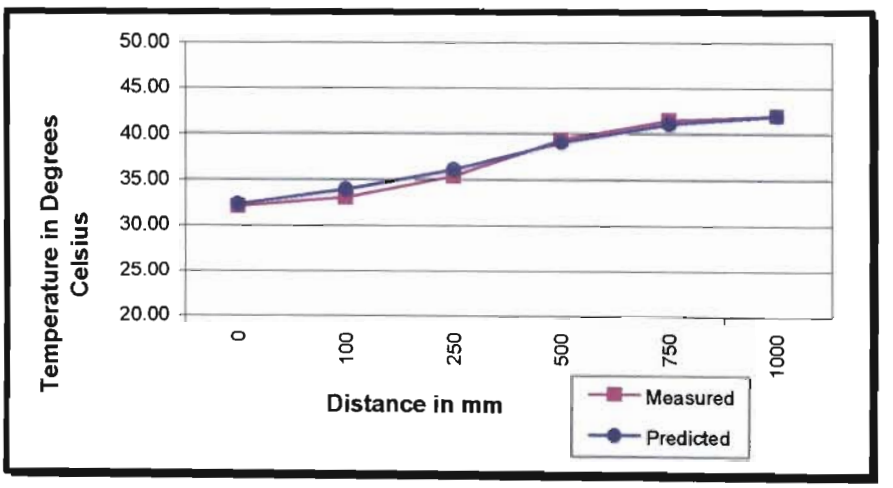

Figure 6.9: Comparison of measured and predicted temperature profiles at time=285 hours.

The observations at this time are similar to those indicated at the previous time.

6.3 General Comments

The comparison between the measured and the predicted temperature profiles for both the temperature versus time and temperature versus distance curves have been discussed. At distances where the boundary conditions have been imposed the predicted and measured temperature curves agree very well. Similar agreements are observed at the other positions at greater times. The great concern is the error that is experienced at distances positions 100, 250, 500 and 750 mm for smaller times. Further analysis have been carried out to determine whether cause of the errors is not linked to the Green element method or the choice of the heat of hydration curve, which is the Heat rate versus Nurse-Saul equivalence hours.

Three analysis were carried out. The first involved selection of the Heat rate versus normal time curve as an input describing the heat of hydration. The results obtained showed that the error increased by 1.2% for times less than approximately 60 hours, at times greater than 60 hours the results were unchanged. The Heat rate versus Arrhenius equivalence hours was selected for the second analysis and the results showed a negligible increase in error as compared to the results from the Heat rate versus Nurse-Saul equivalence hours input. These comparisons are given in figure 6.10 below for position, x= 750mm.

The third analysis involved using the green element method approach of improving the results obtained from the Heat rate versus Nurse-Saul equivalence hours input. This approach is known as degridding. The degridding approach was achieved by increasing the number of nodes at distances where the errors are experienced.

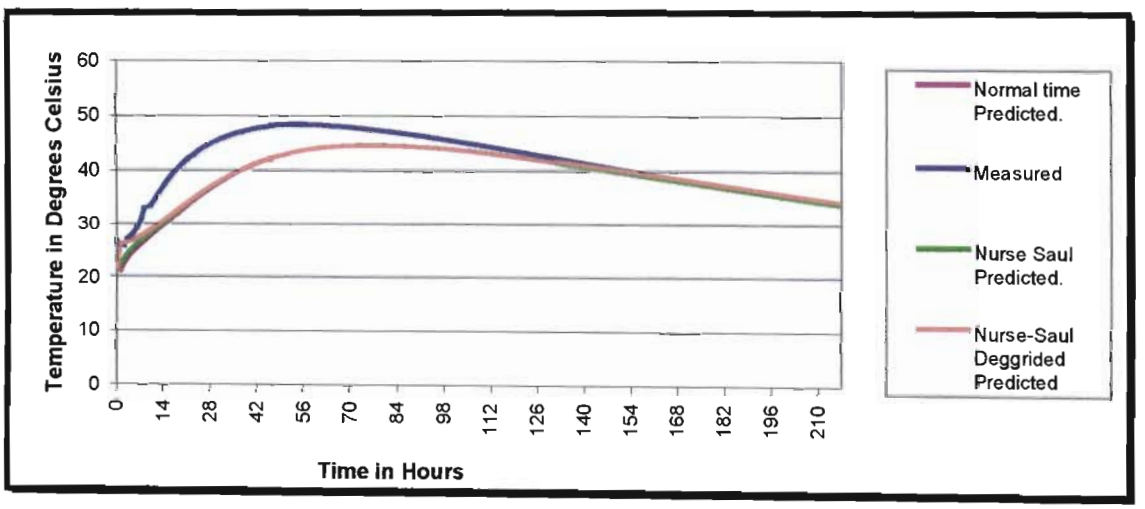

Figure 6.10: Comparison of measured and predicted temperature profiles at x=750mm using various heat rate curves.

The results showed a decrease in error of 2% only for times less than approximately 184.667 hours. Similarly, for times greater than 184.667 hours the results were unchanged. The curves for other position are found in appendix B.

The results confirm that the error may be associated mainly with the thermal conductivity and the value of the initial temperature as discussed earlier.

CHAPTER 7 – CONCLUSION

The study on heat transfer and numerical prediction of temperature development in hardening concrete gives a indication that it is possible to predict with reasonable accuracy the temperature development in hardening concrete in the field. The work presented in this thesis can be of great use for estimation of temperature gradients caused by the hydration heat in developing concrete, which consequently results into crack formation. The avoidance of such cracks is developed mainly for concrete structures such as, large concrete dams, massive hydraulic structures, concrete walls subjected to fires and concrete nuclear power station.

High accuracy performance is required for temperature predictions in hardening concrete and can only be achieved by both non-complicated and reliable test for determining hydration heat and numerical technique. It is more significant when the numerical model and hydration curve determination methods are used as a basis for numerical analysis of thermal cracking and for fire safety assessments in nuclear reactors and tall buildings. The adiabatic calorimeter used in this research demonstrates the ability to measure heat of hydration of a concrete with respect to time. In addition, it was manufactured from equipment that is of a low cost and easy to assemble. G.Y. Gibbon and Y Ballim[8] describe improvements made to the adiabatic calorimeter to enable the determination heat of hydration and thermal conductivity with respect to time.

The Green element method has the ability to solve most engineering problems that are more practically based and complex in nature without being combined with another numerical method. These engineering problems exhibit properties such as, non-linearity, transient nature and heterogeneity. Transformation of a Green element method solution procedure into computer based Fortran program, doubles the advantages that the method usually posses when the solution is obtained by hand.

Combination of the adiabatic calorimeter and the computerized Green element method has been used in this thesis to predict the measured temperature profiles with acceptable practical accuracy. According to Wang and Dingler[9], 20 – 30% of error is considered excellent accuracy in practical problems. The main source or error is from the input data variable.

It can thus be concluded that high levels of accuracy that is required for prediction of temperature distribution can be achieved by using a combination of the adiabatic calorimeter and the computerized Green element method incorporating carefully selected input data. Apart from fire safety assessments and nuclear power station temperature predictions and crack prevention, the results may also be used to help in construction planning. This refers to the design of curing measures that are required to prevent concrete from freezing in cold weather, or to achieve the desired strength at an early age and to maintain the specified temperature differential limits in a structure.

CHAPTER 8 – RECOMMENDATIONS

The main source of error encountered in prediction of measured temperature distribution is undoubtedly the input data variables. Some of these variables have been mentioned in chapter 6. Many key parameters, such as the thermal conductivities of concrete and formwork/insulation materials, specific heat capacity, convection heat transfer coefficient, ambient air temperature, initial temperature etc, vary in wide ranges.

Most researchers have brought the attention that thermal conductivity of concrete depends on numerous variables such as moisture content, aggregate type and content, porosity, density, temperature and time. To date, limited work has been done in developing an expression that relates the thermal conductivity with all these parameters.

It must be appreciated that the thermal conductivity is one of the main input variables that are incorporated during the element by element analysis performed by most numerical technique, if not all. So an incorrect thermal conductivity can result in large errors in the output. To ensure that a reasonable thermal conductivity is used, the researcher is required to research on the thermal conductivity that take into consideration, the variables that have a greater effect on it, namely, the moisture content, type and content of aggregate and temperature.

Also it is very important to note that special attention should be paid in the selection of the initial temperature. Heat is generated immediately when water reacts with cement, the temperature of the mix will also vary, hence it will be incorrect to wait until the beam or any sample is cast before the initial temperature is recorded. The initial temperature should be measured as soon as the mixing of the concrete constituents has been completed.

Limited research has shown that the specific heat capacity is dependent on degree of hydration. It then becomes essential to incorporate such effect when selecting of the specific heat capacity is done.

It is recommended that for future temperature prediction using the Green Element Method and Adiabatic Calorimeter or any other appropriate methods, the effects on the input variables mention above should be taken into consideration.

It is recommended that future research should consider case of a two and three-dimensional heat flow problem incorporating the effects of time on thermal conductivity of concrete using the Green Element Method and Adiabatic Calorimeter. The three-dimensional heat research describes a more realistic situation and will bear a great impact in the field of heat transfer.

CHPTER 9-REFERENCES

1) Huang C.L.D, Gamal N.A and. Fenton D.L. Responses of concrete walls to fire. Int. Journal oh Heat and Mass Transfer. Vol. 34, No. 3. 1991. pg. 649-661.

2) van Breugel, K. Prediction of temperature development in hardened concrete. Prevention of Thermal cracking in concrete at early ages. Springenchmid, R (Ed.). RILEM report No. 15. E&FN Spon, London. 1998. pg .51-75.

3) Harrison, T.A. Early-age thermal crack control in concrete. Const. Ind. Res. Info. Assoc. Report No. 91.

4) Morabito, P, Methods to determine the heat of hydration in concrete. Prevention of Thermal cracking in concrete at early ages. Springenchmid, R (Ed.). RILEM report No. 15. E&FN Spon, London. 1998. pp.1-25.

5) Koenders, EAB and van Breugel, K. Numerical and experimental adiabatic hydration curve determination. Proc.of Int. RILEM Symposium, Thermal crack in concrete at early ages. Springenchmid,R (Ed.), Munich,1994. E&FN Spon, London, pg. 3-10.

6) Fultrons' Concrete Technology.

7) Morabito, P and Barberis, F. Measurement of adiabatic temperature rise in concrete. Pro.of Int. Conf: Concerete 2000-Economic and Durable Construction through Excellence. Dhir,RK and Jones, MR (Eds.), Dundee, Scotland, Sept.1993. pp. 749-759.

8) Gibbon, G.J, Ballim, Y and Grieve, G.R.H . A low-cost, computer controlled adiabatic calorimeter for determining the heat of hydration in concrete. ASTM Journal of Testing and Evaluation, Vol. 25, No. 2, March1997, pp 261-266.

9) Wang, Ch, Dingler, WH. Prediction of temperature distribution in hardening concrete. Pro.of Int. RILEM Symposium, Thermal crack in concrete at early ages. Springenchmid,R (Ed.), Munich,1994. E&FN Spon, London,pp. 21-28.

10) Carnpbell-Allen, D and Thorne, CP. Thermal conductivity of concrete. Mag. of Conc. Res. V 15,No. 43, March 1963

11) Gibbon G.J. "Laboratory test procedure to predict the thermal behavior of concrete". Ph.D. Thesis, University of the Witwatersrand, Johannesburg. 1995.

12) Gibbon, G.J, Ballim, Y. Laboratory test procedures to predict the thermal behaviour of concrete. Journal of SAICE v38, No.3, 1996. pg 21-23.

13) Ballim, Y. Personal Information. Professor at University of the Witwatersrand, Johannesburg

14) Fernando, A.B. Pedro, A and Mirambell. E. Heat of hydration Effects in Concrete Structures. ACI Materials Journal, V89, No. 2, March-April 1992.

15) Nardini, D. and Brebbia, C.A Boundary Integral Formulation of Mass Matrices for Dynamic Analysis, Topics in Boundary Element Research, edited by C.A Brebbia, 2, Springer Verlag, New York, 1985.

16) Wrobel, L. C. and Brebbia, C.A and Nardini, D. The Dual Reciprocity Boundary Element Formulation for Transient Heat Conduction, Pro. VI Int. Conference on Finite Element in Water Resources, pp. 801-812, Springer Verlag, New York, 1986.

17) Brebbia, C. A. and Nardini, D. Dynamic Analysis in Soil Mechanics by an Alternative Boundary Element Procedure, Int. Jnl., Soil Dynam. Earthquake Engr.2 pp. 228-233,1983

18) Dargush, G. F. and Benerjee, P. K. Application of Boundary Element Method to Transient Heat Conduction, Int. Jnl. Num. Nthds, Engr., 31, pp. 1231-1247,1991.

19) Benerjee, P. K. and Butterfield, R. Boundary Element Methods in Geomechanics, G Gudehus (ed.), Finite Element Methods in Geomechanics, London, 1977.

20) Brebbia, C. A., Telles, J. C. F. and Wrobel, L. C. Boundary Element Techniques, Springer Verlag, Berlin, 1984.

21) Azevode, J. P. S. and Wrobel, L. C. Non-Linear Heat Conduction in Composite Bodies: A Boundary Element Formulation, Int. Jnl. Num. Mthds. Engr., 26, pp. 1938,1988.

22) Onyejekwe, O. O. A Green Element Description of Mass Transfer in Reacting Systems, Numerical Heat Transfer, part B30, pp. 483-498, 1996.

23) Onyejekwe, O. O. A green Element Treatment of Isothermal Flow with Second Order Reaction, Int. Communication Heat and Mass Transfer, 97, pp. 251-264, 1997.

24) Onyejekwe, O. O. Effective Numerical Treatment of Non-Linearity: A Green element Approach, Proceed. 2nd South Africa Conference on Applied Mechanics, 13-15 January, University of Cape Town, Rondebosch, South Africa, pp. 729-737, 1998.

25) Onyejekwe, O. O. Green Element Computation of the Sturm-Liouville Equations, Advances in Engineering Software, 28, pp. 615-620, 1997.

26) Onyejekwe, O. O A Finite Element Study of the H-Base Unsaturated Flow Equation, Proceed. FEMSA 95 13th Symposium on Finite Elements in South Africa, 2, pp. 394-406, 1995.

27) Onyejekwe O. O. A Green Element Formulation Applied to Advection-Diffusion-Reaction Problems, Proceed. 1st South Africa Conference on Applied Mechanics (SACAM" 96), 1-5 July, Midrand, South Africa, 1996.

28) Onyejekwe, O. O. A Green Element Application to the Diffusion Equation, 35th Heat Transfer and Fluid Mech. Institute, California State University, Sacramento, California, May pp. 75-90, 1995.

29) Onyejekwe, O. O. A Green Element Implementation of Non-Linear Transport Equation, Proceed. Of the 12th Engineering Mech. Conference, La Jolla, Califonia, 17-20 May, pp. 1645-1648, 1998.

30) Onyejekwe, O. O. Sol\ving the Non-Linear Heat Equation with the Boundary Untegral Method, Proceed. 11th International Heat Transfer Conference, 23-28 August, Kyongju, Korea, 1998.

31) Oyejekwe, O. O. A Boundary Element- Finite Element Equation Solutions to Flow in Heterogenous Media, Transport in Porous Media (Accepted for publication and currently in print), 1998.

32) Onyejekwe, O. O. Boundary Integral Procedures for Unsaturated Flow Problems, Transport porous media, 1998.

33) Onyejekwe, O. O. Unsaturated Flow in Porous media, Proceedings, Computer Methods And Water Resources IV, Computational Mechanics Publication, Byblos, Lebanon, 1997.

34) Taigbenu, A.E. and Onyejekwe, O. O. Transient 1-D Transport Equation Simulated by a Mixed Green Element Formulation, Int. Jnl. Num. Mths. Fluids, 25, pg.437-454.1997.

35) Taigbenu, A.E. and Onyejekwe, O. O. Mixed Green Element Formulation for the Transient Burger's equation. Int. Jnl. Num. Mths. Fluids, 24, pg.563-578.1997.

36) Taigbenu, A.E. and Onyejekwe, O. O. Green Element Simulations of the Transient and Non-Linear Unsaturated Flow Equation. Applied Math Modeling, 19, pg. 675-684.1995.

37) Taigbenu, A.E. and Onyejekwe, O. O. Green's Functions Based Integral Approaches to Non-Linear Boundary Value Problems(II). Applied Math Modeling.1998.

38) Karama, A. B., Onyejekwe, O. O., Bouckaert, C and Buckley, C.J. The use of Computational Fluid Dynamics in Determining the Efficiency of an Activated Sludge Reactor, Proc.4th Int Conf. on Computer Methods in Water Resources, Byblos, Lebanon, 16-18 June, 1997.

39) Onyejekwe, O. O. and Teshome, D.S. A Green Element Solution of the Boussineq Equation, Physics Conf. University of Durban Westville, 1 July, 1997.

40) De Schutter. G, Taerwe. L. Specific heat and thermal diffusivity of hardening concrete. Mag. Conc. Res. Sept. 1995, Vol 47, No 172, pg 203-208.

APPENDICES

Appendix A – Heat of Hydration Curves and Profiles

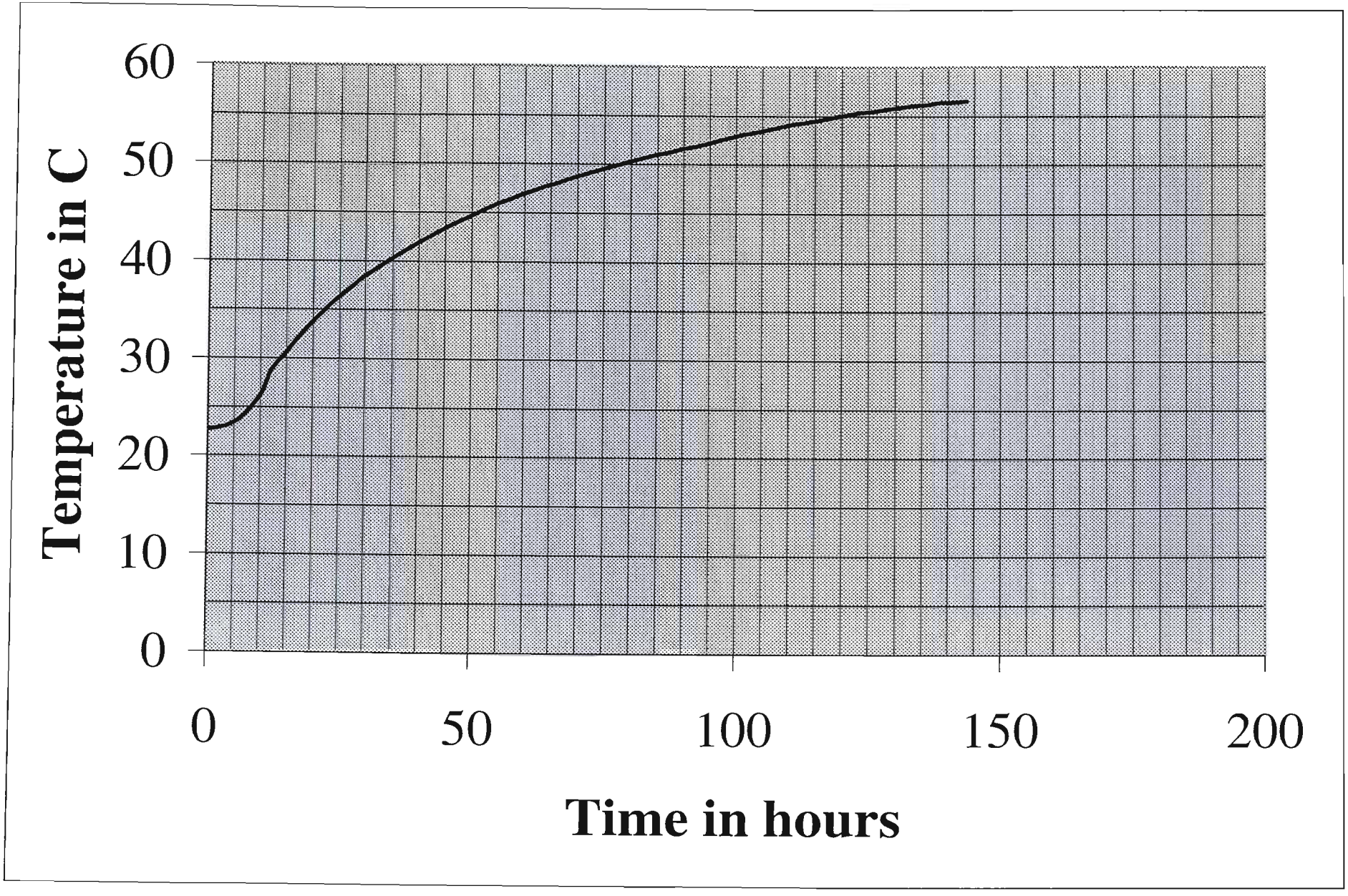
Temperature in C
60
50
40
30
20
10
0
0
50
100
150
200
Time in hours

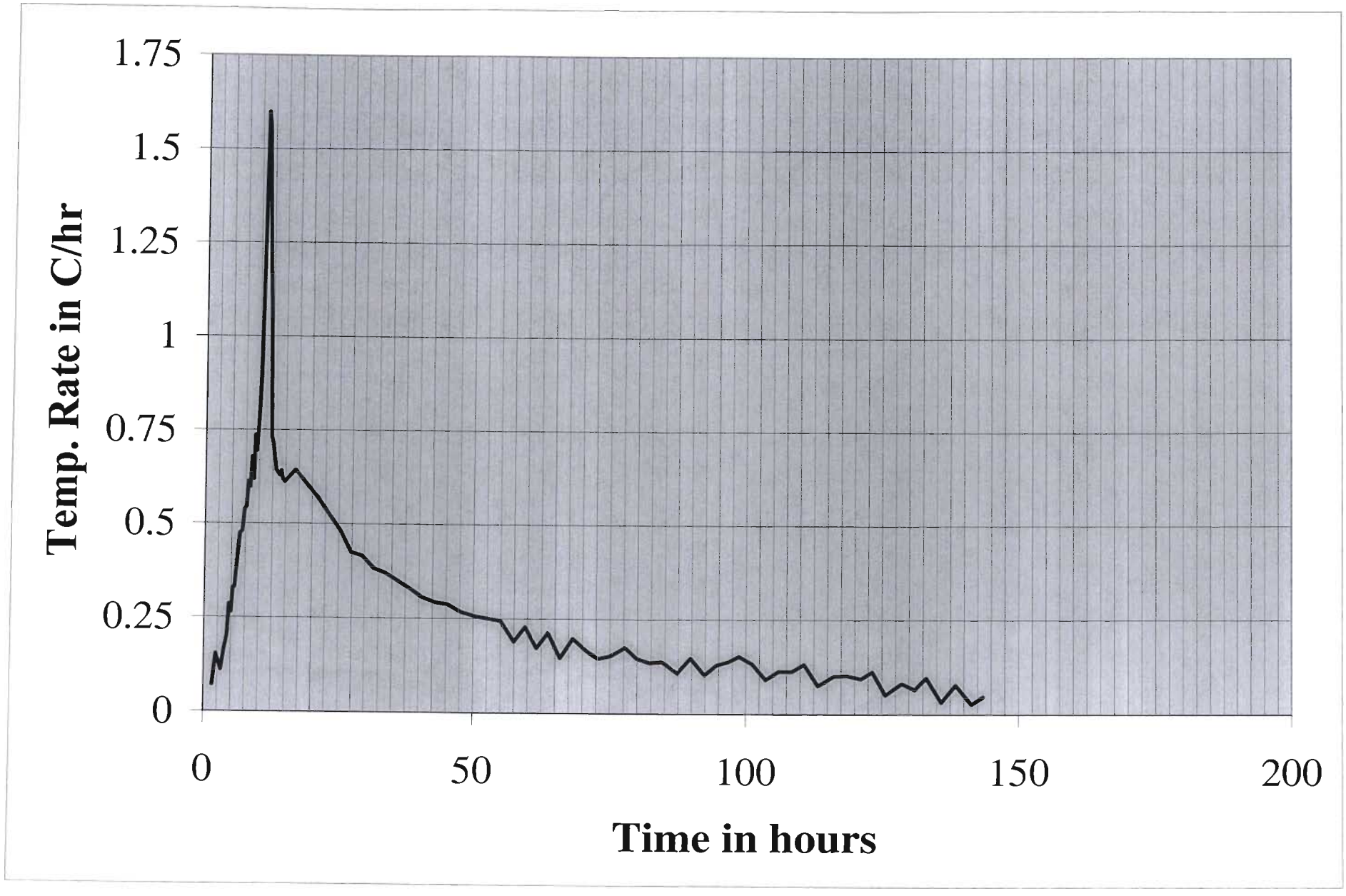
1.75
1.5
1.25
1
0.75
0.5
0.25
0
Temp. Rate in C/hr
0
50
100
150
200
Time in hours

										Smoothed	Corrected
					Sample	S. tank	L. tank	time	dT/dt	dT/dt	T
0	0	0	1	53	22.668	18.919	19.676	0.000277778			22.668
0	1	34	51	43	22.78	22.761	19.729	1.580833333	0.07086116	0.07086116	22.78
0	2	14	50	74	22.882	22.934	19.696	2.247222222	0.15306378	0.15306378	22.882
0	3	9	29	30	22.983	23.105	19.56	3.158055556	0.11088747	0.11088747	22.983
0	3	45	54	23	23.084	23.097	19.717	3.765	0.16640732	0.16640732	23.084
0	4	15	49	64	23.185	23.286	19.763	4.263611111	0.20256267	0.20256267	23.185
0	4	37	3	91	23.286	23.271	19.773	4.6175	0.28540031	0.28540031	23.286
0	5	0	1	61	23.387	23.478	19.871	5.000277778	0.26386067	0.26386067	23.387
0	5	18	26	93	23.488	23.476	19.883	5.307222222	0.32904977	0.32904977	23.488
0	5	36	36	48	23.588	23.648	19.87	5.61	0.33027523	0.33027523	23.588
0	6	5	50	75	23.788	23.828	19.916	6.097222222	0.41049031	0.41049031	23.788
0	6	31	32	7	23.991	23.988	19.854	6.525555556	0.47392996	0.47392996	23.991
0	6	56	40	65	24.192	24.162	19.787	6.944444444	0.47984085	0.47984085	24.192
0	7	19	30	0	24.396	24.509	19.748	7.325	0.53605839	0.53605839	24.396
0	7	41	51	66	24.599	24.67	19.719	7.6975	0.54496644	0.54496644	24.599
0	8	1	38	66	24.801	24.846	19.689	8.027222222	0.6126369	0.6126369	24.801
0	8	21	43	83	25.001	25.032	19.635	8.361944444	0.59751037	0.59751037	25.001
0	8	39	30	32	25.202	25.198	19.659	8.658333333	0.67816307	0.67816307	25.202
0	8	59	5	78	25.404	25.358	19.578	8.984722222	0.61889362	0.61889362	25.404
0	9	15	28	51	25.605	25.715	19.571	9.257777778	0.73611394	0.73611394	25.605
0	9	32	56	54	25.807	25.879	19.517	9.548888889	0.69389313	0.69389313	25.807
0	9	55	54	51	26.109	26.221	19.509	9.931666667	0.78896952	0.78896952	26.109
0	10	16	26	93	26.415	26.388	19.436	10.27388889	0.89415584	0.89415584	26.415
0	10	33	45	46	26.724	26.689	19.385	10.5625	1.07064485	1.07064485	26.724
0	10	51	54	25	27.126	27.226	19.346	10.865	1.32892562	1.32892562	27.126
0	11	10	45	0	27.628	27.619	19.339	11.17916667	1.59787798	1.59787798	27.628
0	11	26	12	31	28.03	27.97	19.275	11.43666667	1.56116505	1.56116505	28.03
0	11	45	11	90	28.432	28.521	19.271	11.75305556	1.27058824	1.27058824	28.432
0	12	2	50	37	28.744	28.822	19.219	12.04722222	1.06062323	1.06062323	28.744
0	12	19	16	83	28.944	28.942	19.186	12.32111111	0.73022312	0.73022312	28.944
0	12	36	4	28	29.144	29.255	19.138	12.60111111	0.71428571	0.71428571	29.144
0	12	53	55	5	29.345	29.357	19.083	12.89861111	0.67563025	0.67563025	29.345
0	13	12	40	31	29.546	29.621	19.068	13.21111111	0.6432	0.6432	29.546
0	13	31	38	4	29.747	29.723	19.065	13.52722222	0.63585237	0.63585237	29.747
0	13	50	43	95	29.947	30.019	18.997	13.84527778	0.62882096	0.62882096	29.947
0	14	9	43	76	30.15	30.099	18.981	14.16194444	0.64105263	0.64105263	30.15
0	14	29	7	47	30.35	30.368	18.917	14.48527778	0.6185567	0.6185567	30.35
0	14	50	7	79	30.564	30.651	18.872	14.83527778	0.61142857	0.61142857	30.564
0	16	52	12	43	31.872	31.967	18.686	16.87	0.64283959	0.64283959	31.872
0	18	55	59	24	33.125	33.209	18.503	18.93305556	0.60735156	0.60735156	33.125
0	21	6	22	11	34.364	34.465	18.803	21.10611111	0.5701649	0.5701649	34.364
0	23	12	54	41	35.471	35.395	19.042	23.215	0.52492097	0.52492097	35.471
1	1	24	14	68	36.522	36.624	19.467	25.40388889	0.48015228	0.48015228	36.522
1	3	24	27	5	37.371	37.402	19.843	27.4075	0.42373492	0.42373492	37.371
1	5	35	26	51	38.277	38.283	20.031	29.59055556	0.41501463	0.41501463	38.277
1	7	45	10	5	39.102	39.171	19.953	31.75277778	0.3815519	0.3815519	39.102
1	9	47	30	96	39.856	39.945	19.844	33.79166667	0.36980926	0.36980926	39.856
1	11	49	0	39	40.568	40.617	19.776	35.81666667	0.35160494	0.35160494	40.568
1	14	2	55	6	41.309	41.335	19.73	38.04861111	0.33199751	0.33199751	41.309
1	16	31	29	14	42.068	42.16	19.477	40.52472222	0.30652906	0.30652906	42.068
1	19	1	53	56	42.802	42.777	19.383	43.03138889	0.29281915	0.29281915	42.802
1	21	15	9	56	43.442	43.401	19.868	45.2525	0.28814407	0.28814407	43.442
1	23	44	31	42	44.108	44.07	20.18	47.74194444	0.26752957	0.26752957	44.108
2	2	18	50	76	44.767	44.874	20.612	50.31388889	0.25622637	0.25622637	44.767
2	4	51	53	70	45.405	45.426	20.928	52.86472222	0.25011434	0.25011434	45.405
2	7	1	1	38	45.931	45.844	20.909	55.01694444	0.24439855	0.24439855	45.931
2	9	27	36	71	46.394	46.379	20.555	57.46	0.18951677	0.18951677	46.394
2	11	31	58	34	46.868	46.867	20.556	59.53277778	0.22867864	0.22867864	46.868
2	13	37	2	98	47.228	47.251	20.446	61.61722222	0.17270789	0.17270789	47.228
2	15	44	5	26	47.679	47.603	20.335	63.73472222	0.21298701	0.21298701	47.679
2	17	55	23	6	48	48.047	20.221	65.92305556	0.14668698	0.14668698	48
2	20	14	31	29	48.46	48.376	20.494	68.24194444	0.19837087	0.19837087	48.46
2	22	53	44	16	48.896	48.95	20.758	70.89555556	0.16430441	0.16430441	48.896
3	0	57	53	59	49.198	49.155	21.183	72.96472222	0.14595248	0.14595248	49.198
3	3	7	16	82	49.527	49.625	21.648	75.12111111	0.15256988	0.15256988	49.527
3	5	46	19	63	49.991	49.901	21.771	77.77194444	0.1750393	0.1750393	49.991
3	7	53	19	39	50.301	50.231	21.741	79.88861111	0.14645669	0.14645669	50.301
3	10	11	32	20	50.612	50.593	21.558	82.19222222	0.13500543	0.13500543	50.612

3	12	32	58	96	50.936	50.948	21.453	84.54944444	0.13744992	0.13744992	50.936
3	15	18	19	38	51.232	51.314	21.254	87.30527778	0.10740853	0.10740853	51.232
3	17	46	29	73	51.596	51.5	20.996	89.77472222	0.14740157	0.14740157	51.596
3	20	20	58	8	51.861	51.84	21.18	92.34944444	0.10292372	0.10292372	51.861
3	22	33	17	67	52.146	52.273	21.439	94.55472222	0.12923542	0.12923542	52.146
4	0	37	13	49	52.43	52.52	21.684	96.62027778	0.13749328	0.13749328	52.43
4	2	44	22	80	52.753	52.672	21.859	98.73944444	0.1524184	0.1524184	52.753
4	5	10	55	60	53.077	53.03	22.02	101.1819444	0.13265097	0.13265097	53.077
4	7	40	39	22	53.304	53.253	21.316	103.6775	0.09096171	0.09096171	53.304
4	10	5	27	83	53.578	53.645	21.153	106.0908333	0.11353591	0.11353591	53.578
4	12	25	48	40	53.842	53.88	21.037	108.43	0.11286071	0.11286071	53.842
4	14	43	25	35	54.144	54.101	20.73	110.7236111	0.1316701	0.1316701	54.144
4	17	14	50	30	54.334	54.33	20.427	113.2472222	0.07528894	0.07528894	54.334
4	20	11	54	76	54.632	54.697	20.811	116.1983333	0.10097892	0.10097892	54.632
4	22	36	4	97	54.877	54.942	21.122	118.6011111	0.10196532	0.10196532	54.877
5	1	10	43	26	55.119	55.067	21.681	121.1786111	0.09388943	0.09388943	55.119
5	3	14	35	56	55.351	55.386	21.773	123.2430556	0.1123789	0.1123789	55.351
5	5	39	18	13	55.474	55.484	21.255	125.655	0.0509962	0.0509962	55.474
5	8	37	54	81	55.717	55.685	21.043	128.6316667	0.08163494	0.08163494	55.717
5	11	0	17	86	55.873	55.818	20.805	131.0047222	0.06573803	0.06573803	55.873
5	13	6	11	99	56.076	55.98	20.487	133.1030556	0.09674345	0.09674345	56.076
5	15	51	25	65	56.164	56.194	20.102	135.8569444	0.03195481	0.03195481	56.164
5	18	28	51	35	56.368	56.304	19.814	138.4808333	0.07774719	0.07774719	56.368
5	21	22	20	94	56.448	56.431	20.347	141.3722222	0.02766836	0.02766836	56.448
5	23	28	15	78	56.546	56.645	20.532	143.4708333	0.04669755	0.04669755	56.546

CEMII V-B

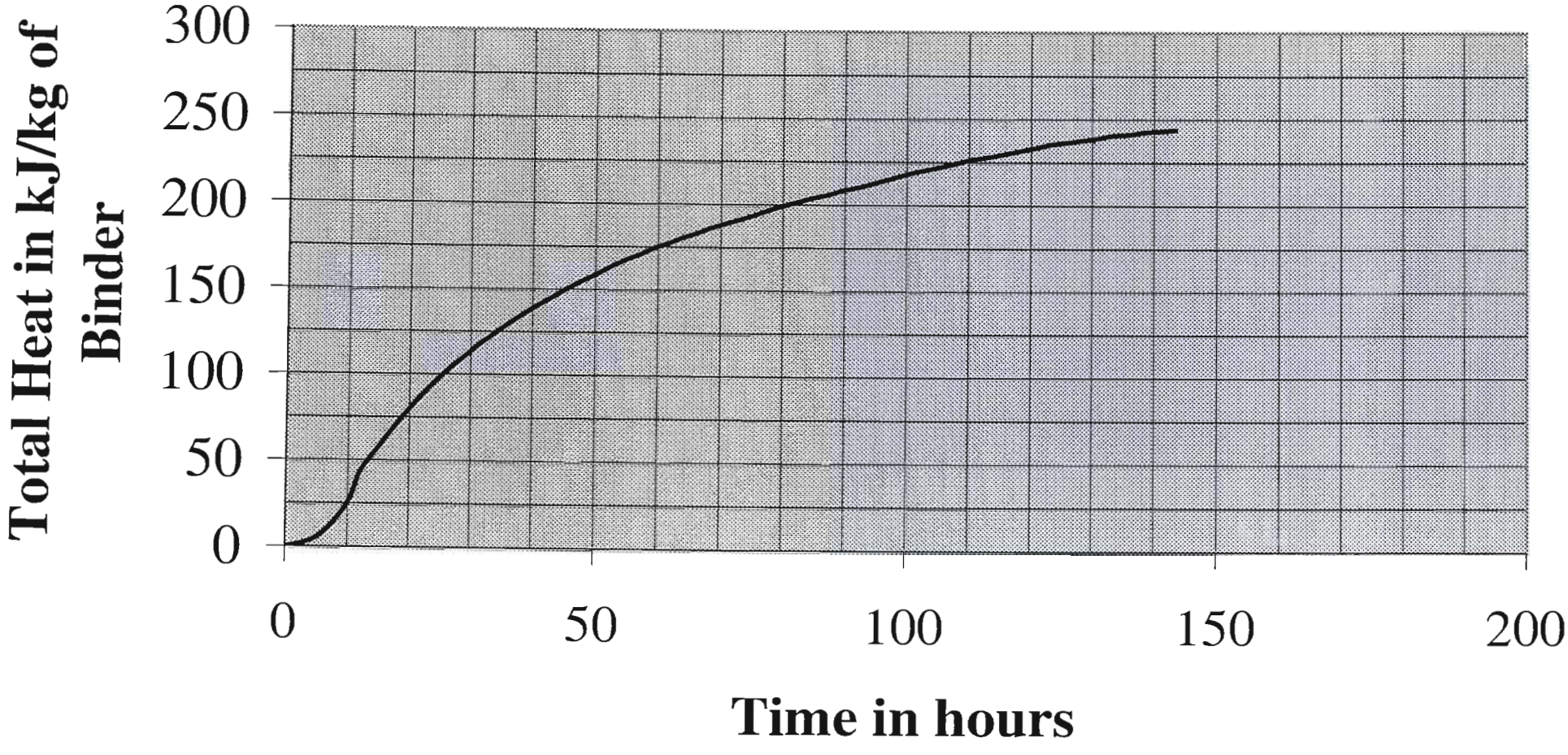
Total Heat in kJ/kg of Binder
300
250
200
150
100
50
0
0
50
100
150
200
Time in hours

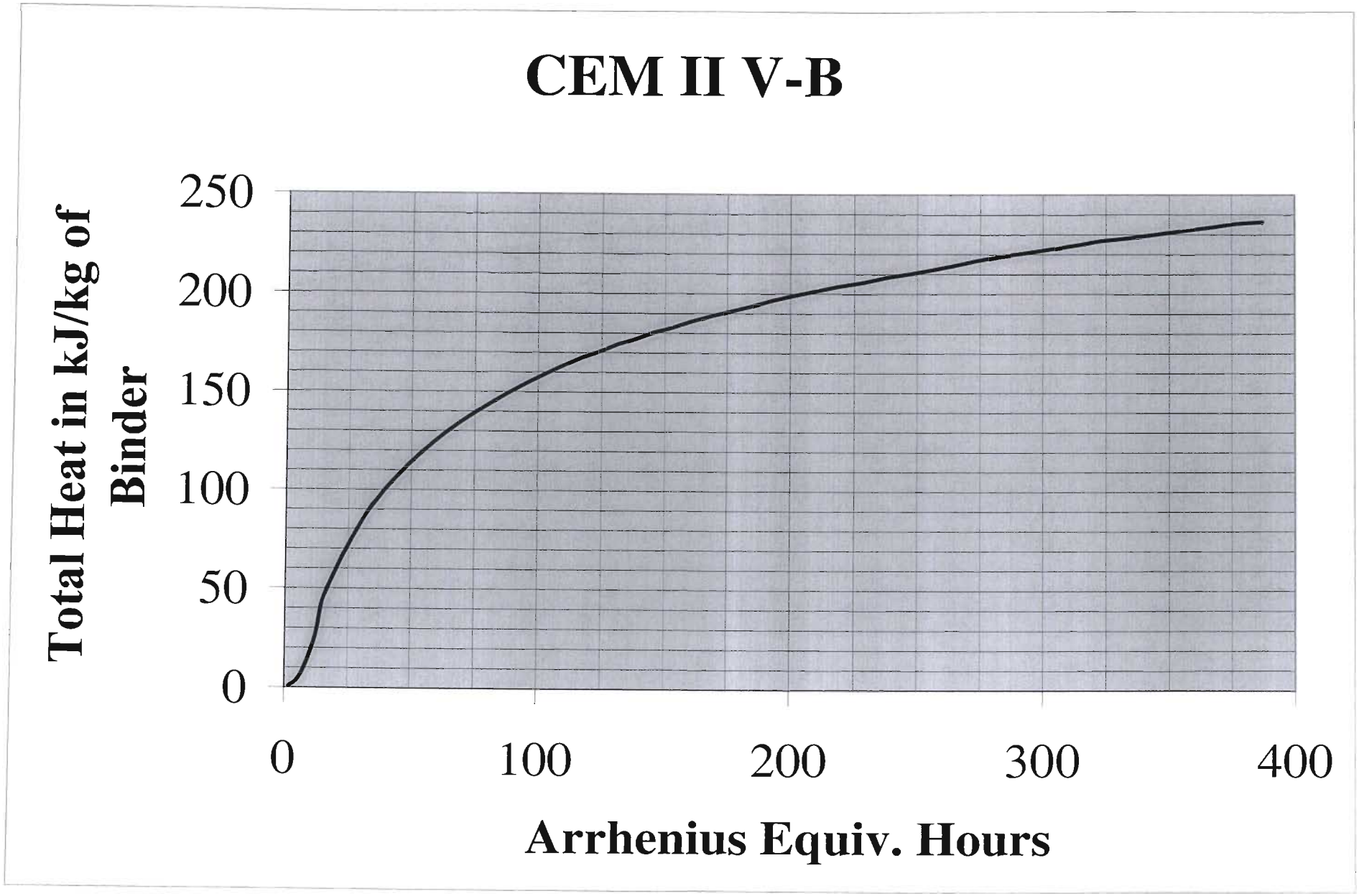
CEM II V-B
Total Heat in kJ/kg of Binder
250
200
150
100
50
0
0
100
200
300
400
Arrhenius Equiv. Hours

CEM II V-B

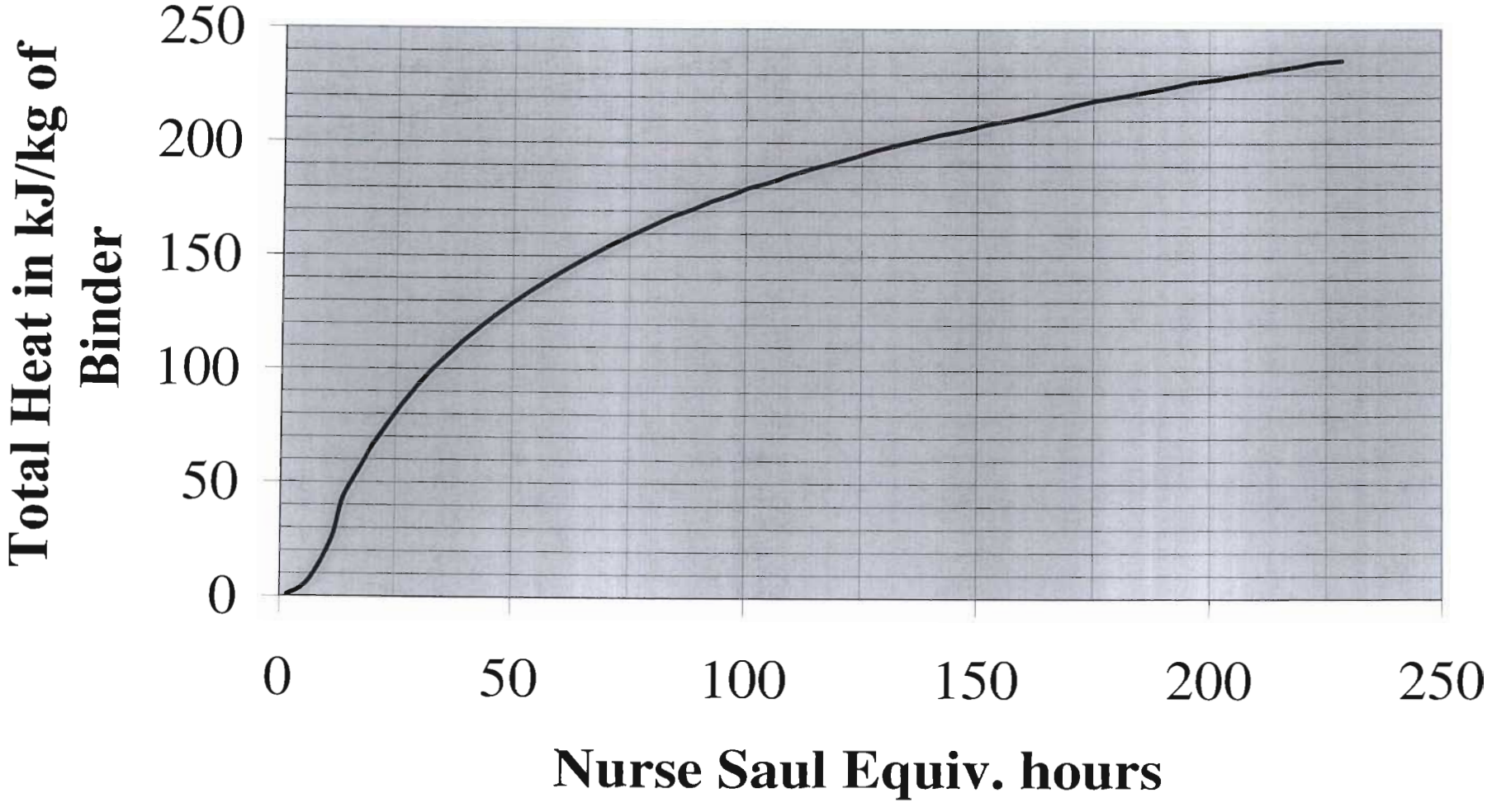
Total Heat in kJ/kg of Binder
250
200
150
100
50
0
0
50
100
150
200
250
Nurse Saul Equiv. hours

CEMENT TYPE :		Cem II B-V				
EXTENDER TYPE :						
SAND TYPE 1 :		Granite				
SAND TYPE 2		0				
STONE TYPE 1 :		Granite				
STONE TYPE 2 :		0				
ADMIXTURE TYPE :		0			Cp	
CEMENT CONTENT :			0.748	kg	880	
EXTENDER CONTENT :				kg	880	
SAND 1 CONTENT :			2.200	kg	750	
SAND 2 CONTENT :			0	kg	750	
STONE 1 CONTENT :			1.650	kg	750	
STONE 2 CONTENT :			0	kg	750	
WATER CONTENT :			0.440	kg	4187	
ADMIXTURE CONTENT :			0	kg	4187	
SAMPLE MASS :			5.038	kg	1069.5	J/kg.K
SAMPLE TEMPERATURE :			22	deg. C		
				Factor:	7.203235	

Sample	time	Total Heat	Heat Rate	Nurse/Saul Maturity	Arrhenius Maturity
22.668	0.000277778	0	0		
22.78	1.580833333	0.806762353	0.142	1.72407	1.798638791
22.882	2.247222222	1.541492353	0.306	2.453343787	2.560544935
22.983	3.158055556	2.269019118	0.222	3.453211079	3.606783688
23.084	3.765	2.996545882	0.333	4.121527722	4.307202187
23.185	4.263611111	3.724072647	0.405	4.672235384	4.885279632
23.286	4.6175	4.451599412	0.571	5.06429119	5.297476827
23.387	5.000277778	5.179126176	0.528	5.489640236	5.74539376
23.488	5.307222222	5.906652941	0.658	5.831755398	6.106239704
23.588	5.61	6.626976471	0.661	6.170240769	6.463822053
23.788	6.097222222	8.067623529	0.821	6.717358843	7.04452655
23.991	6.525555556	9.529880294	0.948	7.201225593	7.559802845
24.192	6.944444444	10.97773059	0.960	7.677243944	8.068362836
24.396	7.325	12.44719059	1.073	8.112269685	8.53470045
24.599	7.6975	13.90944735	1.090	8.540613644	8.995404881
24.801	8.027222222	15.36450088	1.226	8.921992347	9.406964599
25.001	8.361944444	16.80514794	1.196	9.311397023	9.828576538
25.202	8.658333333	18.25299824	1.357	9.658186843	10.2053223
25.404	8.984722222	19.70805176	1.238	10.04227041	10.62401389
25.605	9.257777778	21.15590206	1.473	10.36542711	10.97748776
25.807	9.548888889	22.61095559	1.388	10.71190755	11.35778817
26.109	9.931666667	24.78633265	1.579	11.170705	11.86469448
26.415	10.27388889	26.99052265	1.789	11.5843604	12.32417627
26.724	10.5625	29.21632235	2.142	11.93617254	12.71709117
27.126	10.865	32.11202294	2.659	12.30849962	13.13639717
27.628	11.17916667	35.72804706	3.197	12.69991987	13.58174773
28.03	11.43666667	38.62374765	3.124	13.02461879	13.95336205
28.432	11.75305556	41.51944824	2.542	13.42781424	14.41818655
28.744	12.04722222	43.76685765	2.122	13.80619102	14.85637803
28.944	12.32111111	45.20750471	1.461	14.16082235	15.26798833
29.144	12.60111111	46.64815176	1.429	14.52523302	15.69251611
29.345	12.89861111	48.09600206	1.352	14.91440764	16.14759364
29.546	13.21111111	49.54385235	1.287	15.32529827	16.62986743
29.747	13.52722222	50.99170265	1.272	15.74305491	17.12204692
29.947	13.84527778	52.43234971	1.258	16.1655069	17.62162421
30.15	14.16194444	53.89460647	1.283	16.58824106	18.12346978
30.35	14.48527778	55.33525353	1.238	17.02204662	18.64039061
30.564	14.83527778	56.87674588	1.223	17.49404495	19.20520826
31.872	16.87	66.29857765	1.286	20.28961764	22.68118881

33.125	18.93305556	75.32423147	1.215	23.21217652	26.40148023
34.364	21.10611111	84.24904	1.141	26.38081748	30.53366607
35.471	23.215	92.22302147	1.050	29.53835137	34.73700271
36.522	25.40388889	99.79362176	0.961	32.8943923	39.29765368
37.371	27.4075	105.9091685	0.848	36.02980993	43.62360573
38.277	29.59055556	112.4352997	0.830	39.50989156	48.51850158
39.102	31.75277778	118.3779688	0.763	43.01914219	53.53544679
39.856	33.79166667	123.8092082	0.740	46.38188163	58.41573553
40.568	35.81666667	128.9379118	0.704	49.77119163	63.40662032
41.309	38.04861111	134.2755091	0.664	53.5609217	69.07674556
42.068	40.52472222	139.7427647	0.613	57.82713734	75.564458
42.802	43.03138889	145.0299394	0.586	62.2083729	82.33038253
43.442	45.2525	149.64001	0.577	66.14136838	88.48226267
44.108	47.74194444	154.4373647	0.535	70.60369755	95.56423609
44.767	50.31388889	159.1842968	0.513	75.27070507	103.0762731
45.405	52.86472222	163.7799609	0.500	79.95454524	110.7183724
45.931	55.01694444	167.5688626	0.489	83.94820879	117.302252
46.394	57.46	170.9039606	0.379	88.52181238	124.913957
46.868	59.53277778	174.3182941	0.458	92.43459499	131.4938722
47.228	61.61722222	176.9114588	0.346	96.39837455	138.2051947
47.679	63.73472222	180.1601179	0.426	100.4536341	145.1446693
48	65.92305556	182.4723565	0.294	104.6727043	152.4069592
48.46	68.24194444	185.7858447	0.397	109.1736676	160.2419944
48.896	70.89555556	188.9264553	0.329	114.363954	169.3615066
49.198	72.96472222	191.1018324	0.292	118.4365568	176.5564157
49.527	75.12111111	193.4716968	0.305	122.7035114	184.1508798
49.991	77.77194444	196.8139979	0.350	127.983883	193.655764
50.301	79.88861111	199.0470009	0.293	132.2275174	201.3366595
50.612	82.19222222	201.2872071	0.270	136.8697929	209.7966578
50.936	84.54944444	203.6210553	0.275	141.6450537	218.5620264
51.232	87.30527778	205.7532129	0.215	147.2562978	228.9266681
51.596	89.77472222	208.3751906	0.295	152.3115799	238.344543
51.861	92.34944444	210.2840479	0.206	157.6093712	248.263859
52.146	94.55472222	212.33697	0.259	162.1672026	256.852733
52.43	96.62027778	214.3826888	0.275	166.4558467	264.9849059
52.753	98.73944444	216.7093338	0.305	170.8772408	273.431209
53.077	101.1819444	219.0431821	0.265	175.9995703	283.2865994
53.304	103.6775	220.6783165	0.182	181.2560838	293.4430015
53.578	106.0908333	222.6520029	0.227	186.3595598	303.3670623
53.842	108.43	224.5536571	0.226	191.3271701	313.0824778
54.144	110.7236111	226.7290341	0.263	196.2196719	322.7177175
54.334	113.2472222	228.0976488	0.151	201.6234804	333.3952287
54.632	116.1983333	230.2442129	0.202	207.966697	346.022097
54.877	118.6011111	232.0090056	0.204	213.1530528	356.3977335
55.119	121.1786111	233.7521885	0.188	218.7374643	367.6291919
55.351	123.2430556	235.4233391	0.225	223.2265987	376.7034036
55.474	125.655	236.3093371	0.102	228.4856426	387.3538709
55.717	128.6316667	238.0597232	0.163	234.9941739	400.6177271
55.873	131.0047222	239.1834279	0.132	240.1986802	411.2535891
56.076	133.1030556	240.6456847	0.194	244.8132299	420.7295151
56.164	135.8569444	241.2795694	0.064	250.8828011	433.2066607
56.368	138.4808333	242.7490294	0.156	256.6786218	445.1852865
56.448	141.3722222	243.3252882	0.055	263.0790002	458.4243791
56.546	143.4708333	244.0312053	0.093	267.7307116	468.0685136

Appendix B – Measured and Predicted Temperature Profiles and Profiles

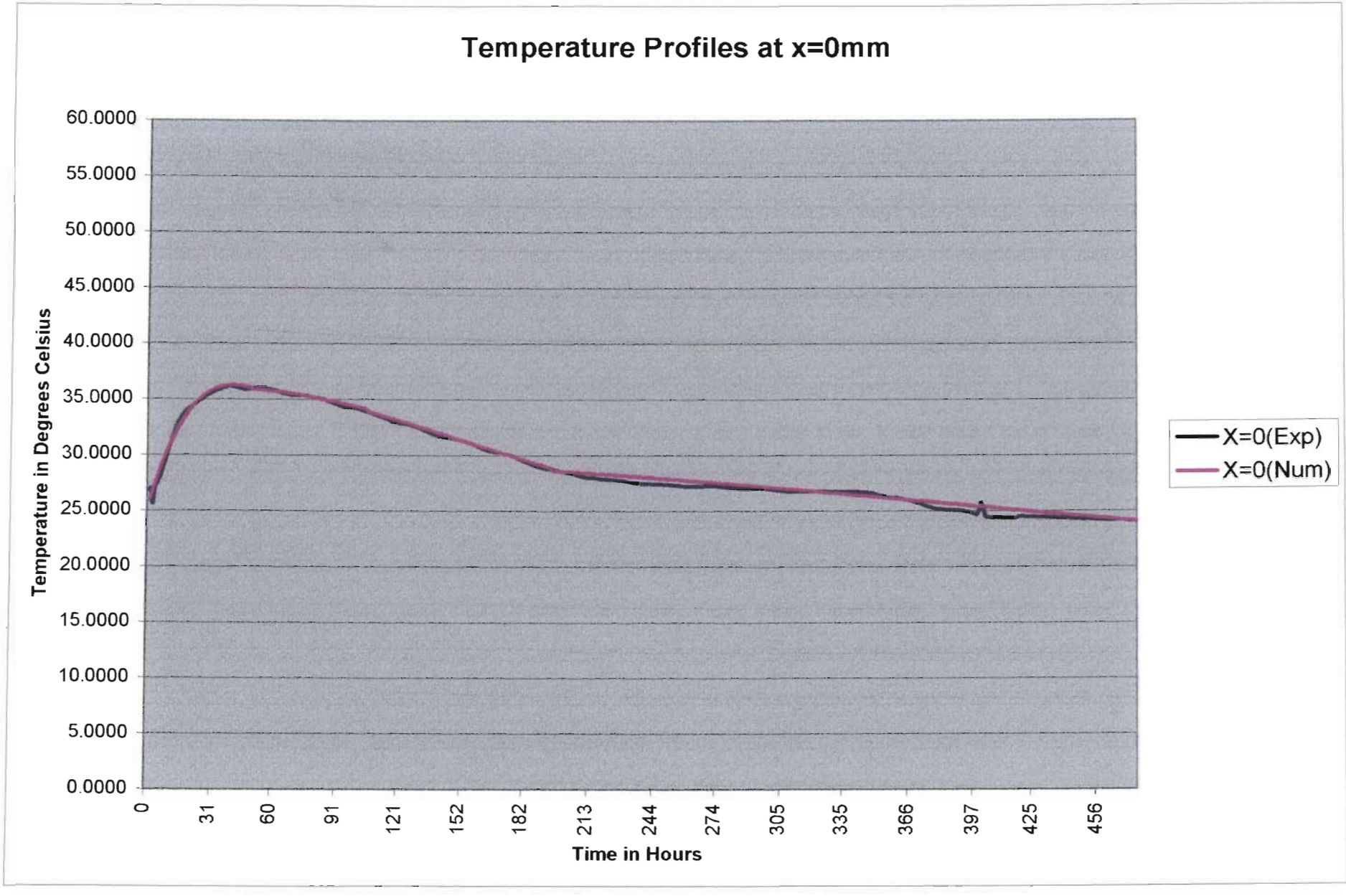
Temperature Profiles at x=0mm
60.0000
55.0000
50.0000
45.0000
40.0000
35.0000
30.0000
25.0000
20.0000
15.0000
10.0000
5.0000
0.0000
Temperature in Degrees Celsius
0
31
60
91
121
152
182
213
244
274
305
335
366
397
425
456
Time in Hours
X=0(Exp)
X=0(Num)

Time(Hours)	X=0(Exp)	X=0(Num)	% Error	X=0(Num.ns)	% Error
0.00	26.84	26.01	3.11	26.01	3.11
1.00	27.00	26.12	3.26	26.12	3.26
2.00	25.60	26.76	4.53	26.76	4.53
3.00	27.20	27.37	0.62	27.37	0.62
4.00	27.53	27.96	1.57	27.96	1.57
5.00	27.86	28.52	2.36	28.52	2.36
6.00	28.39	29.06	2.33	29.06	2.33
7.00	29.11	29.57	1.58	29.57	1.58
8.00	29.54	30.06	1.76	30.06	1.76
9.00	30.39	30.52	0.44	30.52	0.44
10.00	30.97	30.96	0.01	30.96	0.01
11.00	31.46	31.38	0.23	31.38	0.23
12.00	32.01	31.78	0.70	31.78	0.70
13.00	32.48	32.16	0.99	32.16	0.99
14.00	32.90	32.52	1.17	32.52	1.17
15.00	33.27	32.85	1.25	32.85	1.25
16.00	33.59	33.17	1.24	33.17	1.24
17.00	33.84	33.47	1.10	33.47	1.10
18.00	34.05	33.75	0.89	33.75	0.89
19.00	34.22	34.01	0.62	34.01	0.62
20.00	34.37	34.26	0.32	34.26	0.32
21.00	34.47	34.48	0.03	34.48	0.03
22.00	34.64	34.69	0.16	34.69	0.16
23.00	34.78	34.89	0.32	34.89	0.32
24.00	34.92	35.07	0.44	35.07	0.44
25.00	35.05	35.23	0.52	35.23	0.52
26.00	35.19	35.38	0.56	35.38	0.56
27.00	35.32	35.52	0.56	35.52	0.56
28.00	35.43	35.64	0.60	35.64	0.60
29.00	35.55	35.75	0.58	35.75	0.58
30.00	35.63	35.85	0.61	35.85	0.61
31.00	35.73	35.94	0.59	35.94	0.59
32.00	35.81	36.01	0.55	36.01	0.55
33.00	35.89	36.08	0.52	36.08	0.52
34.00	35.96	36.13	0.47	36.13	0.47
35.00	36.02	36.18	0.43	36.18	0.43
36.00	36.08	36.21	0.38	36.21	0.38
37.00	36.13	36.24	0.31	36.24	0.31
38.00	36.19	36.26	0.20	36.26	0.20
39.00	36.20	36.27	0.19	36.27	0.19
40.00	36.16	36.27	0.31	36.27	0.31
41.00	36.14	36.27	0.36	36.27	0.36
42.00	36.10	36.26	0.45	36.26	0.45
43.00	36.05	36.25	0.56	36.25	0.56
44.00	35.99	36.23	0.66	36.23	0.66
45.00	35.95	36.21	0.72	36.21	0.72
46.00	35.88	36.18	0.84	36.18	0.84
46.33	35.90	36.17	0.77	36.17	0.77
46.67	35.90	36.16	0.72	36.16	0.72
48.67	35.97	36.09	0.35	36.09	0.35
50.67	36.01	35.93	0.22	35.93	0.22
52.67	36.00	35.91	0.27	35.91	0.27
54.67	36.00	35.88	0.34	35.88	0.34
56.67	35.99	35.85	0.41	35.85	0.41
58.67	35.94	35.81	0.36	35.81	0.36
60.67	35.85	35.77	0.23	35.77	0.23
62.67	35.74	35.72	0.06	35.72	0.06
64.67	35.54	35.67	0.38	35.67	0.38
66.67	35.49	35.62	0.37	35.62	0.37
68.67	35.42	35.56	0.41	35.56	0.41
70.67	35.39	35.50	0.33	35.50	0.33
72.67	35.38	35.44	0.17	35.44	0.17
74.67	35.39	35.38	0.05	35.38	0.05
76.67	35.35	35.31	0.12	35.31	0.12
78.67	35.27	35.24	0.08	35.24	0.08
80.67	35.16	35.17	0.03	35.17	0.03

82.67	35.14	35.09	0.13	35.09	0.13
84.67	35.06	35.02	0.13	35.02	0.13
86.67	34.90	34.94	0.12	34.94	0.12
88.67	34.76	34.86	0.30	34.86	0.30
90.67	34.60	34.78	0.52	34.78	0.52
92.67	34.46	34.70	0.72	34.70	0.72
94.67	34.35	34.62	0.81	34.62	0.81
96.67	34.28	34.54	0.77	34.54	0.77
98.67	34.26	34.46	0.59	34.46	0.59
100.67	34.21	34.38	0.50	34.38	0.50
102.67	34.13	34.30	0.48	34.30	0.48
104.67	34.03	34.22	0.55	34.02	0.05
106.67	33.90	33.91	0.03	33.91	0.03
108.67	33.77	33.81	0.13	33.81	0.13
110.67	33.63	33.71	0.24	33.71	0.24
112.67	33.49	33.60	0.32	33.60	0.32
114.67	33.37	33.50	0.39	33.50	0.39
116.67	33.18	33.39	0.64	33.39	0.64
118.67	33.01	33.28	0.81	33.28	0.81
120.67	32.93	33.17	0.73	33.17	0.73
122.67	32.90	33.06	0.50	33.06	0.50
124.67	32.84	32.95	0.35	32.95	0.35
126.67	32.77	32.84	0.21	32.84	0.21
128.67	32.66	32.73	0.21	32.73	0.21
130.67	32.51	32.62	0.32	32.62	0.32
132.67	32.38	32.50	0.38	32.50	0.38
134.67	32.23	32.39	0.49	32.39	0.49
136.67	32.09	32.27	0.59	32.27	0.59
138.67	31.92	32.16	0.74	32.16	0.74
140.67	31.76	32.04	0.89	32.04	0.89
142.67	31.66	31.93	0.83	31.93	0.83
144.67	31.60	31.81	0.66	31.81	0.66
146.67	31.57	31.70	0.38	31.70	0.38
148.67	31.52	31.58	0.18	31.58	0.18
150.67	31.46	31.46	0.01	31.46	0.01
152.67	31.37	31.35	0.08	31.35	0.08
154.67	31.26	31.23	0.09	31.23	0.09
156.67	31.12	31.11	0.04	31.11	0.04
158.67	31.00	31.00	0.01	31.00	0.01
160.67	30.82	30.88	0.20	30.88	0.20
162.67	30.63	30.76	0.42	30.76	0.42
164.67	30.48	30.64	0.53	30.64	0.53
166.67	30.39	30.53	0.44	30.53	0.44
168.67	30.34	30.41	0.24	30.41	0.24
170.67	30.28	30.30	0.06	30.30	0.06
172.67	30.18	30.18	0.01	30.18	0.01
174.67	30.08	30.06	0.06	29.95	0.44
176.67	29.98	29.95	0.10	29.84	0.48
178.67	29.83	29.84	0.02	29.72	0.36
180.67	29.65	29.72	0.23	29.61	0.15
182.67	29.51	29.61	0.32	29.50	0.06
184.67	29.36	29.50	0.44	29.38	0.06
186.67	29.20	29.38	0.64	29.27	0.26
188.67	29.07	29.27	0.71	29.16	0.33
190.67	28.96	29.16	0.69	29.05	0.31
192.67	28.85	29.05	0.70	28.66	0.65
194.67	28.79	28.94	0.53	28.64	0.53
196.67	28.76	28.64	0.44	28.61	0.52
198.67	28.68	28.61	0.25	28.59	0.33
200.67	28.59	28.59	0.00	28.57	0.08
202.67	28.50	28.57	0.23	28.54	0.15
204.67	28.41	28.54	0.45	28.52	0.36
206.67	28.33	28.52	0.66	28.49	0.57
208.67	28.24	28.49	0.90	28.47	0.81
210.67	28.13	28.47	1.20	28.44	1.11
212.67	28.05	28.44	1.41	28.42	1.32
214.67	28.02	28.42	1.41	28.39	1.31

216.67	27.99	28.39	1.41	28.36	1.32
218.67	27.94	28.36	1.51	28.34	1.41
220.67	27.91	28.34	1.55	28.31	1.45
222.67	27.88	28.31	1.56	28.28	1.46
224.67	27.84	28.28	1.59	28.26	1.49
226.67	27.82	28.26	1.57	28.23	1.47
228.67	27.78	28.23	1.61	28.20	1.51
230.67	27.73	28.20	1.71	28.18	1.61
232.67	27.66	28.18	1.86	28.15	1.76
234.67	27.58	28.15	2.06	28.12	1.96
236.67	27.52	28.12	2.18	28.09	2.08
238.67	27.49	28.09	2.18	28.06	2.08
240.67	27.48	28.06	2.11	28.04	2.00
242.67	27.46	28.04	2.08	28.01	1.98
244.67	27.45	28.01	2.04	27.98	1.93
246.67	27.43	27.98	1.99	27.95	1.88
248.67	27.41	27.95	1.95	27.92	1.84
250.67	27.40	27.92	1.89	27.89	1.79
252.67	27.38	27.89	1.86	27.86	1.76
254.67	27.35	27.86	1.86	27.83	1.75
256.67	27.32	27.83	1.88	27.80	1.77
258.67	27.27	27.80	1.93	27.77	1.82
260.67	27.25	27.77	1.93	27.74	1.82
262.67	27.24	27.74	1.85	27.71	1.74
264.67	27.23	27.71	1.77	27.68	1.65
266.67	27.24	27.68	1.62	27.65	1.50
268.67	27.25	27.65	1.47	27.62	1.35
270.67	27.26	27.62	1.31	27.59	1.20
272.67	27.27	27.59	1.18	27.56	1.07
274.67	27.26	27.56	1.09	27.52	0.98
276.67	27.24	27.52	1.06	27.49	0.94
278.67	27.20	27.49	1.06	27.46	0.95
280.67	27.15	27.46	1.16	27.43	1.04
282.67	27.08	27.43	1.28	27.40	1.16
284.67	27.04	27.40	1.30	27.32	1.01
285.00	27.04	27.39	1.29	27.39	1.29
287.00	27.03	27.36	1.20	27.36	1.20
289.00	27.04	27.33	1.07	27.33	1.07
291.00	27.03	27.30	0.97	27.30	0.97
293.00	27.03	27.26	0.86	27.26	0.86
295.00	27.03	27.23	0.73	27.23	0.73
297.00	27.03	27.20	0.62	27.20	0.62
299.00	27.01	27.16	0.56	27.16	0.56
301.00	26.97	27.13	0.59	27.13	0.59
303.00	26.91	27.10	0.69	27.10	0.69
305.00	26.85	27.07	0.79	27.07	0.79
307.00	26.79	27.03	0.88	27.03	0.88
309.00	26.74	27.00	0.97	27.00	0.97
311.00	26.76	26.96	0.78	26.96	0.78
313.00	26.77	26.93	0.61	26.93	0.61
315.00	26.78	26.90	0.43	26.90	0.43
317.00	26.79	26.86	0.27	26.86	0.27
319.00	26.78	26.83	0.18	26.83	0.18
321.00	26.78	26.80	0.08	26.80	0.08
323.00	26.77	26.76	0.04	26.76	0.04
325.00	26.77	26.73	0.15	26.73	0.15
327.00	26.76	26.69	0.24	26.69	0.24
329.00	26.74	26.66	0.30	26.66	0.30
331.00	26.73	26.62	0.38	26.62	0.38
333.00	26.72	26.59	0.48	26.59	0.48
335.00	26.71	26.55	0.60	26.55	0.60
337.00	26.72	26.52	0.75	26.52	0.75
339.00	26.74	26.48	0.95	26.48	0.95
341.00	26.74	26.45	1.10	26.45	1.10
343.00	26.73	26.41	1.16	26.41	1.16
345.00	26.69	26.38	1.16	26.38	1.16
347.00	26.65	26.34	1.15	26.34	1.15

349.00	26.59	26.31	1.06	26.31	1.06
351.00	26.50	26.27	0.86	26.27	0.86
353.00	26.39	26.24	0.56	26.24	0.56
355.00	26.26	26.20	0.23	26.20	0.23
357.00	26.21	26.17	0.15	26.17	0.15
359.00	26.19	26.13	0.21	26.13	0.21
361.00	26.17	26.10	0.30	26.10	0.30
363.00	26.10	26.06	0.15	26.06	0.15
365.00	26.02	26.03	0.01	26.03	0.01
367.00	25.94	25.99	0.20	25.99	0.20
369.00	25.83	25.95	0.49	25.95	0.49
371.00	25.70	25.92	0.83	25.92	0.83
373.00	25.57	25.88	1.21	25.88	1.21
375.00	25.46	25.85	1.54	25.85	1.54
377.00	25.32	25.81	1.93	25.81	1.93
379.00	25.21	25.78	2.23	25.78	2.23
381.00	25.14	25.74	2.39	25.74	2.39
383.00	25.11	25.70	2.38	25.70	2.38
385.00	25.09	25.67	2.30	25.67	2.30
387.00	25.08	25.63	2.21	25.63	2.21
389.00	25.05	25.60	2.16	25.60	2.16
391.00	25.02	25.56	2.16	25.56	2.16
393.00	24.98	25.52	2.18	25.52	2.18
395.00	24.91	25.49	2.34	25.49	2.34
397.00	24.79	25.45	2.68	25.45	2.68
399.00	24.65	25.42	3.10	25.42	3.10
401.00	25.69	25.38	1.21	25.38	1.21
403.00	24.44	25.34	3.71	25.34	3.71
405.00	24.41	25.31	3.70	25.31	3.70
407.00	24.38	25.27	3.65	25.27	3.65
409.00	24.38	25.24	3.51	25.24	3.51
411.00	24.36	25.20	3.43	25.20	3.43
413.00	24.35	25.16	3.34	25.16	3.34
415.00	24.34	25.13	3.25	25.13	3.25
417.00	24.31	25.09	3.21	25.09	3.21
419.00	24.50	25.06	2.27	25.06	2.27
421.00	24.49	25.02	2.19	25.02	2.19
423.00	24.47	24.98	2.10	24.98	2.10
425.00	24.46	24.95	2.02	24.95	2.02
427.00	24.44	24.91	1.93	24.91	1.93
429.00	24.43	24.88	1.85	24.88	1.85
431.00	24.41	24.84	1.77	24.84	1.77
433.00	24.40	24.81	1.68	24.81	1.68
435.00	24.38	24.77	1.60	24.77	1.60
437.00	24.37	24.73	1.52	24.73	1.52
439.00	24.35	24.70	1.43	24.70	1.43
441.00	24.34	24.66	1.35	24.66	1.35
443.00	24.32	24.63	1.27	24.63	1.27
445.00	24.31	24.59	1.18	24.59	1.18
447.00	24.29	24.56	1.10	24.56	1.10
449.00	24.27	24.52	1.02	24.52	1.02
451.00	24.26	24.49	0.93	24.49	0.93
453.00	24.24	24.45	0.85	24.45	0.85
455.00	24.23	24.42	0.77	24.42	0.77
457.00	24.21	24.38	0.69	24.38	0.69
459.00	24.20	24.35	0.61	24.35	0.61
461.00	24.18	24.31	0.52	24.31	0.52
463.00	24.17	24.28	0.44	24.28	0.44
465.00	24.15	24.24	0.36	24.24	0.36
467.00	24.16	24.21	0.17	24.21	0.17
469.00	24.15	24.17	0.08	24.17	0.08
471.00	24.12	24.14	0.07	24.14	0.07
473.00	24.08	24.10	0.08	24.10	0.08
475.00	24.06	24.07	0.02	24.07	0.02

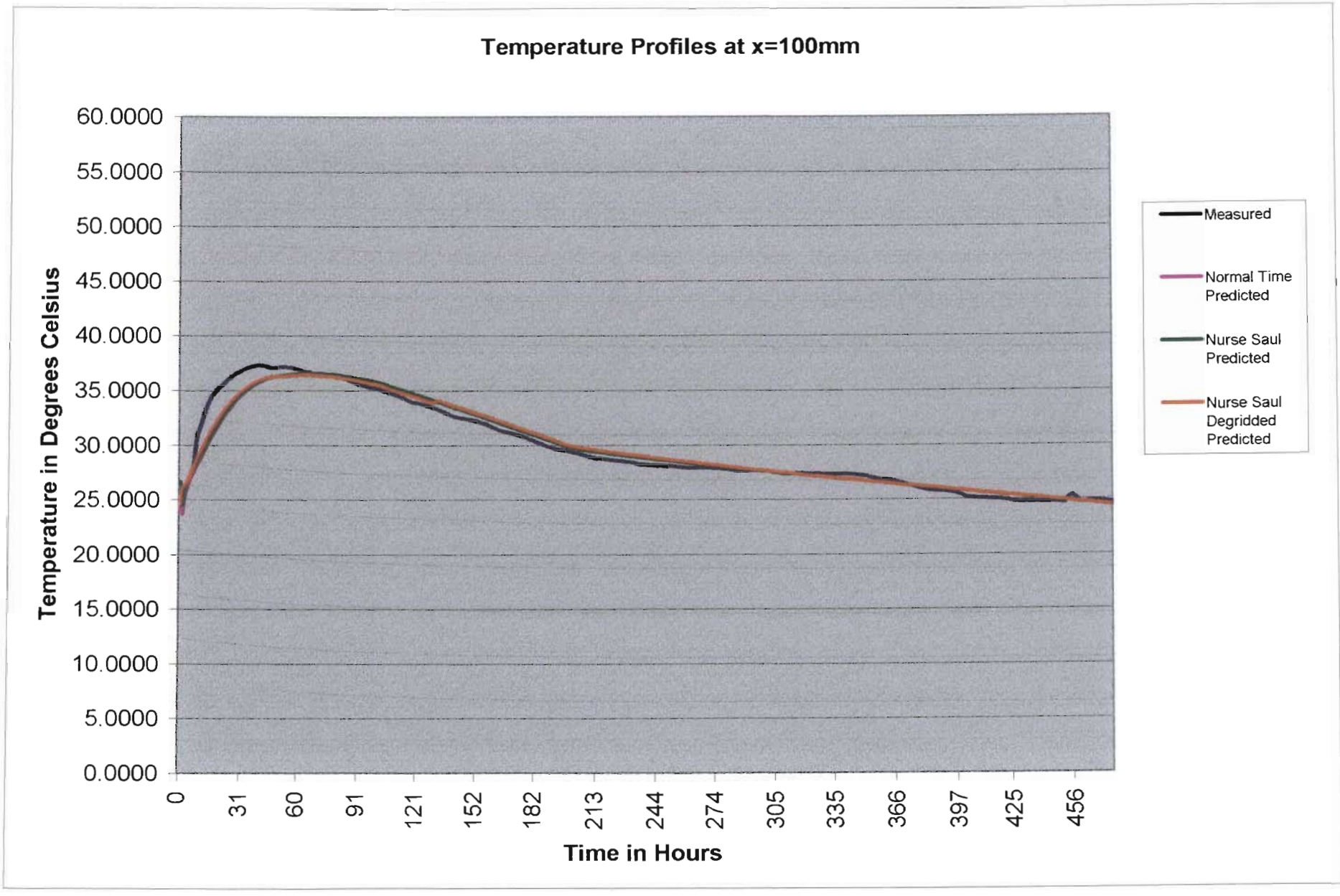
Temperature Profiles at x=100mm
Temperature in Degrees Celsius
60.0000
55.0000
50.0000
45.0000
40.0000
35.0000
30.0000
25.0000
20.0000
15.0000
10.0000
5.0000
0.0000
0
31
60
91
121
152
182
213
244
274
305
335
366
397
425
456
Time in Hours
Measured
Normal Time Predicted
Nurse Saul Predicted
Nurse Saul Degridded Predicted

Time(Hours)	X=100(Exp)	X=100(Num)	% Error	X=100(Numns)	% Error	X=100(Num.deg)	% Error
0.00	25.66	24.53	4.41	26.65	3.88	24.53	4.41
1.00	26.01	23.69	8.94	24.51	5.77	26.08	0.24
2.00	26.11	25.22	3.40	25.83	1.07	26.28	0.65
3.00	26.34	26.00	1.29	26.51	0.63	26.61	1.03
4.00	26.71	26.53	0.69	26.97	0.97	26.99	1.05
5.00	27.15	26.96	0.69	27.36	0.77	27.39	0.89
6.00	27.73	27.36	1.34	27.72	0.03	27.80	0.24
7.00	28.48	27.74	2.59	28.07	1.41	28.20	0.96
8.00	30.24	28.11	7.05	28.42	6.03	28.60	5.43
9.00	31.12	28.48	8.49	28.77	7.56	29.00	6.83
10.00	31.74	28.85	9.11	29.11	8.26	29.38	7.43
11.00	32.26	29.21	9.46	29.46	8.68	29.76	7.76
12.00	32.84	29.56	9.99	29.80	9.27	30.12	8.28
13.00	33.36	29.92	10.32	30.14	9.66	30.48	8.63
14.00	33.81	30.26	10.49	30.47	9.88	30.82	8.83
15.00	34.19	30.60	10.50	30.80	9.93	31.16	8.87
16.00	34.52	30.93	10.39	31.12	9.86	31.48	8.80
17.00	34.78	31.26	10.13	31.43	9.64	31.80	8.58
18.00	35.02	31.57	9.84	31.73	9.38	32.10	8.34
19.00	35.21	31.87	9.49	32.02	9.06	32.39	8.03
20.00	35.38	32.17	9.08	32.31	8.68	32.66	7.68
21.00	35.49	32.45	8.55	32.59	8.18	32.93	7.20
22.00	35.67	32.72	8.25	32.85	7.89	33.19	6.95
23.00	35.79	32.99	7.83	33.11	7.50	33.43	6.60
24.00	36.05	33.24	7.79	33.35	7.48	33.66	6.61
25.00	36.20	33.48	7.51	33.58	7.22	33.88	6.39
26.00	36.34	33.71	7.23	33.81	6.95	34.09	6.17
27.00	36.46	33.93	6.95	34.02	6.69	34.29	5.96
28.00	36.58	34.14	6.67	34.23	6.44	34.48	5.74
29.00	36.69	34.34	6.42	34.42	6.19	34.65	5.54
30.00	36.79	34.52	6.15	34.60	5.94	34.82	5.34
31.00	36.88	34.70	5.90	34.77	5.70	34.98	5.15
32.00	36.96	34.87	5.67	34.93	5.49	35.12	4.98
33.00	37.05	35.02	5.47	35.09	5.30	35.26	4.84
34.00	37.12	35.17	5.25	35.23	5.09	35.38	4.67
35.00	37.18	35.30	5.04	35.36	4.89	35.50	4.51
36.00	37.23	35.43	4.84	35.48	4.70	35.61	4.37
37.00	37.27	35.55	4.63	35.60	4.50	35.70	4.21
38.00	37.32	35.66	4.46	35.70	4.33	35.79	4.09
39.00	37.34	35.76	4.25	35.80	4.13	35.87	3.93
40.00	37.34	35.85	4.00	35.89	3.88	35.95	3.73
41.00	37.33	35.93	3.76	35.97	3.65	36.01	3.54
42.00	37.30	36.01	3.48	36.04	3.38	36.07	3.30
43.00	37.27	36.07	3.20	36.11	3.11	36.12	3.07
44.00	37.22	36.13	2.91	36.17	2.82	36.17	2.82
45.00	37.18	36.19	2.66	36.22	2.58	36.21	2.61
46.00	37.11	36.24	2.36	36.27	2.28	36.24	2.35
46.33	37.11	36.24	2.34	36.30	2.17	36.20	2.46
46.67	37.10	36.25	2.27	36.25	2.27	36.26	2.25
48.67	37.12	36.32	2.15	36.32	2.15	36.30	2.20
50.67	37.14	36.35	2.14	36.35	2.14	36.31	2.25
52.67	37.14	36.38	2.04	36.38	2.04	36.32	2.21
54.67	37.13	36.43	1.89	36.43	1.89	36.35	2.10
56.67	37.11	36.47	1.71	36.47	1.71	36.38	1.97
58.67	37.06	36.51	1.49	36.51	1.49	36.40	1.79
60.67	37.00	36.54	1.25	36.54	1.25	36.41	1.58
62.67	36.90	36.56	0.93	36.56	0.93	36.42	1.30
64.67	36.72	36.57	0.41	36.57	0.41	36.42	0.81
66.67	36.66	36.58	0.24	36.58	0.24	36.42	0.67
68.67	36.57	36.57	0.00	36.57	0.00	36.41	0.45
70.67	36.52	36.56	0.12	36.56	0.12	36.39	0.36
72.67	36.49	36.55	0.16	36.55	0.16	36.36	0.34
74.67	36.47	36.52	0.14	36.52	0.14	36.33	0.38
76.67	36.42	36.49	0.18	36.49	0.18	36.30	0.35
78.67	36.35	36.46	0.29	36.46	0.29	36.26	0.27
80.67	36.25	36.42	0.46	36.42	0.46	36.21	0.10

82.67	36.19	36.37	0.50	36.37	0.50	36.16	0.08
84.67	36.12	36.32	0.55	36.32	0.55	36.11	0.04
86.67	35.98	36.27	0.80	36.27	0.80	36.05	0.20
88.67	35.84	36.21	1.02	36.21	1.02	35.99	0.40
90.67	35.69	36.15	1.27	36.15	1.27	35.93	0.65
92.67	35.54	36.08	1.53	36.08	1.53	35.86	0.90
94.67	35.42	36.02	1.70	36.02	1.70	35.79	1.06
96.67	35.32	35.95	1.78	35.95	1.78	35.72	1.13
98.67	35.27	35.87	1.72	35.87	1.72	35.65	1.07
100.67	35.20	35.80	1.71	35.80	1.71	35.57	1.06
102.67	35.12	35.73	1.74	35.73	1.74	35.49	1.08
104.67	35.02	35.65	1.80	35.65	1.80	35.42	1.14
106.67	34.90	35.50	1.71	35.50	1.71	35.23	0.93
108.67	34.76	35.35	1.71	35.35	1.71	35.10	0.98
110.67	34.62	35.24	1.79	35.24	1.79	34.99	1.07
112.67	34.48	35.13	1.88	35.13	1.88	34.89	1.16
114.67	34.35	35.03	1.97	35.03	1.97	34.78	1.25
116.67	34.20	34.92	2.11	34.92	2.11	34.67	1.39
118.67	34.03	34.81	2.30	34.81	2.30	34.56	1.57
120.67	33.92	34.70	2.30	34.70	2.30	34.45	1.58
122.67	33.85	34.59	2.18	34.59	2.18	34.34	1.46
124.67	33.77	34.47	2.09	34.47	2.09	34.23	1.37
126.67	33.69	34.36	1.99	34.36	1.99	34.12	1.27
128.67	33.59	34.25	1.95	34.25	1.95	34.00	1.23
130.67	33.45	34.13	2.02	34.13	2.02	33.89	1.30
132.67	33.32	34.01	2.07	34.01	2.07	34.12	2.40
134.67	33.18	33.89	2.16	33.89	2.16	34.01	2.50
136.67	33.03	33.77	2.25	33.77	2.25	33.89	2.60
138.67	32.88	33.65	2.36	33.65	2.36	33.78	2.73
140.67	32.72	33.53	2.49	33.53	2.49	33.66	2.88
142.67	32.60	33.41	2.50	33.41	2.50	33.54	2.90
144.67	32.51	33.29	2.39	33.29	2.39	33.42	2.80
146.67	32.45	33.17	2.20	33.17	2.20	33.30	2.63
148.67	32.39	33.04	2.02	33.04	2.02	33.18	2.45
150.67	32.32	32.92	1.85	32.92	1.85	33.06	2.30
152.67	32.24	32.80	1.73	32.80	1.73	32.94	2.19
154.67	32.13	32.67	1.68	32.67	1.68	32.82	2.14
156.67	32.01	32.55	1.69	32.55	1.69	32.70	2.16
158.67	31.88	32.42	1.69	32.42	1.69	32.58	2.17
160.67	31.72	32.30	1.81	32.30	1.81	32.45	2.30
162.67	31.55	32.17	1.98	32.17	1.98	32.33	2.48
164.67	31.39	32.05	2.10	32.05	2.10	32.21	2.61
166.67	31.28	31.92	2.06	31.92	2.06	32.08	2.57
168.67	31.20	31.80	1.92	31.80	1.92	31.96	2.43
170.67	31.13	31.67	1.73	31.67	1.73	31.84	2.26
172.67	31.03	31.55	1.66	31.55	1.66	31.71	2.19
174.67	30.94	31.43	1.58	31.43	1.58	31.59	2.11
176.67	30.84	31.30	1.51	31.30	1.51	31.47	2.05
178.67	30.70	31.18	1.55	31.18	1.55	31.34	2.10
180.67	30.54	31.05	1.68	31.05	1.68	31.22	2.23
182.67	30.39	30.93	1.77	30.93	1.77	31.10	2.32
184.67	30.25	30.81	1.84	30.81	1.84	30.98	2.40
186.67	30.09	30.69	1.98	30.69	1.98	30.86	2.54
188.67	29.95	30.57	2.05	30.57	2.05	30.73	2.61
190.67	29.84	30.44	2.02	30.44	2.02	30.61	2.59
192.67	29.72	30.32	2.03	30.32	2.03	30.49	2.60
194.67	29.64	30.20	1.90	30.20	1.90	30.37	2.47
196.67	29.59	30.02	1.46	30.02	1.46	30.20	2.07
198.67	29.52	29.88	1.23	29.88	1.23	30.06	1.83
200.67	29.42	29.79	1.26	29.79	1.26	29.96	1.84
202.67	29.33	29.72	1.34	29.72	1.34	29.89	1.90
204.67	29.24	29.66	1.43	29.66	1.43	29.82	1.97
206.67	29.16	29.60	1.53	29.60	1.53	29.76	2.07
208.67	29.06	29.55	1.65	29.55	1.65	29.70	2.19
210.67	28.96	29.49	1.83	29.49	1.83	29.64	2.36
212.67	28.87	29.44	1.98	29.44	1.98	29.59	2.49
214.67	28.81	29.39	1.99	29.39	1.99	29.53	2.50

216.67	28.78	29.34	1.94	29.34	1.94	29.48	2.44
218.67	28.72	29.29	1.96	29.29	1.96	29.43	2.45
220.67	28.68	29.24	1.96	29.24	1.96	29.38	2.44
222.67	28.64	29.19	1.93	29.19	1.93	29.33	2.40
224.67	28.60	29.15	1.91	29.15	1.91	29.28	2.38
226.67	28.57	29.10	1.87	29.10	1.87	29.23	2.33
228.67	28.52	29.05	1.86	29.05	1.86	29.18	2.31
230.67	28.48	29.01	1.86	29.01	1.86	29.14	2.31
232.67	28.42	28.96	1.93	28.96	1.93	29.09	2.37
234.67	28.34	28.92	2.06	28.92	2.06	29.04	2.49
236.67	28.27	28.88	2.14	28.88	2.14	29.00	2.57
238.67	28.23	28.83	2.13	28.83	2.13	28.95	2.55
240.67	28.21	28.79	2.06	28.79	2.06	28.90	2.48
242.67	28.18	28.75	2.01	28.75	2.01	28.86	2.41
244.67	28.16	28.70	1.94	28.70	1.94	28.82	2.34
246.67	28.13	28.66	1.87	28.66	1.87	28.77	2.26
248.67	28.11	28.62	1.81	28.62	1.81	28.73	2.19
250.67	28.09	28.58	1.73	28.58	1.73	28.68	2.11
252.67	28.07	28.53	1.67	28.53	1.67	28.64	2.04
254.67	28.04	28.49	1.62	28.49	1.62	28.60	1.99
256.67	28.01	28.45	1.59	28.45	1.59	28.55	1.96
258.67	27.96	28.41	1.60	28.41	1.60	28.51	1.96
260.67	27.93	28.37	1.58	28.37	1.58	28.47	1.93
262.67	27.91	28.33	1.51	28.33	1.51	28.43	1.85
264.67	27.89	28.29	1.41	28.29	1.41	28.38	1.75
266.67	27.89	28.25	1.28	28.25	1.28	28.34	1.61
268.67	27.89	28.21	1.13	28.21	1.13	28.30	1.45
270.67	27.90	28.17	0.97	28.17	0.97	28.26	1.29
272.67	27.90	28.13	0.82	28.13	0.82	28.22	1.14
274.67	27.89	28.09	0.71	28.09	0.71	28.18	1.02
276.67	27.87	28.05	0.63	28.05	0.63	28.13	0.93
278.67	27.85	28.01	0.58	28.01	0.58	28.09	0.88
280.67	27.80	27.97	0.61	27.97	0.61	28.05	0.91
282.67	27.74	27.93	0.68	27.93	0.68	28.01	0.97
284.67	27.70	27.89	0.69	27.89	0.69	27.97	0.99
285.00	27.68	27.90	0.78	27.90	0.78	27.90	0.78
287.00	27.67	27.86	0.69	27.86	0.69	27.86	0.69
289.00	27.67	27.83	0.58	27.83	0.58	27.83	0.58
291.00	27.66	27.79	0.49	27.79	0.49	27.79	0.49
293.00	27.65	27.76	0.39	27.76	0.39	27.76	0.39
295.00	27.65	27.72	0.27	27.72	0.27	27.72	0.27
297.00	27.64	27.69	0.16	27.69	0.16	27.69	0.16
299.00	27.63	27.65	0.07	27.65	0.07	27.65	0.07
301.00	27.60	27.61	0.06	27.61	0.06	27.61	0.06
303.00	27.55	27.58	0.10	27.58	0.10	27.58	0.10
305.00	27.49	27.54	0.18	27.54	0.18	27.54	0.18
307.00	27.44	27.50	0.23	27.50	0.23	27.50	0.23
309.00	27.38	27.47	0.31	27.47	0.31	27.47	0.31
311.00	27.38	27.43	0.20	27.43	0.20	27.43	0.20
313.00	27.38	27.39	0.05	27.39	0.05	27.39	0.05
315.00	27.39	27.36	0.11	27.36	0.11	27.36	0.11
317.00	27.39	27.32	0.26	27.32	0.26	27.32	0.26
319.00	27.39	27.28	0.38	27.28	0.38	27.28	0.38
321.00	27.38	27.25	0.48	27.25	0.48	27.25	0.48
323.00	27.37	27.21	0.60	27.21	0.60	27.21	0.60
325.00	27.37	27.17	0.71	27.17	0.71	27.17	0.71
327.00	27.36	27.14	0.81	27.14	0.81	27.14	0.81
329.00	27.34	27.10	0.89	27.10	0.89	27.10	0.89
331.00	27.33	27.06	0.97	27.06	0.97	27.06	0.97
333.00	27.32	27.03	1.06	27.03	1.06	27.03	1.06
335.00	27.31	26.99	1.18	26.99	1.18	26.99	1.18
337.00	27.31	26.95	1.32	26.95	1.32	26.95	1.32
339.00	27.32	26.92	1.49	26.92	1.49	26.92	1.49
341.00	27.33	26.88	1.63	26.88	1.63	26.88	1.63
343.00	27.31	26.84	1.73	26.84	1.73	26.84	1.73
345.00	27.29	26.80	1.76	26.80	1.76	26.80	1.76
347.00	27.26	26.77	1.79	26.77	1.79	26.77	1.79

349.00	27.21	26.73	1.75	26.73	1.75	26.73	1.75
351.00	27.14	26.69	1.64	26.69	1.64	26.69	1.64
353.00	27.04	26.66	1.43	26.66	1.43	26.66	1.43
355.00	26.93	26.62	1.16	26.62	1.16	26.62	1.16
357.00	26.87	26.59	1.04	26.59	1.04	26.59	1.04
359.00	26.83	26.55	1.05	26.55	1.05	26.55	1.05
361.00	26.81	26.51	1.12	26.51	1.12	26.51	1.12
363.00	26.75	26.48	1.04	26.48	1.04	26.48	1.04
365.00	26.69	26.44	0.94	26.44	0.94	26.44	0.94
367.00	26.61	26.40	0.78	26.40	0.78	26.40	0.78
369.00	26.52	26.37	0.59	26.37	0.59	26.37	0.59
371.00	26.41	26.33	0.30	26.33	0.30	26.33	0.30
373.00	26.29	26.30	0.01	26.30	0.01	26.30	0.01
375.00	26.19	26.26	0.28	26.26	0.28	26.26	0.28
377.00	26.06	26.22	0.61	26.22	0.61	26.22	0.61
379.00	25.95	26.19	0.90	26.19	0.90	26.19	0.90
381.00	25.87	26.15	1.08	26.15	1.08	26.15	1.08
383.00	25.82	26.12	1.13	26.12	1.13	26.12	1.13
385.00	25.79	26.08	1.11	26.08	1.11	26.08	1.11
387.00	25.77	26.04	1.05	26.04	1.05	26.04	1.05
389.00	25.75	26.01	1.01	26.01	1.01	26.01	1.01
391.00	25.72	25.97	1.00	25.97	1.00	25.97	1.00
393.00	25.68	25.94	1.01	25.94	1.01	25.94	1.01
395.00	25.62	25.90	1.10	25.90	1.10	25.90	1.10
397.00	25.52	25.86	1.33	25.86	1.33	25.86	1.33
399.00	25.40	25.83	1.67	25.83	1.67	25.83	1.67
401.00	25.17	25.79	2.47	25.79	2.47	25.79	2.47
403.00	25.19	25.76	2.24	25.76	2.24	25.76	2.24
405.00	25.14	25.72	2.31	25.72	2.31	25.72	2.31
407.00	25.10	25.69	2.31	25.69	2.31	25.69	2.31
409.00	25.09	25.65	2.23	25.65	2.23	25.65	2.23
411.00	25.07	25.61	2.16	25.61	2.16	25.61	2.16
413.00	25.05	25.58	2.09	25.58	2.09	25.58	2.09
415.00	25.04	25.54	2.02	25.54	2.02	25.54	2.02
417.00	25.01	25.51	1.98	25.51	1.98	25.51	1.98
419.00	24.99	25.47	1.92	25.47	1.92	25.47	1.92
421.00	24.96	25.44	1.90	25.44	1.90	25.44	1.90
423.00	24.90	25.40	1.99	25.40	1.99	25.40	1.99
425.00	24.84	25.37	2.14	25.37	2.14	25.37	2.14
427.00	24.78	25.33	2.21	25.33	2.21	25.33	2.21
429.00	24.76	25.30	2.15	25.30	2.15	25.30	2.15
431.00	24.76	25.26	2.02	25.26	2.02	25.26	2.02
433.00	24.76	25.22	1.89	25.22	1.89	25.22	1.89
435.00	24.76	25.19	1.75	25.19	1.75	25.19	1.75
437.00	24.76	25.15	1.60	25.15	1.60	25.15	1.60
439.00	24.76	25.12	1.44	25.12	1.44	25.12	1.44
441.00	24.76	25.08	1.30	25.08	1.30	25.08	1.30
443.00	24.76	25.05	1.17	25.05	1.17	25.05	1.17
445.00	24.75	25.01	1.04	25.01	1.04	25.01	1.04
447.00	24.74	24.98	0.96	24.98	0.96	24.98	0.96
449.00	24.70	24.94	0.95	24.94	0.95	24.94	0.95
451.00	24.68	24.90	0.89	24.90	0.89	24.90	0.89
453.00	25.15	24.87	1.13	24.87	1.13	24.87	1.13
455.00	25.33	24.83	1.96	24.83	1.96	24.83	1.96
457.00	25.11	24.80	1.25	24.80	1.25	24.80	1.25
459.00	24.70	24.76	0.24	24.76	0.24	24.76	0.24
461.00	24.73	24.73	0.01	24.73	0.01	24.73	0.01
463.00	24.76	24.69	0.26	24.69	0.26	24.69	0.26
465.00	24.78	24.66	0.51	24.66	0.51	24.66	0.51
467.00	24.80	24.62	0.71	24.62	0.71	24.62	0.71
469.00	24.79	24.58	0.83	24.58	0.83	24.58	0.83
471.00	24.77	24.55	0.89	24.55	0.89	24.55	0.89
473.00	24.74	24.51	0.91	24.51	0.91	24.51	0.91
475.00	24.71	24.48	0.96	24.48	0.96	24.48	0.96

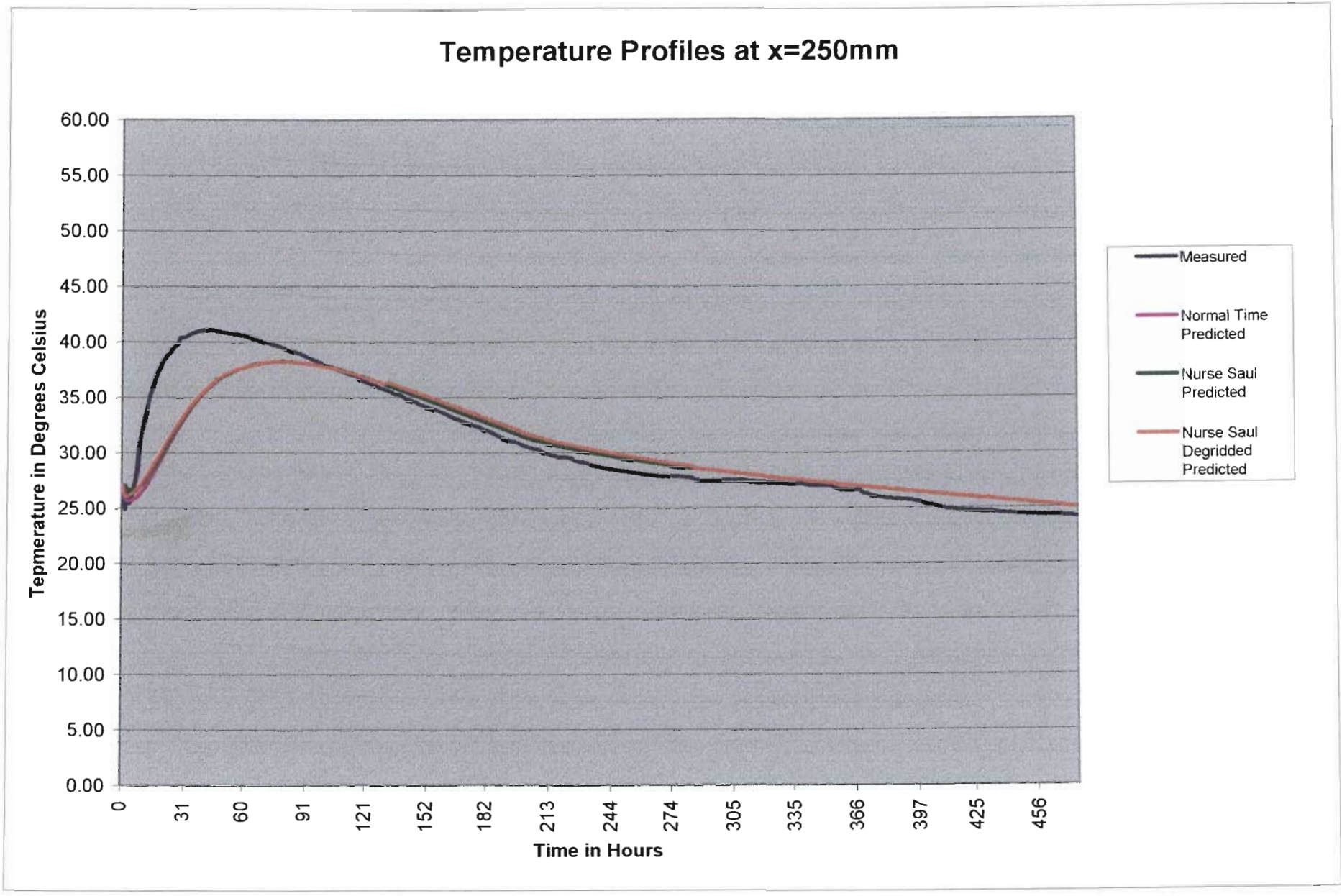
Temperature Profiles at x=250mm
Tepmerature in Degrees Celsius
60.00
55.00
50.00
45.00
40.00
35.00
30.00
25.00
20.00
15.00
10.00
5.00
0.00
0
31
60
91
121
152
182
213
244
274
305
335
366
397
425
456
Time in Hours
Measured
Normal Time Predicted
Nurse Saul Predicted
Nurse Saul Degridded Predicted

Time(Hours)	X=250(Exp)	X=250(Num)	% Error	X=250(Num.ns)	% Error	X=250(Num.deg)	% Error
0.00	26.42	27.03	2.31	27.03	2.31	27.03	2.31
1.00	24.87	25.84	3.90	27.04	8.72	26.06	4.80
2.00	26.70	25.62	4.05	26.74	0.13	26.08	2.31
3.00	25.42	25.63	0.83	26.65	4.84	26.14	2.85
4.00	25.96	25.70	0.98	26.64	2.62	26.25	1.13
5.00	26.68	25.80	3.30	26.67	0.06	26.39	1.08
6.00	27.57	25.93	5.92	26.73	3.01	26.57	3.61
7.00	28.65	26.10	8.90	26.84	6.30	26.77	6.55
8.00	30.74	26.29	14.47	26.99	12.20	27.00	12.18
9.00	31.74	26.52	16.45	27.17	14.40	27.24	14.17
10.00	32.73	26.77	18.23	27.37	16.37	27.50	16.00
11.00	33.49	27.04	19.28	27.61	17.57	27.76	17.10
12.00	34.27	27.32	20.27	27.86	18.70	28.05	18.16
13.00	35.05	27.63	21.17	28.13	19.74	28.33	19.15
14.00	35.71	27.94	21.75	28.41	20.43	28.63	19.82
15.00	36.33	28.27	22.19	28.71	20.97	28.93	20.36
16.00	36.89	28.60	22.48	29.01	21.35	29.24	20.74
17.00	37.36	28.93	22.56	29.33	21.51	29.55	20.91
18.00	37.76	29.27	22.47	29.64	21.50	29.86	20.92
19.00	38.11	29.61	22.30	29.96	21.40	30.17	20.83
20.00	38.46	29.95	22.11	30.28	21.26	30.49	20.73
21.00	38.72	30.29	21.76	30.60	20.97	30.80	20.46
22.00	38.94	30.63	21.35	30.92	20.61	31.11	20.13
23.00	39.09	30.96	20.78	31.23	20.09	31.41	19.64
24.00	39.40	31.29	20.57	31.55	19.93	31.71	19.51
25.00	39.58	31.62	20.13	31.85	19.53	32.01	19.13
26.00	39.77	31.93	19.70	32.16	19.14	32.30	18.78
27.00	39.94	32.24	19.26	32.45	18.73	32.59	18.40
28.00	40.38	32.55	19.39	32.75	18.90	32.87	18.60
29.00	40.38	32.84	18.66	33.03	18.20	33.14	17.93
30.00	40.38	33.13	17.95	33.31	17.52	33.40	17.28
31.00	40.50	33.41	17.49	33.58	17.09	33.66	16.87
32.00	40.60	33.68	17.04	33.84	16.65	33.91	16.47
33.00	40.69	33.94	16.58	34.09	16.22	34.16	16.06
34.00	40.77	34.20	16.13	34.33	15.80	34.39	15.66
35.00	40.84	34.44	15.67	34.57	15.36	34.62	15.24
36.00	40.90	34.67	15.23	34.80	14.93	34.83	14.84
37.00	40.96	34.90	14.80	35.01	14.52	35.04	14.45
38.00	41.01	35.11	14.39	35.22	14.12	35.24	14.07
39.00	41.06	35.32	13.98	35.42	13.73	35.43	13.70
40.00	41.10	35.51	13.59	35.61	13.36	35.61	13.35
41.00	41.13	35.70	13.20	35.79	12.99	35.79	12.99
42.00	41.15	35.88	12.81	35.96	12.60	35.95	12.62
43.00	41.16	36.05	12.42	36.13	12.22	36.11	12.26
44.00	41.15	36.20	12.02	36.28	11.84	36.26	11.89
45.00	41.14	36.35	11.62	36.42	11.45	36.40	11.52
46.00	41.11	36.50	11.23	36.56	11.07	36.53	11.15
46.33	41.10	36.51	11.17	36.65	10.83	36.35	11.56
46.67	41.05	36.55	10.94	36.55	10.94	36.61	10.80
48.67	40.99	36.80	10.23	36.80	10.23	36.84	10.12
50.67	40.94	37.01	9.61	37.01	9.61	37.04	9.52
52.67	40.89	37.19	9.07	37.19	9.07	37.21	9.01
54.67	40.84	37.34	8.56	37.34	8.56	37.36	8.51
56.67	40.77	37.49	8.05	37.49	8.05	37.50	8.02
58.67	40.70	37.63	7.55	37.63	7.55	37.63	7.54
60.67	40.62	37.75	7.08	37.75	7.08	37.75	7.08
62.67	40.53	37.85	6.59	37.85	6.59	37.85	6.61
64.67	40.35	37.95	5.96	37.95	5.96	37.94	5.98
66.67	40.28	38.02	5.61	38.02	5.61	38.01	5.64
68.67	40.15	38.09	5.12	38.09	5.12	38.07	5.16
70.67	40.01	38.14	4.68	38.14	4.68	38.12	4.72
72.67	39.88	38.18	4.27	38.18	4.27	38.16	4.32
74.67	39.77	38.21	3.92	38.21	3.92	38.19	3.97
76.67	39.67	38.23	3.63	38.23	3.63	38.21	3.68
78.67	39.56	38.23	3.35	38.23	3.35	38.21	3.40
80.67	39.43	38.23	3.05	38.23	3.05	38.21	3.10

82.67	39.30	38.22	2.74	38.22	2.74	38.20	2.80
84.67	39.17	38.20	2.47	38.20	2.47	38.18	2.53
86.67	39.04	38.17	2.22	38.17	2.22	38.15	2.27
88.67	38.90	38.14	1.95	38.14	1.95	38.12	2.00
90.67	38.75	38.10	1.67	38.10	1.67	38.08	1.72
92.67	38.58	38.05	1.38	38.05	1.38	38.03	1.42
94.67	38.42	38.00	1.08	38.00	1.08	37.98	1.13
96.67	38.25	37.94	0.81	37.94	0.81	37.93	0.85
98.67	38.11	37.88	0.58	37.88	0.58	37.87	0.63
100.67	37.97	37.82	0.40	37.82	0.40	37.80	0.44
102.67	37.84	37.75	0.24	37.75	0.24	37.73	0.28
104.67	37.71	37.68	0.08	37.68	0.08	37.66	0.12
106.67	37.57	37.59	0.04	37.59	0.04	37.57	0.01
108.67	37.43	37.48	0.15	37.48	0.15	37.46	0.09
110.67	37.28	37.37	0.25	37.37	0.25	37.35	0.20
112.67	37.12	37.26	0.38	37.26	0.38	37.25	0.33
114.67	37.05	37.15	0.28	37.15	0.28	37.14	0.24
116.67	36.98	37.04	0.18	37.04	0.18	37.03	0.14
118.67	36.63	36.93	0.81	36.93	0.81	36.92	0.77
120.67	36.46	36.82	0.97	36.82	0.97	36.80	0.93
122.67	36.31	36.70	1.08	36.70	1.08	36.69	1.05
124.67	36.16	36.58	1.16	36.58	1.16	36.57	1.12
126.67	36.03	36.46	1.20	36.46	1.20	36.45	1.17
128.67	35.89	36.34	1.24	36.34	1.24	36.33	1.22
130.67	35.76	36.21	1.28	36.21	1.28	36.20	1.25
132.67	35.61	36.09	1.35	36.09	1.35	36.31	1.98
134.67	35.45	35.96	1.43	35.96	1.43	36.20	2.10
136.67	35.30	35.83	1.51	35.83	1.51	36.08	2.21
138.67	35.23	35.71	1.35	35.71	1.35	35.96	2.08
140.67	35.06	35.58	1.47	35.58	1.47	35.84	2.23
142.67	34.81	35.44	1.82	35.44	1.82	35.72	2.61
144.67	34.72	35.31	1.71	35.31	1.71	35.59	2.52
146.67	34.57	35.18	1.76	35.18	1.77	35.47	2.60
148.67	34.38	35.05	1.94	35.05	1.94	35.34	2.80
150.67	34.26	34.91	1.91	34.91	1.91	35.22	2.80
152.67	34.14	34.78	1.87	34.78	1.87	35.09	2.78
154.67	34.02	34.64	1.84	34.64	1.84	34.96	2.76
156.67	33.89	34.51	1.83	34.51	1.83	34.83	2.77
158.67	33.75	34.37	1.83	34.37	1.83	34.69	2.80
160.67	33.61	34.23	1.85	34.23	1.85	34.56	2.83
162.67	33.46	34.10	1.91	34.10	1.91	34.43	2.90
164.67	33.29	33.96	2.00	33.96	2.00	34.30	3.02
166.67	33.12	33.82	2.11	33.82	2.11	34.16	3.14
168.67	32.98	33.68	2.13	33.68	2.13	34.03	3.17
170.67	32.83	33.55	2.19	33.55	2.19	33.89	3.25
172.67	32.70	33.41	2.18	33.41	2.18	33.76	3.25
174.67	32.59	33.27	2.08	33.27	2.08	33.62	3.16
176.67	32.43	33.13	2.18	33.13	2.18	33.49	3.28
178.67	32.33	33.00	2.04	33.00	2.04	33.35	3.15
180.67	32.14	32.86	2.23	32.86	2.23	33.22	3.34
182.67	32.04	32.72	2.13	32.72	2.13	33.08	3.25
184.67	31.89	32.59	2.19	32.59	2.19	32.95	3.33
186.67	31.66	32.45	2.50	32.45	2.50	32.81	3.65
188.67	31.49	32.31	2.62	32.31	2.62	32.68	3.77
190.67	31.32	32.18	2.72	32.18	2.72	32.54	3.89
192.67	31.17	32.04	2.80	32.04	2.80	32.41	3.97
194.67	31.02	31.91	2.86	31.91	2.86	32.27	4.04
196.67	30.99	31.77	2.49	31.77	2.49	32.13	3.68
198.67	30.88	31.61	2.37	31.61	2.37	31.99	3.58
200.67	30.65	31.47	2.69	31.47	2.69	31.84	3.90
202.67	30.53	31.35	2.69	31.35	2.69	31.71	3.89
204.67	30.40	31.24	2.74	31.24	2.74	31.60	3.92
206.67	30.35	31.13	2.57	31.13	2.57	31.49	3.74
208.67	30.30	31.03	2.42	31.03	2.42	31.38	3.57
210.67	30.04	30.94	2.99	30.94	2.99	31.28	4.13
212.67	29.92	30.85	3.11	30.85	3.11	31.19	4.24
214.67	29.80	30.76	3.23	30.76	3.23	31.09	4.35

216.67	29.69	30.68	3.31	30.68	3.31	31.00	4.41
218.67	29.60	30.59	3.37	30.59	3.37	30.92	4.46
220.67	29.59	30.51	3.12	30.51	3.12	30.83	4.19
222.67	29.59	30.44	2.88	30.44	2.88	30.75	3.93
224.67	29.51	30.36	2.89	30.36	2.89	30.67	3.93
226.67	29.26	30.29	3.52	30.29	3.52	30.59	4.54
228.67	29.18	30.21	3.53	30.21	3.53	30.51	4.54
230.67	29.11	30.14	3.55	30.14	3.55	30.43	4.54
232.67	29.03	30.07	3.58	30.07	3.58	30.36	4.55
234.67	28.95	30.00	3.64	30.00	3.64	30.28	4.60
236.67	28.87	29.94	3.71	29.94	3.71	30.21	4.65
238.67	28.78	29.87	3.78	29.87	3.78	30.14	4.71
240.67	28.70	29.80	3.83	29.80	3.83	30.07	4.75
242.67	28.64	29.74	3.86	29.74	3.86	30.00	4.76
244.67	28.58	29.68	3.85	29.68	3.85	29.93	4.74
246.67	28.52	29.62	3.85	29.62	3.85	29.86	4.72
248.67	28.46	29.55	3.83	29.55	3.83	29.80	4.69
250.67	28.41	29.49	3.82	29.49	3.82	29.73	4.67
252.67	28.36	29.43	3.80	29.43	3.80	29.67	4.63
254.67	28.30	29.37	3.78	29.37	3.78	29.61	4.60
256.67	28.25	29.32	3.77	29.32	3.77	29.54	4.57
258.67	28.20	29.26	3.77	29.26	3.77	29.48	4.56
260.67	28.14	29.20	3.76	29.20	3.76	29.42	4.54
262.67	28.09	29.15	3.76	29.15	3.76	29.36	4.53
264.67	28.04	29.09	3.74	29.09	3.74	29.30	4.49
266.67	28.00	29.04	3.70	29.04	3.70	29.24	4.44
268.67	27.96	28.98	3.64	28.98	3.64	29.19	4.37
270.67	27.93	28.93	3.56	28.93	3.56	29.13	4.28
272.67	27.91	28.88	3.47	28.88	3.47	29.07	4.18
274.67	27.88	28.82	3.37	28.82	3.37	29.02	4.07
276.67	27.85	28.77	3.29	28.77	3.29	28.96	3.98
278.67	27.82	28.72	3.22	28.72	3.22	28.91	3.89
280.67	27.78	28.67	3.19	28.67	3.19	28.85	3.85
282.67	27.74	28.62	3.16	28.62	3.16	28.80	3.81
284.67	27.69	28.57	3.16	28.57	3.16	28.75	3.81
285.00	27.59	28.58	3.58	28.58	3.58	28.58	3.58
287.00	27.52	28.54	3.72	28.54	3.72	28.54	3.72
289.00	27.51	28.50	3.62	28.50	3.62	28.50	3.62
291.00	27.50	28.46	3.51	28.46	3.51	28.46	3.51
293.00	27.50	28.42	3.37	28.42	3.37	28.42	3.37
295.00	27.49	28.38	3.23	28.38	3.23	28.38	3.23
297.00	27.49	28.34	3.09	28.34	3.09	28.34	3.09
299.00	27.49	28.30	2.94	28.30	2.94	28.30	2.94
301.00	27.49	28.26	2.79	28.26	2.79	28.26	2.79
303.00	27.49	28.22	2.64	28.22	2.64	28.22	2.64
305.00	27.49	28.18	2.49	28.18	2.49	28.18	2.49
307.00	27.49	28.14	2.34	28.14	2.34	28.14	2.34
309.00	27.49	28.10	2.19	28.10	2.19	28.10	2.19
311.00	27.44	28.05	2.22	28.05	2.22	28.05	2.22
313.00	27.39	28.01	2.26	28.01	2.26	28.01	2.26
315.00	27.36	27.97	2.23	27.97	2.23	27.97	2.23
317.00	27.35	27.93	2.11	27.93	2.11	27.93	2.11
319.00	27.35	27.89	1.99	27.89	1.99	27.89	1.99
321.00	27.33	27.85	1.91	27.85	1.91	27.85	1.91
323.00	27.31	27.81	1.83	27.81	1.83	27.81	1.83
325.00	27.28	27.77	1.80	27.77	1.80	27.77	1.80
327.00	27.26	27.73	1.70	27.73	1.70	27.73	1.70
329.00	27.25	27.68	1.61	27.68	1.61	27.68	1.61
331.00	27.20	27.64	1.65	27.64	1.65	27.64	1.65
333.00	27.17	27.60	1.59	27.60	1.59	27.60	1.59
335.00	27.16	27.56	1.49	27.56	1.49	27.56	1.49
337.00	27.15	27.52	1.37	27.52	1.37	27.52	1.37
339.00	27.15	27.48	1.24	27.48	1.24	27.48	1.24
341.00	27.06	27.44	1.41	27.44	1.41	27.44	1.41
343.00	27.02	27.41	1.42	27.41	1.42	27.41	1.42
345.00	27.00	27.37	1.35	27.37	1.35	27.37	1.35
347.00	26.99	27.33	1.24	27.33	1.24	27.33	1.24

349.00	26.99	27.29	1.12	27.29	1.12	27.29	1.12
351.00	26.98	27.25	0.99	27.25	0.99	27.25	0.99
353.00	26.98	27.21	0.85	27.21	0.85	27.21	0.85
355.00	26.78	27.17	1.45	27.17	1.45	27.17	1.45
357.00	26.69	27.14	1.69	27.14	1.69	27.14	1.69
359.00	26.64	27.10	1.73	27.10	1.73	27.10	1.73
361.00	26.61	27.06	1.69	27.06	1.69	27.06	1.69
363.00	26.60	27.02	1.59	27.02	1.59	27.02	1.59
365.00	26.59	26.99	1.48	26.99	1.48	26.99	1.48
367.00	26.59	26.95	1.36	26.95	1.36	26.95	1.36
369.00	26.29	26.91	2.35	26.91	2.35	26.91	2.35
371.00	26.26	26.88	2.34	26.88	2.34	26.88	2.34
373.00	26.09	26.84	2.87	26.84	2.87	26.84	2.87
375.00	26.06	26.80	2.86	26.80	2.86	26.80	2.86
377.00	25.94	26.77	3.19	26.77	3.19	26.77	3.19
379.00	25.92	26.73	3.12	26.73	3.12	26.73	3.12
381.00	25.84	26.69	3.32	26.69	3.32	26.69	3.32
383.00	25.82	26.66	3.24	26.66	3.24	26.66	3.24
385.00	25.76	26.62	3.34	26.62	3.34	26.62	3.34
387.00	25.75	26.59	3.24	26.59	3.24	26.59	3.24
389.00	25.71	26.55	3.27	26.55	3.27	26.55	3.27
391.00	25.70	26.52	3.16	26.52	3.16	26.52	3.16
393.00	25.67	26.48	3.14	26.48	3.14	26.48	3.14
395.00	25.58	26.44	3.36	26.44	3.36	26.44	3.36
397.00	25.53	26.41	3.45	26.41	3.45	26.41	3.45
399.00	25.40	26.37	3.82	26.37	3.82	26.37	3.82
401.00	25.34	26.34	3.93	26.34	3.93	26.34	3.93
403.00	25.28	26.30	4.05	26.30	4.05	26.30	4.05
405.00	25.16	26.27	4.39	26.27	4.39	26.27	4.39
407.00	25.09	26.23	4.57	26.23	4.57	26.23	4.57
409.00	24.95	26.20	4.99	26.20	4.99	26.20	4.99
411.00	24.89	26.16	5.10	26.16	5.10	26.16	5.10
413.00	24.86	26.13	5.12	26.13	5.12	26.13	5.12
415.00	24.79	26.09	5.26	26.09	5.26	26.09	5.26
417.00	24.76	26.06	5.24	26.06	5.24	26.06	5.24
419.00	24.74	26.02	5.18	26.02	5.18	26.02	5.18
421.00	24.71	25.99	5.19	25.99	5.19	25.99	5.19
423.00	24.69	25.95	5.11	25.95	5.11	25.95	5.11
425.00	24.68	25.92	5.01	25.92	5.01	25.92	5.01
427.00	24.67	25.88	4.93	25.88	4.93	25.88	4.93
429.00	24.63	25.85	4.97	25.85	4.97	25.85	4.97
431.00	24.62	25.81	4.85	25.81	4.85	25.81	4.85
433.00	24.62	25.78	4.72	25.78	4.72	25.78	4.72
435.00	24.56	25.74	4.80	25.74	4.80	25.74	4.80
437.00	24.50	25.71	4.92	25.71	4.92	25.71	4.92
439.00	24.48	25.67	4.86	25.67	4.86	25.67	4.86
441.00	24.45	25.64	4.84	25.64	4.84	25.64	4.84
443.00	24.44	25.60	4.74	25.60	4.74	25.60	4.74
445.00	24.43	25.57	4.66	25.57	4.66	25.57	4.66
447.00	24.42	25.53	4.54	25.53	4.54	25.53	4.54
449.00	24.40	25.49	4.48	25.49	4.48	25.49	4.48
451.00	24.37	25.46	4.46	25.46	4.46	25.46	4.46
453.00	24.37	25.42	4.32	25.42	4.32	25.42	4.32
455.00	24.36	25.39	4.21	25.39	4.21	25.39	4.21
457.00	24.34	25.35	4.13	25.35	4.13	25.35	4.13
459.00	24.34	25.31	3.98	25.31	3.98	25.31	3.98
461.00	24.34	25.28	3.85	25.28	3.85	25.28	3.85
463.00	24.33	25.24	3.73	25.24	3.73	25.24	3.73
465.00	24.33	25.20	3.58	25.20	3.58	25.20	3.58
467.00	24.32	25.16	3.48	25.16	3.48	25.16	3.48
469.00	24.23	25.13	3.72	25.13	3.72	25.13	3.72
471.00	24.21	25.09	3.64	25.09	3.64	25.09	3.64
473.00	24.19	25.05	3.55	25.05	3.55	25.05	3.55
475.00	24.14	25.01	3.59	25.01	3.59	25.01	3.59

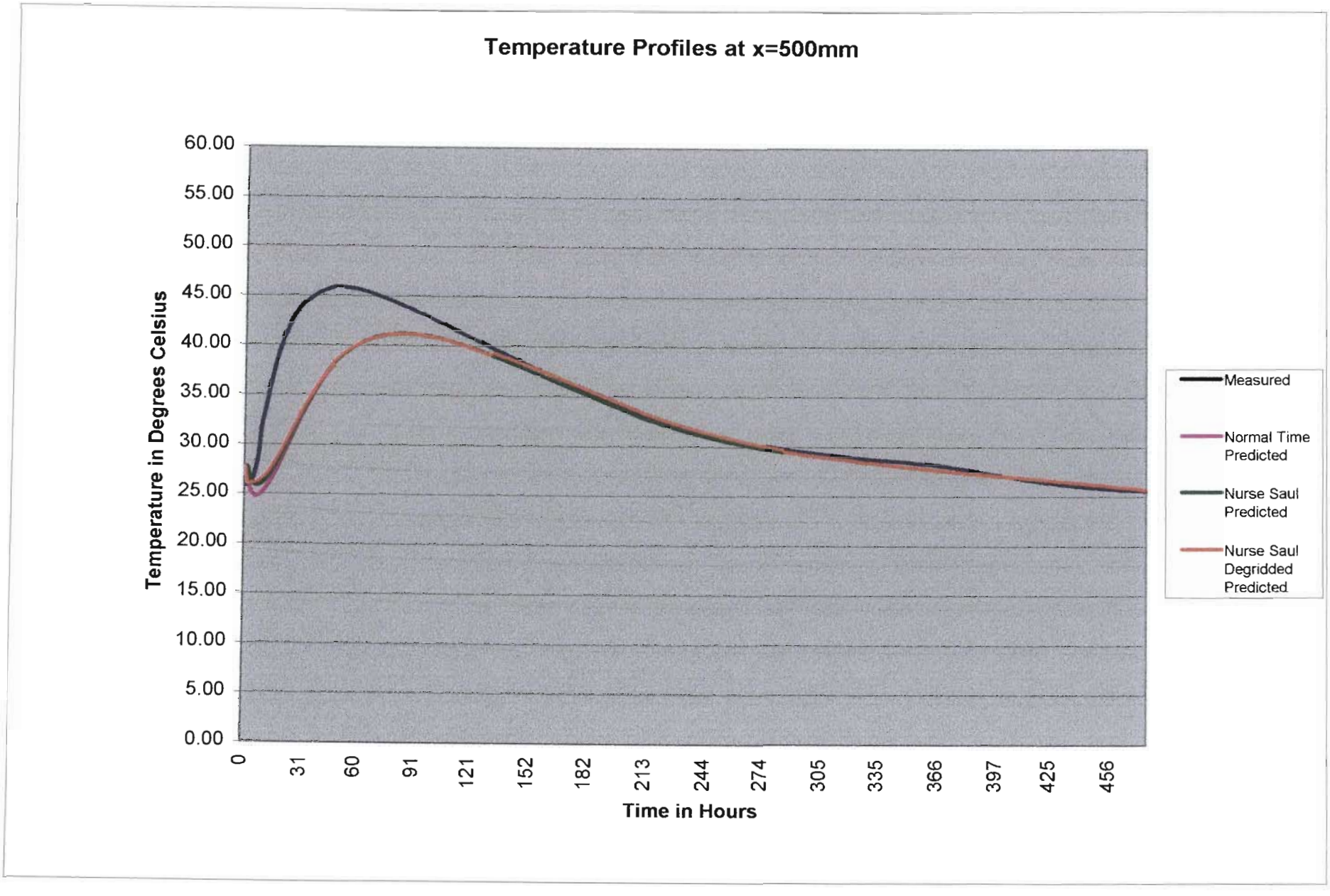
Temperature Profiles at x=500mm
Temperature in Degrees Celsius
60.00
55.00
50.00
45.00
40.00
35.00
30.00
25.00
20.00
15.00
10.00
5.00
0.00
0
31
60
91
121
152
182
213
244
274
305
335
366
397
425
456
Time in Hours
Measured
Normal Time Predicted
Nurse Saul Predicted
Nurse Saul Degridded Predicted

Time(Hours)	X=500(Exp)	X=500(Num)	% Error	X=500(Num.ns)	% Error	X=500(Num.deg)	% Error
0.00	25.81	27.73	7.46	27.73	7.46	27.73	7.46
1.00	25.89	26.50	2.35	27.74	7.15	26.06	0.66
2.00	25.95	25.66	1.14	26.90	3.64	26.06	0.44
3.00	26.18	25.14	3.98	26.35	0.66	26.08	0.41
4.00	26.67	24.87	6.74	26.05	2.34	26.10	2.14
5.00	27.36	24.78	9.44	25.90	5.35	26.15	4.43
6.00	28.26	24.80	12.25	25.86	8.49	26.23	7.20
7.00	29.41	24.91	15.31	25.91	11.90	26.33	10.45
8.00	31.58	25.07	20.62	26.02	17.62	26.47	16.17
9.00	32.65	25.28	22.57	26.17	19.84	26.65	18.40
10.00	33.61	25.53	24.04	26.37	21.54	26.85	20.13
11.00	34.57	25.82	25.33	26.61	23.04	27.07	21.69
12.00	35.49	26.13	26.38	26.87	24.28	27.33	22.99
13.00	36.38	26.46	27.27	27.16	25.35	27.60	24.13
14.00	37.21	26.81	27.96	27.47	26.19	27.90	25.03
15.00	37.99	27.18	28.47	27.80	26.84	28.21	25.75
16.00	38.71	27.56	28.81	28.14	27.30	28.54	26.28
17.00	39.35	27.95	28.97	28.50	27.58	28.88	26.63
18.00	39.94	28.35	29.01	28.87	27.72	29.23	26.83
19.00	40.47	28.76	28.94	29.25	27.74	29.58	26.90
20.00	41.00	29.18	28.84	29.63	27.73	29.95	26.95
21.00	41.44	29.59	28.59	30.02	27.55	30.32	26.84
22.00	41.85	30.01	28.28	30.41	27.32	30.69	26.65
23.00	42.20	30.43	27.90	30.81	27.00	31.07	26.39
24.00	42.59	30.85	27.57	31.20	26.73	31.44	26.17
25.00	42.91	31.26	27.15	31.60	26.36	31.82	25.85
26.00	43.20	31.67	26.69	31.99	25.96	32.19	25.49
27.00	43.48	32.08	26.22	32.38	25.54	32.56	25.12
28.00	43.72	32.48	25.71	32.76	25.07	32.92	24.70
29.00	43.94	32.87	25.19	33.14	24.59	33.28	24.26
30.00	44.16	33.26	24.68	33.51	24.12	33.64	23.83
31.00	44.35	33.64	24.14	33.87	23.62	33.99	23.36
32.00	44.53	34.01	23.62	34.23	23.13	34.33	22.91
33.00	44.69	34.38	23.08	34.58	22.62	34.66	22.44
34.00	44.84	34.73	22.55	34.92	22.11	34.99	21.96
35.00	44.99	35.07	22.04	35.25	21.63	35.31	21.52
36.00	45.11	35.40	21.52	35.58	21.14	35.62	21.05
37.00	45.22	35.73	21.00	35.89	20.64	35.91	20.58
38.00	45.34	36.04	20.51	36.19	20.18	36.20	20.14
39.00	45.42	36.34	20.00	36.48	19.69	36.48	19.68
40.00	45.50	36.63	19.50	36.76	19.21	36.75	19.22
41.00	45.58	36.91	19.04	37.03	18.76	37.01	18.80
42.00	45.65	37.17	18.57	37.29	18.31	37.26	18.37
43.00	45.71	37.43	18.12	37.54	17.87	37.50	17.95
44.00	45.77	37.67	17.69	37.78	17.46	37.73	17.56
45.00	45.81	37.91	17.25	38.00	17.04	37.95	17.15
46.00	45.85	38.13	16.84	38.22	16.63	38.16	16.76
46.33	45.85	38.16	16.78	38.34	16.38	37.88	17.38
46.67	45.90	38.23	16.71	38.23	16.71	38.30	16.56
48.67	45.91	38.62	15.87	38.62	15.87	38.67	15.76
50.67	45.91	38.97	15.10	38.97	15.10	39.01	15.03
52.67	45.88	39.28	14.38	39.28	14.38	39.31	14.31
54.67	45.84	39.58	13.66	39.58	13.66	39.59	13.63
56.67	45.78	39.84	12.97	39.84	12.97	39.84	12.96
58.67	45.71	40.08	12.33	40.08	12.33	40.07	12.34
60.67	45.63	40.28	11.71	40.28	11.71	40.27	11.74
62.67	45.54	40.47	11.14	40.47	11.14	40.45	11.18
64.67	45.44	40.63	10.58	40.63	10.58	40.61	10.63
66.67	45.33	40.77	10.07	40.77	10.07	40.74	10.12
68.67	45.19	40.88	9.52	40.88	9.52	40.86	9.59
70.67	45.06	40.98	9.04	40.98	9.04	40.95	9.11
72.67	44.91	41.06	8.57	41.06	8.57	41.03	8.64
74.67	44.77	41.13	8.12	41.13	8.12	41.10	8.19
76.67	44.62	41.18	7.71	41.18	7.71	41.15	7.78
78.67	44.47	41.21	7.32	41.21	7.32	41.18	7.39
80.67	44.32	41.24	6.95	41.24	6.95	41.20	7.02

82.67	44.16	41.25	6.59	41.25	6.59	41.21	6.66
84.67	43.99	41.24	6.25	41.24	6.25	41.21	6.32
86.67	43.85	41.23	5.97	41.23	5.97	41.20	6.04
88.67	43.68	41.21	5.67	41.21	5.67	41.18	5.74
90.67	43.52	41.17	5.38	41.17	5.38	41.15	5.44
92.67	43.34	41.13	5.09	41.13	5.09	41.11	5.15
94.67	43.18	41.08	4.85	41.08	4.85	41.06	4.91
96.67	42.99	41.03	4.57	41.03	4.57	41.00	4.63
98.67	42.82	40.97	4.34	40.97	4.34	40.94	4.39
100.67	42.65	40.90	4.10	40.90	4.10	40.87	4.16
102.67	42.47	40.82	3.87	40.82	3.87	40.80	3.92
104.67	42.29	40.74	3.66	40.74	3.66	40.72	3.70
106.67	42.12	40.66	3.45	40.66	3.45	40.64	3.50
108.67	41.95	40.57	3.27	40.57	3.27	40.55	3.33
110.67	41.77	40.47	3.11	40.47	3.11	40.44	3.18
112.67	41.59	40.36	2.98	40.36	2.98	40.33	3.04
114.67	41.41	40.24	2.84	40.24	2.84	40.21	2.90
116.67	41.23	40.11	2.70	40.11	2.70	40.09	2.76
118.67	41.05	39.98	2.60	39.98	2.60	39.96	2.65
120.67	40.86	39.85	2.48	39.85	2.48	39.83	2.52
122.67	40.68	39.72	2.36	39.72	2.36	39.70	2.40
124.67	40.49	39.58	2.24	39.58	2.24	39.57	2.28
126.67	40.32	39.44	2.17	39.44	2.17	39.43	2.21
128.67	40.13	39.30	2.07	39.30	2.07	39.29	2.10
130.67	39.95	39.16	1.97	39.16	1.97	39.15	2.00
132.67	39.78	39.02	1.91	39.02	1.91	39.33	1.12
134.67	39.59	38.87	1.82	38.87	1.82	39.20	0.99
136.67	39.42	38.72	1.77	38.72	1.77	39.07	0.89
138.67	39.23	38.57	1.67	38.57	1.67	38.93	0.75
140.67	39.05	38.42	1.61	38.42	1.61	38.80	0.66
142.67	38.88	38.27	1.55	38.27	1.55	38.66	0.57
144.67	38.70	38.12	1.48	38.12	1.48	38.52	0.46
146.67	38.52	37.97	1.44	37.97	1.44	38.37	0.38
148.67	38.34	37.81	1.37	37.81	1.37	38.23	0.29
150.67	38.17	37.66	1.34	37.66	1.34	38.08	0.23
152.67	37.99	37.50	1.28	37.50	1.28	37.94	0.14
154.67	37.82	37.35	1.26	37.35	1.26	37.79	0.10
156.67	37.66	37.19	1.25	37.19	1.25	37.64	0.06
158.67	37.48	37.03	1.19	37.03	1.19	37.49	0.02
160.67	37.32	36.87	1.20	36.87	1.20	37.34	0.03
162.67	37.16	36.72	1.19	36.72	1.19	37.18	0.06
164.67	36.99	36.56	1.17	36.56	1.17	37.03	0.11
166.67	36.82	36.40	1.14	36.40	1.14	36.88	0.15
168.67	36.64	36.24	1.09	36.24	1.09	36.72	0.23
170.67	36.48	36.08	1.09	36.08	1.09	36.57	0.24
172.67	36.31	35.92	1.08	35.92	1.08	36.41	0.27
174.67	36.14	35.76	1.06	35.76	1.06	36.25	0.31
176.67	35.98	35.60	1.06	35.60	1.06	36.10	0.32
178.67	35.81	35.44	1.04	35.44	1.04	35.94	0.36
180.67	35.66	35.28	1.06	35.28	1.06	35.79	0.35
182.67	35.50	35.13	1.06	35.13	1.06	35.63	0.36
184.67	35.33	34.97	1.03	34.97	1.03	35.47	0.40
186.67	35.17	34.81	1.01	34.81	1.01	35.32	0.43
188.67	35.01	34.65	1.02	34.65	1.02	35.16	0.43
190.67	34.85	34.49	1.01	34.49	1.01	35.00	0.45
192.67	34.67	34.34	0.96	34.34	0.96	34.85	0.50
194.67	34.51	34.18	0.96	34.18	0.96	34.69	0.52
196.67	34.35	34.03	0.94	34.03	0.94	34.54	0.55
198.67	34.20	33.87	0.97	33.87	0.97	34.38	0.53
200.67	34.03	33.71	0.95	33.71	0.95	34.22	0.57
202.67	33.88	33.54	1.00	33.54	1.00	34.06	0.53
204.67	33.74	33.38	1.07	33.38	1.07	33.90	0.47
206.67	33.59	33.23	1.07	33.23	1.07	33.75	0.46
208.67	33.45	33.08	1.10	33.08	1.10	33.59	0.43
210.67	33.30	32.94	1.09	32.94	1.09	33.44	0.43
212.67	33.16	32.80	1.08	32.80	1.08	33.30	0.42
214.67	33.02	32.67	1.08	32.67	1.08	33.16	0.41

216.67	32.88	32.53	1.06	32.54	1.06	33.02	0.41
218.67	32.74	32.41	1.02	32.41	1.02	32.88	0.44
220.67	32.61	32.29	1.01	32.29	1.01	32.75	0.43
222.67	32.49	32.17	0.99	32.17	0.99	32.63	0.43
224.67	32.36	32.05	0.96	32.05	0.96	32.50	0.43
226.67	32.25	31.94	0.96	31.94	0.96	32.38	0.42
228.67	32.13	31.83	0.93	31.83	0.93	32.26	0.42
230.67	32.02	31.72	0.93	31.72	0.93	32.15	0.40
232.67	31.91	31.61	0.92	31.61	0.92	32.03	0.39
234.67	31.79	31.51	0.89	31.51	0.89	31.92	0.40
236.67	31.68	31.41	0.86	31.41	0.86	31.81	0.41
238.67	31.59	31.31	0.88	31.31	0.88	31.70	0.37
240.67	31.48	31.21	0.85	31.21	0.85	31.60	0.39
242.67	31.37	31.12	0.82	31.12	0.82	31.50	0.39
244.67	31.29	31.02	0.84	31.02	0.84	31.40	0.35
246.67	31.19	30.93	0.81	30.93	0.81	31.30	0.36
248.67	31.09	30.84	0.80	30.84	0.80	31.20	0.35
250.67	31.00	30.76	0.79	30.76	0.79	31.11	0.35
252.67	30.92	30.67	0.82	30.67	0.82	31.02	0.30
254.67	30.84	30.59	0.81	30.59	0.81	30.92	0.29
256.67	30.75	30.50	0.80	30.50	0.80	30.84	0.28
258.67	30.67	30.42	0.81	30.42	0.81	30.75	0.25
260.67	30.59	30.34	0.81	30.34	0.81	30.66	0.24
262.67	30.52	30.26	0.83	30.26	0.83	30.58	0.19
264.67	30.44	30.19	0.84	30.19	0.84	30.49	0.18
266.67	30.36	30.11	0.84	30.11	0.84	30.41	0.16
268.67	30.29	30.04	0.85	30.04	0.85	30.33	0.13
270.67	30.23	29.96	0.87	29.96	0.87	30.25	0.09
272.67	30.17	29.89	0.91	29.89	0.91	30.18	0.03
274.67	30.11	29.82	0.95	29.82	0.95	30.10	0.02
276.67	30.05	29.75	0.98	29.75	0.98	30.03	0.07
278.67	30.00	29.68	1.07	29.68	1.07	29.95	0.16
280.67	29.94	29.62	1.09	29.62	1.09	29.88	0.20
282.67	29.89	29.55	1.13	29.55	1.13	29.81	0.25
284.67	29.83	29.48	1.15	29.48	1.15	29.74	0.29
285.00	29.78	29.51	0.91	29.51	0.91	29.51	0.91
287.00	29.73	29.46	0.91	29.46	0.91	29.46	0.91
289.00	29.66	29.41	0.86	29.41	0.86	29.41	0.86
291.00	29.61	29.36	0.84	29.36	0.84	29.36	0.84
293.00	29.55	29.31	0.83	29.31	0.83	29.31	0.83
295.00	29.51	29.26	0.86	29.26	0.86	29.26	0.86
297.00	29.47	29.21	0.89	29.21	0.89	29.21	0.89
299.00	29.42	29.16	0.89	29.16	0.89	29.16	0.89
301.00	29.38	29.11	0.92	29.11	0.92	29.11	0.92
303.00	29.34	29.06	0.95	29.06	0.95	29.06	0.95
305.00	29.29	29.01	0.96	29.01	0.96	29.01	0.96
307.00	29.24	28.96	0.98	28.96	0.98	28.96	0.98
309.00	29.20	28.91	0.98	28.91	0.98	28.91	0.98
311.00	29.15	28.86	0.98	28.86	0.98	28.86	0.98
313.00	29.10	28.81	0.98	28.81	0.98	28.81	0.98
315.00	29.06	28.76	1.02	28.76	1.02	28.76	1.02
317.00	29.00	28.71	1.00	28.71	1.00	28.71	1.00
319.00	28.96	28.67	1.03	28.67	1.03	28.67	1.03
321.00	28.94	28.62	1.10	28.62	1.10	28.62	1.10
323.00	28.89	28.57	1.09	28.57	1.09	28.57	1.09
325.00	28.87	28.53	1.18	28.53	1.18	28.53	1.18
327.00	28.81	28.48	1.15	28.48	1.15	28.48	1.15
329.00	28.79	28.43	1.23	28.43	1.23	28.43	1.23
331.00	28.75	28.39	1.26	28.39	1.26	28.39	1.26
333.00	28.71	28.34	1.28	28.34	1.28	28.34	1.28
335.00	28.69	28.30	1.36	28.30	1.36	28.30	1.36
337.00	28.64	28.26	1.34	28.26	1.34	28.26	1.34
339.00	28.62	28.21	1.42	28.21	1.42	28.21	1.42
341.00	28.59	28.17	1.47	28.17	1.47	28.17	1.47
343.00	28.56	28.13	1.51	28.13	1.51	28.13	1.51
345.00	28.53	28.09	1.55	28.09	1.55	28.09	1.55
347.00	28.50	28.05	1.59	28.05	1.59	28.05	1.59

349.00	28.48	28.00	1.67	28.00	1.67	28.00	1.67
351.00	28.45	27.96	1.72	27.96	1.72	27.96	1.72
353.00	28.42	27.92	1.75	27.92	1.75	27.92	1.75
355.00	28.38	27.88	1.76	27.88	1.76	27.88	1.76
357.00	28.34	27.85	1.74	27.85	1.74	27.85	1.74
359.00	28.29	27.81	1.71	27.81	1.71	27.81	1.71
361.00	28.26	27.77	1.73	27.77	1.73	27.77	1.73
363.00	28.21	27.73	1.69	27.73	1.69	27.73	1.69
365.00	28.16	27.69	1.65	27.69	1.65	27.69	1.65
367.00	28.12	27.66	1.65	27.66	1.65	27.66	1.65
369.00	28.07	27.62	1.61	27.62	1.61	27.62	1.61
371.00	28.02	27.58	1.57	27.58	1.57	27.58	1.57
373.00	27.97	27.54	1.53	27.54	1.53	27.54	1.53
375.00	27.91	27.51	1.44	27.51	1.44	27.51	1.44
377.00	27.85	27.47	1.34	27.47	1.34	27.47	1.34
379.00	27.80	27.44	1.29	27.44	1.29	27.44	1.29
381.00	27.72	27.40	1.14	27.40	1.14	27.40	1.14
383.00	27.65	27.37	1.04	27.37	1.04	27.37	1.04
385.00	27.59	27.33	0.93	27.33	0.93	27.33	0.93
387.00	27.53	27.30	0.84	27.30	0.84	27.30	0.84
389.00	27.46	27.26	0.72	27.26	0.72	27.26	0.72
391.00	27.40	27.23	0.61	27.23	0.61	27.23	0.61
393.00	27.34	27.19	0.54	27.19	0.54	27.19	0.54
395.00	27.27	27.16	0.40	27.16	0.40	27.16	0.40
397.00	27.22	27.13	0.37	27.13	0.37	27.13	0.37
399.00	27.17	27.09	0.29	27.09	0.29	27.09	0.29
401.00	27.09	27.06	0.11	27.06	0.11	27.06	0.11
403.00	27.04	27.02	0.08	27.02	0.08	27.02	0.08
405.00	26.98	26.99	0.04	26.99	0.04	26.99	0.04
407.00	26.91	26.96	0.18	26.96	0.18	26.96	0.18
409.00	26.85	26.92	0.28	26.92	0.28	26.92	0.28
411.00	26.78	26.89	0.42	26.89	0.42	26.89	0.42
413.00	26.72	26.85	0.50	26.85	0.50	26.85	0.50
415.00	26.67	26.82	0.56	26.82	0.56	26.82	0.56
417.00	26.60	26.79	0.68	26.79	0.68	26.79	0.68
419.00	26.57	26.75	0.70	26.75	0.70	26.75	0.70
421.00	26.52	26.72	0.76	26.72	0.76	26.72	0.76
423.00	26.45	26.68	0.88	26.68	0.88	26.68	0.88
425.00	26.41	26.65	0.89	26.65	0.89	26.65	0.89
427.00	26.36	26.61	0.95	26.61	0.95	26.61	0.95
429.00	26.31	26.58	1.01	26.58	1.01	26.58	1.01
431.00	26.26	26.54	1.09	26.54	1.09	26.54	1.09
433.00	26.22	26.51	1.12	26.51	1.12	26.51	1.12
435.00	26.17	26.47	1.16	26.47	1.16	26.47	1.16
437.00	26.13	26.44	1.17	26.44	1.17	26.44	1.17
439.00	26.08	26.40	1.25	26.40	1.25	26.40	1.25
441.00	26.06	26.37	1.19	26.37	1.19	26.37	1.19
443.00	26.01	26.33	1.22	26.33	1.22	26.33	1.22
445.00	25.98	26.29	1.21	26.29	1.21	26.29	1.21
447.00	25.95	26.26	1.19	26.26	1.19	26.26	1.19
449.00	25.92	26.22	1.15	26.22	1.15	26.22	1.15
451.00	25.88	26.18	1.16	26.18	1.16	26.18	1.16
453.00	25.85	26.14	1.12	26.14	1.12	26.14	1.12
455.00	25.82	26.10	1.10	26.10	1.10	26.10	1.10
457.00	25.79	26.06	1.05	26.06	1.05	26.06	1.05
459.00	25.77	26.02	1.01	26.02	1.01	26.02	1.01
461.00	25.74	25.98	0.94	25.98	0.94	25.98	0.94
463.00	25.72	25.94	0.89	25.94	0.89	25.94	0.89
465.00	25.70	25.90	0.79	25.90	0.79	25.90	0.79
467.00	25.67	25.86	0.74	25.86	0.74	25.86	0.74
469.00	25.67	25.82	0.60	25.82	0.60	25.82	0.60
471.00	25.64	25.78	0.52	25.78	0.52	25.78	0.52
473.00	25.63	25.73	0.39	25.73	0.39	25.73	0.39
475.00	25.62	25.69	0.29	25.69	0.29	25.69	0.29

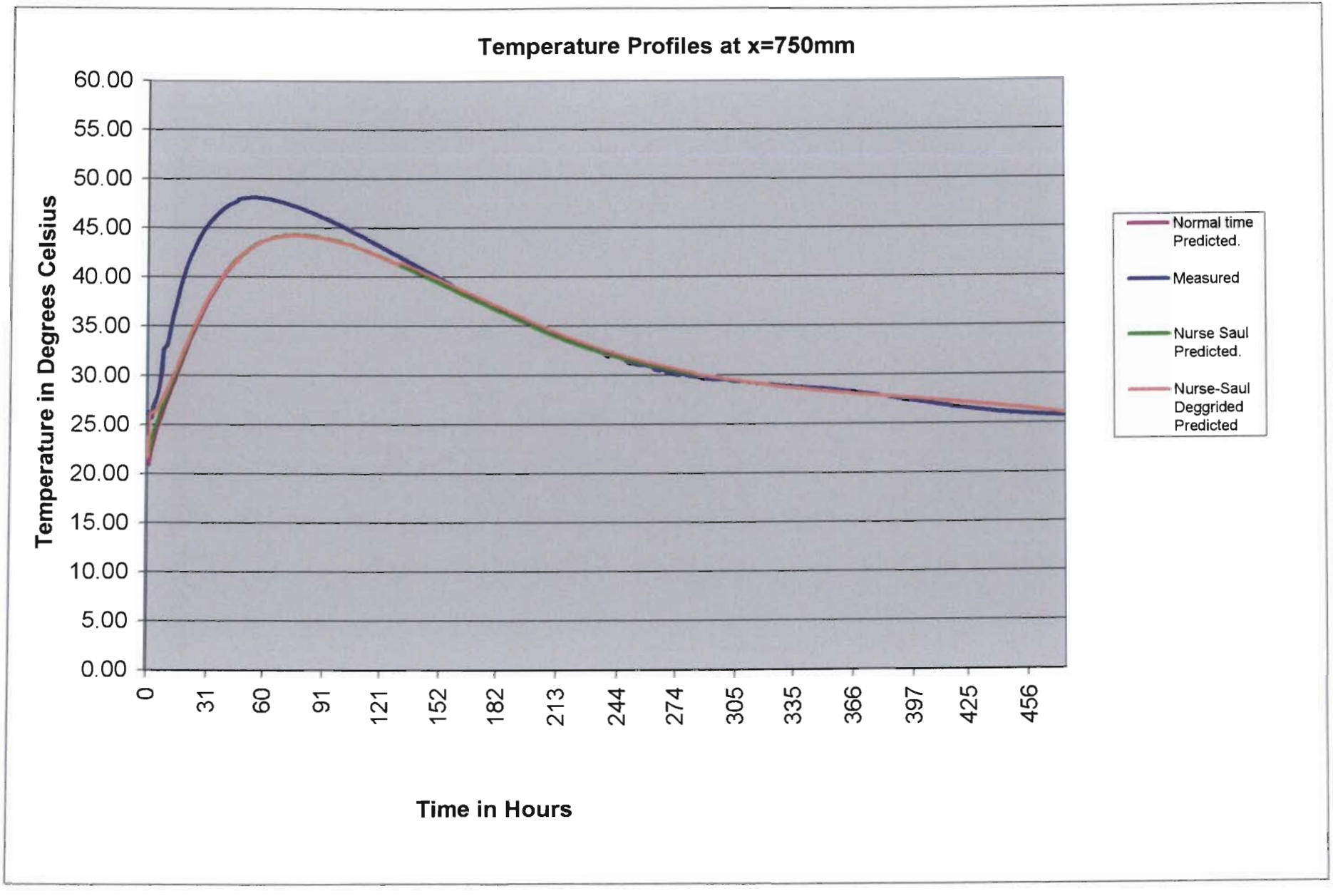
Temperature Profiles at x=750mm
Temperature in Degrees Celsius
60.00
55.00
50.00
45.00
40.00
35.00
30.00
25.00
20.00
15.00
10.00
5.00
0.00
0
31
60
91
121
152
182
213
244
274
305
335
366
397
425
456
Time in Hours
Normal time Predicted.
Measured
Nurse Saul Predicted.
Nurse-Saul Deggrided Predicted

Time(Hours)	X=750(Exp)	X=750(Num)	% Error	X=750(Num.ns)	% Error	X=750(Num.deg)	% Error
0.00	26.40	21.72	17.73	21.72	17.73	21.72	17.73
1.00	25.70	20.94	18.52	22.03	14.28	26.08	1.47
2.00	25.70	22.21	13.58	23.19	9.76	26.13	1.68
3.00	26.86	23.18	13.71	24.08	10.36	26.25	2.27
4.00	27.38	23.96	12.47	24.80	9.41	26.45	3.38
5.00	28.13	24.64	12.41	25.42	9.63	26.71	5.03
6.00	29.10	25.25	13.24	25.98	10.71	27.03	7.13
7.00	30.35	25.82	14.91	26.52	12.62	27.38	9.78
8.00	32.67	26.38	19.25	27.04	17.24	27.76	15.01
9.00	32.92	26.93	18.20	27.55	16.32	28.17	14.42
10.00	33.17	27.47	17.18	28.05	15.42	28.60	13.77
11.00	34.10	28.01	17.87	28.56	16.26	29.04	14.84
12.00	35.13	28.54	18.76	29.06	17.28	29.50	16.04
13.00	36.08	29.08	19.41	29.57	18.05	29.96	16.97
14.00	36.99	29.61	19.94	30.08	18.69	30.43	17.73
15.00	37.83	30.14	20.32	30.58	19.17	30.91	18.31
16.00	38.62	30.67	20.57	31.08	19.51	31.38	18.74
17.00	39.34	31.20	20.71	31.58	19.73	31.86	19.03
18.00	40.01	31.71	20.74	32.08	19.83	32.33	19.20
19.00	40.63	32.23	20.69	32.57	19.85	32.80	19.28
20.00	41.21	32.73	20.57	33.05	19.79	33.27	19.27
21.00	41.74	33.23	20.39	33.53	19.67	33.73	19.20
22.00	42.24	33.72	20.18	34.01	19.50	34.18	19.08
23.00	42.60	34.20	19.73	34.47	19.10	34.63	18.72
24.00	43.15	34.67	19.65	34.92	19.07	35.07	18.73
25.00	43.56	35.13	19.35	35.37	18.81	35.50	18.51
26.00	43.94	35.58	19.03	35.80	18.53	35.92	18.26
27.00	44.30	36.02	18.70	36.23	18.22	36.33	17.99
28.00	44.63	36.44	18.35	36.64	17.90	36.73	17.70
29.00	44.93	36.85	17.98	37.04	17.57	37.12	17.40
30.00	45.22	37.25	17.62	37.43	17.23	37.49	17.08
31.00	45.49	37.64	17.25	37.81	16.89	37.86	16.77
32.00	45.73	38.02	16.88	38.17	16.54	38.21	16.44
33.00	45.97	38.38	16.51	38.52	16.20	38.56	16.12
34.00	46.18	38.72	16.15	38.86	15.86	38.88	15.81
35.00	46.38	39.06	15.80	39.19	15.52	39.20	15.49
36.00	46.57	39.38	15.45	39.50	15.19	39.50	15.18
37.00	46.75	39.68	15.11	39.80	14.86	39.80	14.87
38.00	46.91	39.98	14.78	40.09	14.55	40.07	14.57
39.00	47.06	40.26	14.45	40.36	14.24	40.34	14.28
40.00	47.20	40.52	14.14	40.62	13.94	40.59	13.99
41.00	47.33	40.78	13.84	40.87	13.65	40.83	13.72
42.00	47.44	41.02	13.55	41.10	13.37	41.06	13.45
43.00	47.55	41.25	13.26	41.32	13.10	41.28	13.19
44.00	47.65	41.46	12.99	41.53	12.83	41.49	12.93
45.00	47.73	41.66	12.72	41.73	12.57	41.68	12.68
46.00	47.81	41.85	12.46	41.92	12.32	41.86	12.44
46.33	47.83	41.88	12.45	41.90	12.40	41.62	13.00
46.67	47.95	41.94	12.55	41.94	12.55	41.98	12.47
48.67	48.04	42.27	12.02	42.27	12.02	42.29	11.97
50.67	48.10	42.54	11.55	42.54	11.55	42.58	11.48
52.67	48.14	42.89	10.90	42.89	10.90	42.89	10.91
54.67	48.15	43.17	10.34	43.17	10.34	43.16	10.36
56.67	48.14	43.40	9.84	43.40	9.84	43.39	9.86
58.67	48.11	43.60	9.37	43.60	9.37	43.59	9.41
60.67	48.06	43.77	8.94	43.77	8.94	43.75	8.97
62.67	48.00	43.91	8.53	43.91	8.53	43.89	8.57
64.67	47.88	44.02	8.06	44.02	8.06	44.00	8.11
66.67	47.83	44.12	7.78	44.12	7.78	44.09	7.82
68.67	47.73	44.19	7.42	44.19	7.42	44.16	7.47
70.67	47.62	44.24	7.08	44.24	7.08	44.22	7.14
72.67	47.49	44.28	6.77	44.28	6.77	44.26	6.82
74.67	47.37	44.30	6.47	44.30	6.47	44.28	6.52
76.67	47.23	44.31	6.19	44.31	6.19	44.29	6.24
78.67	47.10	44.31	5.93	44.31	5.93	44.28	5.98
80.67	46.95	44.29	5.67	44.29	5.67	44.26	5.73

82.67	46.80	44.26	5.43	44.26	5.43	44.23	5.49
84.67	46.64	44.21	5.21	44.21	5.21	44.19	5.26
86.67	46.48	44.16	4.99	44.16	4.99	44.14	5.04
88.67	46.32	44.10	4.78	44.10	4.78	44.08	4.83
90.67	46.15	44.03	4.58	44.03	4.58	44.01	4.63
92.67	45.97	43.96	4.38	43.96	4.38	43.94	4.43
94.67	45.79	43.87	4.19	43.87	4.19	43.85	4.23
96.67	45.61	43.79	3.99	43.79	3.99	43.77	4.03
98.67	45.42	43.69	3.81	43.69	3.81	43.67	3.85
100.67	45.23	43.59	3.63	43.59	3.63	43.57	3.66
102.67	45.04	43.49	3.45	43.49	3.45	43.47	3.49
104.67	44.85	43.38	3.28	43.38	3.28	43.37	3.31
106.67	44.66	43.27	3.10	43.27	3.10	43.24	3.17
108.67	44.46	43.12	3.02	43.12	3.02	43.10	3.07
110.67	44.26	42.97	2.91	42.97	2.91	42.95	2.96
112.67	44.06	42.82	2.80	42.82	2.80	42.80	2.84
114.67	43.85	42.67	2.69	42.67	2.69	42.65	2.73
116.67	43.64	42.51	2.59	42.51	2.59	42.50	2.63
118.67	43.44	42.35	2.49	42.35	2.49	42.34	2.52
120.67	43.23	42.19	2.39	42.19	2.39	42.18	2.42
122.67	43.02	42.03	2.30	42.03	2.30	42.02	2.33
124.67	42.81	41.86	2.21	41.86	2.21	41.85	2.24
126.67	42.61	41.70	2.13	41.70	2.13	41.69	2.16
128.67	42.40	41.53	2.06	41.53	2.06	41.52	2.08
130.67	42.19	41.36	1.98	41.36	1.98	41.35	2.00
132.67	41.99	41.19	1.90	41.19	1.90	41.45	1.27
134.67	41.77	41.01	1.82	41.01	1.82	41.29	1.16
136.67	41.56	40.84	1.74	40.84	1.74	41.12	1.05
138.67	41.35	40.66	1.67	40.66	1.67	40.96	0.95
140.67	41.15	40.49	1.60	40.49	1.60	40.79	0.86
142.67	40.94	40.31	1.53	40.31	1.53	40.62	0.76
144.67	40.73	40.13	1.46	40.13	1.46	40.45	0.67
146.67	40.52	39.95	1.39	39.95	1.39	40.28	0.58
148.67	40.31	39.78	1.33	39.78	1.33	40.11	0.50
150.67	40.11	39.60	1.27	39.60	1.27	39.94	0.42
152.67	39.90	39.42	1.22	39.42	1.22	39.76	0.35
154.67	39.70	39.24	1.17	39.24	1.17	39.59	0.28
156.67	39.50	39.06	1.12	39.06	1.12	39.41	0.21
158.67	39.29	38.87	1.06	38.87	1.06	39.24	0.14
160.67	39.09	38.69	1.02	38.69	1.02	39.06	0.08
162.67	38.89	38.51	0.97	38.51	0.97	38.88	0.02
164.67	38.69	38.33	0.92	38.33	0.92	38.71	0.05
166.67	38.48	38.15	0.87	38.15	0.87	38.53	0.11
168.67	38.28	37.97	0.83	37.97	0.83	38.35	0.17
170.67	38.09	37.79	0.79	37.79	0.79	38.17	0.22
172.67	37.89	37.61	0.76	37.61	0.76	37.99	0.27
174.67	37.70	37.43	0.72	37.43	0.72	37.81	0.31
176.67	37.51	37.25	0.70	37.25	0.70	37.64	0.35
178.67	37.31	37.07	0.67	37.07	0.67	37.46	0.39
180.67	37.12	36.89	0.64	36.89	0.64	37.28	0.42
182.67	36.93	36.71	0.61	36.71	0.61	37.10	0.46
184.67	36.74	36.53	0.57	36.53	0.57	36.93	0.51
186.67	36.55	36.35	0.54	36.35	0.54	36.75	0.55
188.67	36.36	36.17	0.50	36.17	0.50	36.57	0.59
190.67	36.17	36.00	0.46	36.00	0.46	36.40	0.64
192.67	35.98	35.82	0.43	35.82	0.43	36.22	0.68
194.67	35.79	35.65	0.40	35.65	0.40	36.05	0.72
196.67	35.61	35.47	0.37	35.47	0.37	35.88	0.76
198.67	35.43	35.28	0.41	35.28	0.41	35.69	0.74
200.67	35.25	35.10	0.43	35.10	0.43	35.50	0.72
202.67	35.07	34.91	0.44	34.91	0.44	35.32	0.71
204.67	34.89	34.73	0.46	34.73	0.46	35.14	0.71
206.67	34.72	34.56	0.46	34.56	0.46	34.96	0.71
208.67	34.55	34.39	0.46	34.39	0.46	34.79	0.70
210.67	34.38	34.22	0.46	34.22	0.46	34.62	0.70
212.67	34.21	34.05	0.45	34.05	0.44	34.45	0.71
214.67	34.04	33.89	0.43	33.89	0.43	34.28	0.72

216.67	33.88	33.74	0.41	33.74	0.41	34.12	0.73
218.67	33.72	33.59	0.39	33.59	0.39	33.97	0.73
220.67	33.56	33.44	0.37	33.44	0.37	33.81	0.74
222.67	33.41	33.29	0.34	33.29	0.34	33.66	0.76
224.67	33.26	33.15	0.32	33.15	0.32	33.51	0.76
226.67	33.11	33.01	0.29	33.01	0.29	33.37	0.77
228.67	32.97	32.88	0.27	32.88	0.27	33.22	0.78
230.67	32.83	32.75	0.25	32.75	0.25	33.09	0.79
232.67	32.69	32.62	0.22	32.62	0.22	32.95	0.80
234.67	32.55	32.49	0.19	32.49	0.19	32.82	0.81
236.67	32.42	32.37	0.15	32.37	0.15	32.69	0.84
238.67	32.21	32.25	0.11	32.25	0.11	32.56	1.09
240.67	32.01	32.13	0.38	32.13	0.38	32.44	1.34
242.67	32.38	32.01	1.12	32.01	1.12	32.31	0.19
244.67	32.08	31.90	0.56	31.90	0.56	32.20	0.36
246.67	31.78	31.79	0.02	31.79	0.02	32.08	0.94
248.67	31.66	31.68	0.05	31.68	0.05	31.96	0.95
250.67	31.37	31.57	0.63	31.57	0.63	31.85	1.52
252.67	31.26	31.47	0.68	31.47	0.68	31.74	1.55
254.67	31.14	31.37	0.72	31.37	0.72	31.64	1.58
256.67	31.03	31.27	0.77	31.27	0.77	31.53	1.61
258.67	31.11	31.17	0.18	31.17	0.18	31.43	1.01
260.67	31.01	31.07	0.21	31.07	0.21	31.33	1.02
262.67	30.91	30.98	0.24	30.98	0.24	31.23	1.04
264.67	30.59	30.89	0.96	30.89	0.96	31.13	1.75
266.67	30.49	30.80	1.00	30.80	1.00	31.04	1.78
268.67	30.62	30.71	0.30	30.71	0.30	30.94	1.07
270.67	30.30	30.62	1.05	30.62	1.05	30.85	1.81
272.67	30.22	30.54	1.07	30.54	1.07	30.76	1.82
274.67	30.13	30.46	1.09	30.46	1.09	30.68	1.82
276.67	30.04	30.38	1.10	30.38	1.10	30.59	1.82
278.67	30.20	30.30	0.33	30.30	0.33	30.51	1.03
280.67	30.01	30.22	0.70	30.22	0.70	30.43	1.40
282.67	29.91	30.14	0.77	30.14	0.77	30.35	1.45
284.67	29.87	30.07	0.68	30.07	0.68	30.27	1.35
285.00	29.84	30.10	0.85	30.10	0.85	30.10	0.85
287.00	29.82	30.03	0.72	30.03	0.72	30.03	0.72
289.00	29.69	29.97	0.97	29.97	0.97	29.97	0.97
291.00	29.62	29.91	0.98	29.91	0.98	29.91	0.98
293.00	29.59	29.85	0.89	29.85	0.89	29.85	0.89
295.00	29.57	29.79	0.74	29.79	0.74	29.79	0.74
297.00	29.56	29.73	0.57	29.73	0.57	29.73	0.57
299.00	29.56	29.67	0.38	29.67	0.38	29.67	0.38
301.00	29.55	29.61	0.20	29.61	0.20	29.61	0.20
303.00	29.44	29.55	0.37	29.55	0.37	29.55	0.37
305.00	29.39	29.50	0.36	29.50	0.36	29.50	0.36
307.00	29.36	29.44	0.26	29.44	0.26	29.44	0.26
309.00	29.35	29.39	0.12	29.39	0.12	29.39	0.12
311.00	29.34	29.33	0.02	29.33	0.02	29.33	0.02
313.00	29.25	29.28	0.08	29.28	0.08	29.28	0.08
315.00	29.21	29.22	0.04	29.22	0.04	29.22	0.04
317.00	29.16	29.17	0.04	29.17	0.04	29.17	0.04
319.00	29.12	29.12	0.00	29.12	0.00	29.12	0.00
321.00	29.09	29.07	0.08	29.07	0.08	29.07	0.08
323.00	29.04	29.02	0.08	29.02	0.08	29.02	0.08
325.00	29.02	28.97	0.17	28.97	0.17	28.97	0.17
327.00	28.97	28.92	0.15	28.92	0.15	28.92	0.15
329.00	28.94	28.88	0.24	28.88	0.24	28.88	0.24
331.00	28.91	28.83	0.26	28.83	0.26	28.83	0.26
333.00	28.87	28.78	0.29	28.78	0.29	28.78	0.29
335.00	28.85	28.74	0.37	28.74	0.37	28.74	0.37
337.00	28.80	28.69	0.35	28.69	0.35	28.69	0.35
339.00	28.77	28.65	0.43	28.65	0.43	28.65	0.43
341.00	28.75	28.61	0.48	28.61	0.48	28.61	0.48
343.00	28.71	28.57	0.51	28.57	0.51	28.57	0.51
345.00	28.69	28.53	0.56	28.53	0.56	28.53	0.56
347.00	28.65	28.48	0.59	28.48	0.59	28.48	0.59

349.00	28.64	28.44	0.67	28.44	0.67	28.44	0.67
351.00	28.61	28.40	0.72	28.40	0.72	28.40	0.72
353.00	28.58	28.37	0.74	28.37	0.74	28.37	0.74
355.00	28.54	28.33	0.74	28.33	0.74	28.33	0.74
357.00	28.49	28.29	0.72	28.29	0.72	28.29	0.72
359.00	28.45	28.25	0.68	28.25	0.68	28.25	0.68
361.00	28.41	28.22	0.69	28.22	0.69	28.22	0.69
363.00	28.36	28.18	0.65	28.18	0.65	28.18	0.65
365.00	28.31	28.14	0.60	28.14	0.60	28.14	0.60
367.00	28.27	28.11	0.59	28.11	0.59	28.11	0.59
369.00	28.23	28.07	0.54	28.07	0.54	28.07	0.54
371.00	28.18	28.04	0.49	28.04	0.49	28.04	0.49
373.00	28.13	28.00	0.44	28.00	0.44	28.00	0.44
375.00	28.07	27.97	0.35	27.97	0.35	27.97	0.35
377.00	28.00	27.94	0.23	27.94	0.23	27.94	0.23
379.00	27.95	27.90	0.17	27.90	0.17	27.90	0.17
381.00	27.87	27.87	0.02	27.87	0.02	27.87	0.02
383.00	27.81	27.84	0.10	27.84	0.10	27.84	0.10
385.00	27.74	27.80	0.22	27.80	0.22	27.80	0.22
387.00	27.68	27.77	0.32	27.77	0.32	27.77	0.32
389.00	27.62	27.74	0.44	27.74	0.44	27.74	0.44
391.00	27.55	27.71	0.56	27.71	0.56	27.71	0.56
393.00	27.50	27.67	0.64	27.67	0.64	27.67	0.64
395.00	27.42	27.64	0.79	27.64	0.79	27.64	0.79
397.00	27.38	27.61	0.83	27.61	0.83	27.61	0.83
399.00	27.32	27.58	0.92	27.58	0.92	27.58	0.92
401.00	27.24	27.54	1.10	27.54	1.10	27.54	1.10
403.00	27.20	27.51	1.14	27.51	1.14	27.51	1.14
405.00	27.13	27.48	1.27	27.48	1.27	27.48	1.27
407.00	27.06	27.45	1.42	27.45	1.42	27.45	1.42
409.00	27.00	27.41	1.52	27.41	1.52	27.41	1.52
411.00	26.93	27.38	1.67	27.38	1.67	27.38	1.67
413.00	26.88	27.35	1.75	27.35	1.75	27.35	1.75
415.00	26.83	27.31	1.81	27.31	1.81	27.31	1.81
417.00	26.76	27.28	1.94	27.28	1.94	27.28	1.94
419.00	26.72	27.25	1.96	27.25	1.96	27.25	1.96
421.00	26.67	27.21	2.02	27.21	2.02	27.21	2.02
423.00	26.61	27.18	2.14	27.18	2.14	27.18	2.14
425.00	26.57	27.14	2.16	27.14	2.16	27.14	2.16
427.00	26.52	27.11	2.21	27.11	2.21	27.11	2.21
429.00	26.47	27.07	2.27	27.07	2.27	27.07	2.27
431.00	26.41	27.03	2.34	27.03	2.34	27.03	2.34
433.00	26.37	27.00	2.38	27.00	2.38	27.00	2.38
435.00	26.33	26.96	2.41	26.96	2.41	26.96	2.41
437.00	26.29	26.92	2.41	26.92	2.41	26.92	2.41
439.00	26.23	26.88	2.48	26.88	2.48	26.88	2.48
441.00	26.21	26.84	2.42	26.84	2.42	26.84	2.42
443.00	26.17	26.80	2.43	26.80	2.43	26.80	2.43
445.00	26.13	26.76	2.41	26.76	2.41	26.76	2.41
447.00	26.10	26.72	2.38	26.72	2.38	26.72	2.38
449.00	26.07	26.68	2.33	26.68	2.33	26.68	2.33
451.00	26.04	26.64	2.32	26.64	2.32	26.64	2.32
453.00	26.01	26.60	2.26	26.60	2.26	26.60	2.26
455.00	25.97	26.55	2.22	26.55	2.22	26.55	2.22
457.00	25.95	26.51	2.16	26.51	2.16	26.51	2.16
459.00	25.92	26.46	2.09	26.46	2.09	26.46	2.09
461.00	25.90	26.42	2.00	26.42	2.00	26.42	2.00
463.00	25.87	26.37	1.92	26.37	1.92	26.37	1.92
465.00	25.85	26.32	1.80	26.32	1.80	26.32	1.80
467.00	25.83	26.27	1.72	26.27	1.72	26.27	1.72
469.00	25.82	26.22	1.54	26.22	1.54	26.22	1.54
471.00	25.80	26.17	1.43	26.17	1.43	26.17	1.43
473.00	25.79	26.12	1.27	26.12	1.27	26.12	1.27
475.00	25.77	26.06	1.13	26.06	1.13	26.06	1.13

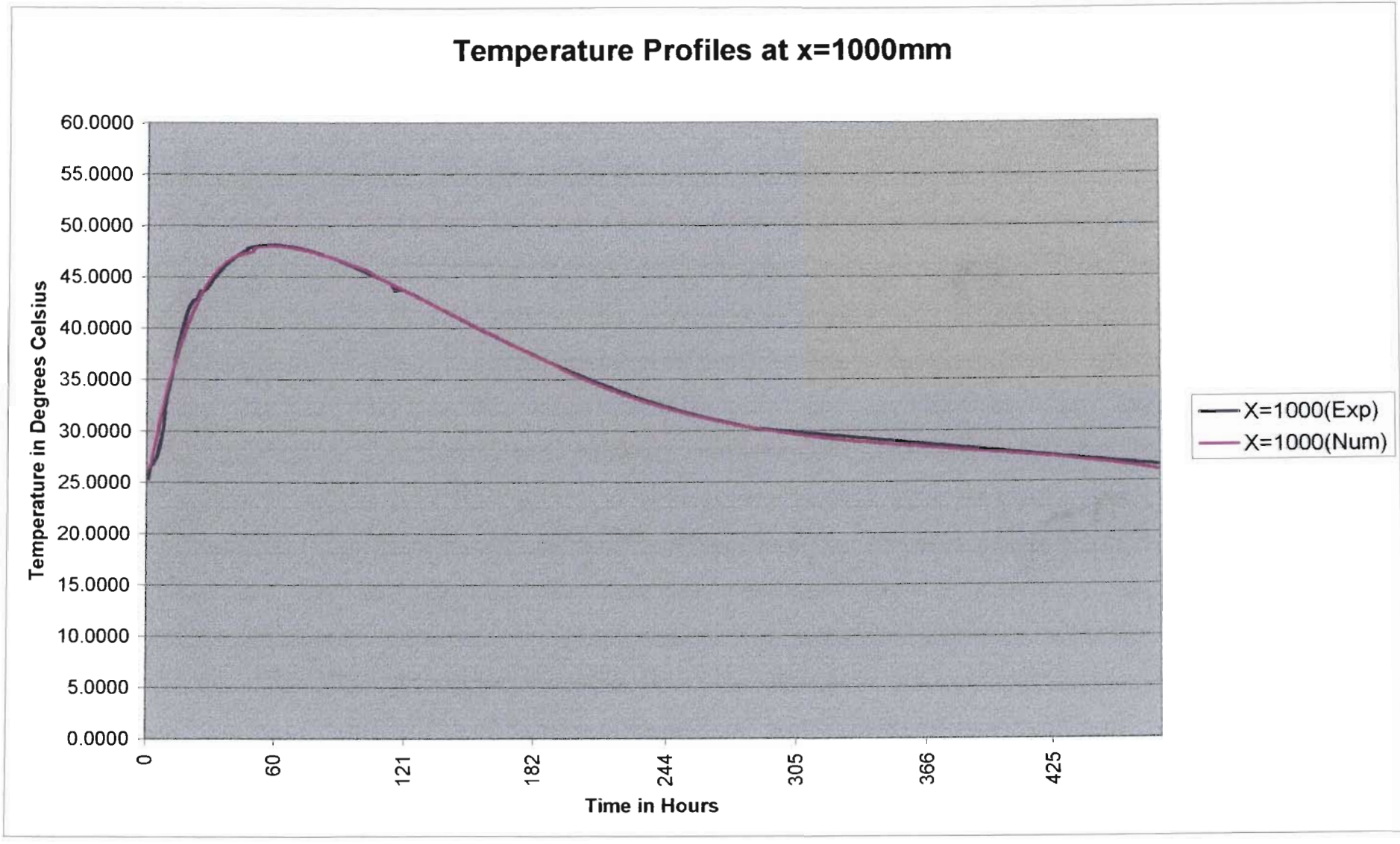
Temperature Profiles at x=1000mm
60.0000
55.0000
50.0000
45.0000
40.0000
35.0000
30.0000
25.0000
20.0000
15.0000
10.0000
5.0000
0.0000
Temperature in Degrees Celsius
0
60
121
182
244
305
366
425
Time in Hours
X=1000(Exp)
X=1000(Num)

Time(Hours)	X=1000(Exp)	X=1000(Num)	% Error	X=1000(Num.ns)	% Error
0.0000	25.2360	26.4001	4.6127	26.4001	4.6127
1.0000	26.5835	26.457	0.4760	26.457	0.4760
2.0000	26.6941	27.5505	3.2082	27.5505	3.2082
3.0000	26.9697	28.606	6.0672	28.606	6.0672
4.0000	27.4497	29.6243	7.9223	29.6243	7.9223
5.0000	28.1506	30.606	8.7223	30.606	8.7223
6.0000	29.0768	31.5517	8.5116	31.5517	8.5116
7.0000	30.2380	32.4621	7.3553	32.4621	7.3553
8.0000	32.5231	33.3378	2.5051	33.3378	2.5051
9.0000	33.6767	34.1796	1.4933	34.1796	1.4933
10.0000	34.6487	34.9879	0.9790	34.9879	0.9790
11.0000	35.6207	35.7635	0.4010	35.7635	0.4010
12.0000	36.6402	36.5071	0.3632	36.5071	0.3632
13.0000	37.5874	37.2192	0.9795	37.2192	0.9795
14.0000	38.4910	37.9005	1.5340	37.9005	1.5340
15.0000	39.3351	38.5517	1.9915	38.5517	1.9915
16.0000	40.1212	39.1734	2.3623	39.1734	2.3623
17.0000	40.8521	39.7662	2.6581	39.7662	2.6581
18.0000	41.5320	40.3309	2.8920	40.3309	2.8920
19.0000	42.1557	40.868	3.0547	40.868	3.0547
20.0000	42.4447	41.3782	2.5126	41.3782	2.5126
21.0000	42.7336	41.8622	2.0392	41.8622	2.0392
22.0000	42.7298	42.3205	0.9579	42.3205	0.9579
23.0000	43.1424	42.7539	0.9006	42.7539	0.9006
24.0000	43.6254	43.163	1.0598	43.163	1.0598
25.0000	43.5480	43.5484	0.0009	43.5484	0.0009
26.0000	43.6870	43.9109	0.5126	43.9109	0.5126
27.0000	43.8259	44.2509	0.9697	44.2509	0.9697
28.0000	44.1565	44.5692	0.9345	44.5692	0.9345
29.0000	44.4667	44.8665	0.8992	44.8665	0.8992
30.0000	44.7568	45.1433	0.8635	45.1433	0.8635
31.0000	45.0313	45.4003	0.8194	45.4003	0.8194
32.0000	45.2880	45.6383	0.7736	45.6383	0.7736
33.0000	45.5303	45.8577	0.7190	45.8577	0.7190
34.0000	45.7580	46.0593	0.6584	46.0593	0.6584
35.0000	45.9721	46.2437	0.5909	46.2437	0.5909
36.0000	46.1737	46.4116	0.5153	46.4116	0.5153
37.0000	46.3625	46.5636	0.4338	46.5636	0.4338
38.0000	46.5392	46.7003	0.3461	46.7003	0.3461
39.0000	46.7056	46.8224	0.2501	46.8224	0.2501
40.0000	46.8590	46.9306	0.1528	46.9306	0.1528
41.0000	47.0036	47.0255	0.0465	47.0255	0.0465
42.0000	47.1366	47.1077	0.0612	47.1077	0.0612
43.0000	47.2601	47.1779	0.1738	47.1779	0.1738
44.0000	47.3737	47.2368	0.2889	47.2368	0.2889
45.0000	47.4770	47.2849	0.4047	47.2849	0.4047
46.0000	47.5702	47.323	0.5196	47.323	0.5196
46.3333	47.6006	47.3335	0.5612	47.2964	0.6391
46.6667	47.7540	47.3431	0.8605	47.3064	0.9374
48.6667	47.8762	47.3802	1.0360	47.3462	1.1070
50.6667	47.9713	47.8928	0.1637	47.8928	0.1637
52.6667	48.0411	47.9393	0.2120	47.9393	0.2120
54.6667	48.0854	47.9691	0.2419	47.9691	0.2419
56.6667	48.1096	47.983	0.2632	47.9830	0.2632
58.6667	48.1124	47.9817	0.2716	47.9817	0.2716
60.6667	48.0966	47.966	0.2715	47.9660	0.2715
62.6667	48.0634	47.9365	0.2640	47.9365	0.2640
64.6667	47.9365	47.8941	0.0884	47.8940	0.0886
66.6667	47.9495	47.8393	0.2299	47.8393	0.2299
68.6667	47.8712	47.7731	0.2049	47.7731	0.2049
70.6667	47.7808	47.6961	0.1772	47.6961	0.1772
72.6667	47.6817	47.609	0.1525	47.6090	0.1525
74.6667	47.5743	47.5126	0.1297	47.5126	0.1297
76.6667	47.4598	47.4076	0.1100	47.4076	0.1100
78.6667	47.3394	47.2948	0.0942	47.2948	0.0942
80.6667	47.2114	47.1749	0.0773	47.1749	0.0773

82.6667	47.0754	47.0486	0.0570	47.0485	0.0572
84.6667	46.9343	46.9166	0.0376	46.9166	0.0376
86.6667	46.7890	46.7797	0.0198	46.7797	0.0198
88.6667	46.6380	46.6387	0.0016	46.6387	0.0016
90.6667	46.4796	46.4942	0.0314	46.4942	0.0314
92.6667	46.3167	46.347	0.0655	46.3470	0.0655
94.6667	46.1472	46.1978	0.1097	46.1978	0.1097
96.6667	45.9740	46.0474	0.1596	46.0474	0.1596
98.6667	45.7977	45.8965	0.2157	45.8965	0.2157
100.6667	45.6204	45.7458	0.2749	45.7458	0.2749
102.6667	45.4416	45.5961	0.3400	45.5961	0.3400
104.6667	45.2601	45.4481	0.4153	45.2846	0.0541
106.6667	45.0767	45.0877	0.0244	45.0877	0.0244
108.6667	44.8886	44.8898	0.0026	44.8897	0.0024
110.6667	44.6959	44.6908	0.0114	44.6908	0.0114
112.6667	44.4993	44.491	0.0187	44.4910	0.0187
114.6667	44.3004	44.2904	0.0226	44.2903	0.0228
116.6667	43.6950	44.0889	0.9015	44.0889	0.9015
118.6667	43.6921	43.8868	0.4455	43.8867	0.4453
120.6667	43.6893	43.6839	0.0124	43.6839	0.0124
122.6667	43.4845	43.4804	0.0094	43.4804	0.0094
124.6667	43.2795	43.2764	0.0071	43.2764	0.0071
126.6667	43.0743	43.0718	0.0059	43.0718	0.0059
128.6667	42.8698	42.8668	0.0069	42.8668	0.0069
130.6667	42.6636	42.6614	0.0052	42.6614	0.0052
132.6667	42.4548	42.4557	0.0022	42.4557	0.0022
134.6667	42.2437	42.2496	0.0139	42.2496	0.0139
136.6667	42.0321	42.0434	0.0268	42.0433	0.0266
138.6667	41.8227	41.8369	0.0339	41.8369	0.0339
140.6667	41.6119	41.6303	0.0442	41.6303	0.0442
142.6667	41.4004	41.4237	0.0563	41.4236	0.0560
144.6667	41.1897	41.217	0.0663	41.2170	0.0663
146.6667	40.9798	41.0104	0.0746	41.0104	0.0746
148.6667	40.7707	40.8039	0.0815	40.8038	0.0813
150.6667	40.5659	40.5975	0.0780	40.5974	0.0778
152.6667	40.3618	40.3913	0.0731	40.3913	0.0731
154.6667	40.1584	40.1854	0.0672	40.1854	0.0672
156.6667	39.9541	39.9798	0.0644	39.9798	0.0644
158.6667	39.7494	39.7746	0.0635	39.7745	0.0632
160.6667	39.5471	39.5698	0.0574	39.5698	0.0574
162.6667	39.3447	39.3655	0.0529	39.3654	0.0526
164.6667	39.1421	39.1617	0.0501	39.1617	0.0501
166.6667	38.9382	38.9585	0.0522	38.9585	0.0522
168.6667	38.7380	38.756	0.0466	38.7560	0.0466
170.6667	38.5395	38.5542	0.0381	38.5541	0.0379
172.6667	38.3439	38.3531	0.0240	38.3531	0.0240
174.6667	38.1492	38.1528	0.0095	37.9534	0.5132
176.6667	37.9566	37.9534	0.0083	37.7549	0.5313
178.6667	37.7647	37.755	0.0256	37.5575	0.5486
180.6667	37.5731	37.5575	0.0416	37.3610	0.5646
182.6667	37.3812	37.361	0.0539	37.1656	0.5766
184.6667	37.1885	37.1657	0.0613	36.9714	0.5838
186.6667	36.9969	36.9715	0.0685	36.7784	0.5905
188.6667	36.8042	36.7784	0.0701	36.5866	0.5913
190.6667	36.6131	36.5867	0.0721	36.3962	0.5924
192.6667	36.4239	36.3962	0.0759	36.1164	0.8441
194.6667	36.2363	36.2071	0.0805	35.9205	0.8714
196.6667	36.0516	35.9205	0.3637	35.7282	0.8971
198.6667	35.8711	35.7282	0.3985	35.5394	0.9248
200.6667	35.6924	35.5395	0.4284	35.3541	0.9479
202.6667	35.5162	35.3542	0.4562	35.1723	0.9683
204.6667	35.3401	35.1723	0.4749	34.9938	0.9800
206.6667	35.1661	34.9938	0.4900	34.8187	0.9879
208.6667	34.9939	34.8187	0.5005	34.6469	0.9915
210.6667	34.8231	34.6469	0.5061	34.4784	0.9899
212.6667	34.6538	34.4784	0.5062	34.3131	0.9832
214.6667	34.4860	34.3131	0.5012	34.1511	0.9710

216.6667	34.3220	34.1511	0.4980	33.9922	0.9610
218.6667	34.1617	33.9922	0.4962	33.8364	0.9523
220.6667	34.0040	33.8364	0.4929	33.6837	0.9420
222.6667	33.8480	33.6838	0.4851	33.5341	0.9273
224.6667	33.6972	33.5341	0.4840	33.3875	0.9191
226.6667	33.5498	33.3875	0.4838	33.2439	0.9118
228.6667	33.4045	33.2439	0.4808	33.1032	0.9020
230.6667	33.2626	33.1032	0.4792	32.9654	0.8935
232.6667	33.1226	32.9654	0.4745	32.8305	0.8818
234.6667	32.9829	32.8305	0.4619	32.6984	0.8624
236.6667	32.8457	32.6984	0.4483	32.5691	0.8420
238.6667	32.7089	32.5691	0.4274	32.4425	0.8145
240.6667	32.5762	32.4425	0.4105	32.3186	0.7908
242.6667	32.4459	32.3186	0.3924	32.1974	0.7660
244.6667	32.3188	32.1974	0.3756	32.0789	0.7423
246.6667	32.1949	32.0789	0.3602	31.9629	0.7205
248.6667	32.0737	31.9629	0.3454	31.8495	0.6989
250.6667	31.9546	31.8495	0.3288	31.7386	0.6758
252.6667	31.8393	31.7386	0.3162	31.6301	0.6570
254.6667	31.7239	31.6301	0.2957	31.5241	0.6298
256.6667	31.6120	31.5241	0.2781	31.4205	0.6058
258.6667	31.5009	31.4206	0.2549	31.3193	0.5765
260.6667	31.3923	31.3193	0.2326	31.2204	0.5476
262.6667	31.2859	31.2204	0.2094	31.1238	0.5182
264.6667	31.1820	31.1238	0.1867	31.0294	0.4895
266.6667	31.0814	31.0294	0.1674	30.9372	0.4640
268.6667	30.9836	30.9372	0.1497	30.8472	0.4402
270.6667	30.8887	30.8472	0.1343	30.7594	0.4185
272.6667	30.7969	30.7594	0.1216	30.6736	0.4002
274.6667	30.7091	30.6736	0.1155	30.5899	0.3881
276.6667	30.6241	30.5899	0.1115	30.5082	0.3783
278.6667	30.5396	30.5082	0.1027	30.4284	0.3640
280.6667	30.4559	30.4284	0.0901	30.3506	0.3456
282.6667	30.3730	30.3507	0.0735	30.2748	0.3233
284.6667	30.2908	30.2748	0.0529	30.1948	0.3170
285.0000	30.2209	30.2623	0.1370	30.2623	0.1370
287.0000	30.1820	30.1886	0.0218	30.1886	0.0218
289.0000	30.1432	30.1167	0.0877	30.1167	0.0877
291.0000	30.1043	30.0466	0.1916	30.0466	0.1916
293.0000	30.0654	29.9782	0.2900	29.9782	0.2900
295.0000	30.0265	29.9115	0.3830	29.9115	0.3830
297.0000	29.9876	29.8465	0.4706	29.8465	0.4706
299.0000	29.9488	29.7831	0.5531	29.7831	0.5531
301.0000	29.9099	29.7213	0.6305	29.7213	0.6305
303.0000	29.8710	29.6610	0.7030	29.6610	0.7030
305.0000	29.8321	29.6023	0.7703	29.6023	0.7703
307.0000	29.7932	29.5450	0.8332	29.5450	0.8332
309.0000	29.7544	29.4892	0.8911	29.4892	0.8911
311.0000	29.7155	29.4348	0.9445	29.4348	0.9445
313.0000	29.6766	29.3817	0.9937	29.3817	0.9937
315.0000	29.6377	29.3299	1.0386	29.3299	1.0386
317.0000	29.5988	29.2794	1.0792	29.2794	1.0792
319.0000	29.5600	29.2302	1.1155	29.2302	1.1155
321.0000	29.5211	29.1821	1.1482	29.1821	1.1482
323.0000	29.4822	29.1353	1.1766	29.1353	1.1766
325.0000	29.4433	29.0895	1.2017	29.0895	1.2017
327.0000	29.4044	29.0448	1.2230	29.0448	1.2230
329.0000	29.3656	29.0012	1.2407	29.0012	1.2407
331.0000	29.3267	28.9586	1.2551	28.9586	1.2551
333.0000	29.2878	28.9170	1.2660	28.9170	1.2660
335.0000	29.2489	28.8763	1.2739	28.8763	1.2739
337.0000	29.2100	28.8365	1.2788	28.8365	1.2788
339.0000	29.1712	28.7976	1.2805	28.7976	1.2805
341.0000	29.1323	28.7594	1.2799	28.7594	1.2799
343.0000	29.0934	28.7221	1.2762	28.7221	1.2762
345.0000	29.0545	28.6855	1.2701	28.6855	1.2701
347.0000	29.0156	28.6496	1.2615	28.6496	1.2615

349.0000	28.9768	28.6144	1.2505	28.6144	1.2505
351.0000	28.9379	28.5798	1.2374	28.5798	1.2374
353.0000	28.8990	28.5458	1.2222	28.5458	1.2222
355.0000	28.8601	28.5123	1.2052	28.5123	1.2052
357.0000	28.8212	28.4794	1.1860	28.4794	1.1860
359.0000	28.7824	28.4469	1.1655	28.4469	1.1655
361.0000	28.7435	28.4148	1.1435	28.4148	1.1435
363.0000	28.7046	28.3832	1.1196	28.3832	1.1196
365.0000	28.6657	28.3519	1.0947	28.3519	1.0947
367.0000	28.6268	28.3209	1.0687	28.3209	1.0687
369.0000	28.5880	28.2903	1.0412	28.2903	1.0412
371.0000	28.5491	28.2598	1.0132	28.2598	1.0132
373.0000	28.5102	28.2296	0.9842	28.2296	0.9842
375.0000	28.4713	28.1995	0.9547	28.1995	0.9547
377.0000	28.4324	28.1696	0.9244	28.1696	0.9244
379.0000	28.3936	28.1397	0.8940	28.1397	0.8940
381.0000	28.3547	28.1099	0.8632	28.1099	0.8632
383.0000	28.3158	28.0801	0.8324	28.0801	0.8324
385.0000	28.2769	28.0503	0.8014	28.0503	0.8014
387.0000	28.2380	28.0204	0.7707	28.0204	0.7707
389.0000	28.1992	27.9904	0.7403	27.9904	0.7403
391.0000	28.1603	27.9603	0.7101	27.9603	0.7101
393.0000	28.1214	27.9300	0.6806	27.9300	0.6806
395.0000	28.0825	27.8995	0.6517	27.8995	0.6517
397.0000	28.0436	27.8687	0.6238	27.8687	0.6238
399.0000	28.0048	27.8377	0.5965	27.8377	0.5965
401.0000	27.9659	27.8063	0.5706	27.8063	0.5706
403.0000	27.9270	27.7745	0.5460	27.7745	0.5460
405.0000	27.8881	27.7423	0.5228	27.7423	0.5228
407.0000	27.8492	27.7097	0.5010	27.7097	0.5010
409.0000	27.8104	27.6766	0.4809	27.6766	0.4809
411.0000	27.7715	27.6429	0.4630	27.6429	0.4630
413.0000	27.7326	27.6087	0.4467	27.6087	0.4467
415.0000	27.6937	27.5739	0.4326	27.5739	0.4326
417.0000	27.6548	27.5385	0.4206	27.5385	0.4206
419.0000	27.6160	27.5023	0.4115	27.5023	0.4115
421.0000	27.5771	27.4655	0.4046	27.4655	0.4046
423.0000	27.5382	27.4279	0.4005	27.4279	0.4005
425.0000	27.4993	27.3895	0.3993	27.3895	0.3993
427.0000	27.4604	27.3503	0.4010	27.3503	0.4010
429.0000	27.4216	27.3102	0.4061	27.3102	0.4061
431.0000	27.3827	27.2692	0.4144	27.2692	0.4144
433.0000	27.3438	27.2272	0.4264	27.2272	0.4264
435.0000	27.3049	27.1843	0.4417	27.1843	0.4417
437.0000	27.2660	27.1403	0.4611	27.1403	0.4611
439.0000	27.2272	27.0953	0.4843	27.0953	0.4843
441.0000	27.1883	27.0492	0.5115	27.0492	0.5115
443.0000	27.1494	27.0019	0.5433	27.0019	0.5433
445.0000	27.1105	26.9535	0.5791	26.9535	0.5791
447.0000	27.0716	26.9039	0.6196	26.9039	0.6196
449.0000	27.0328	26.8529	0.6653	26.8529	0.6653
451.0000	26.9939	26.8007	0.7156	26.8007	0.7156
453.0000	26.9550	26.7472	0.7709	26.7472	0.7709
455.0000	26.9161	26.6923	0.8315	26.6923	0.8315
457.0000	26.8772	26.6360	0.8975	26.6360	0.8975
459.0000	26.8384	26.5782	0.9693	26.5782	0.9693
461.0000	26.7995	26.5190	1.0466	26.5190	1.0466
463.0000	26.7606	26.4582	1.1300	26.4582	1.1300
465.0000	26.7217	26.3959	1.2193	26.3959	1.2193
467.0000	26.6828	26.3320	1.3148	26.3320	1.3148
469.0000	26.6440	26.2664	1.4170	26.2664	1.4170
471.0000	26.6051	26.1992	1.5255	26.1992	1.5255
473.0000	26.5662	26.1302	1.6411	26.1302	1.6411
475.0000	26.5273	26.0595	1.7635	26.0595	1.7635

Appendix C – Fortran Program and Alterations

APPENDIX C – FORTRAN PROGRAM

D.1 The Main Program.

```
      PROGRAM HEAT BEAM
      IMPLICIT REAL *4(A-H,O-Z)
      INTEGER*1 NTYP
      INTEGER*2 NWRITE
      CHARACTER*80 TITLE
      CHARACTER*12 FNAME
      PARAMETER (MXELN=200,MXNODES=201,MXROW=400,MXCOL=5)

C     This program solves the time dependent diffusion and transport equations
C     in 1-D spatial dimension by the Green Element Method.
C     The computational domain is discretized by piece-wise linear elements.

      COMMON /A/ H(MXROW,MXCOL)
      DIMENSION X(MXNODES),CHI(MXNODES),CHI0(MXNODES),CHN(MXNODES)
      DIMENSION CHN0(MXNODES),RHS(MXROW),NTYP(2),OLDDSDT(MXNODES)
      DIMENSION SIZE(MXELN),RECH(MXNODES)
      DIMENSION TDIV(5),TLEVEL(5),NWRITE(5),NSP(10)

C     MXBAND = Half bandwidth of the set of discrete equations
C     NGLOBE = Total number of nodes in the computational domain
C     NCOL = 2*MXBAND+1  MXROW >= NGLOBE;
C     H is the coefficient matrix
C     X is a row vector of the x-coordinate of the nodes
C     CHI is a row vector of the dependent variable at the nodes
C     CHN is a row vector of the derivative of the dependent variable in the flow
C     direction.
C     CHI0 is a row vector of the dependent variable at the nodes at initial
C     time
C     CHN0 is a row vector of the derivative of the dependent variable in the flow
C     direction at the initial time.
C     OLDDSDT is a row vector of the temporal derivative at each node at initial
C     time
C     RHS is the right-hand side of the matrix equation

C     ********** Format Statements **********

 1000 FORMAT(//)
 2000 FORMAT('..... NUMBER OF NODES  =',I3/)
 2055  FORMAT('..... DIFFERENCE SCHEME =',F5.2/)
 2150 FORMAT('..... NATURE OF BOUNDARY CONDS. (STEADY=0; UNSTEADY=1) ='
     1  ,I3/,7X,'INITIAL TIME =',F9.4,';   TIME LIMIT =',F9.4/)
 2450 FORMAT(5X,I3,4X,F10.2,6X,F12.4)
 4300 FORMAT(5X,'NODE',7X,'X-COOD.',8X,'PRIMARY VAR.')
 2800 FORMAT(/' ..... TIME .....=',F9.4)
 3111 FORMAT(/' ..... STEADY STATE SOLUTIONS .....')
```

```
      PIE = 4.0*ATAN(1.0)
      WRITE(*,'(A)')'    Supply input file name: '
      READ(*,'(A)') FNAME
      OPEN(5,FILE=FNAME,STATUS='OLD')
      WRITE(*,'(A)')'    Supply output file name: '
      READ(*,'(A)') FNAME
      OPEN(6,FILE=FNAME,STATUS='UNKNOWN')

      READ (5,'(A)') TITLE
      WRITE (6,'(A)')TITLE
      READ (5,*) KEY1,KEY2


          T1=12.6669
          T2=15.3253
          T3=267.7307
          T4=50.6667
          T5=104.6667
          T6=194.6667
          T7=475
C     DIFF = Diffusivity of the flow medium
      READ(5,*) DIFF

C     VELX = Uniform velocity in the x-direction
      READ(5,*) VELX
c     velx0 = velx

C     DECAY = Rate of first-order decay
      READ(5,*) DECAY

C     INAT = 1 if it is a time-dependent problem; = 0 if it is steady
      READ(5,*) INAT
      IF(INAT .EQ. 1) THEN
C     NSUB = Number of divisions of the time dimension; TIME = Initial time;
C     ICOND = 1 if the boundary data change with time; = 0 if boundary data are
C     steady
          READ(5,*) NSUB,TIME,ICOND

C     NWRITE is the number of time steps to skip before solution is printed
C     TDIV is the time step of each time subdivision
C     TLEVEL if the time limit of each time subdivision
          READ(5,*) (NWRITE(I),TDIV(I),TLEVEL(I),I=1,NSUB)
          TLIMIT = TLEVEL(NSUB)

C     ISCHEME = 2 for the 2-level time scheme; = 3 for the 3-level time scheme
          READ(5,*) ISCHEME

C     THETA = Finite difference time weighing factor; it takes any value
C     between 0.0 and 1.0 for the 2-level scheme and between 1.0 and 2.0 for
C     the 3-level scheme.
```

```
      READ(5,*) THETA
      IF(ISCHEME .EQ. 2) THEN
        TSCALE = 1.0
      ELSE IF(ISCHEME .EQ. 3) THEN
        TSCALE = THETA
        THETA = 1.0
      END IF
    ELSE IF(INAT .EQ. 0) THEN
      NSTEP = 1
      NSUB = 1
      THETA = 1.0
      NWRITE(1) = 1
    END IF
    TMINUS = 1.-THETA

C    NSEG = Number of segments into which the 1-D spatial dimension is divided
    READ(5,*) NSEG
    IBEG = 1
C    X is the x-coordinate of the beginning node of the segment
C    NSP = Number of additional nodes generated excluding the end nodes
    READ (5,*) X(1),NSP(1)
    XA = X(1)
    DO I=1,NSEG
      IPANELS=NSP(I)+1
      IEND = IPANELS+IBEG
      M = I+1
      READ (5,*) X(IEND),NSP(M)
      XB = X(IEND)

C    GENERATE EXTRA BOUNDARY NODES BETWEEN END NODES
      IF (NSP(I) .GT. 0) THEN
        DX0 = (XB-XA)/REAL(IPANELS)
        KB = IBEG+1
        KN = IEND-1
        DO K=KB,KN
          X(K) = X(K-1)+DX0
        END DO
      END IF
      XA = XB
      IBEG = IEND
    END DO
C    NGLOBE = total number of nodes
    NGLOBE = IEND
    IF(NGLOBE .GT. MXROW) THEN
      WRITE(*,'(A,I3)')' **** Error - Too many nodes ****',NGLOBE
      STOP
    END IF
    WRITE (6,2000) NGLOBE
    IF(INAT .EQ. 1) WRITE(6,2150) ICOND,TIME,TLIMIT
C    NELEM = Number of Elements
```

```
      NELEM = NGLOBE-1
      MXBAND = 2
C     MXBAND = Half bandwidth of the coefficient matrix
C     NCOL = Bandwidth of coefficient matrix
      NCOL = 2*MXBAND+1
C     Input Boundary Data
C     CALL DATA(CHI,NTYP,MXNODES,CHN,NGLOBE)
      IF(INAT .EQ. 1) THEN
C     Initialize the solution at initial time
          DO I=1,NGLOBE
            CHI0(I) = 0.0
            CHN0(I) = 0.0
          END DO
C     NFINIT = 1 if initial data are input at each node, or are given by a
C     functional relationship; = 0 if the data at initial time are uniform.
          READ(5,*) NFINIT
C     Input data at the initial time
          CALL INITRAN(NFINIT,CHI0,CHN0,NGLOBE,MXNODES)
c       do i=1,nglobe
c         chi0(i) = exp(-(x(i)-0.)**2/(2.*0.1**2))
c         chn0(i) = -(x(i)-0.0)/(0.1**2)*chi0(i)
c       end do
          IF(NTYP(1) .EQ. 1) THEN
            CHI(1) = CHI0(1)
            CHN0(1) = CHN(1)
          ELSE
            CHI0(1) = CHI(1)
            CHN(1) = CHN0(1)
          END IF
          IF(NTYP(2) .EQ. 1) THEN
            CHI(NGLOBE) = CHI0(NGLOBE)
            CHN0(NGLOBE) = CHN(NGLOBE)
          ELSE
            CHI0(NGLOBE) = CHI(NGLOBE)
            CHN(NGLOBE) = CHN0(NGLOBE)
          END IF
          OLDDSDT(1) = 0.0
          OLDDSDT(NGLOBE) = 0.0
          DO I=2,NELEM
            OLDDSDT(I) = 0.0
            CHI(I) = CHI0(I)
            CHN(I) = CHN0(I)
          END DO
      END IF
C     Input recharge data
C     NRECH = 1 if the recharge data are input at each node, or given by a
C     functional relationship.; = 0 if the recharge data are uniform.
      READ(5,*) NRECH
      CALL RECHARGE(NRECH,RECH,MXNODES,NGLOBE)
C     Integrations on the elements
```

```
      CALL INTG(SIZE,NELEM,X,MXNODES,MXELN)
      XMAX = SIZE(1)
      DO M=2,NELEM
           IF(SIZE(M) .GT. XMAX) XMAX = SIZE(M)
      END DO

      IF (KEY1 .EQ. 1) THEN
           IF(INAT .EQ. 1) WRITE(6,2055) THETA*TSCALE
C       Nodal data information
           WRITE(6,4300)
           DO 500 I=1,NGLOBE
             WRITE(6,2450)I,X(I),CHI(I)
 500    CONTINUE
      END IF

      NEND = 2*NELEM
      DO I=1,NSUB
           MT = 1
           IF(INAT .EQ. 1) THEN
             DELT = TDIV(I)
             NSTEP = (TLEVEL(I)-TIME)/DELT+0.5
             WEIGHT = TSCALE
             TSCALE = 1.0
           END IF
           DO J=1,NSTEP
             IF(INAT .EQ. 1) THEN
               IF(J .EQ. 2) TSCALE = WEIGHT
               TIME = TIME+DELT
c           velx = 4.*sin(4.*pie*time)
             END IF
C          The boundary conditions are time dependent


C          The recharge function is time dependent and uses three functions
           IF(TIME .LE. T1) THEN
           CALL RECHARGET1(RECH,TIME,MXNODES,NGLOBE)
           END IF

           IF(TIME .GT.T1.AND.TIME.LE.T2) THEN
           CALL RECHARGET2(RECH,TIME,MXNODES,NGLOBE)
           END IF



           IF(TIME .GT.T2.AND.TIME.LE.T3) THEN
           CALL RECHARGET3(RECH,TIME,MXNODES,NGLOBE)
           END IF
```

```
C       The boundary conditions are time dependent and divided into four analytical equations

        IF(TIME .LE. T4) THEN
        CALL DATA4(CHI,NTYP,MXNODES,CHN,NGLOBE,TIME)
        END IF

        IF(TIME .GT.T4.AND.TIME.LE.T5) THEN
        CALL DATA5(CHI,NTYP,MXNODES,CHN,NGLOBE,TIME)
        END IF

        IF(TIME .GT.T5.AND.TIME.LE.T6) THEN
        CALL DATA6(CHI,NTYP,MXNODES,CHN,NGLOBE,TIME)

        END IF

        IF(TIME .GT.T6.AND.TIME.LE.T7) THEN
        CALL DATA7(CHI,NTYP,MXNODES,CHN,NGLOBE,TIME)

        END IF

C   ASSMBL does the matrix assembly
C   RIGHT computes the right hand side of the matrix equation
C   SOLVE decomposes and solves for the nodal unknowns
C   SORT assigns the computed solution to the proper node.
          DO L=1,NEND
            RHS(L) = 0.0
            DO K=1,NCOL
                 H(L,K) = 0.0
            END DO
          END DO
          CALL ASSMBL(H,NTYP,THETA,TSCALE,DELT,NELEM,MXROW,MXCOL,
     1          MXELN,INAT,MXBAND,DIFF,VELX,NEND,SIZE,DECAY,
     2          XMAX)

          CALL RIGHT(RHS,NTYP,THETA,TSCALE,DELT,MXNODES,CHI,CHI0,
     1         CHN,CHN0,OLDDSDT,NELEM,MXROW,MXELN,INAT,
     2         TMINUS,DIFF,VELX,NGLOBE,NEND,SIZE,DECAY,RECH,
     3         XMAX)

          IF(KEY2 .EQ. 1 .AND. J .EQ. 1) THEN
            WRITE(*,'(//A)')' H & RHS matrices'
            DO L=1,NEND
                 WRITE(*,'(I3,1X,5(1X,F11.3),2X,F12.4)')
     1        L,(H(L,K),K=1,NCOL),RHS(L)
            END DO
          END IF
          KKK = 0
          CALL SOLVE (KKK,H,RHS,NEND,MXBAND,MXROW,MXCOL)
          CALL SORT(CHI,CHN,RHS,NELEM,MXROW,MXNODES,NTYP,
     1         NGLOBE,NEND)
```

```
            IF(J/NWRITE(I) .EQ. MT) THEN
              MT = MT+1
              IF(INAT .EQ. 1) THEN
                   WRITE (6,2800) TIME
              ELSE
                   WRITE(6,3111)
              END IF

C     Output of solutions
              write(6,2)
              do I=1,nglobe
                   write(6,1) I,x(I),chi(I),chn(I)
c             write(6,1) x(I),chi(I)
              end do
             END IF
 1   format(3x,i4,3x,f12.3,3x,f12.4,4x,f12.4)
c 1   format(1x,f8.3,2x,e14.8)
 2   format(1x,'Node No.',5x,'Location',5x,' Primary ',7x,'Flux',
    1      /29x,' Variable')

C     Update data at initial time level
c          velx0 = velx
             IF(INAT .EQ. 1) THEN
               DO L=1,NGLOBE
                    OLDDSDT(L) = TSCALE/DELT*(CHI(L)-CHI0(L))+
    1                 (1.0-TSCALE)*OLDDSDT(L)
                    CHI0(L) = CHI(L)
                    CHN0(L) = CHN(L)
               END DO
             END IF
           END DO
      END DO
      END

          SUBROUTINE DATA4(CHI,NTYP,MXNODES,CHN,NGLOBE,TIME)
          IMPLICIT REAL *4(A-H,O-Z)
      INTEGER *1 NTYP
      DIMENSION CHI(MXNODES),CHN(MXNODES),NTYP(2)

          NTYP (1) = 2
          NTYP (2) = 2
          TMP = 0.0

      IF(NTYP(1) .EQ. 1) THEN
            CHN(1) = TMP
      ELSE IF(NTYP(1) .EQ. 2) THEN
          CHI(1) =0.000087*(TIME**3)-0.0137*(TIME**2)+0.6793*TIME+25.454
      END IF
```

```
C     READ(5,*) NTYP(2),TMP
      IF(NTYP(2) .EQ. 1) THEN
            CHN(NGLOBE) = TMP
      ELSE IF(NTYP(2) .EQ. 2) THEN
          CHI(NGLOBE)=0.0001079*(TIME**3)-0.0196*(TIME**2)+1.1515
          * *TIME+25.325
      END IF
      RETURN
      END

          SUBROUTINE DATA5(CHI,NTYP,MXNODES,CHN,NGLOBE,TIME)
          IMPLICIT REAL *4(A-H,O-Z)
      INTEGER *1 NTYP
      DIMENSION CHI(MXNODES),CHN(MXNODES),NTYP(2)

                    NTYP (1) = 2
                    NTYP (2) = 2
                    TMP = 0.0

      IF(NTYP(1) .EQ. 1) THEN
            CHN(1) = TMP
      ELSE IF(NTYP(1) .EQ. 2) THEN
            CHI(1) =0.0000044*(TIME**3)-0.0013*(TIME**2)+0.0874*TIME+34.267

      END IF

C     READ(5,*) NTYP(2),TMP
      IF(NTYP(2) .EQ. 1) THEN
            CHN(NGLOBE) = TMP
      ELSE IF(NTYP(2) .EQ. 2) THEN
     CHI(NGLOBE) =0.0000153*(TIME**3)-0.0045*(TIME**2)+0.3657
          * *TIME+38.926

      END IF
     RETURN
     END


          SUBROUTINE DATA6(CHI,NTYP,MXNODES,CHN,NGLOBE,TIME)
          IMPLICIT REAL *4(A-H,O-Z)
     INTEGER *1 NTYP
     DIMENSION CHI(MXNODES),CHN(MXNODES),NTYP(2)

          NTYP (1) = 2
          NTYP (2) = 2
          TMP = 0.0

     IF(NTYP(1) .EQ. 1) THEN
            CHN(1) = TMP
     ELSE IF(NTYP(1) .EQ. 2) THEN
```

```
          CHI(1)=0.000001*(TIME**3)-0.00047*(TIME**2)+0.0151*TIME+36.437

      END IF

C     READ(5,*) NTYP(2),TMP
      IF(NTYP(2) .EQ. 1) THEN
            CHN(NGLOBE) = TMP
      ELSE IF(NTYP(2) .EQ. 2) THEN
     CHI(NGLOBE)=0.00000115*(TIME**3)-0.000494*(TIME**2)-0.0326
          * *TIME+52.79


      END IF
      RETURN
      END

          SUBROUTINE DATA7(CHI,NTYP,MXNODES,CHN,NGLOBE,TIME)
     IMPLICIT REAL *4(A-H,O-Z)
      INTEGER *1 NTYP
      DIMENSION CHI(MXNODES),CHN(MXNODES),NTYP(2)

          NTYP (1) = 2
          NTYP (2) = 2
          TMP = 0.0

      IF(NTYP(1) .EQ. 1) THEN
            CHN(1) = TMP
      ELSE IF(NTYP(1) .EQ. 2) THEN
          CHI(1)=0.00000005*(TIME**3)-0.00006*(TIME**2)+0.006*TIME+29.398

      END IF

C     READ(5,*) NTYP(2),TMP
      IF(NTYP(2) .EQ. 1) THEN
            CHN(NGLOBE) = TMP
      ELSE IF(NTYP(2) .EQ. 2) THEN
     CHI(NGLOBE)=-0.0000008*(TIME**3)+0.000916*(TIME**2)-0.3645*
    *TIME+78.262

               END IF
      RETURN
      END


     SUBROUTINE INITRAN(NFINIT,CHI0,CHN0,NGLOBE,MXROW)
     IMPLICIT REAL*4 (A-H,O-Z)
     DIMENSION CHI0(MXROW),CHN0(MXROW)
     IF(NFINIT .EQ. 0) THEN
           READ(5,*) POT
           DO 100 I=1,NGLOBE
             CHI0(I) = POT
```

```
 100   CONTINUE
       ELSE IF(NFINIT .EQ. 1) THEN
            READ(5,*) (CHI0(I),I=1,NGLOBE)
       END IF

C      NNODES = No. of external of nodes at which initial flux values should
C              be specified
       READ(5,*) NNODES
       IF(NNODES .GE. 1) THEN
C      Specify node number, and initial flux value the NNODES
            DO I=1,NNODES
C      J = Node number;   U = flux Value
               READ(5,*) J,U
               CHN0(J) = U
            END DO
       END IF
       RETURN
       END

       SUBROUTINE RECHARGE(NRECH,RECH,MXROW,NGLOBE)
       IMPLICIT REAL*4 (A-H,O-Z)
       DIMENSION RECH(MXROW)
       IF(NRECH .EQ. 0) THEN
            READ(5,*) RAIN
            DO I=1,NGLOBE
              RECH(I) = RAIN
            END DO
       ELSE IF(NRECH .EQ. 1) THEN
            READ(5,*) (RECH(I),I=1,NGLOBE)
c
c         do i=1,nglobe
c           rech(i) = x(i)*0.5
c         end do
       END IF
       RETURN
       END

            SUBROUTINE RECHARGET1(RECH,TIME,MXROW,NGLOBE)
            IMPLICIT REAL*4 (A-H,O-Z)
            DIMENSION RECH(MXROW)
            DO I=1,NGLOBE
            RECH(I)=(0.0003*(TIME**5)-0.0106*(TIME**4)+0.1215*(TIME**3)
            *-0.6175*(TIME**2)+1.4715*TIME-1.0806)/2425500

            END DO
            RETURN
        END

            SUBROUTINE RECHARGET2(RECH,TIME,MXROW,NGLOBE)
            IMPLICIT REAL*4 (A-H,O-Z)
            DIMENSION RECH(MXROW)
```

```
      DO I=1,NGLOBE
      RECH(I) =(-0.0862*(TIME**5)+5.7354*(TIME**4)-151.84*(TIME**3)
      *+1998*(TIME**2)-13061*TIME+33920)/2425500

      END DO
      RETURN
    END

      SUBROUTINE RECHARGET3(RECH,TIME,MXROW,NGLOBE)
      IMPLICIT REAL*4 (A-H,O-Z)
      DIMENSION RECH(MXROW)
      DO I=1,NGLOBE
      RECH(I)=(-0.000000000003*(TIME**5)+0.000000003*(TIME**4)-0.000001
      **(TIME**3)+0.0003*(TIME**2)-0.0316*TIME+1.7307)/2425500


      END DO
      RETURN
    END

    SUBROUTINE INTG(SIZE,NELEM,X,MXNODES,MXELN)
    IMPLICIT REAL *4(A-H,O-Z)
    DIMENSION SIZE(MXELN),X(MXNODES)

    DO M=1,NELEM
        DELX = X(M+1)-X(M)
        SIZE(M) = DELX

C   Boundary integrations for the diffusion term (Evaluate limits)
c     RLN(M,1,1) = 1.0
c     RLN(M,1,2) = -(1.0+DELX)
c     RLN(M,2,2) = -RLN(M,1,1)
c     RLN(M,2,1) = -RLN(M,1,2)

C   Performing line integration to account for the temporal term
c     W(M,1,1) = DELX*(DELX+3.0)/6.0
c     W(M,1,2) = DELX*(2.0*DELX+3.0)/6.0
c     W(M,2,2) = W(M,1,1)
c     W(M,2,1) = W(M,1,2)

C   Accounting for the advective term
c     WX(M,1,1) = -(2.+DELX)/2.
c     WX(M,1,2) = (2.+DELX)/2.
c     WX(M,2,1) = -WX(M,1,2)
c     WX(M,2,2) = -WX(M,1,1)
    END DO
    RETURN
    END
    SUBROUTINE ASSMBL(H,NTYP,THETA,TSCALE,DELT,NELEM,MXROW,MXCOL,
   1          MXELN,INAT,MXBAND,DIFF,VELX,NEND,SIZE,DECAY,
   2          XMAX)
```

```
      IMPLICIT REAL *4(A-H,O-Z)
      INTEGER*1 NTYP
      DIMENSION NTYP(2),SIZE(MXELN),H(MXROW,MXCOL)

      NENM = NEND-1
      DO M=1,NELEM
            DO L=1,2
              I = 2*(M-1)+L
              J = MXBAND-L
              DO K=1,2
                J = J+1
                R = ABS(REAL(L-K))
                RN = (-1.)**(L+K-1)
                RLN = (-1.)**(K+1)*(XMAX+R*SIZE(M))
                WT = SIZE(M)/6.*(3.*XMAX+SIZE(M)*(1.+R))
                H(I,J) = (DIFF*RN+DECAY*WT)*THETA
                IF(INAT .EQ. 1) H(I,J) = H(I,J)+TSCALE/DELT*WT
                J = J+1
                H(I,J) = (DIFF*RLN+VELX*WT)*THETA
              END DO
            END DO
      END DO
      IF(NTYP(1) .EQ. 1) THEN
            H(1,MXBAND+1) = H(1,MXBAND)
            H(2,MXBAND) = H(2,MXBAND-1)
      END IF
      IF(NTYP(2) .EQ. 2) THEN
            H(NEND,MXBAND+1) = H(NEND,MXBAND+2)
            H(NENM,MXBAND+2) = H(NENM,MXBAND+3)
      END IF
      H(1,MXBAND) = 0.0
      H(2,MXBAND-1) = 0.0
      H(NENM,MXBAND+3) = 0.0
      H(NEND,MXBAND+2) = 0.0
      RETURN
      END

      SUBROUTINE RIGHT(RHS,NTYP,THETA,TSCALE,DELT,MXNODES,CHI,CHI0,
     1            CHN,CHN0,OLDDSDT,NELEM,MXROW,MXELN,INAT,
     2            TMINUS,DIFF,VELX,NGLOBE,NEND,SIZE,DECAY,RECH,
     3            XMAX)
      IMPLICIT REAL *4(A-H,O-Z)
      INTEGER *1 NTYP
      DIMENSION SIZE(MXELN),NTYP(2)
      DIMENSION CHI(MXNODES),CHI0(MXNODES),RHS(MXROW),RECH(MXNODES)
      DIMENSION CHN(MXNODES),CHN0(MXNODES),OLDDSDT(MXNODES)

      NENM = NEND-1
      IF(NTYP(1) .EQ. 2) THEN
            DO L=1,2
              R = ABS(REAL(L-1))
```

```
        RN = (-1.)**L
        WT = SIZE(1)/6.*(3.*XMAX+SIZE(1)*(1.+R))
        RHS(L) = -(DIFF*RN+DECAY*WT)*CHI(1)*THETA
        IF(INAT .EQ. 1) THEN
          RHS(L) = RHS(L)-TSCALE/DELT*WT*CHI(1)
        END IF
      END DO
    ELSE IF(NTYP(1) .EQ. 1) THEN
      DO L=1,2
        R = ABS(REAL(L-1))
        RLN = XMAX+R*SIZE(1)
        WT = SIZE(1)/6.*(3.*XMAX+SIZE(1)*(1.+R))
        RHS(L) = -(DIFF*RLN+VELX*WT)*CHN(1)*THETA
      END DO
    END IF
    IF(NTYP(2) .EQ. 2) THEN
      DO L=1,2
        I = NENM+L-1
        R = ABS(REAL(L-2))
        RN = (-1.)**(L+1)
        WT = SIZE(NELEM)/6.*(3.*XMAX+SIZE(NELEM)*(1.+R))
        RHS(I) = -(DIFF*RN+DECAY*WT)*CHI(NGLOBE)*THETA
        IF(INAT .EQ. 1) THEN
          RHS(I) = RHS(I)-TSCALE/DELT*WT*CHI(NGLOBE)
        END IF
      END DO
    ELSE IF(NTYP(2) .EQ. 1) THEN
      DO L=1,2
        I = NENM+L-1
        R = ABS(REAL(L-2))
        WT = SIZE(NELEM)/6.*(3.*XMAX+SIZE(NELEM)*(1.+R))
        RLN = -(XMAX+R*SIZE(NELEM))
        RHS(I) = -(DIFF*RLN+VELX*WT)*CHN(NGLOBE)*THETA
      END DO
    END IF
    DO M = 1,NELEM
      DO L=1,2
        I = 2*(M-1)+L
        DO K=1,2
          J = M+K-1
          R = ABS(REAL(L-K))
          WT = SIZE(M)/6.*(3.*XMAX+SIZE(M)*(1.+R))
          RHS(I) = RHS(I)-WT*RECH(J)
          IF(INAT .EQ. 1) THEN
              RN = (-1.)**(L+K-1)
              RLN = (-1.)**(K+1)*(XMAX+R*SIZE(M))
              DSDT = TSCALE/DELT*CHI0(J)-(1.0-TSCALE)*OLDDSDT(J)
              RHS(I) = RHS(I)-((DIFF*RN+DECAY*WT)*CHI0(J)+
1             (DIFF*RLN+VELX*WT)*CHN0(J))*TMINUS+WT*DSDT
          END IF
        END DO
```

```
      END DO
    END DO
    RETURN
    END

    SUBROUTINE SORT(CHI,CHN,RHS,NELEM,MXROW,MXNODES,NTYP,
   1            NGLOBE,NEND)
    IMPLICIT REAL *4(A-H,O-Z)
    INTEGER *1 NTYP
    DIMENSION CHI(MXNODES),CHN(MXNODES),RHS(MXROW),NTYP(2)

    IF(NTYP(1) .EQ. 1) THEN
      CHI(1) = RHS(1)
    ELSE
      CHN(1) = RHS(1)
    END IF
    IF(NTYP(2) .EQ. 1) THEN
      CHI(NGLOBE) = RHS(NEND)
    ELSE
      CHN(NGLOBE) = RHS(NEND)
    END IF
    DO M=2,NELEM
      I = 2*(M-1)
      CHI(M) = RHS(I)
      CHN(M) = RHS(I+1)
    END DO
    RETURN
    END
    SUBROUTINE SOLVE(KKK,C,R,NNP,IHALFB,MAXNP,MAXBW)

C   Subroutine  SOLVE
C   Purpose :-
C   (1) Decompose the coefficient matrix
C   (2) Modify the right hand side of the equations

    IMPLICIT REAL*4 (A-H,O-Z)
    DIMENSION C(MAXNP,MAXBW),R(MAXNP)

C   KKK = 0; Decompose and back-substitute,  KKK = 2 Back-substitute only
    IHBP = IHALFB+1
C   Decompose matrix C by banded Gaussian elimination for Non-symmetric
C   matrix.

    IF(KKK .EQ. 2) GO TO 50
    NU=NNP-IHALFB
    DO 20 NI=1,NU
      IF(ABS(C(NI,IHBP)) .LT. 1.E-30) THEN
        WRITE(6,'(/A,/A,F9.4,A,I3)')' The matrix is singular',
   1    '   Pivot element =',C(NI,IHBP),'    Row =',NI
        STOP
      END IF
```

```
          PIVOTI=1.0/C(NI,IHBP)
          NJ=NI+1
          IB=IHBP
          NK = NI+IHALFB
          NK=NI+IHALFB
          DO 10 NL=NJ,NK
            IB=IB-1
            A=-C(NL,IB)*PIVOTI
            C(NL,IB)=A
            JB=IB+1
            KB=IB+IHALFB
            LB=IHBP-IB
            DO 55 MB=JB,KB
              NB=LB+MB
              C(NL,MB)=C(NL,MB)+A*C(NI,NB)
 55       CONTINUE
 10     CONTINUE
 20   CONTINUE
      NR=NU+1
      NU=NNP-1
      NK=NNP
      DO 40 NI=NR,NU
          IF(ABS(C(NI,IHBP)) .LT. 1.E-30) THEN
            WRITE(*,'(/A,/A,F9.4,A,I3)')' The matrix is singular',
     1     '     Pivot element =',C(NI,IHBP),'     Row =',NI
            STOP
          END IF
          PIVOTI=1.0/(C(NI,IHBP))
          NJ=NI+1
          IB=IHBP
          DO 30 NL=NJ,NK
            IB=IB-1
            A=-C(NL,IB)*PIVOTI
            C(NL,IB)=A
            JB=IB+1
            KB=IB+IHALFB
            LB=IHBP-IB
            DO 65 MB=JB,KB
              NB=LB+MB
              C(NL,MB)=C(NL,MB)+A*C(NI,NB)
 65       CONTINUE
 30     CONTINUE
 40   CONTINUE
      IF(KKK-1) 50,44,50
 44   RETURN

C.....UPDATE RIGHT-HAND SIDE VECTOR, R

 50   NU=NNP+1
      IBAND=2*IHALFB+1
      DO 70 NI=2,IHBP
```

```
      IB=IHBP-NI+1
      NJ=1
      SUM=0.0
      DO 60 JB=IB,IHALFB
        SUM=SUM+C(NI,JB)*R(NJ)
        NJ=NJ+1
60    CONTINUE
      R(NI)=R(NI)+SUM
70 CONTINUE
  IB=1
  NL=IHBP+1
  DO 90 NI=NL,NNP
      NJ=NI-IHBP+1
      SUM=0.0
      DO 80 JB=IB,IHALFB
        SUM=SUM+C(NI,JB)*R(NJ)
        NJ=NJ+1
80    CONTINUE
      R(NI)=R(NI)+SUM
90 CONTINUE

C.....BACK SOLVE

  R(NNP)=R(NNP)/C(NNP,IHBP)
  DO 110 IB=2,IHBP
      NI=NU-IB
      NJ=NI
      MB=IHALFB+IB
      SUM=0.0
      DO 100 JB=NL,MB
        NJ=NJ+1
        SUM=SUM+C(NI,JB)*R(NJ)
100   CONTINUE
      R(NI)=(R(NI)-SUM)/C(NI,IHBP)
110 CONTINUE
  MB=IBAND
  DO 130 IB=NL,NNP
      NI=NU-IB
      NJ=NI
      SUM=0.0
      DO 120 JB=NL,MB
        NJ=NJ+1
        SUM=SUM+C(NI,JB)*R(NJ)
120   CONTINUE
      R(NI)=(R(NI)-SUM)/C(NI,IHBP)
130 CONTINUE
  RETURN
  END
```

D.2 Alteration to the Main Program.

This appendix deals with the Alteration that have been made to the main program as they appear in D.1. The alterations are given in the following sections.

D.2.1 Alteration to the program to account for the time dependent boundary conditions and splitting of the curves

T4=50.6667
T5=104.6667
T6=194.6667
T7=475

T4, T5, T6 AND T7, are times at which subroutines are called when ever program reaches a time domain at which that particular subroutine operate under.

The boundary conditions are time dependent and divided into four analytical equations

```
IF(TIME .LE. T4) THEN
CALL DATA4(CHI,NTYP,MXNODES,CHN,NGLOBE,TIME)
END IF

IF(TIME .GT.T4.AND.TIME.LE.T5) THEN
CALL DATA5(CHI,NTYP,MXNODES,CHN,NGLOBE,TIME)
END IF

IF(TIME .GT.T5.AND.TIME.LE.T6) THEN
CALL DATA6(CHI,NTYP,MXNODES,CHN,NGLOBE,TIME)

END IF

IF(TIME .GT.T6.AND.TIME.LE.T7) THEN
CALL DATA7(CHI,NTYP,MXNODES,CHN,NGLOBE,TIME)

END IF
```

The statements above assist in identifying the subroutine that is required by the program during particular time limits where that subroutine is operational.

```
SUBROUTINE DATA4(CHI,NTYP,MXNODES,CHN,NGLOBE,TIME)
      IMPLICIT REAL *4(A-H,O-Z)
    INTEGER *1 NTYP
    DIMENSION CHI(MXNODES),CHN(MXNODES),NTYP(2)

      NTYP (1) = 2
      NTYP (2) = 2
      TMP = 0.0

    IF(NTYP(1) .EQ. 1) THEN
       CHN(1) = TMP
    ELSE IF(NTYP(1) .EQ. 2) THEN
      CHI(1) =0.000087*(TIME**3)-0.0137*(TIME**2)+0.6793*TIME+25.454
    END IF

C    READ(5,*) NTYP(2),TMP
    IF(NTYP(2) .EQ. 1) THEN
       CHN(NGLOBE) = TMP
    ELSE IF(NTYP(2) .EQ. 2) THEN
      CHI(NGLOBE)=0.0001079*(TIME**3)-0.0196*(TIME**2)+1.1515
      * *TIME+25.325
    END IF
    RETURN
    END


      SUBROUTINE DATA5(CHI,NTYP,MXNODES,CHN,NGLOBE,TIME)
      IMPLICIT REAL *4(A-H,O-Z)
    INTEGER *1 NTYP
    DIMENSION CHI(MXNODES),CHN(MXNODES),NTYP(2)

            NTYP (1) = 2
            NTYP (2) = 2
            TMP = 0.0

    IF(NTYP(1) .EQ. 1) THEN
       CHN(1) = TMP
    ELSE IF(NTYP(1) .EQ. 2) THEN
       CHI(1) =0.0000044*(TIME**3)-0.0013*(TIME**2)+0.0874*TIME+34.267


    END IF

C    READ(5,*) NTYP(2),TMP
    IF(NTYP(2) .EQ. 1) THEN
       CHN(NGLOBE) = TMP
    ELSE IF(NTYP(2) .EQ. 2) THEN
    CHI(NGLOBE) =0.0000153*(TIME**3)-0.0045*(TIME**2)+0.3657
      * *TIME+38.926
```

```
      END IF
      RETURN
      END


SUBROUTINE DATA6(CHI,NTYP,MXNODES,CHN,NGLOBE,TIME)
          IMPLICIT REAL *4(A-H,O-Z)
      INTEGER *1 NTYP
      DIMENSION CHI(MXNODES),CHN(MXNODES),NTYP(2)

          NTYP (1) = 2
          NTYP (2) = 2
          TMP = 0.0


      IF(NTYP(1) .EQ. 1) THEN
            CHN(1) = TMP
      ELSE IF(NTYP(1) .EQ. 2) THEN
           CHI(1)=0.000001*(TIME**3)-0.00047*(TIME**2)+0.0151*TIME+36.437

      END IF

C     READ(5,*) NTYP(2),TMP
      IF(NTYP(2) .EQ. 1) THEN
            CHN(NGLOBE) = TMP
      ELSE IF(NTYP(2) .EQ. 2) THEN
     CHI(NGLOBE)=0.00000115*(TIME**3)-0.000494*(TIME**2)-0.0326
          * *TIME+52.79

      END IF
      RETURN
      END


SUBROUTINE DATA7(CHI,NTYP,MXNODES,CHN,NGLOBE,TIME)
     IMPLICIT REAL *4(A-H,O-Z)
      INTEGER *1 NTYP
      DIMENSION CHI(MXNODES),CHN(MXNODES),NTYP(2)

          NTYP (1) = 2
          NTYP (2) = 2
          TMP = 0.0

     IF(NTYP(1) .EQ. 1) THEN
            CHN(1) = TMP
     ELSE IF(NTYP(1) .EQ. 2) THEN
          CHI(1)=0.00000005*(TIME**3)-0.00006*(TIME**2)+0.006*TIME+29.398

     END IF
```

```
C     READ(5,*) NTYP(2),TMP
      IF(NTYP(2) .EQ. 1) THEN
            CHN(NGLOBE) = TMP
       ELSE IF(NTYP(2) .EQ. 2) THEN
     CHI(NGLOBE)=-0.0000008*(TIME**3)+0.000916*(TIME**2)-0.3645*
     *TIME+78.262


      END IF
      RETURN
      END
```

The subroutines above that describe the time depended boundary conditions and operate at particular times indicated above.

D.2.2 Alteration to the program to account for the time dependent recharge function and splitting of the heat rate curve.

```
T1=12.6669
T2=15.3253
T3=267.7307
```

T1, T2, AND T3, are times at which subroutines are called when ever program reaches a time domain at which that particular subroutine operate under.

```
c       The recharge function is time dependent and uses three functions
        IF(TIME .LE. T1) THEN
        CALL RECHARGET1(RECH,TIME,MXNODES,NGLOBE)
        END IF

        IF(TIME .GT.T1.AND.TIME.LE.T2) THEN
        CALL RECHARGET2(RECH,TIME,MXNODES,NGLOBE)
        END IF


        IF(TIME .GT.T2.AND.TIME.LE.T3) THEN
        CALL RECHARGET3(RECH,TIME,MXNODES,NGLOBE)
        END IF
```

The statements above assist in identifying the subroutine that is required by the program during particular time limits where that subroutine is operational.

```
SUBROUTINE RECHARGET1(RECH,TIME,MXROW,NGLOBE)
      IMPLICIT REAL*4 (A-H,O-Z)
      DIMENSION RECH(MXROW)
      DO I=1,NGLOBE
      RECH(I)=(0.0003*(TIME**5)-0.0106*(TIME**4)+0.1215*(TIME**3)
      *-0.6175*(TIME**2)+1.4715*TIME-1.0806)/2425500

      END DO
      RETURN
    END
```

```
      SUBROUTINE RECHARGET2(RECH,TIME,MXROW,NGLOBE)
      IMPLICIT REAL*4 (A-H,O-Z)
      DIMENSION RECH(MXROW)
      DO I=1,NGLOBE
      RECH(I) =(-0.0862*(TIME**5)+5.7354*(TIME**4)-151.84*(TIME**3)
      *+1998*(TIME**2)-13061*TIME+33920)/2425500


      END DO
      RETURN
END

      SUBROUTINE RECHARGET3(RECH,TIME,MXROW,NGLOBE)
      IMPLICIT REAL*4 (A-H,O-Z)
      DIMENSION RECH(MXROW)
      DO I=1,NGLOBE
      RECH(I)=(-0.000000000003*(TIME**5)+0.000000003*(TIME**4)-0.000001
      **(TIME**3)+0.0003*(TIME**2)-0.0316*TIME+1.7307)/2425500


      END DO
      RETURN
END
```

The subroutines above describe the time depended recharge functions and operate at particular times indicated above.

D.3 Input Data Files.

D.3.1 Input Data File For Time Between O and 46 hours.

1-D. Diffusion-advection problem	
0 0	Key1, Key2
0.004303	DIFF
0.0	VELX
0.0	DECAY
1	Inat
1 5 0	nsub, time, icond
1 1 60	nwrite, tdiv, tlevel
3	TIME SCHEME
1.25	THETA
3	NSEG
0.0 0	X(1), NSP(1)
0.1 0	X(IEND), NSP(M)
0.25 2	X(1), NSP(1)
1.0 0	X(IEND), NSP(M)
0	NFINIT
26.0609	POT
0	NNODES
0	NRECH
0	RECH

D.3.2 Input Data File For Time Between 46.6667 and 284.6667 hours.

1-D. Diffusion-advection problem	
0 0	Key1, Key2
0.004303	DIFF
0.0	VELX
0.0	DECAY
1	Inat
1 46.6667 1	nsub, time, icond
1 2 284.6667	nwrite, tdiv, tlevel
3	TIME SCHEME
1.25	THETA
3	NSEG
0.0 0	X(1), NSP(1)
0.1 0	X(IEND), NSP(M)
0.25 2	X(1), NSP(1)
1.0 0	X(IEND), NSP(M)
0	NFINIT
26.0609	POT
0	NNODES
0	NRECH
0	RECH

D.3.3 Input Data File For Time Between 285 and 475 hours.

1-D. Diffusion-advection problem	
0 0	Key1, Key2
0.004303	DIFF
0.0	VELX
0.0	DECAY
1	Inat
1 285 1	nsub, time, icond
1 2 475	nwrite, tdiv, tlevel
3	TIME SCHEME
1.25	THETA
3	NSEG
0.0 0	X(1), NSP(1)
0.1 0	X(IEND), NSP(M)
0.25 2	X(1), NSP(1)
1.0 0	X(IEND), NSP(M)
0	NFINIT
26.0609	POT
0	NNODES
0	NRECH
0	RECH

D.4 Output File

The out file for temperature have been converted to Excel Spreadsheet and are found on appendix

Appendix D – GEM Examples Solved by Hand

Linear Equations Examples

Part 1 : Linear equation without a source term

In Section 1 Part 1 we developed a Green Element model that we shall use in this chapter to solve linear problems through a homogeneous domain.

Our first example is a 1-D Poisson equation with no recharge. The example is given by

$$\frac{d^2\phi}{dx^2} = 0; \qquad \phi(x=0) = 0 \qquad and \qquad \phi(x=1) = 1$$

The exact solution to the problem is given by

$$\phi = x, \qquad and \qquad \frac{d\phi}{dx} = \varphi = 1$$

Solution

We shall discretize the computational domain over which the differential equation is valid into 4 equal elements, so that the spatial element size is uniform, that is

$\ell = \bar{\ell} = 0.25$. As shown below

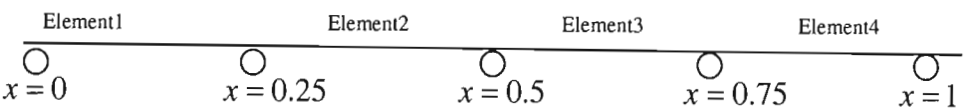

Green Element equation for this problem is obtained from eq. (1.24) in Section 1 and restated below

$$\sum_{e=1}^{M} R_{ij}^{(e)}\phi_j^{(e)} + L_{ij}^{(e)}\varphi_j^{(e)} + F_i^{(e)} = 0 \qquad i, j = 1,2$$

Since there is no recharge, $F_i^{(e)} = 0$ and the third term of the above equation becomes 0.

Eight equations are required to solve eight unknowns.

Step 1: Calculate the values of the coefficients, $R_{ij}^{(e)}$ and $L_{ij}^{(e)}$

According to equations (1.25) and (1.26), repectively.

$$R_{ij}^{(e)} = \begin{bmatrix} -1 & 1 \\ 1 & -1 \end{bmatrix} \qquad and \qquad L_{ij}^{(e)} = 0.25 \begin{bmatrix} 1 & -2 \\ 2 & -1 \end{bmatrix}$$

Step 2: Fornulate elementary equations

Element 1:

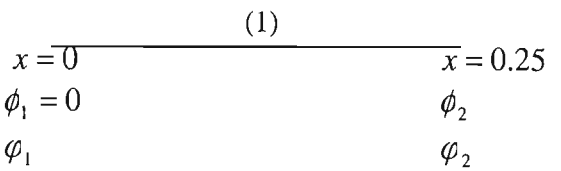

$$R_{11}\phi_1 + R_{12}\phi_2 + L_{11}\varphi_1 + L_{12}\varphi_2 = 0$$

$$\phi_2 + 0.25\varphi_1 - 0.5\varphi_2 = 0$$

$$R_{21}\phi_1 + R_{22}\phi_2 + L_{21}\phi_1 + L_{22}\phi_2 = 0$$

$$-\phi_2 + 0.5\varphi_1 - 0.25\varphi_2 = 0$$

Element 2:

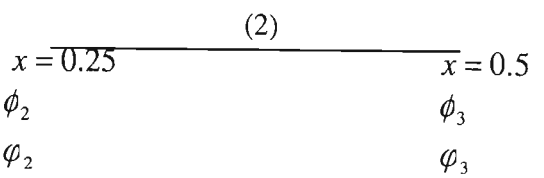

$$R_{11}\phi_2 + R_{12}\phi_3 + L_{11}\varphi_2 + L_{12}\varphi_3 = 0$$

$$-\phi_2 + \phi_3 + 0.25\varphi_2 - 0.5\varphi_3 = 0$$

$$R_{21}\phi_2 + R_{22}\phi_3 + L_{21}\varphi_2 + L_{22}\varphi_3 = 0$$

$$\phi_2 - \phi_3 + 0.5\varphi_2 - 0.25\varphi_3 = 0$$

Element 3:

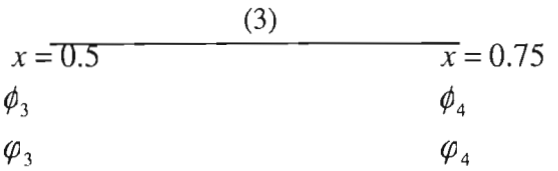

$$R_{11}\phi_3 + R_{12}\phi_4 + L_{11}\varphi_3 + L_{12}\varphi_4 = 0$$

$$-\phi_3 + \phi_4 + 0.25\varphi_3 - 0.5\varphi_4 = 0$$

$$R_{21}\phi_3 + R_{22}\phi_4 + L_{21}\varphi_3 + L_{22}\varphi_4 = 0$$

$$\phi_3 - \phi_4 + 0.5\varphi_3 - 0.25\varphi_4 = 0$$

Element 4:

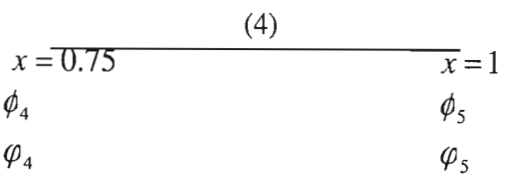

$$R_{11}\phi_4 + R_{12}\phi_5 + L_{11}\varphi_4 + L_{12}\varphi_5 = 0$$

$$-\phi_4 + 1 + 0.25\varphi_4 - 0.5\varphi_5 = 0$$

$$-\phi_4 + 0.25\varphi_4 - 0.5\varphi_5 = -1$$

$$R_{21}\phi_4 + R_{22}\phi_5 + L_{21}\varphi_4 + L_{22}\varphi_5 = 0$$

$$\phi_4 - 1 + 0.5\varphi_4 - 0.25\varphi_5 = 0$$

$$\phi_4 + 0.5\varphi_4 - 0.25\varphi_5 = 1$$

Step 3: Assemble global matrix from the equations obtained in Step 2 and solve.

$$\begin{bmatrix} 1 & 0.25 & -0.5 & 0 & 0 & 0 & 0 & 0 \\ -1 & 0.5 & -0.25 & 0 & 0 & 0 & 0 & 0 \\ -1 & 0 & 0.25 & 1 & -0.5 & 0 & 0 & 0 \\ 1 & 0 & 0.5 & -1 & -0.25 & 0 & 0 & 0 \\ 0 & 0 & 0 & -1 & 0.25 & 1 & -0.5 & 0 \\ 0 & 0 & 0 & 1 & 0.5 & -1 & -0.25 & 0 \\ 0 & 0 & 0 & 0 & 0 & -1 & 0.25 & -0.5 \\ 0 & 0 & 0 & 0 & 0 & 1 & 0.5 & -0.25 \end{bmatrix} \begin{Bmatrix} \phi_2 \\ \varphi_1 \\ \varphi_2 \\ \phi_3 \\ \varphi_3 \\ \phi_4 \\ \varphi_4 \\ \varphi_5 \end{Bmatrix} = \begin{Bmatrix} 0 \\ 0 \\ 0 \\ 0 \\ 0 \\ 0 \\ -1 \\ 1 \end{Bmatrix}$$

Step 4: Tabulate the results obtained from Step 3 and compare against exact solution and Gem solutions obtained by using a domain that is discretized into 4 elements.

Solution	Exact Solution	**GEM** Solution
Of ϕ at x=0.25	0.25	0.25
x=0.5	0.5	0.5
x=0.75	0.75	0.75
Of φ at x=0	1	1
X=0.25	1	1
X=0.5	1	1
x=0.75	1	1
X=1	1	1

Part 2 : Linear equation with a Distributed Source Term

Our second example is a 1-D Poisson equation with a distributed source, and is obtained from The Green Element Method text book by A.E.Taigbenu, Exercise 2.4(b) and is given by the following equation

$$\frac{d^2\phi}{dx^2}+1=0; \qquad \phi(x=0)=1 \qquad and \qquad \phi(1)=0$$

The exact solution to the above problem is given by

$$\phi=1-\frac{x}{2}-\frac{x^2}{2} \qquad and \qquad \frac{d\phi}{dx}=-\frac{1}{2}-x$$

Solution

We shall discretize the computational domain over which the differential equation is valid into 4 equal elements, so that the spatial element size is uniform, that is

$\ell=\bar{\ell}=0.25$. Green Element equation for this problem is obtained from eq. (1.24) in Section 1 and restated below

$$\sum_{e=1}^{M} R_{ij}^{(e)}\phi_j^{(e)}+L_{ij}^{(e)}\varphi_j^{(e)}+F_i^{(e)}=0 \qquad i,j=1,2$$

Eight equations are required to solve eight unknowns.

Step 1: Calculate the values of the coefficients, $R_{ij}^{(e)}$ and $L_{ij}^{(e)}$

According to equations (1.25) and (1.26), repectively

$$R_{ij}^{(e)}=\begin{bmatrix}-1 & 1\\ 1 & -1\end{bmatrix} \qquad and \qquad L_{ij}^{(e)}=\frac{1}{3}\begin{bmatrix}1 & -2\\ 2 & -1\end{bmatrix}$$

and $F_i^{(e)}$ in accordance with eqs. (1.31) and (1.32) for distributed source/sink

$$F_1^{(e)}=\frac{1}{K}\int_{x_1^{(e)}}^{x_2^{(e)}} f(x)\left(x-x_1^{(e)}+\bar{\ell}\right)dx$$

$$F_2^{(e)}=\frac{1}{K}\int_{x_1^{(e)}}^{x_2^{(e)}} f(x)\left(x_2^{(e)}-x+\bar{\ell}\right)dx$$

Noting that K=1 and f(x)=-1, we can now compute the values of F_1 and F_2 for each element.

$$F_1^{(e)} = \int_{x_1^{(e)}}^{x_2^{(e)}} (-1)\left(x - x_1^{(e)} + \bar{\ell} \right) dx = \left[-\frac{x^2}{2} + x_1^{(e)} x - \bar{\ell} x \right]_{x_1^{(e)}}^{x_2^{(e)}} = \left[-0.5x^2 + x_1^{(e)} x - 0.25x \right]_{x_1^{(e)}}^{x_2^{(e)}}$$

$$F_2^{(e)} = \int_{x_1^{(e)}}^{x_2^{(e)}} (-1)\left(x_2^{(e)} - x + \bar{\ell} \right) dx = \left[-x_2^{(e)} x + \frac{x^2}{2} - \bar{\ell} x \right]_{x_1^{(e)}}^{x_2^{(e)}} = \left[-x_2^{(e)} x + 0.5x^2 - 0.25x \right]_{x_1^{(e)}}^{x_2^{(e)}}$$

Substituting the values of x_1 and x_2 for each element into the above equations yield the following results

$$F_1^{(1)} = F_2^{(1)} = F_1^{(2)} = F_2^{(2)} = F_1^{(3)} = F_2^{(3)} = F_1^{(4)} = F_2^{(4)} = -0.0938$$

Step 2: Fornulate element equations

Element 1:

$$R_{11}\phi_1 + R_{12}\phi_2 + L_{11}\varphi_1 + L_{12}\varphi_2 + F_1 = 0$$
$$-1 + \phi_2 + 0.25\varphi_1 - 0.5\varphi_2 - 0.0938 = 0$$
$$\phi_2 + 0.25\varphi_1 - 0.5\varphi_2 = 1.0938$$

$$R_{21}\phi_1 + R_{22}\phi_2 + L_{21}\phi_1 + L_{22}\phi_2 + F_2 = 0$$
$$1 - \phi_2 + 0.5\varphi_1 - 0.25\varphi_2 - 0.0938 = 0$$
$$-\phi_2 + 0.5\varphi_1 - 0.25\varphi_2 = -0.9062$$

Element 2:

$$R_{11}\phi_2 + R_{12}\phi_3 + L_{11}\varphi_2 + L_{12}\varphi_3 + F_1 = 0$$
$$-\phi_2 + \phi_3 + 0.25\varphi_2 - 0.5\varphi_3 = 0.0938$$

$$R_{21}\phi_2 + R_{22}\phi_3 + L_{21}\varphi_2 + L_{22}\varphi_3 + F_2 = 0$$
$$\phi_2 - \phi_3 + 0.5\varphi_2 - 0.25\varphi_3 = 0.0938$$

Element 3:

$$R_{11}\phi_3 + R_{12}\phi_4 + L_{11}\varphi_3 + L_{12}\varphi_4 + F_1 = 0$$

$$-\phi_3 + \phi_4 + 0.25\varphi_3 - 0.5\varphi_4 = 0.0938$$

$$R_{21}\phi_3 + R_{22}\phi_4 + L_{21}\varphi_3 + L_{22}\varphi_4 + F_2 = 0$$

$$\phi_3 - \phi_4 + 0.5\varphi_3 - 0.25\varphi_4 = 0.0938$$

Element 4:

$$R_{11}\phi_4 + R_{12}\phi_5 + L_{11}\varphi_4 + L_{12}\varphi_5 + F_1 = 0$$

$$-\phi_4 + 0 + 0.25\varphi_4 - 0.5\varphi_5 - 0.0938 = 0$$

$$-\phi_4 + 0.25\varphi_4 - 0.5\varphi_5 = 0.0938$$

$$R_{21}\phi_4 + R_{22}\phi_5 + L_{21}\varphi_4 + L_{22}\varphi_5 + F_2 = 0$$

$$\phi_4 - 0 + 0.5\varphi_4 - 0.25\varphi_5 - 0.0938 = 0$$

$$\phi_4 + 0.5\varphi_4 - 0.25\varphi_3 = 0.0938$$

Step 3: Assemble global matrix from the equations obtained in Step 2 and solve.

$$\begin{bmatrix} 1 & 0.25 & -0.5 & 0 & 0 & 0 & 0 & 0 \\ -1 & 0.5 & -0.25 & 0 & 0 & 0 & 0 & 0 \\ -1 & 0 & 0.25 & 1 & -0.5 & 0 & 0 & 0 \\ 1 & 0 & 0.5 & -1 & -0.25 & 0 & 0 & 0 \\ 0 & 0 & 0 & -1 & 0.25 & 1 & -0.5 & 0 \\ 0 & 0 & 0 & 1 & 0.5 & -1 & -0.25 & 0 \\ 0 & 0 & 0 & 0 & 0 & -1 & 0.25 & -0.5 \\ 0 & 0 & 0 & 0 & 0 & 1 & 0.5 & -0.25 \end{bmatrix} \begin{Bmatrix} \phi_2 \\ \varphi_1 \\ \varphi_2 \\ \phi_3 \\ \varphi_3 \\ \phi_4 \\ \varphi_4 \\ \varphi_5 \end{Bmatrix} = \begin{Bmatrix} 1.0938 \\ -0.9062 \\ 0.0938 \\ 0.0938 \\ 0.0938 \\ 0.0938 \\ 0.0938 \\ 0.0938 \end{Bmatrix}$$

Step 4: Tabulate the results obtained from Step 3 and compare against exact solution and Gem solutions obtained by using a domain that is discretized into 3 elements.

Solution	Exact Solution	**GEM** Solution
Of ϕ at x=0.25	0.8438	0.8438
x=0.5	0.625	0.6251
x=0.75	0.3438	0.3438
Of φ at x=0	-0.5	-0.4997
X=0.25	-0.75	-0.7499
X=0.5	-1	-1
x=0.75	-1.25	-1.251
X=1	-1.5	-1.5003

Part 3 : Linear equation with a Distributed Source Term

Our second example is a 1-D Poisson equation with a distributed source, and is obtained from The Green Element Method text book by A.E.Taigbenu, Exercise 2.4(c) and is given by the following equation

$$\frac{d^2\phi}{dx^2} = (x^2 - 1); \qquad \phi(x=0) = 0 \qquad and \qquad \phi(1) = 0$$

The exact solution to the above problem is given by

$$\phi = 0.0833x^4 - 0.5x^2 + 04167x \qquad \varphi = 0.3333x^3 - x + 04167$$

Solution

We shall discretize the computational domain over which the differential equation is valid into 4 equal elements, so that the spatial element size is uniform, that is $\ell = \bar{\ell} = 0.25$. Green Element equation for this problem is obtained from eq. (1.24) in Section 1 and restated below

$$\sum_{e=1}^{M} R_{ij}^{(e)}\phi_j^{(e)} + L_{ij}^{(e)}\varphi_j^{(e)} + F_i^{(e)} = 0 \qquad i, j = 1,2$$

Eight equations are required to solve eight unknowns.

Step 1: Calculate the values of the coefficients, $R_{ij}^{(e)}$ and $L_{ij}^{(e)}$

According to equations (1.25) and (1.26), repectively

$$R_{ij}^{(e)} = \begin{bmatrix} -1 & 1 \\ 1 & -1 \end{bmatrix} \qquad and \qquad L_{ij}^{(e)} = \frac{1}{3}\begin{bmatrix} 1 & -2 \\ 2 & -1 \end{bmatrix}$$

and $F_i^{(e)}$ in accordance with eqs. (1.31) and (1.32) for distributed source/sink

$$F_1^{(e)} = \frac{1}{K}\int_{x_1^{(e)}}^{x_2^{(e)}} f(x)\left(x - x_1^{(e)} + \bar{\ell}\right)dx$$

$$F_2^{(e)} = \frac{1}{K}\int_{x_1^{(e)}}^{x_2^{(e)}} f(x)\left(x_2^{(e)} - x + \bar{\ell}\right)dx$$

Noting that K=1 and f(x)=-1, we can now compute the values of F_1 and F_2 for each element.

$$F_1^{(e)} = \int_{x_1^{(e)}}^{x_2^{(e)}} \left(x^2 - 1\right)\left(x - x_1^{(e)} + \bar{\ell}\right)dx = \left[0.25x^4 - 0.3333x_1^{(e)}x^3 + 0.3333\bar{\ell}x^3 - 0.5x^2 + x_1^{(e)}x - \bar{\ell}x\right]_{x_1^{(e)}}^{x_2^{(e)}}$$

$$F_1^{(e)} = \int_{x_1^{(e)}}^{x_2^{(e)}} \left(x^2 - 1\right)\left(x - x_1^{(e)} + \bar{\ell}\right)dx = \left[0.25x^4 - 0.3333x_1^{(e)}x^3 + 0.0833\bar{\ell}x^3 - 0.5x^2 + x_1^{(e)}x - 0.25x\right]_{x_1^{(e)}}^{x_2^{(e)}}$$

$$F_2^{(e)} = \int_{x_1^{(e)}}^{x_2^{(e)}} \left(x^2 - 1\right)\left(x - x_1^{(e)} + \bar{\ell}\right) dx = \left[0.3333 x_2^{(e)} x^3 - 0.25x^4 + 0.3333\bar{\ell}\, x^3 - x_2^{(e)} x + 0.5x^2 - \bar{\ell}\, x\right]_{x_1^{(e)}}^{x_2^{(e)}}$$

$$F_2^{(e)} = \int_{x_1^{(e)}}^{x_2^{(e)}} \left(x^2 - 1\right)\left(x - x_1^{(e)} + \bar{\ell}\right) dx = \left[0.3333 x_2^{(e)} x^3 - 0.25x^4 + 0.0833x^3 - x_2^{(e)} x + 0.5x^2 - 0.25x\right]_{x_1^{(e)}}^{x_2^{(e)}}$$

Substituting the values of x_1 and x_2 for each element into the above equations yield the following results

$F_1^{(1)} = -0.0915$ $\quad F_2^{(1)} = -0.0921$ $\quad F_1^{(2)} = -0.0791$ $\quad F_2^{(2)} = -0.0811$

$F_1^{(3)} = -0.0549$ $\quad F_2^{(3)} = -0.0584$ $\quad F_1^{(4)} = -0.0193$ $\quad F_2^{(4)} = -0.0238$

Step 2: Fornulate element equations

Element 1:

$$R_{11}\phi_1 + R_{12}\phi_2 + L_{11}\varphi_1 + L_{12}\varphi_2 + F_1 = 0$$

$$0 + \phi_2 + 0.25\varphi_1 - 0.5\varphi_2 - 0.09915 = 0$$

$$\phi_2 + 0.25\varphi_1 - 0.5\varphi_2 = 0.0915$$

$$R_{21}\phi_1 + R_{22}\phi_2 + L_{21}\phi_1 + L_{22}\phi_2 + F_2 = 0$$

$$0 - \phi_2 + 0.5\varphi_1 - 0.25\varphi_2 - 0.0938 = 0$$

$$-\phi_2 + 0.5\varphi_1 - 0.25\varphi_2 = -0.9062$$

Element 2:

$$R_{11}\phi_2 + R_{12}\phi_3 + L_{11}\varphi_2 + L_{12}\varphi_3 + F_1 = 0$$

$$-\phi_2 + \phi_3 + 0.25\varphi_2 - 0.5\varphi_3 = 0.0791$$

$$R_{21}\phi_2 + R_{22}\phi_3 + L_{21}\varphi_2 + L_{22}\varphi_3 + F_2 = 0$$

$$\phi_2 - \phi_3 + 0.5\varphi_2 - 0.25\varphi_3 = 0.0811$$

Element 3:

$$R_{11}\phi_3 + R_{12}\phi_4 + L_{11}\varphi_3 + L_{12}\varphi_4 + F_1 = 0$$

$$-\phi_3 + \phi_4 + 0.25\varphi_3 - 0.5\varphi_4 = 0.0549$$

$$R_{21}\phi_3 + R_{22}\phi_4 + L_{21}\varphi_3 + L_{22}\varphi_4 + F_2 = 0$$

$$\phi_3 - \phi_4 + 0.5\varphi_3 - 0.25\varphi_4 = 0.0584$$

Element 4:

$$R_{11}\phi_4 + R_{12}\phi_5 + L_{11}\varphi_4 + L_{12}\varphi_5 + F_1 = 0$$

$$-\phi_4 + 0 + 0.25\varphi_4 - 0.5\varphi_5 - 0.0193 = 0$$

$$-\phi_4 + 0.25\varphi_4 - 0.5\varphi_5 = 0.0193$$

$$R_{21}\phi_4 + R_{22}\phi_5 + L_{21}\varphi_4 + L_{22}\varphi_5 + F_2 = 0$$

$$\phi_4 - 0 + 0.5\varphi_4 - 0.25\varphi_5 - 0.0238 = 0$$

$$\phi_4 + 0.5\varphi_4 - 0.25\varphi_5 = 0.0238$$

Step 3: Assemble global matrix from the equations obtained in Step 2 and solve.

$$\begin{bmatrix} 1 & 0.25 & -0.5 & 0 & 0 & 0 & 0 & 0 \\ -1 & 0.5 & -0.25 & 0 & 0 & 0 & 0 & 0 \\ -1 & 0 & 0.25 & 1 & -0.5 & 0 & 0 & 0 \\ 1 & 0 & 0.5 & -1 & -0.25 & 0 & 0 & 0 \\ 0 & 0 & 0 & -1 & 0.25 & 1 & -0.5 & 0 \\ 0 & 0 & 0 & 1 & 0.5 & -1 & -0.25 & 0 \\ 0 & 0 & 0 & 0 & 0 & -1 & 0.25 & -0.5 \\ 0 & 0 & 0 & 0 & 0 & 1 & 0.5 & -0.25 \end{bmatrix} \begin{Bmatrix} \phi_2 \\ \varphi_1 \\ \varphi_2 \\ \phi_3 \\ \varphi_3 \\ \phi_4 \\ \varphi_4 \\ \varphi_5 \end{Bmatrix} = \begin{Bmatrix} 0.0915 \\ 0.0921 \\ 0.0791 \\ 0.0811 \\ 0.0549 \\ 0.0584 \\ 0.0193 \\ 0.0238 \end{Bmatrix}$$

Step 4: Tabulate the results obtained from Step 3 and compare against exact solution and Gem solutions obtained by using a domain that is discretized into 3 elements.

Solution	Exact Solution	**GEM** Solution
Of ϕ at x=0.25	0.0732	0.0733
x=0.5	0.0886	0.0866
x=0.75	0.0576	0.0576
Of φ at x=0	0.4167	0.4168
X=0.25	0.1719	0.1720
X=0.5	-0.416	-0.416
x=0.75	-01927	-0.1927
X=1	-0.2500	-0.2502

Part 4 : Linear equation with a Concentrated Source Term

We shall solve a 1-D Poisson equation with a concentrated source given by the following relationship

$$\frac{d^2\phi}{dx^2} = \delta(x-0.6) \qquad \phi(x=0)=0 \qquad and \qquad \phi(x=1)=0$$

Exact Solution

The above problem is similar to a case of a simply supported beam which is subjected to a point load with magnitude of 1 acting at position 0.5. (i.e. $\frac{d^2\phi}{dx^2}$ can be considered as a loading equation, where $\frac{d\phi}{dx}$ is the shear force at any point x and ϕ is the bending moment at any point x). (Please note that load acting downwards will be assigned a positive sign and bending above the neutral axis will be considered to be positive)

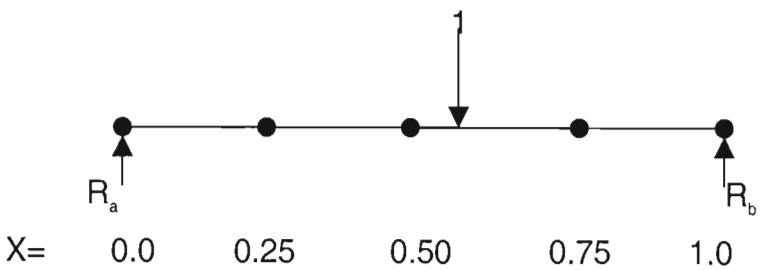

Moments at A=0: R_b = 1x0.6 = 0.6 upwards

Sum of vertical Forces=0: R_a= 1-0.6 = 0.4 upwards

From the simple mechanics theories with can determine the Bending Moment (ϕ) and Shear Force (φ) at points x=0, 0.25, 0.5, 0.75 and 1.0.

$\phi(x=0) = \phi(x=1) = 0$

$\phi(x=0.25) = -0.4 * 0.25 = -0.1$

$\phi(x=0.5) = -0.4 * 0.5+ = -0.2$

$\phi(x=0.75) = -0.6 * 0.25 = -0.15$

$\varphi(x=0) = \varphi(x=0.25)\varphi = (x=0.5) = -0.4$

$\varphi(x=0.75) = \varphi(x=1) = 1 - 0.4 = 0.6$

GEM Solution

We shall discretize the computational domain over which the differential equation is valid into 4 equal elements, so that the spatial element size is uniform, that is $\ell = \bar{\ell} = 0.25$.

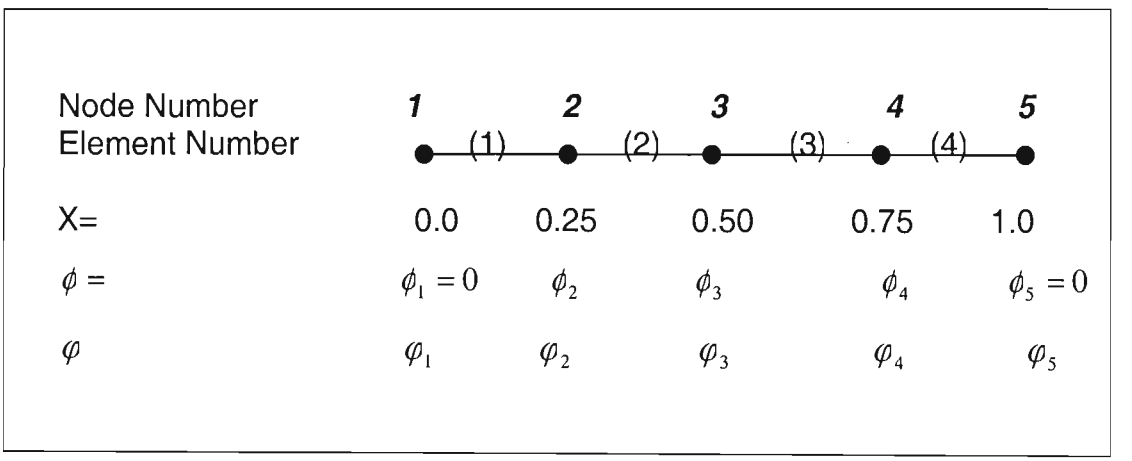

Green Element equation for this problem is obtained from eq. (1.24) in Chapter 1 and restated below

$$\sum_{e=1}^{M} R_{ij}^{(e)} \phi_j^{(e)} + L_{ij}^{(e)} \varphi_j^{(e)} + F_i^{(e)} = 0 \qquad i, j = 1,2$$

Eight equations are reqiured as there is eight unknowns.

Step 1: Calculate the values of the coefficients, $R_{ij}^{(e)}$ and $L_{ij}^{(e)}$, according to equations (1.25) and (1.26), repectively

$$R_{ij}^{(e)} = \begin{bmatrix} -1 & 1 \\ 1 & -1 \end{bmatrix} \qquad and \qquad L_{ij}^{(e)} = \frac{1}{3}\begin{bmatrix} 1 & -2 \\ 2 & -1 \end{bmatrix}$$

and $F_i^{(e)}$ in accordance with eqs. (1.33) and (1.34) for point source/sink

$$F_1^{(e)} = \frac{1}{K}\sum_{j=1}^{N_p^{(e)}} Q_j\left(x_j - x_1^{(e)} + \bar{\ell}\right)$$

$$F_2^{(e)} = \frac{1}{K}\sum_{j=1}^{N_p^{(e)}} Q_j\left(x_2^{(e)} - x_j + \bar{\ell}\right)$$

Noting that K=1, we can now compute the values of F_1 and F_2 for each element.

$$F_1^{(1)} = F_2^{(1)} = F_1^{(2)} = F_2^{(2)} = 0$$

$$F_1^{(3)} = 1(0.6 - 0.5 + 0.25) = 0.35 \qquad \textit{and} \qquad F_2^{(3)} = 1(0.75 - 0.6 + 0.25) = 0.4$$

$$F_1^{(4)} = F_2^{(4)} = 0$$

<u>Step 2:</u> Formulate element equations

Element 1:

$$R_{11}\phi_1 + R_{12}\phi_2 + L_{11}\varphi_1 + L_{12}\varphi_2 + F_1 = 0$$

$$\phi_2 + 0.25\varphi_1 - 0.5\varphi_2 = 0$$

$$R_{21}\phi_1 + R_{22}\phi_2 + L_{21}\phi_1 + L_{22}\phi_2 + F_2 = 0$$

$$\phi_2 + 0.5\varphi_1 - 0.25\varphi_2 = 0$$

Element 2:

$$R_{11}\phi_2 + R_{12}\phi_3 + L_{11}\varphi_2 + L_{12}\varphi_3 + F_1 = 0$$

$$-\phi_2 + \phi_3 + 0.25\varphi_2 - 0.5\varphi_3 = 0$$

$$R_{21}\phi_2 + R_{22}\phi_3 + L_{21}\varphi_2 + L_{22}\varphi_3 + F_2 = 0$$

$$\phi_2 - \phi_3 + 0.5\varphi_2 - 0.25\varphi_3 = 0$$

Element 3:

$$R_{11}\phi_3 + R_{12}\phi_4 + L_{11}\varphi_3 + L_{12}\varphi_4 + F_1 = 0$$

$$-\phi_3 + \phi_4 + 0.25\varphi_3 - 0.5\varphi_4 = -0.35$$

$$R_{21}\phi_3 + R_{22}\phi_4 + L_{21}\varphi_3 + L_{22}\varphi_4 + F_2 = 0$$

$$\phi_3 - \phi_4 + 0.5\varphi_2 - 0.25\varphi_3 = -0.4$$

Element 4:

$$R_{11}\phi_4 + R_{12}\phi_5 + L_{11}\varphi_4 + L_{12}\varphi_5 + F_1 = 0$$

$$-\phi_4 + 0.25\varphi_4 - 0.5\varphi_5 = 0$$

$$R_{21}\phi_4 + R_{22}\phi_5 + L_{21}\varphi_4 + L_{22}\varphi_5 + F_2 = 0$$

$$\phi_4 - \phi_5 + 0.5\varphi_4 - 0.25\varphi_5 = 0$$

Step 3: Assemble global matrix from the equations obtained in Step 2 and solve.

$$\begin{bmatrix} 1 & 0.25 & -0.5 & 0 & 0 & 0 & 0 & 0 \\ -1 & 0.5 & -0.25 & 0 & 0 & 0 & 0 & 0 \\ -1 & 0 & 0.25 & 1 & -0.5 & 0 & 0 & 0 \\ 1 & 0 & 0.5 & -1 & -0.25 & 0 & 0 & 0 \\ 0 & 0 & 0 & -1 & 0.25 & 1 & -0.5 & 0 \\ 0 & 0 & 0 & 1 & 0.5 & -1 & -0.25 & 0 \\ 0 & 0 & 0 & 0 & 0 & -1 & 0.25 & -0.5 \\ 0 & 0 & 0 & 0 & 0 & 1 & 0.5 & -0.25 \end{bmatrix} \begin{Bmatrix} \phi_2 \\ \varphi_1 \\ \varphi_2 \\ \phi_3 \\ \varphi_3 \\ \phi_4 \\ \varphi_4 \\ \varphi_5 \end{Bmatrix} = \begin{Bmatrix} 0 \\ 0 \\ 0 \\ 0 \\ -0.35 \\ -0.4 \\ 0 \\ 0 \end{Bmatrix}$$

Step 4: Tabulate the results obtained from Step 3 and compare against exact solution and Gem solutions obtained by using a domain that is discretized into 4 elements.

Solution	Exact Solution	**GEM** Solution
Of ϕ at x=0.25	-0.1	-0.1
x=0.5	-0.2	-0.2
x=0.75	-0.15	-0.15
Of φ at x=0	-0.4	-0.4
X=0.25	-0.4	-0.4
X=0.5	-0.4	-0.4
x=0.75	0.6	0.6
X=1	0.6	0.6

Applications of Green Element to a Linear Heterogeneous Problems

The heterogeneous problem to be solved is one which is governed the following expression

$$\frac{d}{dx}\left[K\frac{d\phi}{dx}\right]=0; \qquad \phi(x=0)=0 \qquad \phi(x=1)=1$$

where $K=1+x$

Exact Solution

The exact solution to the governing equation is given below

$$\phi(x)=\frac{\ln(1+x)}{\ln 2}$$

$$\varphi(x)=\frac{1}{(1+x)\ln 2}$$

Green Element Solution

We shall discretize the domain into 4 equal elements so that $\ell=\bar{\ell}=0.25$ as shown below:

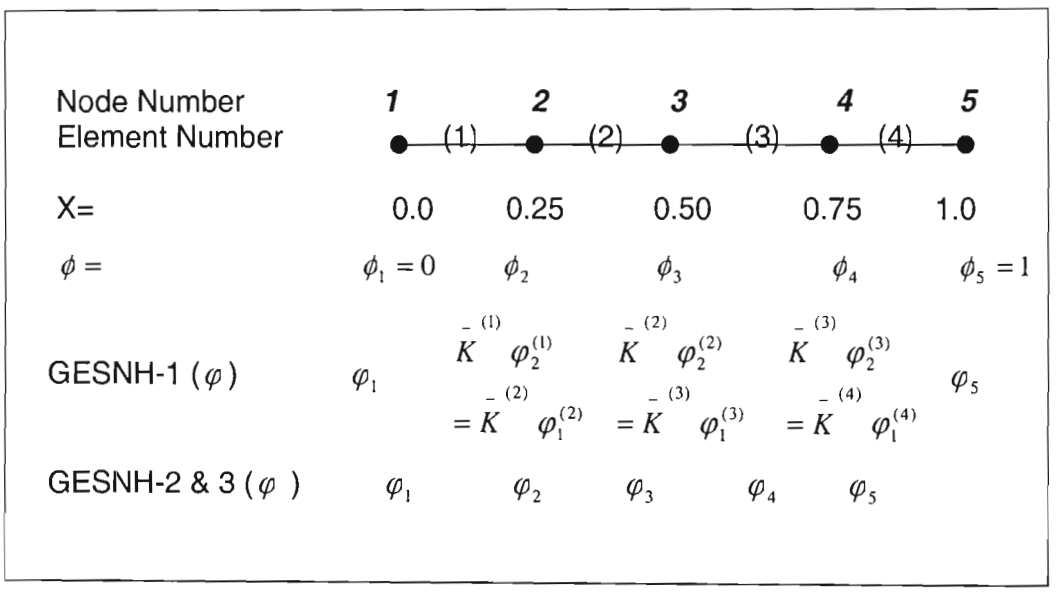

Part 1 : First Green Element Model (GESHN-1)

The system of discrete element equations is given by eq. (2.13) and restated below

$$R_{ij}^{(e)}\phi_j^{(e)} + L_{ij}^{(e)}\varphi_j^{(e)} + \frac{1}{\bar{K}}F_i^{(e)} = 0; \qquad i,j = 1,2 \qquad e = 1,2,3,4$$

Since there is no recharge, $F_i^{(e)} = 0$ and thus the 3rd of the equation becomes 0

Step 1: Calculate the values of the coefficients, $R_{ij}^{(e)}$ and $L_{ij}^{(e)}$, according to equations (1.25) and (1.26), repectively.

$$R_{ij}^{(e)} = \begin{bmatrix} -1 & 1 \\ 1 & -1 \end{bmatrix} \qquad and \qquad L_{ij}^{(e)} = \frac{1}{3}\begin{bmatrix} 1 & -2 \\ 2 & -1 \end{bmatrix}$$

Step 2: To account for the heterogeneous nature of the problem, we must compute $\bar{K}$ for each element, note that $K = 1 + x$.

At

x=0; $K = 1 + 0 = 1$

X=0.25 $K = 1 + 0.25 = 1.25$ $\bar{K}^{(1)} = \frac{1 + 1.25}{2} = 1.125$

X=0.5 $K = 1 + 0.5 = 1.5$ $\bar{K}^{(2)} = \frac{1.25 + 1.5}{2} = 1.375$

X=0.75 $K = 1 + 0.75 = 1.75$ $\bar{K}^{(3)} = \frac{1.5 + 1.75}{2} = 1.625$

X=1.0 $K = 1 + 1 = 2$ $\bar{K}^{(4)} = \frac{1.75 + 2}{2} = 1.875$

For shared nodes Compatibility requires that:

$$\phi_2^1 = \phi_1^2 = \varphi_2$$

thus

$$\bar{K}^{(1)}\phi_2^1 = \bar{K}^{(2)}\phi_1^2$$

hence

$$\phi_2^1 = \bar{K}^{(2)} / \bar{K}^{(1)}\phi_1^2 = 1.222\phi_1^2 = \phi_2$$

Similarly:

$$\phi_2^2 = \phi_1^3 = \varphi_3$$

thus

$$\bar{K}^{(2)}\ \phi_2^2 = \bar{K}^{(3)}\ \phi_1^3$$

hence

$$\phi_2^2 = \bar{K}^{(3)} / \bar{K}^{(2)}\ \phi_1^3 = 1.182\phi_1^3 = \phi_3$$

and

$$\phi_2^3 = \phi_1^4 = \varphi_4$$

thus

$$\bar{K}^{(3)}\ \phi_2^3 = \bar{K}^{(4)}\ \phi_1^4$$

hence

$$\phi_2^3 = \bar{K}^{(4)} / \bar{K}^{(3)}\ \phi_1^4 = 1.154\phi_1^4 = \phi_4$$

<u>Step 3:</u> Formulate element equations

Element 1:

$$R_{11}\phi_1 + R_{12}\phi_2 + L_{11}\varphi_1 + L_{12}\left(\frac{\bar{K}^{(2)}}{\bar{K}^{(1)}}\right)\varphi_2 = 0$$

$$0 + \phi_2 + 0.25\varphi_1 - 0.5(1.222)\varphi_2 = 0$$

$$\phi_2 + 0.25\varphi_1 - 0.61\varphi_2 = 0$$

$$R_{21}\phi_1 + R_{22}\phi_2 + L_{21}\phi_1 + L_{22}\left(\frac{\bar{K}^{(2)}}{\bar{K}^{(1)}}\right)\phi_2 = 0$$

$$-\phi_2 + 0.5\varphi_1 - 0.25\,(1.222\,)\varphi_2 = 0$$

$$-\phi_2 + 0.5\varphi_1 - 0.305\,\varphi_2 = 0$$

Element 2:

$$R_{11}\phi_2 + R_{12}\phi_3 + L_{11}\varphi_2 + L_{12}\left(\frac{\bar{K}^{(3)}}{\bar{K}^{(2)}}\right)\varphi_3 = 0$$

$$-\phi_2 + \phi_3 + 0.25\varphi_2 - 0.591\varphi_3 = 0$$

$$R_{21}\phi_2 + R_{22}\phi_3 + L_{21}\varphi_2 + L_{22}\left(\frac{\bar{K}^{(3)}}{\bar{K}^{(2)}}\right)\varphi_3 = 0$$

$$\phi_2 - \phi_3 + 0.5\varphi_2 - 0.296\varphi_3 = 0$$

Element 3:

$$R_{11}\phi_3 + R_{12}\phi_4 + L_{11}\varphi_3 + L_{12}\left(\frac{\bar{K}^{(4)}}{\bar{K}^{(3)}}\right)\varphi_4 = 0$$

$$-\phi_3 + \phi_4 + 0.25\varphi_3 - 0.577\varphi_4 = 0$$

$$R_{21}\phi_3 + R_{22}\phi_4 + L_{21}\varphi_3 + L_{22}\left(\frac{\bar{K}^{(4)}}{\bar{K}^{(3)}}\right)\varphi_4 = 0$$

$$\phi_3 - \phi_4 + 0.5\varphi_3 - 0.289\varphi_4 = 0$$

Element 4:

$$R_{11}\phi_4 + R_{12}\phi_5 + L_{11}\varphi_4 + L_{12}\varphi_5 = 0$$

$$-\phi_4 + 1 + 0.25\varphi_4 - 0.5\varphi_5 = 0$$

$$-\phi_4 + 0.25\varphi_4 - 0.5\varphi_5 = -1$$

$$R_{21}\phi_4 + R_{22}\phi_5 + L_{21}\varphi_4 + L_{22}\varphi_5 = 0$$

$$\phi_4 - 1 + 0.5\varphi_4 - 0.25\varphi_5 = 0$$

$$\phi_4 + 0.5\varphi_4 - 0.25\varphi_5 = 1$$

<u>Step 4:</u> Assemble global matrix from the equations obtained in Step 3 and solve.

$$\begin{bmatrix} 1 & 0.25 & -0.61 & 0 & 0 & 0 & 0 & 0 \\ -1 & 0.5 & -0.305 & 0 & 0 & 0 & 0 & 0 \\ -1 & 0 & 0.25 & 1 & -0.591 & 0 & 0 & 0 \\ 1 & 0 & 0.5 & -1 & -0.296 & 0 & 0 & 0 \\ 0 & 0 & 0 & -1 & 0.25 & 1 & -0.577 & 0 \\ 0 & 0 & 0 & 1 & 0.5 & -1 & -0.289 & 0 \\ 0 & 0 & 0 & 0 & 0 & -1 & 0.25 & -0.5 \\ 0 & 0 & 0 & 0 & 0 & 1 & 0.5 & -0.25 \end{bmatrix} \begin{Bmatrix} \phi_2 \\ \varphi_1 \\ \varphi_2 \\ \phi_3 \\ \varphi_3 \\ \phi_4 \\ \varphi_4 \\ \varphi_5 \end{Bmatrix} = \begin{Bmatrix} 0 \\ 0 \\ 0 \\ 0 \\ 0 \\ 0 \\ -1 \\ 1 \end{Bmatrix}$$

Part 2 : First Green Element Model (GESHN-2)

The system of discrete element equations is given by eq. (2.33) and restated below

$$R_{ij}^{(e)}\phi_j^{(e)} + \left(L_{ij}^{(e)} - V_{inj}^{(e)}\theta_n^{(e)}\right)\varphi_j^{(e)} + U_{ijn}^{(e)}\Psi_j^{(e)} f_n^{(e)} = 0; \qquad i, j, n = 1,2$$

Since there is no recharge, $F_i^{(e)} = 0$ and thus the 3rd of the equation becomes 0

Step 1: Calculate the values of the coefficients

$$R_{ij}^{(e)} = \begin{bmatrix} -1 & 1 \\ 1 & -1 \end{bmatrix} \qquad and \qquad L_{ij}^{(e)} = 0.25\begin{bmatrix} 1 & -2 \\ 2 & -1 \end{bmatrix}$$

$$\theta_n \equiv \ln K = \ln(1+x)$$

$x = 0$

$\theta_1^{(1)} = \ln(1+0) = 0$

$\theta_2^{(1)} = \ln(1+0.25) = 0.22314$

$x = 0.25$

$\theta_1^{(2)} = \ln(1+0.25) = 0.22314$

$\theta_2^{(2)} = \ln(1+0.5) = 0.40547$

$x = 0.75$

$\theta_1^{(3)} = \ln(1+0.5) = 0.40547$

$\theta_2^{(3)} = \ln(1+0.75) = 0.55962$

$x = 1$

$\theta_1^{(4)} = \ln(1+0.75) = 0.55962$

$\theta_2^{(4)} = \ln(1+1) = 0.69315$

$V_{inj}^{(e)}$ are calculated according to eq (2.37)

$$V_{1nj}^{(e)} = \frac{1}{6}\begin{bmatrix} -1 & -1.25 \\ 1 & 1.25 \end{bmatrix}$$

$$V_{2nj}^{(e)} = \frac{1}{6}\begin{bmatrix} -1.25 & -1 \\ 1.25 & 1 \end{bmatrix}$$

Step 3: Calculate the values of $V_{inj}^{(e)}\theta_j^{(e)}$

Element	i	n	j	V	ø	V_{inj}ø
1	1	1	1	-0.1667	0.00000	0.00000
	1	1	2	-0.2083	0.00000	0.00000
	1	2	1	0.1667	0.22314	0.03719
	1	2	2	0.2083	0.22314	0.04649
	2	1	1	-0.2083	0.00000	0.00000
	2	1	2	-0.1667	0.00000	0.00000
	2	2	1	0.2083	0.22314	0.04649
	2	2	2	0.1667	0.22314	0.03719
2	1	1	1	-0.1667	0.22314	-0.03719
	1	1	2	-0.2083	0.22314	-0.04649
	1	2	1	0.1667	0.40547	0.06758
	1	2	2	0.2083	0.40547	0.08447
	2	1	1	-0.2083	0.22314	-0.04649
	2	1	2	-0.1667	0.22314	-0.03719
	2	2	1	0.2083	0.40547	0.08447
	2	2	2	0.1667	0.40547	0.06758
3	1	1	1	-0.1667	0.40547	-0.06758
	1	1	2	-0.2083	0.40547	-0.08447
	1	2	1	0.1667	0.55962	0.09327
	1	2	2	0.2083	0.55962	0.11659
	2	1	1	-0.2083	0.40547	-0.08447
	2	1	2	-0.1667	0.40547	-0.06758
	2	2	1	0.2083	0.55962	0.11659
	2	2	2	0.1667	0.55962	0.09327
4	1	1	1	-0.1667	0.55962	-0.09327
	1	1	2	-0.2083	0.55962	-0.11659
	1	2	1	0.1667	0.69315	0.11553
	1	2	2	0.2083	0.69315	0.14441
	2	1	1	-0.2083	0.55962	-0.11659
	2	1	2	-0.1667	0.55962	-0.09327
	2	2	1	0.2083	0.69315	0.14441
	2	2	2	0.1667	0.69315	0.11553

Step 4: Formulate element equations

Element 1:

$$R_{11}\phi_1 + R_{12}\phi_2 + [L_{11} - (V_{111}\theta_1 + V_{121}\theta_2)]\varphi_1 + [L_{12} - (V_{112}\theta_1 + V_{122}\theta_2)]\varphi_2 = 0$$

$$0 + \phi_2 + [0.25 - (0 + 0.03719)]\varphi_1 + [-0.5 - (0 + 0.04649)]\varphi_2 = 0$$

$$\phi_2 + 0.21281\varphi_1 - 0.54649\varphi_2 = 0$$

$$R_{21}\phi_1 + R_{22}\phi_2 + [L_{21} - (V_{211}\theta_1 + V_{221}\theta_2)]\varphi_1 + [L_{22} - (V_{212}\theta_1 + V_{222}\theta_2)]\varphi_2 = 0$$

$$0 + \phi_2 + [0.5 - (0 + 0.04649)]\varphi_1 + [-0.25 - (0 - 0.03719)]\varphi_2 = 0$$

$$-\phi_2 + 0.45351\varphi_1 - 0.28719\varphi_2 = 0$$

Element 2:

$$R_{11}\phi_2 + R_{12}\phi_3 + [L_{11} - (V_{111}\theta_1 + V_{121}\theta_2)]\varphi_2 + [L_{12} - (V_{112}\theta_1 + V_{122}\theta_2)]\varphi_3 = 0$$

$$-\phi_2 + \phi_3 + [0.25 - (-0.03719 - 0.06758)]\varphi_2 + [-0.5 - (-0.04649 + 0.08447)]\varphi_3 = 0$$

$$-\phi_2 + \phi_3 + 0.21961\varphi_2 - 0.53798\varphi_3 = 0$$

$$R_{21}\phi_2 + R_{22}\phi_3 + [L_{21} - (V_{211}\theta_1 + V_{221}\theta_2)]\varphi_2 + [L_{22} - (V_{212}\theta_1 + V_{222}\theta_2)]\varphi_3 = 0$$

$$\phi_2 - \phi_3 + [0.5 - (-0.04649 + 0.08447)]\varphi_2 + [-0.25 - (-0.03719 + 0.06758)]\varphi_3 = 0$$

$$\phi_2 - \phi_3 + 0.46202\varphi_2 - 0.28039\varphi_3 = 0$$

Element 3:

$$R_{11}\phi_3 + R_{12}\phi_4 + [L_{11} - (V_{111}\theta_1 + V_{121}\theta_2)]\varphi_3 + [L_{12} - (V_{112}\theta_1 + V_{122}\theta_2)]\varphi_4 = 0$$

$$-\phi_3 + \phi_4 + [0.25 - (-0.06758 + 0.09327)]\varphi_3 + [-0.5 - (-0.08447 + 0.11659)]\varphi_4 = 0$$

$$-\phi_3 + \phi_4 + 0.22431\varphi_3 - 0.53212\varphi_4 = 0$$

$$R_{21}\phi_3 + R_{22}\phi_4 + [L_{21} - (V_{211}\theta_1 + V_{221}\theta_2)]\varphi_3 + [L_{22} - (V_{212}\theta_1 + V_{222}\theta_2)]\varphi_4 = 0$$

$$\phi_3 - \phi_4 + [0.5 - (-0.08447 + 0.11659)]\varphi_3 + [-0.25 - (-0.06758 + 0.09327)]\varphi_4 = 0$$

$$\phi_3 - \phi_4 + 0.46788\varphi_3 - 0.27569\varphi_4 = 0$$

Element 4:

$$R_{11}\phi_4 + R_{12}\phi_5 + \left[L_{11} - \left(V_{111}\theta_1 + V_{121}\theta_2\right)\right]\varphi_4 + \left[L_{12} - \left(V_{112}\theta_1 + V_{122}\theta_2\right)\right]\varphi_5 = 0$$

$$-\phi_4 + 1 + \left[0.25 - \left(-0.09327 + 0.11659\right)\right]\varphi_4 + \left[-0.5 - \left(-0.11553 + 0.14441\right)\right]\varphi_5 = 0$$

$$-\phi_4 + 0.22668\varphi_4 - 0.52888\varphi_5 = -1$$

$$R_{21}\phi_4 + R_{22}\phi_5 + \left[L_{21} - \left(V_{211}\theta_1 + V_{221}\theta_2\right)\right]\varphi_4 + \left[L_{22} - \left(V_{212}\theta_1 + V_{222}\theta_2\right)\right]\varphi_5 = 0$$

$$\phi_4 - 1 + \left[0.5 - \left(-0.11659 + 0.14441\right)\right]\varphi_4 + \left[-0.25 - \left(-0.09327 + 0.11659\right)\right]\varphi_5 = 0$$

$$\phi_4 + 0.47218\varphi_4 - 0.27332\varphi_5 = 1$$

Step 5: Assemble global matrix and solve

$$\begin{bmatrix} 1 & 0.21281 & -0.54649 & 0 & 0 & 0 & 0 & 0 \\ -1 & 0.45351 & -0.28719 & 0 & 0 & 0 & 0 & 0 \\ -1 & 0 & 0.21961 & 1 & -0.53798 & 0 & 0 & 0 \\ 1 & 0 & 0.46202 & -1 & -0.28039 & 0 & 0 & 0 \\ 0 & 0 & 0 & -1 & 0.22431 & 1 & -0.53212 & 0 \\ 0 & 0 & 0 & 1 & 0.46788 & -1 & -0.27569 & 0 \\ 0 & 0 & 0 & 0 & 0 & -1 & 0.22668 & -0.52888 \\ 0 & 0 & 0 & 0 & 0 & 1 & 0.47219 & -0.27332 \end{bmatrix} \begin{Bmatrix} \phi_2 \\ \varphi_1 \\ \varphi_2 \\ \phi_3 \\ \varphi_3 \\ \phi_4 \\ \varphi_4 \\ \varphi_5 \end{Bmatrix} = \begin{Bmatrix} 0 \\ 0 \\ 0 \\ 0 \\ 0 \\ 0 \\ -1 \\ 1 \end{Bmatrix}$$

Example 4.3

Implementation of GESNH-3

The system of discrete element equations is given by eq. (2.44) and restated below

$$R_{ij}^{(e)}\phi_j^{(e)} + \left(L_{ij}^{(e)} - S_{imnj}^{(e)}K_m^{(e)}\Psi_n^{(e)}\right)\varphi_j^{(e)} + U_{ijm}^{(e)}\Psi_j^{(e)}f_m^{(e)} = 0; \qquad i,j,m,n = 1,2$$

Since there is no recharge, $f_m^{(e)} = 0$ and the 3rd term of the equation becomes 0.

Step 1: Calculate the values of the coefficients

$$R_{ij}^{(e)} = \begin{bmatrix} -1 & 1 \\ 1 & -1 \end{bmatrix} \qquad and \qquad L_{ij}^{(e)} = \frac{1}{3}\begin{bmatrix} 1 & -2 \\ 2 & -1 \end{bmatrix}$$

$$K_1^{(1)} = e^{-3} \qquad K_2^{(1)} = e^{-2.5}$$
$$K_1^{(2)} = K_2^{(1)} = e^{-2.5} \qquad K_2^{(2)} = e^{-2.0}$$
$$K_1^{(3)} = K_2^{(2)} = e^{-2.0} \qquad K_2^{(3)} = e^{-1.5}$$
$$K_1^{(4)} = K_2^{(3)} = e^{-1.5} \qquad K_2^{(4)} = e^{-1.0}$$

$$\Psi_1^{(1)} = e^{3} \qquad \Psi_2^{(1)} = e^{2.5}$$
$$\Psi_1^{(2)} = \Psi_2^{(1)} = e^{2.5} \qquad \Psi_2^{(2)} = e^{2.0}$$
$$\Psi_1^{(3)} = \Psi_2^{(2)} = e^{2.0} \qquad \Psi_2^{(3)} = e^{1.5}$$
$$\Psi_1^{(4)} = \Psi_2^{(3)} = e^{1.5} \qquad \Psi_2^{(4)} = e^{1.0}$$

$S_{imnj}^{(e)}$ can be calculated using eqs. (2.49) and (2.50)

$$S_{11nj}^{(e)} = -S_{12nj}^{(e)} = -\frac{1}{12}\begin{bmatrix} \frac{5}{4} & \frac{3}{4} \\ \frac{3}{4} & \frac{7}{4} \end{bmatrix}$$

$$S_{11nj}^{(e)} = -S_{12nj}^{(e)} = -\frac{1}{12}\begin{bmatrix} \frac{7}{4} & \frac{3}{4} \\ \frac{3}{4} & \frac{5}{4} \end{bmatrix}$$

Step 3: Calculate the values of $S_{imnj}^{(e)} K_m^{(e)} \Psi_n^{(e)}$

Element	I	m	n	j	S	K	Ψ	$S_{imnj} K_m \Psi_n$
1	1	1	1	1	-0.10417	0.0498	20.08554	-0.10417
	1	1	1	2	-0.06250	0.0498	20.08554	-0.06250
	1	1	2	1	-0.06250	0.0498	12.18249	-0.03791
	1	1	2	2	-0.14583	0.0498	12.18249	-0.08845
	1	2	1	1	-0.10417	0.0821	20.08554	-0.17174
	1	2	1	2	0.06250	0.0821	20.08554	0.10305
	1	2	2	1	0.06250	0.0821	12.18249	0.06250
	1	2	2	2	0.14583	0.0821	12.18249	0.14583
	2	1	1	1	-0.14583	0.0498	20.08554	-0.14583
	2	1	1	2	-0.06250	0.0498	20.08554	-0.06250
	2	1	2	1	-0.06250	0.0498	12.18249	-0.03791
	2	1	2	2	-0.10417	0.0498	12.18249	-0.06318
	2	2	1	1	0.14583	0.0821	20.08554	0.24044
	2	2	1	2	0.06250	0.0821	20.08554	0.10305
	2	2	2	1	0.06250	0.0821	12.18249	0.06250
	2	2	2	2	0.10417	0.0821	12.18249	0.10417
2	1	1	1	1	-0.10417	0.0821	12.18249	-0.10417
	1	1	1	2	-0.06250	0.0821	12.18249	-0.06250
	1	1	2	1	-0.06250	0.0821	7.389056	-0.03791
	1	1	2	2	-0.14583	0.0821	7.389056	-0.08845
	1	2	1	1	-0.10417	0.1353	12.18249	-0.17174
	1	2	1	2	0.06250	0.1353	12.18249	0.10305
	1	2	2	1	0.06250	0.1353	7.389056	0.06250
	1	2	2	2	0.14583	0.1353	7.389056	0.14583
	2	1	1	1	-0.14583	0.0821	12.18249	-0.14583
	2	1	1	2	-0.06250	0.0821	12.18249	-0.06250
	2	1	2	1	-0.06250	0.0821	7.389056	-0.03791
	2	1	2	2	-0.10417	0.0821	7.389056	-0.06318
	2	2	1	1	0.14583	0.1353	12.18249	0.24044
	2	2	1	2	0.06250	0.1353	12.18249	0.10305
	2	2	2	1	0.06250	0.1353	7.389056	0.06250
	2	2	2	2	0.10417	0.1353	7.389056	0.10417

Element	I	m	n	j	S	K	Ψ	$S_{imnj} K_m \Psi_n$
3	1	1	1	1	-0.10417	0.1353	7.389056	-0.10417
	1	1	1	2	-0.06250	0.1353	7.389056	-0.06250
	1	1	2	1	-0.06250	0.1353	4.481689	-0.03791
	1	1	2	2	-0.14583	0.1353	4.481689	-0.08845
	1	2	1	1	-0.10417	0.2231	7.389056	-0.17174
	1	2	1	2	0.06250	0.2231	7.389056	0.10305
	1	2	2	1	0.06250	0.2231	4.481689	0.06250
	1	2	2	2	0.14583	0.2231	4.481689	0.14583
	2	1	1	1	-0.14583	0.1353	7.389056	-0.14583
	2	1	1	2	-0.06250	0.1353	7.389056	-0.06250
	2	1	2	1	-0.06250	0.1353	4.481689	-0.03791
	2	1	2	2	-0.10417	0.1353	4.481689	-0.06318
	2	2	1	1	0.14583	0.2231	7.389056	0.24044
	2	2	1	2	0.06250	0.2231	7.389056	0.10305
	2	2	2	1	0.06250	0.2231	4.481689	0.06250
	2	2	2	2	0.10417	0.2231	4.481689	0.10417
4	1	1	1	1	-0.10417	0.2231	4.481689	-0.10417
	1	1	1	2	-0.06250	0.2231	4.481689	-0.06250
	1	1	2	1	-0.06250	0.2231	2.718282	-0.03791
	1	1	2	2	-0.14583	0.2231	2.718282	-0.08845
	1	2	1	1	-0.10417	0.3679	4.481689	-0.17174
	1	2	1	2	0.06250	0.3679	4.481689	0.10305
	1	2	2	1	0.06250	0.3679	2.718282	0.06250
	1	2	2	2	0.14583	0.3679	2.718282	0.14583
	2	1	1	1	-0.14583	0.2231	4.481689	-0.14583
	2	1	1	2	-0.06250	0.2231	4.481689	-0.06250
	2	1	2	1	-0.06250	0.2231	2.718282	-0.03791
	2	1	2	2	-0.10417	0.2231	2.718282	-0.06318
	2	2	1	1	0.14583	0.3679	4.481689	0.24044
	2	2	1	2	0.06250	0.3679	4.481689	0.10305
	2	2	2	1	0.06250	0.3679	2.718282	0.06250
	2	2	2	2	0.10417	0.3679	2.718282	0.10417

Step 4: Formulate element equations

Element

1: $R_{11}\phi_1 + R_{12}\phi_2 + [L_{11} - (S_{1111}K_1\Psi_1 + S_{1121}K_1\Psi_2 + S_{1211}K_2\Psi_1 + S_{1221}K_2\Psi_2)]\varphi_1$
$[L_{21} - (S_{21111}K_1\Psi_1 + S_{2121}K_1\Psi_2 + S_{1211}K_2\Psi_1 + S_{1221}K_2\Psi_2)]\varphi_1 = 0$

$0 + \phi_2 + [0.25 - (0.5 - 0.41667)]\varphi_1 + [-0.5 - (0.625 - 0.52083)]\varphi_2 = 0$

$\phi_2 + 0.16667\varphi_1 - 0.60417\varphi_2 = 0 \qquad (1)$

$R_{21}\phi_1 + R_{22}\phi_2 + [L_{21} - (V_{211}\theta_1 + V_{221}\theta_2)]\varphi_1 + [L_{22} - (V_{212}\theta_1 + V_{222}\theta_2)]\varphi_2 = 0$

$0 + \phi_2 + [0.5 - (0.625 - 0.52083)]\varphi_1 + [-0.25 - (0.5 - 0.41667)]\varphi_2 = 0$

$-\phi_2 + 0.39583\varphi_1 - 0.33333\varphi_2 = 0 \qquad (2)$

Element 2: $R_{11}\phi_2 + R_{12}\phi_3 + [L_{11} - (V_{111}\theta_1 + V_{121}\theta_2)]\varphi_2 + [L_{12} - (V_{112}\theta_1 + V_{122}\theta_2)]\varphi_3 = 0$

$-\phi_2 + \phi_3 + [0.25 - (0.41667 - 0.33333)]\varphi_2 + [-0.5 - (0.52083 - 0.41667)]\varphi_3 = 0$

$-\phi_2 + \phi_3 + 0.16667\varphi_2 - 0.60416\varphi_3 = 0 \qquad (3)$

$R_{21}\phi_2 + R_{22}\phi_3 + [L_{21} - (V_{211}\theta_1 + V_{221}\theta_2)]\varphi_2 + [L_{22} - (V_{212}\theta_1 + V_{222}\theta_2)]\varphi_3 = 0$

$\phi_2 - \phi_3 + [0.5 - (0.52083 - 0.41667)]\varphi_2 + [-0.25 - (0.41667 - 0.33333)]\varphi_3 = 0$

$\phi_2 - \phi_3 + 0.39584\varphi_2 - 0.33334\varphi_3 = 0 \qquad (4)$

Element 3: $R_{11}\phi_3 + R_{12}\phi_4 + [L_{11} - (V_{111}\theta_1 + V_{121}\theta_2)]\varphi_3 + [L_{12} - (V_{112}\theta_1 + V_{122}\theta_2)]\varphi_4 = 0$

$-\phi_3 + \phi_4 + [0.25 - (0.33333 - 0.25)]\varphi_3 + [-0.5 - (0.41667 - 0.3125)]\varphi_4 = 0$

$-\phi_3 + \phi_4 + 0.16667\varphi_2 - 0.60416\varphi_3 = 0 \qquad (5)$

$R_{21}\phi_3 + R_{22}\phi_4 + [L_{21} - (V_{211}\theta_1 + V_{221}\theta_2)]\varphi_3 + [L_{22} - (V_{212}\theta_1 + V_{222}\theta_2)]\varphi_4 = 0$

$\phi_3 - \phi_4 + [0.5 - (0.41667 - 0.3125)]\varphi_3 + [-0.25 - (0.33333 - 0.25)]\varphi_4 = 0$

$\phi_3 - \phi_4 + 0.39583\varphi_3 - 0.33333\varphi_4 = 0 \qquad (6)$

Element 3: $R_{11}\phi_4 + R_{12}\phi_5 + [L_{11} - (V_{111}\theta_1 + V_{121}\theta_2)]\varphi_4 + [L_{12} - (V_{112}\theta_1 + V_{122}\theta_2)]\varphi_5 = 0$

$$-\phi_4 + 1 + [0.25 - (0.25 - 0.16667)]\varphi_4 + [-0.5 - (0.3125 - 0.20833)]\varphi_5 = 0$$
$$-\phi_4 + 0.16667\varphi_2 - 0.60416\varphi_3 = -1 \qquad (7)$$

$$R_{21}\phi_4 + R_{22}\phi_5 + [L_{21} - (V_{211}6_1 + V_{221}6_2)]\varphi_4 + [L_{22} - (V_{212}6_1 + V_{222}6_2)]\varphi_5 = 0$$
$$\phi - 1 + [0.5 - (0.3125 - 0.20833)]\varphi_4 + [-0.25 - (0.25 - 0.16667)]\varphi_5 = 0$$
$$\phi_4 + 0.39583\varphi_3 - 0.33333\varphi_4 = 1 \qquad (8)$$

Step 5: Assemble global matrix and solve

$$\begin{bmatrix} 0.161 & 1 & -0.604 & 0 & 0 & 0 & 0 & 0 \\ 0.396 & -1 & -0.333 & 0 & 0 & 0 & 0 & 0 \\ 0 & -1 & 0.167 & 1 & -0.604 & 0 & 0 & 0 \\ 0 & 1 & 0.396 & -1 & -0.333 & 0 & 0 & 0 \\ 0 & 0 & 0 & -1 & 0.167 & 1 & -0.604 & 0 \\ 0 & 0 & 0 & 1 & 0.396 & -1 & -0.333 & 0 \\ 0 & 0 & 0 & 0 & 0 & -1 & 0.167 & -0.604 \\ 0 & 0 & 0 & 0 & 0 & 1 & 0.396 & -0.333 \end{bmatrix} \begin{Bmatrix} \varphi_1 \\ \phi_2 \\ \varphi_2 \\ \phi_3 \\ \varphi_3 \\ \phi_4 \\ \varphi_4 \\ \varphi_5 \end{Bmatrix} = \begin{Bmatrix} 0 \\ 0 \\ 0 \\ 0 \\ 0 \\ 0 \\ -1 \\ 1 \end{Bmatrix}$$